Regulation of fission yeast cytokinesis by membrane lipids and septins

Federica Arbizzani

PSL UNIVERSITÉ PARIS

THÈSE DE DOCTORAT
DE L'UNIVERSITÉ PSL

Préparée à l'Institut Curie

dans le laboratoire Architecture du cytosquelette et morphogenèse cellulaire, CNRS UMR 144

Régulation de la cytokinèse par les lipides membranaires et les septines chez la levure S. Pombe

Soutenue par
Federica ARBIZZANI
Le 02 Decembre 2019

Ecole doctorale n° 577
Structure et Dynamique des systèmes vivants

Spécialité
Sciences de la vie et de la santé

Composition du jury :

Anne, PAOLETTI Directeur de recherche, Institut Curie-CNRS UMR 144	*Directeur de thèse*
Pierre, CAPY Professeur, Université Paris-Sud	*Président*
Simonetta, PIATTI Directeur de Recherche, CRBM-CNRS, Université de Montpellier	*Rapporteur*
Arnaud, ECHARD Directeur de recherche, Institut Pasteur-CNRS	*Rapporteur*
Pilar, PEREZ Professeur, IBGF-Universidad Salamanca	*Examinateur*
Sergio, RINCON Professeur Assistant, IBGF-Universidad Salamanca	*Examinateur*

institutCurie
Ensemble, prenons le cancer de vitesse.

ACKNOWLEDGEMENTS

First of all, I would like to thank my supervisor, Anne Paoletti, who has given me the opportunity of working on an interesting topic in the great scientific environment offered by Institute Curie. You are an excellent and rigorous scientist which carefully follows the path of your students, always providing support and advice. I have been very lucky to have you as my mentor.

I also need to thank my co-supervisor, Sergio Rincon, for having been my referent and guide during my PhD. I`ve learned more things from you than anyone else in the lab. You were always available to discuss about science and more. You are a very hardworking scientist and I`m very happy for the position you got in Spain.

Additionally, I have to thank Nicolas Minc and Jean-Baptiste Manneville for accepting to be part of my thesis committee and for the help and inputs you have provided in these occasions.

Of course a big thank goes to our collaborators, Aurelie Bertin and Manos Mavrakis, who worked next to me on the septin project and offered me the occasion to get familiar with new scientific techniques.

Obviously, I want to thank the entire team for the atmosphere not only prolific in terms of science but also for all the friendship, talks, laughs and cakes over the years. Thanks for all the technical help you gave me and for the strong emotional support when I was down or anxious. I wish you all the best for your future plans.

A big thanks also to all the new friends I met here. This time in Paris has been cheered by all the appetizers, picnics, birthdays, concerts and Italian Sunday lunches we had together. I hope we will still manage to spend some time together, despite our displacements in Europe.

A special thanks to Natascia Laura and Chiara, my dearest friends. We met at University, when we were all younger and light-hearted, and we have matured together. I have missed you so much in these years I can`t really describe. Our skype sessions and the few meetings we managed to have from time to time were really important to me. Every time we are together is like nothing has changed, even if half a year or more has passed. I hope sooner or later we will manage to live closer again.

A unique thanks goes to Matteo. These years would not have been the same without you. Our trips in France and around Europe, amazing summer holidays in Crete and Italy, inevitable walks around Paris over the weekends, Netflix sessions, cakes and Italian dishes preparation, parisian restaurant tastings have made these years very happy and unforgettable. Of course, being both PhD student in biology, there have been hard times, but you always managed to support me when I was stressed or stuck. The sweets you brought me from Joel and the cappelletti from your mum were incredibly helpful.

Infine, non puo` mancare un ringraziamento speciale alla mia famiglia. Cinque anni fa, ho lasciato la mia citta` natale e la mia famiglia per perseguire i miei studi e la mia carriera. Sono stati anni difficili e vi sono grata per aver accettato le mie scelte, stando sempre al mio fianco. Non ce l`avrei mai fatta senza il vostro indefesso incoraggiamento e supporto. Con i vostri assidui messaggini e foto mi avete sempre fatto sentire amata e tenuta al corrente di tutti gli eventi e novita` che avvenivano in mia assenza. Le visite natalizie, pasquali ed estive sono state occasioni uniche per farmi apprezzare ogni volta l` importanza e la gioia di essere insieme e condividere momenti felici. Sono incredibilmente fortunata ad avervi accanto. Questa tesi e` dedicata a voi.

Table of contents

I. INTRODUCTION

This section has been articulated into two parts. In the first one, the general elements on cell division will be presented, highlighting the crucial contribution of cytoskeletal elements and membrane reorganization for the success of cytokinesis. Secondly, it will be described specifically the cytokinesis in fission yeast, the model system used in this study.

1. The cell division cycle: progression and machinery

The cell cycle is a key process used by all cellular life forms to proliferate or self-renew. It is an ordered set of events, culminating in the division of the mother cell into two daughter cells. The cell cycle comprises two main stages: interphase composed of G1, S and G2 phases, where cells grow and duplicate their genetic material, and mitosis, during which chromosome segregation is driven by the mitotic spindle. Cytokinesis is the subsequent and final step that leads to the physical separation of the two daughter cells.

The proper succession of the different cell cycle steps is regulated by cyclin-dependent kinases (Cdks) and phosphatases that specifically counteract their actions. Cdk activity is dependent on the association with activating proteins, the cyclins whose expression vary during the cell cycle to modulate Cdk activity. Multiple Cdk and cyclins exist and interact differentially in diverse phases of the cell cycle (Fig1). The G1 cyclins in complex with CDK4, CDK6, and CDK2, establish entry into the cell cycle, whereas S-phase events and the G2/M transition are primarily regulated by CDK1 bound to members of the B-type family of cyclins (Hochegger et al., 2008; Rhind and Russell, 2012).

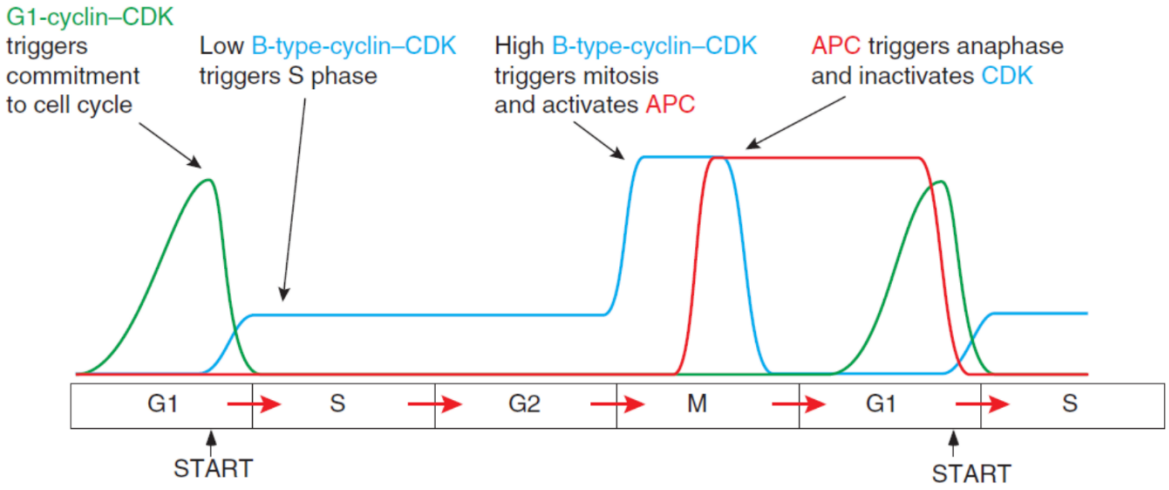

Figure 1 (Adapted from Rhind and Russell 2012): The regulation of the major events of the cell cycle. Waves of kinases and ubiquitine ligase activity are involved: G1-cyclin-CDK1 initiates the cell cycle and activate B-type cyclin-CDK1 activity. Low levels of B-type-cyclin–CDK activity are sufficient to trigger S phase, but tyrosine phosphorylation by Wee1 prevents full activation, preventing premature mitosis. Full CDK activation triggers mitosis and activates APC, which triggers anaphase and feeds back to inactivate CDK activity. Inactivation of CDK allows exit from mitosis and the establishment of interphase chromosome and nuclear structure in G1 phase.

The progression of cells through the cell cycle is also critically controlled by checkpoints operating at the G1/S the G2/M and the metaphase to anaphase transitions. They act as surveillance mechanisms that check the order, integrity, and fidelity of the major events of the cell cycle. Checkpoint dysfunction can have severe outcomes ranging from cell death to aneuploidy, which can result in cancer onset in metazoans (Fujiwara et al., 2005; Hayashi and Karlseder, 2013; Lacroix and Maddox, 2012; Storchova and Pellman, 2004).

1.1 Interphase: getting ready to divide

In order to maintain cell size and guarantee that each daughter cell will receive an appropriate amount of genetic and cytoplasmic material, cells need to double their content before division. This doubling takes places during the three sub-phases of interphase G1, S and G2 (Fig2). In G1 the cells grow and synthetize the mRNAs and proteins required to execute the future steps, but it is also the time of an important decision: enter and complete another cell cycle or stay in a resting phase also known as G0. During S phase the genetic information is copied and the centrosome, the main microtubule (MT) organizing center that directs chromosome movements during mitosis, is duplicated. In G2 the cells undergo additional growth, refill energy supplies and prepare themselves to reorganize the cytoplasmic components for division (Barnum and O'Connell, 2014; Rhind and Russell, 2012). Multiple surveillance mechanisms operate during interphase to monitor that a cell is fully committed to division, that it grows to an appropriate cell size and that the genetic material is accurately replicated and its integrity preserved. In particular, DNA damage correction strategies that maintain Cdk1 inactive can be engaged throughout interphase to allow DNA repair pathways to correct the lesions before entry into S phase or mitosis.

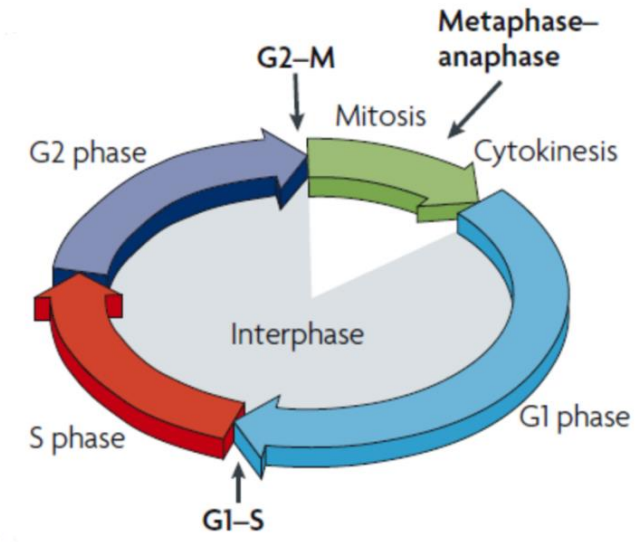

Figure 2: **Scheme of the eukaryotic cell cycle.**
Representation of the main cell cycle phases with the key events highlighted.

1.2 Mitosis: segregating cellular components in two equal sets

Entry into mitosis requires the activation of the Cdk1-Cyclin B complex, also known as Mitosis Promoting Factor (MPF), whose activity is maintained low during G2. This is achieved by multiple regulatory loops operating in parallel that promote the activation of the phosphatase Cdc25, which counteracts the inhibitory activity of the kinase Wee1 and the inhibition of the phosphatase PP2A, which antagonizes Cdk1 activity (Bollen et al., 2009; Wurzenberger and Gerlich, 2011). Once activated, this molecular machinery acts as a master regulator of mitosis by activating a plethora of downstream effectors. This leads to a general reorganization of the entire cell structure.

Mitosis is conventionally divided into four phases: prophase, metaphase, anaphase and telophase (Fig3). Prophase is characterized by the initiation of chromosome condensation and separation of the duplicated centrosomes, leading to the assembly of the mitotic spindle, a bipolar apparatus based on microtubules (MTs), microtubule-associated proteins and molecular motors that provides the mechanical forces necessary for the segregation of the sister chromatids. Bipolar spindle formation is completed in prometaphase, in concert with nuclear envelope breakdown and complete condensation of chromosomes. During metaphase, the MTs of the mitotic spindle bind to the kinetochores of condensed chromosomes in a bi-oriented manner. The kinetochores of sister chromatids attach to MTs emanating from opposite poles of the spindle. The chromosomes move back and forth until they eventually align on the metaphase plane in the center of the spindle. The spindle assembly checkpoint (SAC) monitors chromosome alignment preventing metaphase/anaphase transition in presence of unattached kinetochores. Once all chromosome are aligned on the metaphase plane, anaphase is triggered by activation of the anaphase promoting complex or Cyclosome (APC/C). The APC is an E3 ubiquitin ligase subunit that inactivates CDK1 by degradation of cyclin B and by activating phosphatases (Cdc14 in yeasts; PP1 and PP2A-B55 in animals) that oppose CDK1 activity (Clifford et al., 2008; Wurzenberger and Gerlich, 2011). It is activated by phosphorylation by CDK1 and by interaction with two regulatory subunits: Cdc20 at the metaphase/anaphase transition and Cdh1 during telophase and G1 phase. Upon activation, the APC targets the inhibitor of sister chromatid disjunction, securin, leading to the activation of the protease separase which cleaves the cohesin proteins that hold sister chromatids together and allows the separation of chromosomes in two movements: anaphase A, during which chromosomes are pulled toward the spindle poles by shortening of kinetochore MTs; and anaphase B, during which the spindles are further separated by elongation of interpolar MTs.

As anaphase progresses, the mitotic spindle re-organizes to generate an antiparallel microtubule bundle structure between segregating chromosomes, which is known as the central spindle or spindle midzone. Mitosis ends with telophase, during which nuclear envelope reassembles while the chromosomes start to decondense (Cross and McAinsh, 2014; Rhind and Russell, 2012; Sacristan and Kops, 2014).

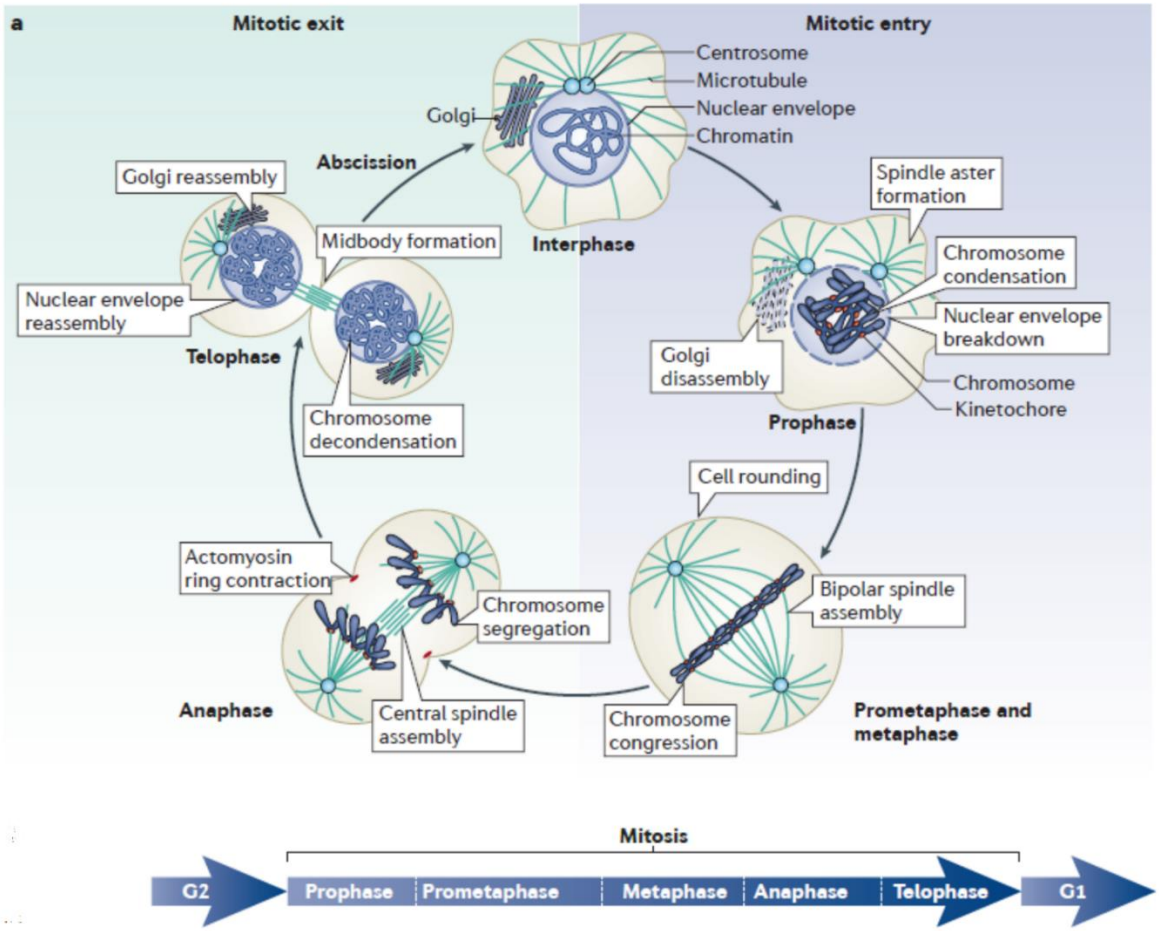

Figure 3 (Adapted from Wurzenberg and Gerlich 2011): **Cellular reorganization during mitotic entry and exit.** Schematic representation of centrosomes, chromatin, microtubules, nuclear envelope and Golgi for a cell progressing through mitosis. Attachment of all chromosomes to opposite spindle poles satisfies the spindle assembly checkpoint and initiates mitotic exit. Key events that occur at each stage of the cell cycle are indicated.

1.3 Cytokinesis: making two independent cellular entities

Cytokinesis begins during late anaphase and is usually completed in G1. It is a critical and irreversible step resulting in the formation of two independent daughter cells. It is therefore under the control of very tight regulatory mechanisms. In fact, cytokinesis is strictly coordinated with mitotic exit and chromosome separation to ensure an equal repartition of the genetic material in the newborn cells (Cullati and Gould, 2019).

Four major events can be distinguished during cytokinesis (Fig4). First, the position of the division plane is defined. In most organisms, this step involves signaling by the central spindle to allow cell division to occur in between the two sets of segregated chromosomes. Second, an actomyosin-based contractile ring (CR) assembles at the division site on the inner face of the plasma membrane. The third step is represented by the constriction of this structure that leads to the formation of the cleavage furrow that

partitions the cell into two. The closure of the CR is well synchronized with membrane trafficking pathways so that new membranes are generated to match the increased surface area of the two daughter cells, which are physically separated in two distinct entities in the last step of cytokinesis called abscission.

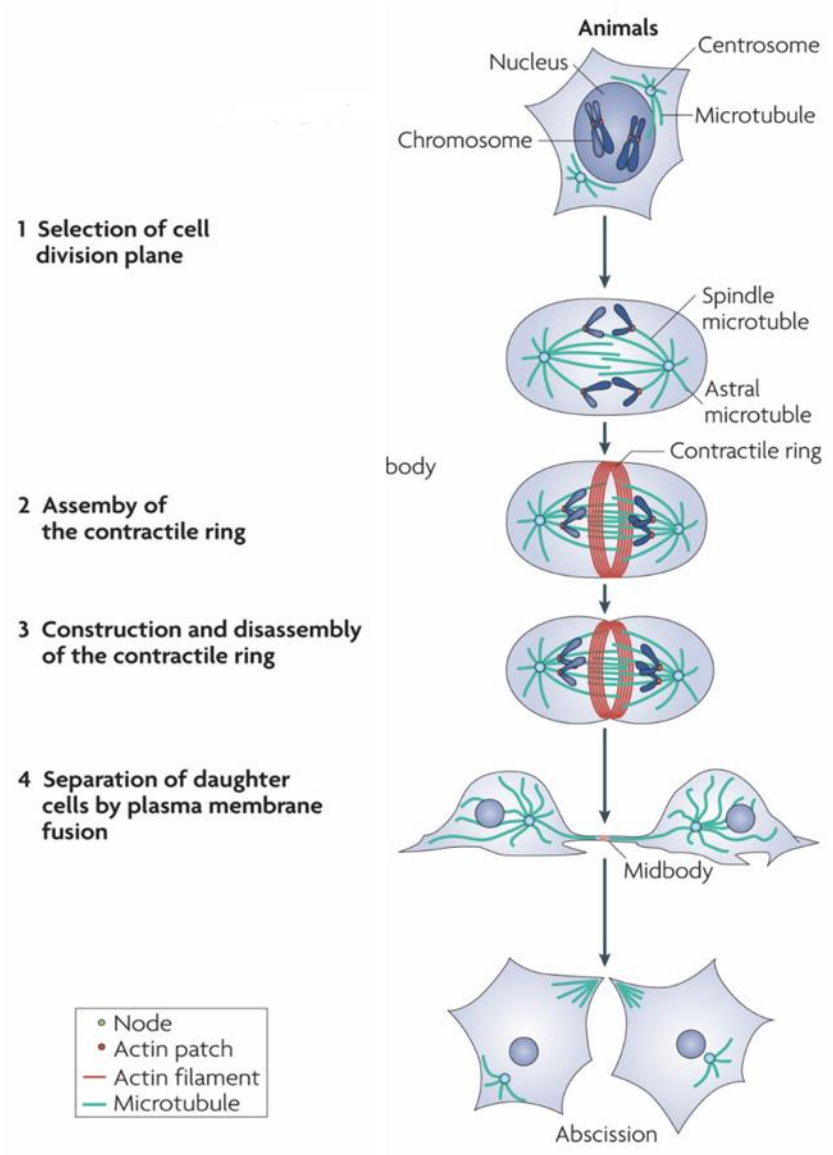

Figure 4 (Adapted from Wu and Pollard 2010): **Strategies for cytokinesis in animal cells.** In fission yeast, the cell division plane is selected by the nucleus specifying the position of nodes around the equator, whereas in animals, spindle and astral microtubules specify the position of the contractile ring. Fission yeast and animal cells assemble a contractile ring of actin filaments and myosin II around the equator of the cell between the chromosomes, which are separated by microtubules of the mitotic apparatus. The ring constricts and the daughter cells separate by membrane fusion.

2. Major cytoskeletal elements involved in cytokinesis

The cytoskeleton is composed of protein monomers that polymerize into polarized (actin, MTs) or non-polarized filaments (intermediate filaments), with key roles in cell spatial organization. Septin filaments have been recognized as the fourth element of the cytoskeleton (Mostowy and Cossart, 2012). The cytoskeleton forms complex three-dimensional networks which control a number of basic cellular functions including cell polarity, cell migration, vesicle transport and cell division. In particular, the cytoskeleton is subject to massive reorganizations during cell division to promote the segregation of chromosomes with the assembly of the mitotic spindle and to drive cytokinesis with the assembly of an acto-myosin-based contractile apparatus. Septins and their partner anillin also contribute to contractile ring assembly and contraction, while MTs, except in plants, do not take directly part into cytokinesis progression, although they participate in signaling the division plane. Their basic properties will not be described here.

2.1 F-actin networks

Actin is a largely conserved protein throughout eukaryotes which exists in two different forms: soluble monomers (G-actin) and filaments (F-actin). These filaments are composed of two strands that intertwine in a double helix, with a diameter of about 7 nm. F-actin networks are highly dynamic and provide mechanical support and forces to accomplish a very large variety of biological functions such as cell morphogenesis, cell motility or cytokinesis (Pollard and Cooper, 2009).

Actin filaments are polar, with a plus end (also known as the barbed end), where monomers preferentially assemble and a minus end (also known as the pointed end), where monomers preferentially disassemble, resulting in net growth, shrinkage or a steady state known as treadmilling (Kueh and Mitchison, 2009). F-actin dynamics is driven by ATP hydrolysis. Actin monomers polymerize preferentially via ATP binding at the barbed end. Although they can polymerize also without ATP by interacting with ADP, they accomplish this process much faster in its presence. Shortly after polymerization, F-actin filaments hydrolyze ATP, releasing phosphate and retaining ADP in the polymer. The resultant ADP-bound polymer is weaker than an ATP-bound polymer and consequently depolymerizes at the pointed end, releasing individual subunits for another round of polymerization and depolymerization.

The assembly and disassembly of actin filaments, their crosslinking into bundles and their association with other cell structures are regulated by a large numbers of actin-binding proteins (Fig5).

Actin nucleation is the critical first step in actin filament assembly since the constitution of actin dimers and trimers is thermodynamically unfavourable, which causes a kinetic barrier to filament formation (Chang and Peter, 2002). To overcome this issue, cells use two distinct classes of nucleators: the Arp2/3

complex, which nucleates branched actin networks, and formins, which are responsible for the organization of linear actin structures (Fig5). They are able to induce the *de novo* formation of actin filaments in response to cellular signaling pathways, allowing precise spatio-temporal control of the initiation of the actin filament.

Arp2/3 is conserved in all eukaryotes and in mammals and forms a complex of seven subunits where two are actin-related subunits (Arp2 and Arp3), while the other five components stabilize this dimeric stable core in an inactive state. It is a unique nucleator since it can imitate an actin dimer or trimer and act as a template for the initiation of a new actin filament that branches off of an existing filament with an angle of 70°, generating branched actin networks.
Since Arp2/3 is intrinsically inactive, it requires the binding of one or more nucleation-promoting factors (NPFs). The WASp/Scar family of proteins are the ones which have been mainly studied: they present a characteristic C-terminal VCA domain sufficient to activate the Arp2/3 complex. This domain contains three segments with different functions: the V region (verprolin homology; also called WH2 for WASp homology 2 domain) binds actin monomers and makes them available in the cytoplasm so that nucleation can start, while in parallel the C and A motifs (central and acidic) bind to two sites on Arp2/3 complex inducing conformational changes that contribute to its activation.
However, in turn also NPFs are autoinhibited and their activity is cooperatively controlled by multiple inputs such as the Rho family GTPase Cdc42, phosphatidylinositol 4, 5-bisphosphate (from now on named PIP2) and proteins containing SH3 domain like the profilin (Higgs and Pollard, 2001; Pollard, 2007; Pollard and Cooper, 2009).
Arp2/3 plays roles in different processes from membrane trafficking and phagocytosis to cell migration and adhesion such as in extensions of lamellipodia (Goley and Welch, 2006; May et al., 2000; Pollard and Borisy, 2003).

Conversely, formins are multiple-domain proteins characterized by two internal formin homology (FH) domains: FH1 motif binds to the profilin bound to actin monomers and transfers this complex to the FH2 domain that stimulates the elongation of linear actin filaments (Kovar, 2006; Vavylonis et al., 2006). A third FH3 domain is instead involved in the localization of formin within the cell (Kato et al., 2001).

Formin activity is mediated by the dimerization of the FH2 domain that assumes a ring-like structure, surrounding the barbed end of the elongating actin filament (Otomo et al., 2005; Xu et al., 2004): mutations that abolish dimerization abrogates the FH2 mediated function (Moseley et al., 2004).
Differently from the Arp2/3 complex, which remains bound at the pointed end, the FH2 domain act as a processive cap at the barbed end, shielding it from other capping proteins since they may interrupt

elongation, while permitting the rapid addition of new subunits (Pruyne et al., 2002; Romero et al., 2004; Zigmond, 2004).

In addition, regulation of formins frequently occurs through autoinhibition, as described for the diaphanous related formins. This relies on an intramolecular interaction between its N-terminal DID (Diaphanous Inhibitory Domain) and C-terminal DAD (Diaphanous Autoregolatory Domain) domains (Li and Higgs, 2003). To overcome this self-regulation mechanism, the N-terminal GTPase binding domain (GBD) of formins binds to small Rho GTPases (Alberts, 2001; Lammers et al., 2005; Wallar et al., 2006). However, additional modes of regulation have also been reported, such as phosphorylation or interactions with other proteins or lipids (Buttery et al., 2012; Matheos et al., 2004; Moseley et al., 2004; Ramalingam et al., 2010; Takeya et al., 2008; Wang et al., 2009).

Formins have key roles in the assembly of various actin-related processes, ranging from polarity to adhesion and cytokinesis (Hotulainen and Lappalainen, 2006; Kobielak et al., 2004; Watanabe et al., 2008). Despite a huge variability in the number of formin genes in different organisms, its structure and function are largely conserved (Chalkia et al., 2008; Chesarone et al., 2010). For instance, formins from singled cell yeast to multicellular organisms are implicated in the generation of F-actin meshworks for the organization of the contractile ring that separates daughter cells during cytokinesis (Bohnert et al., 2013b).

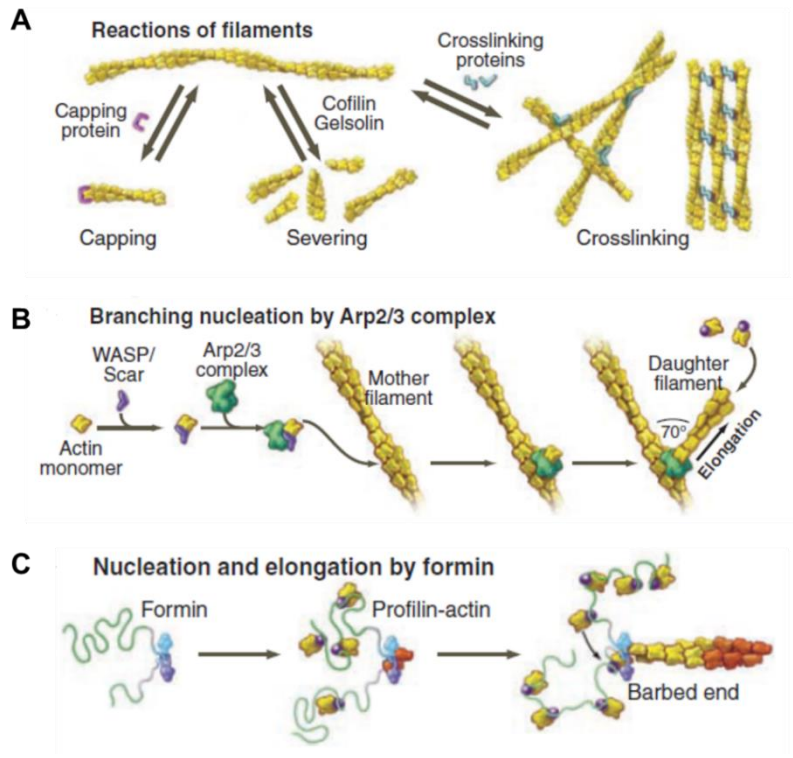

Figure 5 (Adapted from Pollard and Cooper 2009): **Structures of actin and diagrams of fundamental reactions**. (**A**) Reactions of actin filaments. Capping proteins bind to and block barbed ends; cofilin sever filaments; cross-linking proteins assemble networks and bundles of actin filaments (**B**) Nucleation by Arp2/3 complex. Nucleation-promoting factors such as WASp bind an actin monomer and Arp2/3 complex. Binding to the side of a filament completes activation, and the barbed end of the daughter filament grows from Arp2/3 complex (**C**) Nucleation and elongation by formins. Formins initiate polymerization from free actin monomers and remain associated with the growing barbed end. Profilin-actin binds to formin and transfers actin onto the barbed end of the filament.

Once assembled, F-actin filaments are submitted to a number of reactions including capping, severing and crosslinking with impact on their organization.

In particular, while profilin facilitates formin-dependent F-actin assembly by stimulating the exchange of ADP for ATP bound monomers and carrying them at the barbed ends (Wolven et al., 2000; Yarmola and Bubb, 2006), capping proteins bind to free barbed ends to prevent the addition and loss of actin monomers at the end, therefore limiting actin filament elongation (Edwards et al., 2014).

Cofilin regulates actin disassembly in two ways: 1) by enhancing the rate of dissociation of actin monomers from the minus end, increasing the pool of G-actin available (Carlier et al., 1997) and 2) by severing F-actin creating more free ends further enhancing filament disassembly (Andrianantoandro and Pollard, 2006).

Tropomyosin is a conserved α-helical coiled-coiled protein, which is required for the stabilization and maintenance of actin filaments. By dimerizing through end to end contacts, this protein curls around actin filaments to regulate their function (Perry, 2001). Beside this, in specialized structures such as muscle, tropomyosin plays a key role in regulating F-actin interactions with myosin (Lehman et al., 1995; McKillop and Geeves, 1991; McKillop and Geeves, 1993; Perry, 2001). Moreover, it has been reported that N-terminal acetylation of this protein strengthens its ability to regulate acto-myosin activity (East et al., 2011; Monteiro et al., 1994; Skoumpla et al., 2007).

Actin- based motors: Myosin II

Besides playing structural roles, actin filaments also function as tracks for molecular motors that, by converting ATP in mechanical energy, exert tension and drive short range movement of several cargoes such as vesicles and organelles. Myosins are the only described proteins that perform this activity along actin filaments with recognized function in membrane trafficking, cell polarity and motility and cytokinesis (Hartman and Spudich, 2012; Krendel and Mooseker, 2005; Ross et al., 2008). The myosin superfamily is composed of at least 25 different classes. The myosin II subfamily, which includes skeletal, cardiac and smooth muscle myosins, as well as nonmuscle conventional myosin II, is the one with the highest number of members. All myosin II molecules are hexamers consisting of two heavy chains and two pairs of essential and regulatory light chains. Myosin heavy chains are organized in three distinct domains: the N-terminal head catalytic motor domain that mediates actin binding and ATP hydrolysis, the lever arm linker region with IQ motifs interacting with its own light chains or those of regulatory proteins that can regulate myosin motor function (i.e. calmodulin) and the C-terminal tail with an α-helical coiled-coil structure responsible for dimerization and/or cargo binding (Masters et al., 2016). Myosin II forms bipolar filaments that are formed by several myosin molecules that face opposite directions from the midzone of the filament: these thick structures provide the force required to induce

contraction of muscles and to form the contractile ring that separates daughter cells during cytokinesis (Hartman and Spudich, 2012; Vicente-Manzanares et al., 2009). In metazoans, the activity of the nonmuscle myosin II is regulated by phosphorylation by multiple kinases including the myosin light chain kinases (MLCK) and the ROCK kinases, downstream effectors of RhoA (Somlyo and Somlyo, 2003) (see chapter 2.3 and Fig15 for details). These modifications activate the motor catalytic domain of myosin II, which in turn promotes its ability to cross-link and slide actin filaments, ensuring the force necessary for cytokinetic furrow contraction (Bresnick, 1999; Matsumura, 2005).

2.2 Septins

2.2.1 Septins structure and filament organization

Septins were discovered 40 years ago in the budding yeast *Saccharomyces cerevisiae* through a temperature sensitive screen to identify cell division mutants: *cdc3ts*, *cdc10ts*, *cdc11ts* and *cdc12ts* mutants fail to undergo division at the restrictive temperature, resulting in multinucleated and multibudded cells (Hartwell, 1971). In the following years, three related gene products were identified by sequence homology: Shs1, which is also expressed in mitotic cells and Spr3 and Spr28, which are expressed only in cells undergoing meiosis and sporulation (De Virgilio et al., 1996; Mino et al., 1998; Ozsarac et al., 1995). In this model system, the five mitotic septins localize to the presumptive budding site, to the bud tip and to the neck of budding cells: their deletion is lethal for the cell and result in a complete block of cytokinesis.

Later on, phylogenetic analysis identified septin genes in all eukaryotes except higher plants (Pan et al., 2007) and it has been shown that their number is highly variable ranging from two in *Caenorhabditis elegans* to 13 in humans (Fung et al., 2014). To date, mammalian septins display complex expression patterns with tissue-specific or ubiquitous expression and can produce a considerable number of splicing variants. Based on the sequence homology, four different classes have been distinguished: SEPT2, SEPT3, SEPT6 and SEPT7 (Hall et al., 2008; Kinoshita, 2003a).

Septins are conserved GTP-binding proteins of 30-65 kDa and possess a central core characterized by a polybasic region which mediates their interaction with phosphoinositides (PIP2) of membrane surfaces, a GTP-binding domain, which is key in the organization of septin filaments and a conserved region of 53 aminoacids called the Septin Unique Element (SUE) with an unknown role. The N-terminus and C-terminus domains contain respectively a proline-rich domain and a variable α-helical coiled-coil domain that are essential for homo-typic and hetero-typic interactions (Marttinen et al., 2015) (Fig6).

Figure 6 (Adapted from Fung et al 2014): Schematic showing the primary common structure of septin protein family. See text for details.

Septins are known to polymerize into hetero-oligomeric complexes by lateral associations between the G interface, that imply interactions through the GTP-binding domain, and the NC interface, that instead requires associations between the N and C-terminal regions (Bertin et al., 2008; Mostowy and Cossart, 2012). Structural studies have revealed that septins associate in linear apolar rods: single particle EM analysis of the four essential mitotic septins in budding yeast have described that the septin complex is an octameric rod, consisting of two tetramers with a mirror symmetry: Cdc11–Cdc12–Cdc3–Cdc10–Cdc10–Cdc3–Cdc12–Cdc11 (Bertin et al., 2008). Likewise, X-Ray crystallography techniques provided the first proof that also mammalian septins exist as hexameric or octameric complexes with the order: SEPT7–SEPT6–SEPT2–SEPT2–SEPT6–SEPT7 (Sirajuddin et al., 2007), with the septin SEPT9 placed at the terminal position of octameric complexes (Kim et al., 2011; Sellin et al., 2011). Recently, by using Flp-In systems to express septins in HeLa cells, the existing model of septin organization has been found to be inverted with SEPT9 playing a role at the center of heteroligomers (Soroor et al., bioRxiv 2019). This new prediction is not only consistent with the currently known yeast complex but it would also provide compatible ends that would permit hexamers and octamers to co-polymerize.

By end-on and lateral association of hetero-oligomers, septin filaments can pair together and this leads to the formation of higher order structures such as rings and filaments (DeMay et al., 2011)(Fig7).

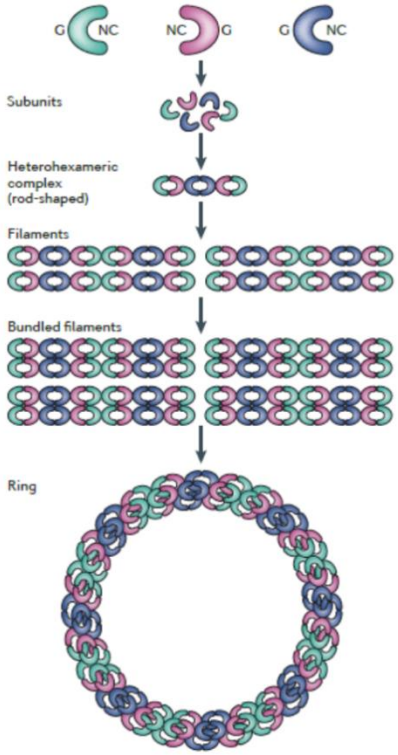

Figure 7 (From Mostowy and Cossart 2012): Septin cytoskeleton dynamics. Septin monomers interact via their G and NC interfaces to form ordered oligomeric complexes, which further assemble into large filamentous structures by end to end or lateral associations. Septins from different groups are depicted in different colors.

2.2.2 Septin-membrane association

Septins are found in intimate association with membranes and are implicated in processes where membrane remodeling occurs. For instance, in *S. cerevisiae,* septins assemble at the bud neck which represents the future division site and delineate where plasma membrane inward pinching takes place.

It has been well established that septins are able to distinguish specific lipid domains and sense micron scale PM curvature. *In vitro* studies have demonstrated that septins bind preferentially to PIP2 which in turn influences filament organization and reinforces their polymerization (Bertin et al., 2010). Reciprocally, another study has revealed that septins affect phospholipid membranes, inducing a higher rate of tubulation in liposomes enriched in PIP2 (Tanaka-Takiguchi et al., 2009).
In addition, it has been shown that both fungal and human septins are enriched at the sites of positive curvature and that the degree of PM curvature correlates with the amount of septins (Bridges et al., 2016). The authors provide two hypotheses to explain the preferential interaction of septins with curved platforms: 1) the septin–lipid association is geometrically favorable when membranes are bended 2) interacting with a curved membrane promotes an energetically favorable septin complex conformation.

In the last year, it has been demonstrated that septins association with curved membranes is cooperative and it has been clarified how septins sense PM curvature: an evolutionary conserved C-terminus alpha helix flanked by a polybasic motif orchestrate membrane association (Cannon et al., 2019; McMurray, 2019).
To date, a theoretical model has proposed that septin filaments do not display a curvature sensitivity *per se*, but they adopt different configuration according to the degree of membrane curvature, thus the geometry and curvature of PM have a key role in tuning septins organization (Beber et al., 2019). This suggests that membrane bending may contribute to regulate septin reorganization occurring during cytokinesis.

2.2.3 Septin interaction with other elements of the cytoskeleton

In addition to membrane association, septins interact with, respond to, and organize the actin and microtubule cytoskeletons. Since septins dynamics is slower compared to MTs and actin (Bridges et al., 2014; Hagiwara et al., 2011), they may constitute a spatial framework for the coordinated organization of other cytoskeleton components.
Septins have been reported to co-localize with MTs in different cell types at different cell cycle stages. Septins are involved in MTs stability by associating with the microtubule associating protein MAP4 and also affect MT organization and post-translational modifications, including regulating MTs

polyglutamylation and acetylation (Spiliotis, 2018). However, it is still not clear if septins interact directly with MTs or if they require adaptor proteins. So far only SEPT9 is known to be a direct interactor, playing key roles in regulating MTs dynamics (Nakos et al., 2018).

It is also well known that F-actin and septins are interdependent: disruption of F-actin organization by treatments with cytochalasin D or latrunculin B leads to alterations in the structure of septin filaments (Fung et al., 2014). Multiple works have established that septins concentrate both to the sites of actin formation and/or reorganization: in interphase, septins are mainly found in actin stress fibers, while in dividing cells they localize to the cleavage furrow. However, similarly to microtubule-associated septins, actin-bound septins only localize to specific subset or to discrete domains of individual filaments, rather than match uniformly the distribution of their cytoskeletal partner (Spiliotis, 2018). This can be explained considering that septins may interact preferentially with polymers characterized by a peculiar orientation, charge or post-translational modification.

Moreover, it has been described that septins are also present in sites that contains branched actin filaments like lamellipodia, filopodia and site of phagocytosis and *in vitro* experiments have revealed that SEPT6 binds to Arp2/3-nucleated filaments better than to linear actin filaments (Hu et al., 2012). Therefore, it is possible that septins interact with Arp2/3 complex directly or indirectly as actin cross-linkers.

Interestingly, a work combining *in vivo* analysis in *Drosophila* and *in vitro* reconstitution assays has revealed that septins are required to maintain cell shape during embryogenesis and that they are able alone to cross-link and bundle actin filaments into ring-like structures (Mavrakis et al., 2014).

2.2.4 Post-translational modifications

Septins filaments rearrangement through the cell cycle needs to be strictly controlled both in space and time: different post-translational modifications, including phosphorylation, sumoylation and acetylation play key regulatory roles in this process (Marquardt et al., 2018) (Fig9).

Phosphorylation is the most abundant septin modification: 59 phosphorylation events have been found to occur in budding yeast septins. Phosphorylation is mainly restricted to the variable N- and C-termini and the not essential Shs1 is the most heavily phosphorylated (Hernandez-Rodriguez and Momany, 2012). Shs1 modifications seem to have an essential role in driving septins ring higher-order rearrangements throughout the cell cycle (Garcia et al., 2011; McQuilken et al., 2017). This complex phosphorylation pattern influences septin localization and function (see chapter 2.2.5 for more details).

Sumoylation is a modification characterized by the covalent attachment of the SUMO moiety, a small ubiquitin-like modifier, to lysines of target proteins. There are four SUMO paralogs in humans (SUMO1-

4); but only one in budding yeast (Smt3) and one in fission yeast (Pmt3) (Alonso et al., 2015; Tanaka et al., 1999). Septins were the first substrates of SUMO identified in yeast. It has been described that just before anaphase, Cdc3, Cdc11 and Shs1 are sumoylated, but only at the mother side of the bud neck, and then desumoylation occurs sharply at cytokinesis (Johnson and Blobel, 1999; Takahashi et al., 1999). Mutants lacking sumoylation sites in all the three septins mentioned displayed ectopic septin rings associated with the previous cell division site, suggesting defects in septin ring disassembly process.
Similarly, it has recently been discovered that all four human septin groups can be sumoylated in their C- and N-termini domains and non sumoylatable versions of SEPT6 and SEPT7 lead to the formation of bundles with aberrant morphology and dynamics. This leads to defects in late stages of cytokinesis since cells with abnormally thick septin bundles are not able to maintain a stable intercellular bridges and become multinucleated (Ribet et al., 2017). In both systems, sumoylation might work as an initiation signal, allowing the recruitment of other proteins that trigger septin reorganization during and after cytokinesis.

Regulation of septins by acetylation is the less investigated post-translational modification. All budding yeast mitotic septins except Cdc11 are acetylated by the lysine acetyltransferase complex NuA4. In NuA4 deletion mutant strains, septins have been shown to mislocalize during the ring-to-hourglass transition, suggesting that acetylation of septins may regulate septin hourglass formation or its stability (Mitchell et al., 2011).

Altogether these data indicate that a complex network of post-translational modifications orchestrate the organization of the septin cytoskeleton (see chapter 2.2.5).

2.2.5 Septins functions

Septins are multi-functional proteins. They function as cellular scaffolds to regulate many biological processes, acting as dynamic platforms to recruit cytoplasmic and cytoskeleton components or as diffusion barriers (Bridges and Gladfelter, 2015; Caudron and Barral, 2009; Mostowy and Cossart, 2012).

This is best exemplified in budding yeast where septins have been thoroughly studied. As mentioned above, in this organism, septins localize at the presumptive division site. This localization is highly dynamic through the cell cycle and undergoes multiple transitions: in early G1, septins initially assemble as a patch-like structure at the presumptive bud site. Upon bud emergence, septins narrow to form a single ring marking the future site of bud growth. Once the bud has formed, the septin ring extends into an hourglass-shaped collar present at the bud neck until the mitotic entry. Before cytokinesis, the septin hourglass splits into two distinct rings that sandwich the CR (Gladfelter et al., 2001). After cell division, the old septin ring is disassembled and the septin subunits are partially replaced and recycled for a new

cycle to begin (McMurray and Thorner, 2009). A haploid yeast cell forms its new bud adjacent to the site of the preceding cell division, following an axial symmetry, and there is evidence that septins play a key role in marking the future division site (Balasubramanian et al., 2004). Evidences show that septin filaments globally reorient by 90° at the onset of cytokinesis: initially found parallel to the mother–bud axis in the hourglass conformation, septins rearrange during splitting adopting a circumferential organization (McQuilken et al., 2017; Ong et al., 2014) (Fig8).

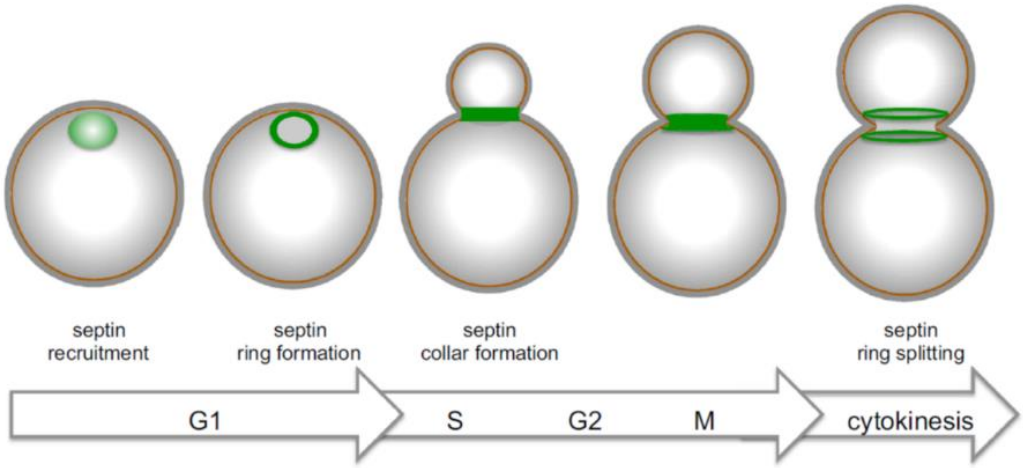

Figure 8 (From Juanes and Piatti 2016): Representation of septin behaviour in the main steps of budding yeast cytokinesis. See text for details.

The initial recruitment of septins to the future bud site, together with the final disassembly of the previous septin ring, depend on the small GTPase Cdc42 and the action of the G1-cyclin-dependent kinases Cdc28 and Pho85 (Egelhofer et al., 2008; Li et al., 2012; Okada et al., 2013; Tang and Reed, 2002). Phosphorylation by the p21-activated Cla4 kinase is required for the ring assembly (Kadota et al., 2004) and mediates the transition to the hourglass collar stage (Versele and Thorner, 2004). Subsequently, the ring splitting is mediated by the Gin4 kinase, which phosphorylates Shs1 at residues different from the ones regulated in G1 (McQuilken et al., 2017; Mortensen et al., 2002). The remnant bud site marks are removed at the end of mitosis by the Rts1-bound PP2A phosphatase, which dephosphorylates Shs1 (Dobbelaere et al., 2003).

Besides this, other kinases have been identified as septin interactors such as Kcc4, Ste20, Hsl1, Elm1 and Kin2 (Glomb and Gronemeyer, 2016). However, the exact window of activity and the biological relevance of the associated modification remain unclear. A first attempt in the identification of septin-associated proteins in specific cell cycle stages of budding yeast has been performed by combining cell synchronization and quantitative mass-spectrometry (Renz et al., 2016). In this study, the kinase Hsl1 was found exclusively in S phase; Gin4 and Bud4 both in S phase and anaphase; the kinase Ste20 together with the SUMO enzyme Smt3 in cells with split rings.

Regarding their function, *S. cerevisiae* septins are essential for cytokinesis for two reasons: 1) they are involved in the recruitment and maintenance of the actomyosin ring and of the protein machinery required for septation fulfilling their function as a platform to recruit cytoskeletal elements and 2) they establish a diffusion barrier between the mother cell and the daughter bud that helps maintain cell polarity and asymmetry, fulfilling in this way the second function of septins.

Indeed, septins create selectively permeable boundaries at the mother-bud neck both at the PM and at the ER that restrict the diffusion of cortical and morphogenesis factors, such as the exocyst and the polarizome complex, which is specifically involved in the regulation of actin dynamics. Additionally, septins play another function at the ER and at the nuclear envelope level: they retain in the mother cell stress and ageing factors, preventing them from entering in the daughter cells. In this way, they control cellular longevity and reset age in newborn cells (Clay et al., 2014; Luedeke et al., 2005; Shcheprova et al., 2008) (Fig10). Altogether, this highlights a key role for septins in *S. cerevisiae* in integrating cell cycle regulation and morphogenesis (Gladfelter et al., 2001; Juanes and Piatti, 2016; McMurray and Thorner, 2009; Oh and Bi, 2011; Versele and Thorner, 2005).

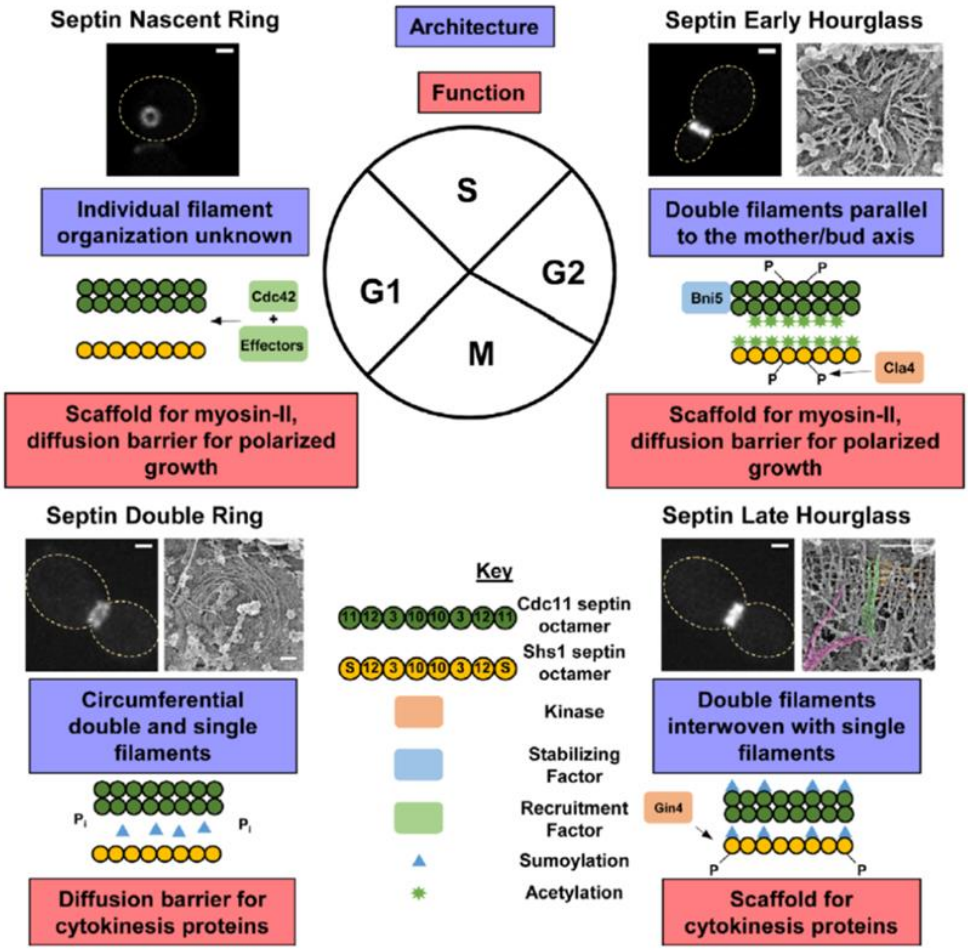

Figure 9 (From Marquardt et al 2018): The septin cycle in yeast: architecture, remodeling, and function starting from the upper left and going clockwise: the nascent septin ring forms in late G1 phase, after the launch of a new cell cycle, through Cdc42-controlled septin recruitment. The exact filament structure is unknown, but most likely is composed of double filaments formed by Cdc11-capped octamers (green rods) and possibly single Shs1-capped octamers (yellow rods). Then, as the bud emerges and grows in S/G2, the septin structure expands to form an hourglass comprised of double filaments (green rods) that are potentially linked laterally by Shs1-capped octamers (yellow rods). This structure is regulated by phosphorylation by Cla4, and acetylation (green stars). Subsequently, as the cell enters anaphase, the septin hourglass exhibits a transitional structure that consists of double filaments (green rods in the cartoon and in the EM image) interwoven with single filaments (yellow rods in the cartoon and in the EM image) akin to a gauze-like structure. This transition is regulated by phosphorylation of Shs1 by Gin4 and sumoylation (blue triangles). Finally, the septins adopt a double ring architecture at the onset of cytokinesis comprised of both double and single filaments arranged circumferentially at the bud neck. This organization is accompanied by a loss of sumoylation and phosphorylation of septins.

Similarly, in mammalian systems, septins contribute to recruit the cytokinetic apparatus to the site of cell division together with the actin-binding protein anillin (see 2.3), and to regulate its contraction (Kinoshita et al., 1997; Maddox et al., 2007; Mavrakis et al., 2014). Later on, septins are also important for the maturation of the intercellular bridge and the midbody formation and eventually for the abscission event in animal cells (Echard et al., 2004; El Amine et al., 2013; Estey et al., 2010; Karasmanis et al., 2019; Renshaw et al., 2014).

In addition, in higher eukaryotes, septins localize to the cortex at boundaries between cell compartments, with pleiotropic roles (Caudron and Barral, 2009; Saarikangas and Barral, 2011) (Fig10): i.e. in the annulus separating the tail from the midbody in spermatozoa, which is key for spermiogenesis and reproduction (Ihara et al., 2005; Kuo et al., 2015); at the base of cilia where they are required for a correct cilium formation and function (Hu et al., 2010); in cage-like structures to respond to microbial infections in *Listeria monocytogenes* and *Shigella flexneri* (Krokowski et al., 2018; Mostowy et al., 2010) and at the base of dendritic protrusions in neurons where septins are key for spine and dendrite maturation (Ewers et al., 2014; Tada et al., 2007).

Moreover, septins, by associating with membranes and cytoskeleton components, have been shown to confer rigidity to the cell: using Atomic Force Microscopy, it has been demonstrated that septins depletion leads to a decrease in cortical stiffness (Mostowy et al., 2011).

By acting as scaffold and signaling platforms at the PM, septins also regulate vesicle trafficking and play two roles in exocytosis: by interacting with the exocyst complex they may act as additional tethering or targeting agents, while as a partner of the SNARE protein syntaxin they can be involved in membrane fusion events (Kartmann and Roth, 2001).

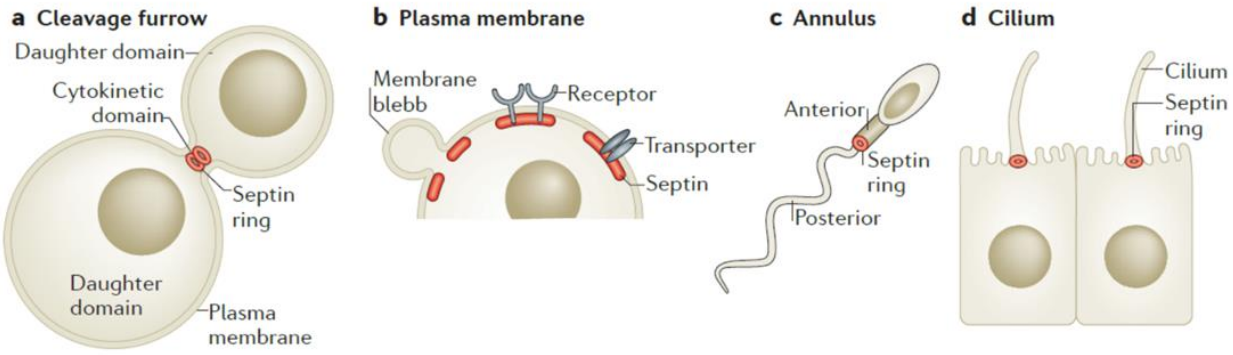

Figure 10 (From Mostowy and Cossart 2012): Septins in several biological processes. Septins can act as scaffolds or diffusion barriers in several biological processes in mammalian cells. (**a**) Cytokinetic cells have two daughter domains and a cytokinetic domain at the cleavage plane. Septin rings may form a diffusion barrier at the cleavage furrow and act as a scaffold for cytokinesis proteins. (**b**) Non-dividing cells have septin assemblies at the plasma membrane, which provide rigidity to the cell and act as a scaffold to restrain membrane-bound proteins, including membrane receptors and transporters. (**c**) The annulus of the mammalian spermatozoon separates the anterior and posterior of the tail. A septin ring forms a diffusion barrier at the annulus, where it is required for mechanical and structural integrity. (**d**) To separate the ciliary membrane from the plasma membrane, a septin ring forms a diffusion barrier at the base of the cilium, and this is required for cilium formation.

2.2.6 Septins involvement in human disease

Given their broad spectrum of function, it is not surprising that septins dysfunctions have been linked to many pathologies such as cancer, neurodegenerative disorders, infections and reproductive disease (Fig11).

Of note, septin expression levels are largely altered in almost every cancer type (Dolat et al., 2014). In the Catalog of Somatic Mutations in Cancer (COSMIC) database, many septins missense mutations occurring especially in the GTP-binding pocket and in the dimerization interfaces were reported after the analysis of different types of solid tumors (Angelis and Spiliotis, 2016). Multiple work has highlighted septins involvement in cellular processes linked to cancer cells such as metastasis, angiogenesis and apoptosis failure (Pous et al., 2016).

Alterations in septin expression were also reported in neurodevelopmental disorders (e.g., Down syndrome, schizophrenia) and septins have been found in the neurofibrillary tangles and Lewy bodies of Alzheimer's and Parkinson's brains (Dolat et al., 2014; Marttinen et al., 2015).

Specific deletions and mutations of SEPT4 and SEPT12, whose expression is fundamental for sperm differentiation and motility, have been linked to male infertility (Lhuillier et al., 2009; Lin et al., 2009).

Finally, multiple works have shown that septins play a role in host-pathogen interactions: during *Listeria monocytogenes* and *Shigella flexneri* infections, septins form a cage that surrounds the actin tails assembled by the bacteria and target them for autophagy (Mostowy and Cossart, 2012). Recent

evidences have discovered that septins are recruited to regions of micrometer-scale membrane curvature of dividing cells where the phosholipid cardiolipin is particularly enriched. Indeed, bacteria mutated for cardiolipin show reduced level of entrapment in septin cages (Krokowski et al., 2018).

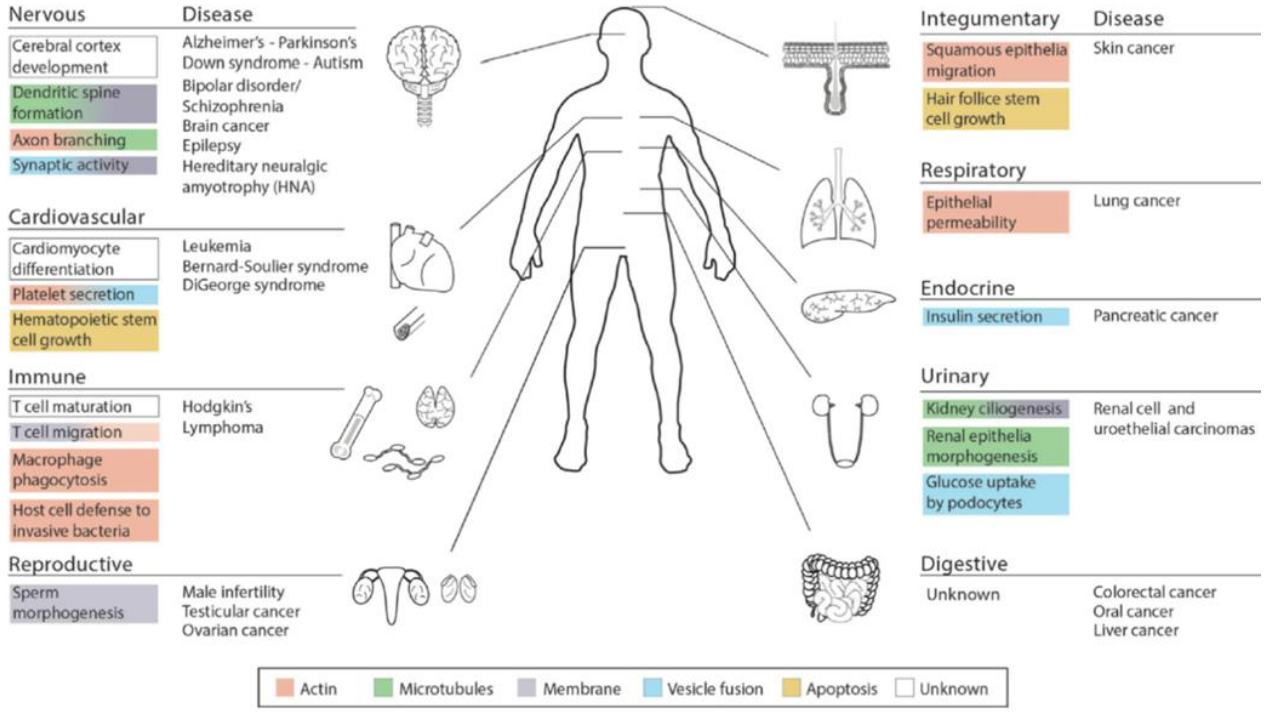

Figure 11 (From Dolat et al 2014): Septin functions in organ systems and their connection to human disease
The schematic diagram depicts the main organ systems of the human body and outlines organ- and cell type-specific structures and processes that require septins. Color codes indicate the intracellular involvement of septins, which includes septin functions in the organization of actin (red), microtubules (green) and cell membranes (gray), vesicle fusion (blue), and apoptosis (yellow). Human diseases are listed based on genetic, histological, genomic, and proteomic evidence that implicates septins in the pathology of various organ disorders.

2.3 Anillin

Besides the F-actin and septin networks described above, cytokinesis also involves anillin, which belongs to a third family of conserved multi-domain proteins that act both as a scaffold and regulatory platform to position and assemble the cytokinetic apparatus and connect it to the underlying PM.

Anillin was first discovered in *Drosophila* as an F-actin interacting protein (Miller et al., 1989) and afterwards homologues have been identified in vertebrates (Oegema et al., 2000; Straight et al., 2005), yeast (Berlin et al., 2003; Paoletti and Chang, 2000; Sohrmann et al., 1996; Tasto et al., 2003) and *C. elegans* (Maddox et al., 2005). The human genome encodes one anillin which contains an N-terminal SH3 domain that binds to proline-rich motifs, separate regions that recognize formin (FBD), F-actin (ABD) and phosphorylated myosin II (MBD) and two nuclear localization sequences (NLS). Anillin C-terminus includes the evolutionary conserved anillin homology domain (AHD), which contains a conserved coiled-coil Rho-binding domain (RBD) and a PH domain at the very end of the protein (D'Avino, 2009; Paoletti and Chang, 2005; Piekny and Maddox, 2010; Watanabe et al., 2010) (Fig12). It has been shown that the PH domain is involved in two functions: 1) recruit anillin to the furrow by a preferential interaction with PIP2, facilitating the accumulation of actin and actin-binding proteins in this area 2) target septins to the division site (Liu et al., 2012).

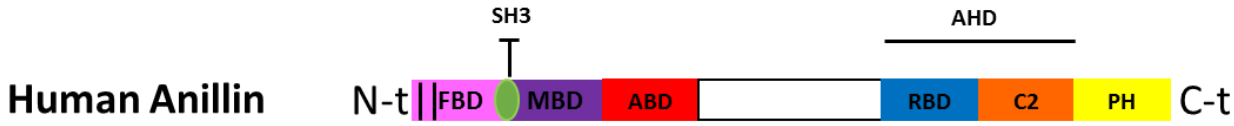

Figure 12: The structure of human Anillin is shown, illustrating all the protein domains characterized. At the N-terminus are present a FBD= formin binding domain, a MBD=myosin II binding domain, a ABD=actin binding domain and SH3= Src-homology-3-binding consensus sequences. The two NLS sequences are shown as black bars in the N-terminus. In the C-terminus the Anillin homology domain (AHD) with the Rho-binding domain (RBD) and the pleckstrin-homology domain (PH).

Recently, structural studies have revealed that the AHD, downstream of the RBD, contains a β-sandwich structure adopting a C2 like domain organization which preferentially interacts with negatively charged lipids such as PIP2 and PS thanks to a long L3 loop, which is amphipathic and positively charged. The authors have identified that a cooperative action of the RBD, which induces a specific orientation of the C-terminal lipidated tail of RhoA, C2 and PH domains anchors anillin at the PM around the cleavage furrow (Fig13). Indeed mutations or deletion of any of this membrane-binding domains prevent association of anillin to the cleavage furrow. Moreover, *in vitro* assays provided the functional proof that anillin acts as a linker between the components of the CR and the PM at the division site: only in presence of anillin, F-actin is able to interact with membrane structures of GUVs and the addition of lipidated RhoA to the mix enhanced this phenomenon (Sun et al., 2015).

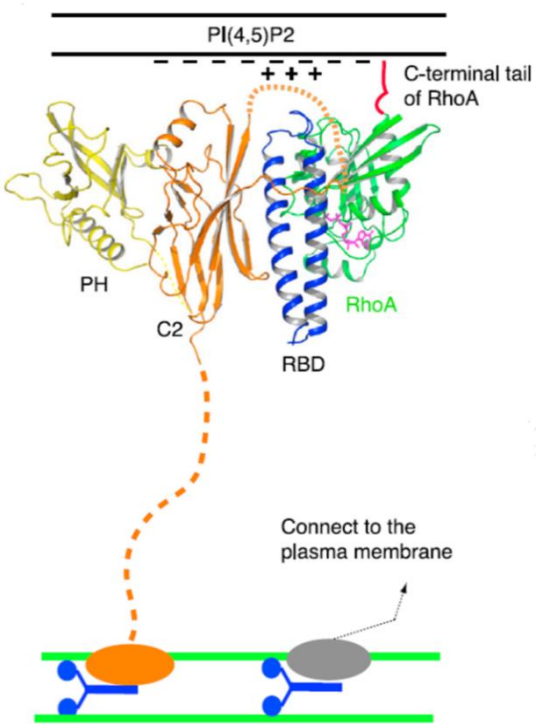

Figure 13 (Adapted from Sun et al. 2015): Model for the Anchorage of Contractile Ring at Division Plane through Anillin. The plasma membranes are schematically shown as double lines. The L3 loop of the C2 domain and the amphipathic sequence are shown as a dotted line and a cylinder, respectively. The C-terminal tail of RhoA is indicated by a red line. The N-terminal domain of anillin (orange oval) interacts with actin filament (green line) and myosin (blue). Additional contractile ring components (gray ovals).

Fly and vertebrate anillins show a dynamic localization: they accumulate in the nucleus in interphase, relocalize on the cortex in metaphase, concentrate at the cleavage furrow in anaphase and at the midbody region in telophase (Field and Alberts, 1995; Oegema et al., 2000)(Fig14). This peculiar distribution indicates that anillin distribution is controlled in a cell–cycle dependent fashion and regulation by phosphorylation has been recently confirmed. Of the many phosphorylation sites identified in the anillin sequence by phosphoproteomics analysis (Gnad et al., 2011; Hornbeck et al., 2012), only one (S635), adjacent to the AH domain, has been found to be critical for its localization and function to perform a correct cytokinesis. Indeed, this phosphorylation regulates the timing of its accumulation at the cell equator and it is key to maintain a stable cytokinetic furrow (Kim et al., 2017). However, the kinase responsible for this modification remains still obscure. Phosphorylation could be important to mediate its function influencing its capacity to adopt a particular conformation/orientation and interact with other proteins.

Anillin perturbation in *Drosophila* or human cultured cells have revealed that it acts as a multi-functional linker interacting with PM, septins, formin, actin and myosin II and coordinating the CR organization during the cleavage furrow formation. Interestingly, anillin is not required for the ingression of the cytokinetic furrow, but it is essential to maintain it stable afterwards to avoid cytokinesis regression. Indeed, loss of function of anillin results in oscillation of the CR along the spindle axis with slow and abortive furrowing (Field et al., 2005a; Golbach et al., 2010; Hickson and O'Farrell, 2008a; Kinoshita et

al., 2002; Oegema et al., 2000; Piekny and Maddox, 2010; Straight et al., 2005; Watanabe et al., 2010; Zhao and Fang, 2005).

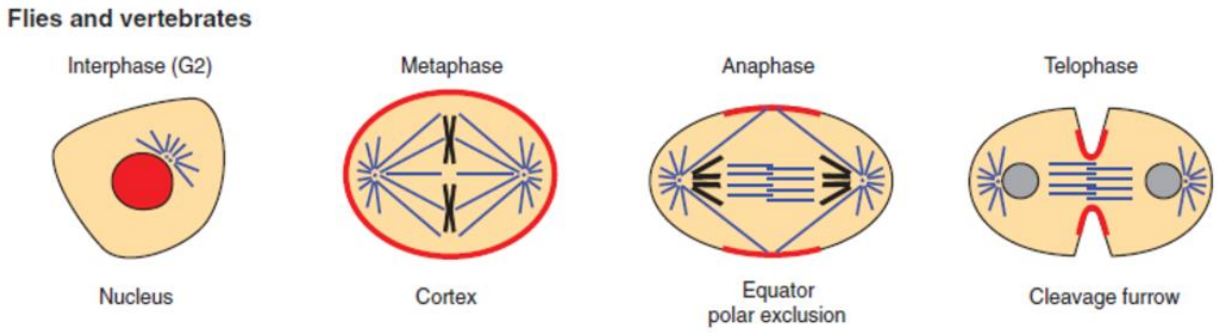

Figure 14 (Adapted from D'Avino et al. 2009): Localization of anillin during the cell cycle in *Drosophila* and vertebrates. The distribution of Anillin-related proteins is depicted in red, nuclei in grey, chromosomes in black, and microtubules, centrosomes and spindle-pole bodies in blue.

Besides this, RNAi in *Drosophila* cultured cells have showed that anillin plays also key roles in late cytokinesis stabilizing the intercellular bridge to avoid membrane blebbing around the cleavage zone and other defects in the distribution and integrity of cytoskeleton components that would result in cytokinesis failure (Echard et al., 2004; Kechad et al., 2012; Somma et al., 2002).

In addition, a role for human anillin in early cytokinetic stages has been discovered: in absence of a central spindle, anillin become essential for the furrow assembly. This suggest that both of them work redundantly to regulate furrow formation either by restricting the recruitment of cytoskeleton components to a limited zone at the cell equator or regulating the ability to contract (Piekny and Glotzer, 2008).

Moreover, it has been demonstrated that anillin is not only necessary for the organization and/or recruitment of structural components of the ring, but it also links the cytokinetic machinery to signaling factors that control cytokinesis (Clifford et al., 2008; Gregory et al., 2008; Piekny and Glotzer, 2008). In metazoans, the position of the division plane is dictated by the orientation of the mitotic spindle in early anaphase.The central spindle acts as a positive regulator of furrow ingression by delivering the centralspindlin complex, which is composed of two proteins: a kinesin-like protein, MKLP1, and a Rho GTPase activating protein (RhoGAP), CYK-4 (White and Glotzer, 2012). The latter subunit activates RhoA, a fundamental regulator of furrow ingression, by relieving its Rho GDP–GTP exchange factor (GEF)-Ect2 from its auto-inhibition. Besides promoting actin polymerization and myosin II activation (Almonacid and Paoletti, 2010; Glotzer, 2005), RhoA recruits anillin at the cell equator, which is crucial for the organization of the structural components of the contractile ring (Piekny and Glotzer, 2008; Piekny and Maddox, 2010) (Fig15). In parallel, in *Drosophila,* it has been shown that the GTPase Rho1,

independently of F-actin, is able to induce anillin accumulation at the medial cortex promoting its interaction with the plasma membrane and septins (Hickson and O'Farrell, 2008b). Interestingly, overexpression of anillin increases Rho activation, suggesting that anillin functions in the regulation of Rho during cytokinesis (Suzuki et al., 2005). Indeed, recent evidences have revealed that anillin enhances Rho signaling at the cell equator reinforcing the dwell time of active Rho bound to the plasma membrane in a PIP2 dependent way (Budnar et al., 2019). In this way, anillin influences Rho binding kinetics and its ability to interact with downstream effectors, regulating cell contractility. Additionally, anillin is regulated by the APC complex, which directs chromosome separation and mitotic exit (Zhao and Fang, 2005). Accordingly, the authors found that the levels of anillin fluctuate in the cell cycle, peaking in mitosis, and decrease drastically when cells enter in G1.

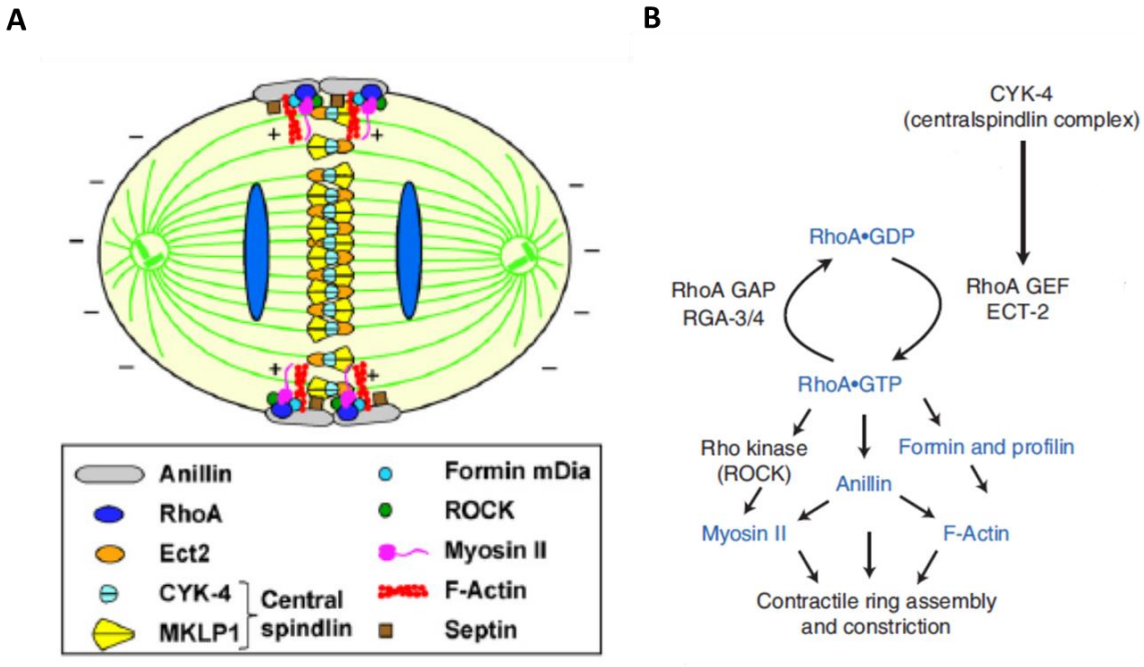

Figure 15 (Adapted from Glotzer 2017 and Almonacid and Paoletti 2010): Cytokinesis in metazoa. (**A**) Graphic representation of the spatial distribution of key proteins involved in the regulation of cytokinesis in animal cells (**B**) The scheme represents the pathways that induce activation and accumulation of contractile ring components. Proteins conserved between metazoa and yeast are highlighted in blue.

Anillin has also been shown to bind septins *in vitro* and recruit them to the actomyosin ring during cell division, thus playing a spatial control in organizing septin filaments (Field et al., 2005a; Kinoshita et al., 2002; Oegema et al., 2000). It is well documented that anillin interacts with septins through a C-terminal region that comprehends the anillin homology (AH) domain upstream of the terminal PH domain (Kinoshita et al., 2002; Piekny and Maddox, 2010). The C-terminal anillin related region of Bud4, the anillin-like protein in budding yeast, in cooperation with central domains, is crucial to direct septin organization during bud growth and bud site selection and to preserve the integrity of the septin ring

during cytokinesis (Kang et al., 2013; Wu et al., 2015). Indeed, in *bud4Δ* mutants the septin double ring disassembles during cytokinesis (Eluere et al., 2012; Kang et al., 2013; Wloka et al., 2011), whereas the overexpression of bud4 leads to the formation of extra septins structures (Kang et al., 2013). Recently, polarized fluorescence microscopy studies have described a key role of Bud4 in the reorientation of septin filaments in the hourglass to double ring transition (McQuilken et al., 2017). In turn septins have a role in marking the landmark of the future bud site in *S. cerevisiae* by localizing Bud4 to this region: evidences show that in septins mutants Bud4 is not properly localized to the mother/bud neck (Frazier et al., 1998; Sanders and Herskowitz, 1996).

Since anillin has a pivotal role in cytokinesis, it is not surprising that it has been associated to cancer. Anillin has been found to be upregulated in diverse human cancers and increased levels of expression have been linked to a higher rate of metastasis (Hall et al., 2005; O`Leary et al., 2013; Olakowski et al., 2009; Suzuki et al., 2005). Anillin knockdown by lentivirus mediated RNAi has revealed a strong inhibition of the proliferation index and of the migration ability of breast cancer cells with a higher population blocked at the G2/M phase (Zhou et al., 2015a). Altogether these data indicate that anillin could be used as a new biomarker of cancer onset and progression that could be targeted as a potential candidate for its treatment. The pathogenic effects of anillin deregulation could be explained considering that an abnormal nuclear or cytosolic amount of anillin could lead to alteration of the reproducibility of the cytokinetic process.

Besides its recognized role in cytokinesis, many other functions are emerging. Interestingly, recent reports have demonstrated that anillin play a critical role in interphase in the regulation of integrity and remodeling of cell-cell junctions in *Xenopus laevis* and in human epithelial cells. In both systems, anillin knockdown leads to a collapse of both adherent and tight junctions and disrupt the apical actomyosin belt, resulting in abnormal cell conformation and strongly disorganized intercellular contact areas (Reyes et al., 2014; Wang et al., 2015).

Moreover, anillin has been found to be essential for neuroblast development in *C. elegans*. By taking advantage of the CRISPR-Cas9 technique, a new role for anillin was uncovered in regulating neuron migration and neurite growth by linking Rho signaling to the actin cytoskeleton. Biochemical analysis demonstrated that RhoG recruits anillin to the leading edge of the Q neuroblast where this scaffold protein stabilizes the actin cytoskeleton by counteracting the activity of cofilin (Tian et al., 2015).

In parallel, a role for anillin in concert with septins has been identified in a late stage of myelin maturation in scaffolding the axon/myelin unit of the central nervous system (CNS), a process which is also PIP2 dependent. By using mice mutated for components or interactors of the CNS myelin, the

authors propose that pathological or aging-linked depletion of the septin/anillin scaffold results in myelin outfoldings that strongly reduces the velocity of impulses propagation (Patzig et al., 2016).

Conversely, no roles for anillin have been identified in the nucleus yet. However, it has been discovered that an importin β2 dependent sequestration in this organelle avoids its cytoplasmic enrichment in interphase, which would otherwise disrupt cell shape by increasing F-actin assembly. Thus, its nuclear confiscation is required to regulate spatially and temporally anillin activity (Chen et al., 2015).

Overall, these evidences suggest that beyond cytokinesis, anillin is also important for several aspects of development in metazoans, in link with the actin and septin cytoskeleton.

3. Reorganization of membrane lipids during cytokinesis

Cytokinesis is accompanied by massive cell shape rearrangement with changes in membrane composition and in the dynamics of trafficking pathways within the cell (Fremont and Echard, 2018; Gerien and Wu, 2018; Neto et al., 2011).

Several technics have been developed to study membrane lipids during cell division. By using high-resolution Atomic Force Microscopy (AFM), it has been discovered that the forces required to penetrate the membrane of dividing cells are substantially greater than those of non-dividing cells. Recently, innovative techniques for lipid analysis and quantification have shown that the lipid composition changes both in space and time during the cell cycle (Muro et al., 2014; Shevchenko and Simons, 2010). By using liquid chromatography coupled to mass spectrometry (LC-MS), it was reported that 11 specific lipid families were enriched more than 4 times in dividing HeLa cells: they include a novel sterol derivative and an ether/ester-linked phosphatidic acid with yet to be determined biological roles and derivatives of sphingolipids, strengthening their already described role in cytokinesis. These techniques have revealed that cells are able to control and modify their lipid composition and distribution during cell division, with both informative and mechanical roles (Atilla-Gokcumen et al., 2014; Echard and Burgess, 2014; Storck et al., 2018). Indeed, multiple evidences have shown that some lipid species form signaling membrane frameworks by interacting with other lipids and/or proteins to regulate the transport and regulation of key proteins, while others provide structural support in membrane curvature remodeling (Albertson et al., 2005; Montagnac et al., 2008; van Meer et al., 2008). In agreement with these results, genome-wide ribosomal analysis have demonstrated that many genes that are involved in lipid metabolism are translationally activated in mitosis both in *Saccharomyces cerevisiae* (Blank et al., 2017) and mammalian cells (Stumpf et al., 2013) and recent evidences have suggested that lipid metabolic reprogramming is a hallmark of cancer cells (Beloribi-Djefaflia et al., 2016).

These data suggest that membrane lipids play an important role during cell division and may regulate cytokinesis. Accordingly, an RNAi screen in HeLa cells has identified 23 genes involved in lipid biosynthesis that lead to cytokinesis failure (Atilla-Gokcumen et al., 2014). In the same work, it has been shown that lipids can impact directly or indirectly on cell mechanical properties.

It is also known that the composition of the plasma membrane (PM) lipids is very specific at the level of the division plane with an enrichment in cholesterol and the sphingolipid Gm1. Cholesterol is composed of a four ring carbon structure and an aliphatic tail, while sphingolipids are characterized by a ceramide hydrophobic backbone and long saturated acyl chains. Due to their chemical structures, these classes of lipids pack together in a favorable manner giving rise to liquid ordered microdomains, also known as lipid rafts, which organize platforms for proteins involved in membrane sorting and trafficking, cell polarization, and signal transduction pathways (Pike, 2003; Rajendran and Simons, 2005)(Fig16).

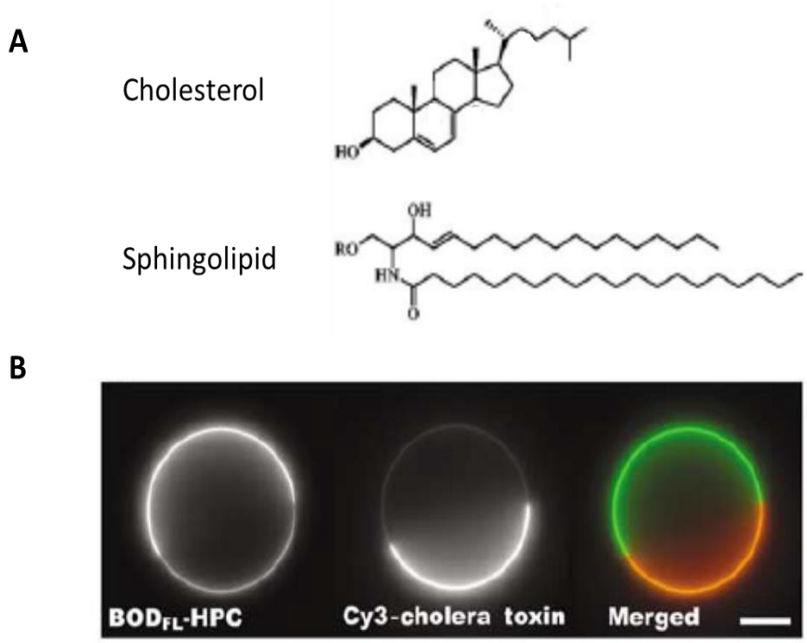

Figure 16 (Adapted from Alvarez et al. 2007 and Roux et al. 2005): **Lipids interaction and phase separation.** (**A**) Comparison of cholesterol and sphingolipid structure. (**B**) Fluorescent image of a GUV, characterized by a 3:1:3 ratio in the order of brain sphingomielin (BSM), cholesterol and dioleylphospatidiylcholine (DOPC) showing the segregation of BODIPY$_{FL}$-C$_5$-hexadecanoyl phosphatidylcholine (BODIPY$_{FL}$-C$_5$-HPC) and the ganglioside GM1 here stained with Cy3-cholera toxin, which segregate specifically in the liquid disordered (Ld) and liquid ordered (Lo) phase respectively.

Interestingly, multiple studies have revealed that cholesterol depletion or inhibition of its synthesis results in cytokinesis inhibition in many systems (Feng et al., 2002; Fernandez et al., 2004). Indeed, the addition of filipin, an agent that binds and sequesters sterols, during the formation of the cleavage furrow results in furrow retraction (Ng et al., 2005). In parallel, old studies revealed that the inhibition by Myriocin of the serine palmitoyl transferase (SPT), that catalyzes the first reaction during sphingolipid biosynthesis leads to cytokinetic defects, which can be rescued by the addition of sphingosine (Miyake et al., 1995; Nakamura et al., 1996). More recently, it has been discovered that sphingolipids reduction

affects cytokinesis completion by altering the localization and thus the role of the PIP2 at the cleavage furrow, resulting in defective cytokinesis (Abe et al., 2012). In addition, it has been shown that inactivation of the glucosyl ceramide synthase by RNAi or by the use of the inhibitor PPMP(1-phenyl-2-hexadecanoylamino-3-morpholino-1-propanol), causes cytokinesis failure with an increase in binucleated cells (Atilla-Gokcumen et al., 2011). These data suggest an involvement of cholesterol and sphingolipids in cytokinesis, but their precise role has not been clarified yet. This may be due to the fact that lipids behave both biosynthetically and structurally as ensembles, making it difficult to identify the role of a single lipid (Klose et al., 2013).

Another type of lipid that plays a crucial role in cytokinesis is that of phospho-inositides (PIs). PIs are intermediates of phosphatidylinositol obtained by phosphorylation of the inositol group in position 3, 4 or 5 and they can be reversibly phosphorylated once, twice or three times. Multiple kinases and phosphatases regulate the synthesis of different types of PIs with a precise temporal and spatial control (Fig17).

Four PIs have been reported to play roles in cytokinesis: PIP2, PI 3, 4, 5-trisphosphate (PIP3), PI4P and PI3P. PIP2 is a major phosphoinositide at the PM and is the only one within its group that is strongly enriched at the cytokinetic furrow (Echard, 2008). PIP2 accomplishes multiple functions during cytokinesis progression due to its capability of interacting with Pleckstrin Homology (PH) and/or basic domains of different cytokinetic elements such as F-actin, anillin and septins, ensuring stability of the furrow after ingression and the solidity of the intercellular bridge (Cauvin and Echard, 2015). One of the main functions of PIP2 is indeed the regulation of the dynamic behaviour of the actin cytoskeleton: it cooperates with various actin-crosslinkers and regulatory proteins such as the Arp2/3 complex, profilin and cofilin stimulating F-actin polymerization when it is present at high levels (Logan and Mandato, 2006; Saarikangas et al., 2010). Indeed it has been found that the overexpression of a GFP-PLC-PH probe, that can be used to follow PIP2 localization, sequesters PIP2, leading to a detachment of actin from the PM with the formation of binucleated cells (Emoto et al., 2005; Field et al., 2005b). Interestingly, PIP2 is also involved in exocytosis and endocytosis processes, which play an essential role throughout cytokinesis in delivering specific cargoes to appropriate targets in proximity of the cytokinetic furrow and of the intercellular bridge (Echard, 2012; Neto et al., 2011; Schiel et al., 2013).
Later on, PIP2 hydrolysis by the PIP2 5-phosphatase OCRL is critical for normal abscission in mammalian cells since it remodels the F-actin cytoskeleton preventing its accumulation at the intercellular bridge, where it would act as a physical barrier blocking bridge resolution and the following abscission (Dambournet et al., 2011). Loss of function of OCRL results in oculocerebrorenal syndrome of Lowe and Dent 2 disease in humans (Pirruccello and De Camilli, 2012), marking the importance of a strict PIP2 levels regulation.

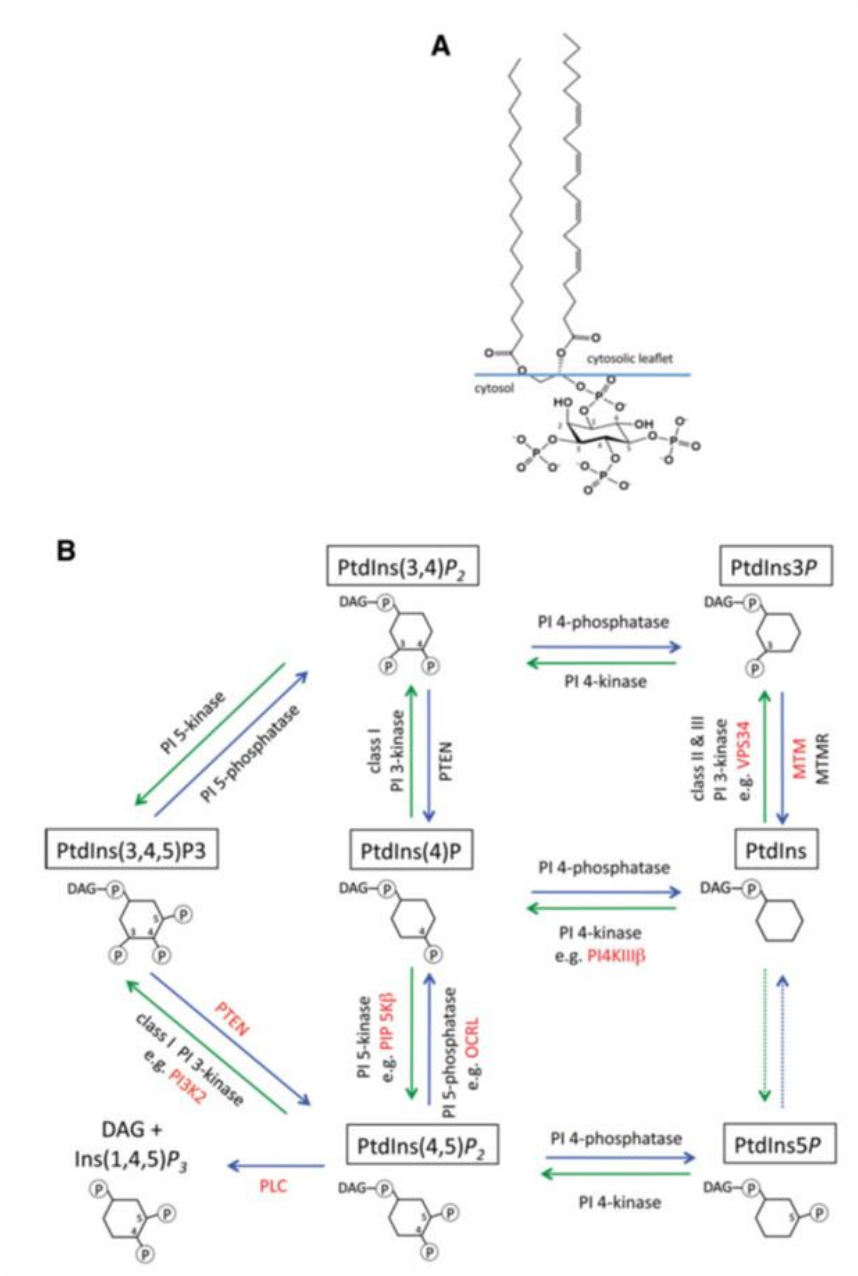

Figure 17 (Adapted from Echard 2012): **Phosphoinositides structure and turnover** (**A**) Representation of the phosphatidylinositol 3, 4, 5-trisphsophate (PIP3). The two acyl chains (18:0 and 20:4 in this case) esterified to glycerol are inserted in the hydrophobic region of the cytoplasmic leaflet of membranes. (**B**) Interconversions between phosphoinositides by kinases (green arrows) and phosphatases (blue arrows). Enzymes involved in cytokinesis are indicated in red. Pathways not demonstrated in vivo are indicated with dash arrows.

The catabolism of PIP2 also depends on another PIP2 5-phosphatase: the synaptojanines. Overexpression of these proteins diminishes the amounts of PIP2 at the cytokinetic membrane furrow, causing an increased number of multinucleated cells (Janetopoulos and Devreotes, 2006).

Of note, another category of enzymes that regulate PIP2 hydrolysis is the phospholipase C (PLC), which converts PIP2 in diacylglicerol (DAG) and inositol 1, 4, 5-triphosphate (IP3). Multiple studies have shown

that PLC function is required for the success of cytokinesis in multiple systems and that several PLC isoforms localize at the cleavage furrow in mammalian cells (Echard, 2012).

The correct localization and turnover of PIP2 and of another PI, PIP3, has a pivotal role in cytokinesis progression. PIP2 is localized at the equator (Field et al., 2005b), while PIP3 at the extremities of the daughter cells (Janetopoulos et al., 2005). Accordingly the PI3-phosphatase PTEN, which dephosphorilates PIP3 in PIP2 is found at the division site, while the PI3-kinase, that catalyzes the opposite reaction, is restricted at the cell poles (Janetopoulos et al., 2005).

Moreover, PIP2 formation can be also obtained by the action of PI-5 kinases that add a phosphate at PI4P. It has been shown that these kinases also localize at the division plane in many systems (Brill et al., 2011; Echard, 2012).

Besides, the PI-4 kinase, another enzyme involved in the PIs pathway, together with its product PI4P, play roles in cytokinesis after furrow ingression in *Drosophila* male germline: in the mutant spermatocytes the furrow ingresses normally, but later on the cleavage furrow regresses due to instability of the intercellular bridge that leads to multinucleated cells (Brill et al., 2000).

Additionally, PI3P is also important for cytokinesis. Indeed, PI3P depletion results in cytokinesis collapse after furrow organization with multinucleated cells. Interestingly, this PI is involved in membrane trafficking by delivering key factors that control intercellular bridge stability and abscission (Brill et al., 2011; Cauvin and Echard, 2015; Nezis et al., 2010).

These data altogether shows that a specific PIs distribution is required for proper cell division.

In parallel, the repartition of another glycerophospholipid, the phosphatidylethanolamine (PE), is largely modified during cytokinesis progression: in interphase it is localized in the internal leaflet of the PM, while it moves to the external one in the division site (Emoto and Umeda, 2000). Reductions in PE levels or its confinement in the external leaflet leads to defects in the abscission event, which can be reversed by the addition of PE or its precursor ethanolamine (Emoto et al., 2005).

These findings suggest that lipids are not passive constituents of the cellular membranes, but thanks to their peculiar geometry, hydrophobicity and charge, they play active roles in regulating membrane shape and function. A unique membrane framework with a specific lipid composition is dynamically assembled throughout the cell cycle (Fig18) and it contributes to key functions for the fidelity of cytokinesis including membrane trafficking, membrane insertion, cytoskeleton dynamic remodeling and signaling.

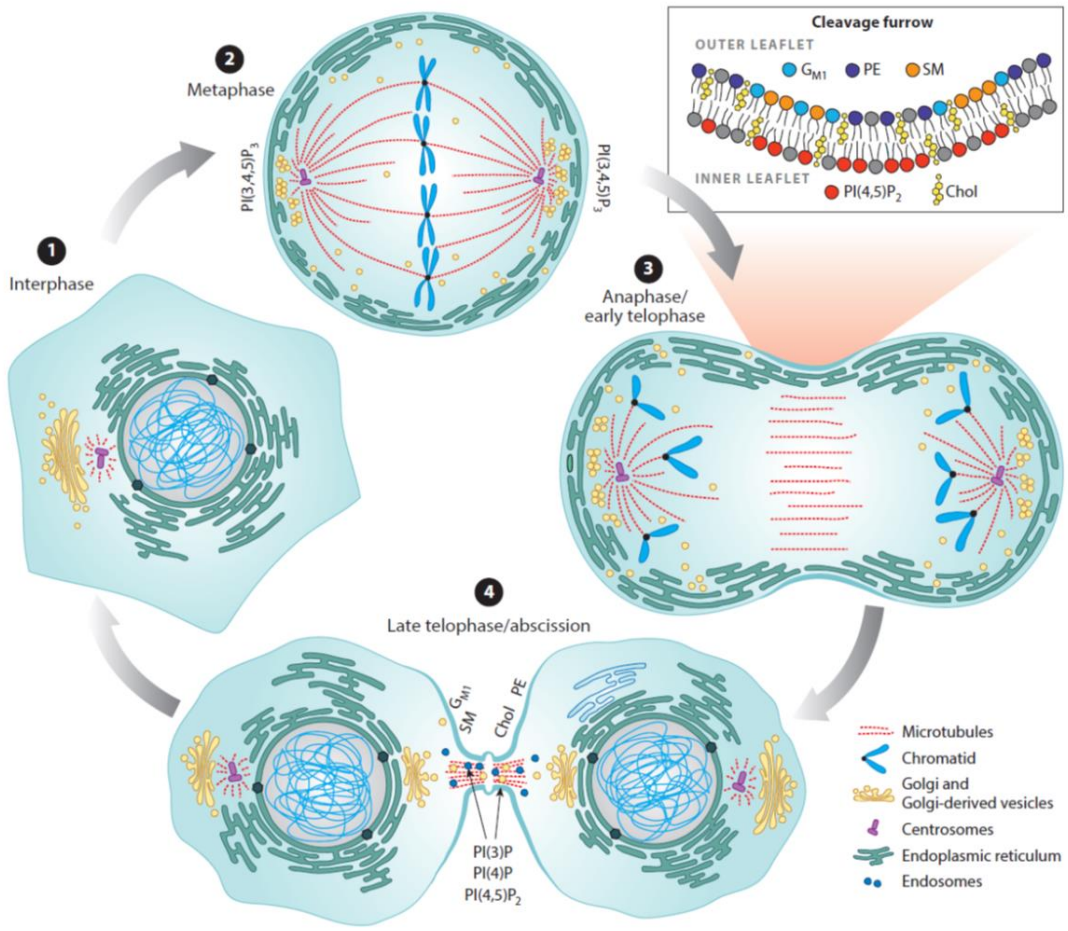

Figure 18 (From Storck et al 2018): **Mammalian cells undergo massive membrane rearrangements during cell division.** In metaphase (2), chromosomes align along the metaphase plate. PI (3,4,5)P3 accumulates at the polar cortex and is required to correctly position the mitotic spindle, which separates the sister chromatids during anaphase (3). A contractile ring then forms, which drives cleavage furrow ingression. Several lipids are enriched at the cleavage furrow. PI(4,5)P2 on the inner membrane leaflet is required to tether the contractile machinery to the membrane. Cholesterol-dependent sphingomyelin (SM) clustering on the outer membrane leaflet is required for PI(4,5)P2 enrichment. Ganglioside GM1 is also enriched at the cytokinetic furrow. Once fully ingressed, the furrow forms a stable midbody bridge during late telophase (4). Several phosphatidylinositol phosphates, including PI(3)P, PI(4)P, and PI(4,5)P2, are present at the midbody. Abscission, the final step of cell division, physically cleaves the intercellular bridge, completing formation of two daughter cells. PE enrichment on the outer membrane leaflet of the furrow is required for abscission.

4. Fission yeast cytokinesis

4.1 Fission yeast cell cycle and morphogenesis

Fission yeast is a simple single cell eukaryotic organism which has been extensively used to study how eukaryotic cells grow and divide because of its stereotyped shape, its easy genetics and short generation time (Almonacid and Paoletti, 2010; Goyal et al., 2011; Hayles and Nurse, 2001; Hayles and Nurse, 2018; Martin, 2009; Pollard and Wu, 2010). This rod-shaped organism exhibits a tight coordination between cell growth and cell cycle progression: cells grow by cell tip extension during a long G2 phase, a peculiarity of fission yeast cell cycle, and stop growing at a critical length of 14 µm to undergo mitosis and divide by medial fission. During this process, they assemble in parallel a MT spindle to segregate chromosomes and an acto-myosin-based contractile ring that drives the division of the cell in two daughter cells of equal size (7µm in length). The constriction of the CR guides plasma membrane invagination and septum formation. Indeed, fungal cells have a rigid external cell wall that antagonizes a high intracellular turgor pressure. Synthesis of septum material at the cell equator produces the force necessary for the membrane rearrangements and cleavage furrow ingression (Fig19). Once cell separation occurs through the digestion of the innermost septum layer by glucanases, fission yeast growth resumes in a monopolar manner from its old cell pole, until it reaches the size of 9 µm in length, when NETO (New End take Off) takes place, allowing the switch to bipolar growth (Garcia et al., 2005; Mitchison and Nurse, 1985; Rincon and Paoletti, 2012).

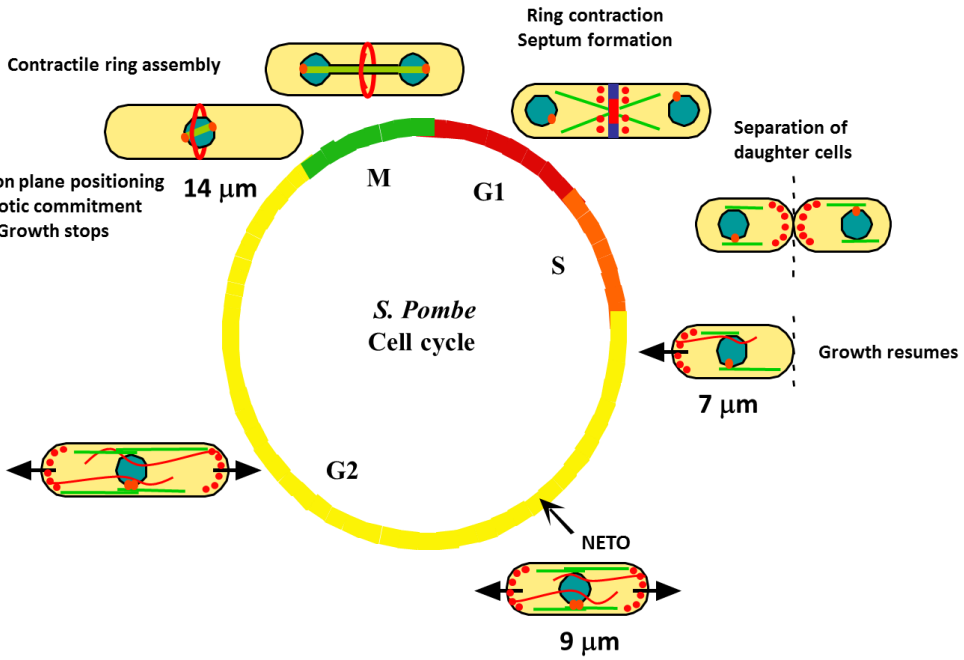

Figure 19: **Scheme of the *S. pombe* cell cycle.** The cell cycle last between 2 and 3 hours and is characterized by several steps. After the cell division (G1/S) phase, the cells grow only from the old tip (black arrow) where the actin patches are localized (red dots). During G2, the NETO process take place and the cell start to grow also at the new tip. At mitotic entry, the cell stops growing and a contractile ring is assembled at the cell middle. Once the ring constricts, the secretory apparatus is redirected towards the center of the cell to support septum formation, whose cleavage leads to cell division.

Fission yeast morphogenesis relies on the one hand on the establishment of cell polarity by the actin and microtubule cytoskeletons during interphase, which defines the cell tips as exclusive growing zones, and on the other hand on mitotic commitment, which regulates cell size at division and controls cell size homeostasis.

In fission yeast there is only one actin isoform (Shortle et al., 1982) that can be polymerized into three different structures: actin patches, actin cables and the actin ring (Kovar et al., 2011; Mishra et al., 2014) (Fig20). Actin patches are short branched polymers, localized to regions of polarized cell growth, where they play key roles in endocytosis contributing to membrane remodeling and cell wall synthesis. However, the identity of cargoes endocytosed at actin patches in fission yeast has not been clarified yet. Actin patches are nucleated by the Arp2/3 complex (Pelham and Chang, 2001), whose activation is stimulated by the fission yeast WASP-like protein Wsp1 and Myo1, which play overlapping roles in actin patches formation (Lee et al., 2000; Sirotkin et al., 2005).

Conversely, actin cables are straight long bundles of short parallel filaments nucleated by the formin For3, running along the long axis of the cell that play roles in intracellular cargo transport throughout the overall cell cycle. They are nucleated by the formin For3 and are used as directional tracks by myosin V to deliver cargoes at actin barbed ends to direct polarized growth (Feierbach and Chang, 2001).

Fission yeast actin cables are a clear example of cytoskeletal crosstalk since their nucleation is established by the sites of cortical contact of interphase MTs plus ends. The polarity complex Tea1-4 is delivered to the cell tips by microtubule plus ends transport. Once the Tea1-Tea4 complex has been anchored to the cortex via the support of the membrane receptor Mod5, it recruits actin-regulating proteins, namely the formin For3 together with its activators: the Rho GTPase Cdc42, Bud6 and Pob1 (Martin, 2009; Martin et al., 2007; Rincon et al., 2009).

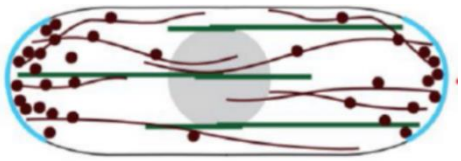

Figure 20 (Adapted from Chang and Martin 2009): **Actin organization during cell cycle in fission yeast**. In interphase, *S. pombe*, F-actin forms two distinct filamentous structures: actin patches, actin cables. Actin patches are assembled at the endocytotic sites, and their distribution is correlated with region of polarized growth. Actin patches appear at the cell growth zones during interphase and the cell division site during late mitosis. Actin cables run along the length of the cell, and are involved in intracellular cargo transport. Actin patches (dots) and cables are noted in brown and microtubules tracks are in green, while sites of active growth are marked in light blue.

It has been estimated that fission yeast cells may contain ~1 million actin molecules per cell. ~35 to 50% are evenly distributed between 30 to 50 actin patches, ~10% are incorporated into the CR, and about 15% are estimated to be organized in actin cables (Sirotkin et al., 2010; Wu and Pollard, 2005).

Multiple evidences have revealed that actin nucleators compete for the limiting supply of actin monomers available (Burke et al., 2014; Moseley, 2014) (Fig21). In particular, depletion of either Arp2/3 complex- or formin-dependent F-actin structures leads to increased F-actin assembly by the other: cells treated with the Arp2/3 inhibitor CK-666 rapidly lose actin patches and organize an extra number of actin cables, whereas formins depletion led to an increased number of Arp2/3 dependent actin patches where the quantity of actin per individual patch is unchanged. In addition, it has been discovered that formins prevail when actin concentration is limited. Indeed, enhancing actin levels favors Arp2/3 activity, whereas decreasing actin levels favors formins (Burke et al., 2014; Moseley, 2014). More recent evidence show that profilin also plays a role in the regulation of F-actin network homeostasis by inhibiting the association of Arp2/3 complex with its activator WASP (Suarez et al., 2015), favoring formin-dependent assembly of F-actin networks.

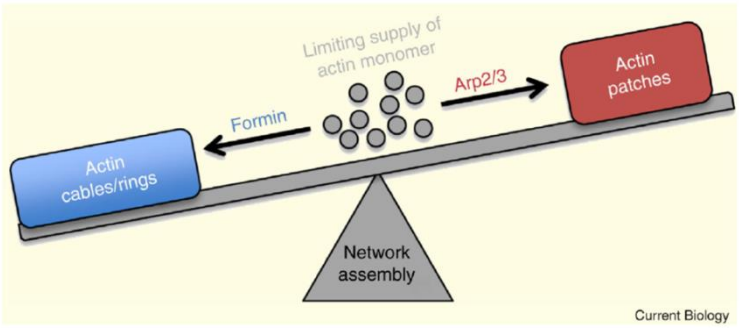

Figure 21 (From Moseley et al 2014): Homeostasis between different actin networks is fueled by competition. Formins and Arp2/3 complex compete for a limiting pool of actin monomers, leading to homeostatic levels of formin-generated actin cables and Arp2/3- assembled actin patches.

One feature of fission yeast morphogenesis, is that growth is a continuous process, only interrupted by mitotic entry. Therefore, any delay in mitotic entry affects cell size at division. This makes of mitotic commitment a morphogenetic tool subject to many physiological inputs controlling cell size homeostasis in addition to DNA damage and replication checkpoints that block mitotic progression to activate mechanisms of reparation at the G2/M transition.

The first one is the stress response pathway (SRP), mediated by TOR (target of rapamicin) signaling, which regulates mitosis commitment in response to osmotic stress and nutrients availability. Rapamycin-induced inhibition of TOR signaling advances mitotic onset, mimicking the reduction in cell size at division seen after nitrogen deprivation. This stimulates the stress Spc1/Sty1 mitogen-activated protein (MAP) kinase pathway, which promotes Polo kinase recruitment at the spindle pole body (SPB), and, in turn, reinforces in a positive feedback the activity of the MPF complex, represented in fission yeast by the Cdc2 kinase (known as Cdk1 in all organisms) and the mitotic cyclin Cdc13. Plo1 phosphorylation by Spc1/Sty1 favors its association with the SPB component Cut12 (Davie and Petersen, 2012; Petersen and Hagan, 2005; Petersen and Nurse, 2007). This interaction is negatively regulated by

the phosphatase Dis2, but during G2, Cdc2 and the NIMA kinase Fin1 phosphorylate Cut12 impairing Dis2 activity and allowing Plo1 to bind to the SPB and induce mitotic entry (Grallert et al., 2013).

The second one is a Wee1 regulatory pathway directly modulating mitotic entry according to cell length. In fission yeast indeed, like in other eukaryotes, Cdc2 is inhibited by the Wee1 kinase and activated by the Cdc25 phosphatase (Gautier et al., 1991; Gould and Nurse, 1989; Russell and Nurse, 1986; Russell and Nurse, 1987). Therefore, mutations in Wee1 and Cdc25 lead to changes in cell size with *wee1-50* and *cdc25-22* mutants dividing respectively at an abnormally short and long cell lengths compared to wild type cells (Nurse and Thuriaux, 1980; Russell and Nurse, 1986). The dual-specificity tyrosine-regulated kinase (DYRK) family kinase Pom1 plays a key role in the transduction of cell size information to Wee1, in order to modulate Cdc2 activity (Martin and Berthelot-Grosjean, 2009; Moseley et al., 2009).

Pom1 forms a polar cortical gradient of decreasing concentration towards the cell middle. Pom1 associates directly with negatively charged phospholipids at the PM through a polybasic domain. Autophosphorylation of this motif results in decreased affinity for the PM. MT-dependent delivery of Tea1-Tea4 protein complex, assisted by the prenylated protein Mod5 and the protein Tea3, promote the association of the PP1 phosphatase Dis2 at the cell tips, where it stimulates Pom1 association with the PM, by de-phosphorylation of Pom1 polybasic domain (Bahler and Pringle, 1998; Celton-Morizur et al., 2006; Hachet et al., 2011; Huang et al., 2007; Martin, 2009; Padte et al., 2006).

Pom1 negatively regulates the position and function of the Wee1 inhibitory kinase Cdr2 (Bhatia et al., 2014; Deng et al., 2014; Rincon et al., 2014), a conserved member of the Brsk/SAD (synapses of the amphid defective) kinases. Cdr2 forms punctuate oligomeric structures called nodes that assemble at the cortical cell equator (Martin and Berthelot-Grosjean, 2009; Morrell et al., 2004a; Moseley et al., 2009). In small cells, Pom1 clusters can easily reach Cdr2 nodes, inhibiting them. Once cells become longer, the inhibition by Pom1 on Cdr2 is alleviated in the medial region of the cell leading to Wee1 inactivation, Cdk1 activation and entry into mitosis (Fig22).

Since the interplay between Pom1 and Cdr2 links cell length and mitotic entry, this pathway has been defined as the Cell Geometry Network (CGN) (Martin and Berthelot-Grosjean, 2009; Moseley et al., 2009).

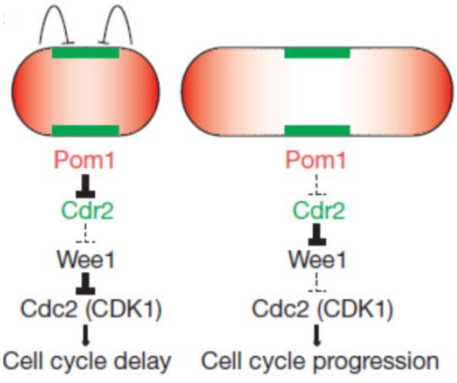

Figure 22 (From Martin and Berthelot-Grosjean 2009): **Pom1 overlaps with Cdr2 and prevents mitosis in small cells.** Model for how fission yeast cells monitor their length to control entry into mitosis. A gradient of Pom1 from cell ends overlaps significantly with Cdr2 at the middle of small cells, leading to Cdr2 inhibition and cell cycle delay. Once the cells reach a longer size, the concentration of Pom1 at the cell middle is no longer sufficient for significant Cdr2 inhibition, allowing cell cycle progression.

In the last years, this important regulatory network has been better characterized. By using live-cell total internal reflection fluorescence (TIRF) microscopy, it has been shown that endogenous Wee1 transiently interacts with cortical Cdr2 nodes in bursts. Since Cdr2 interaction with Wee1 depends on Cdr2 activity (Guzman-Vendrell et al., 2015), burst frequency is negatively regulated by Pom1. Once cells double in size, Pom1 inhibition is relieved, Cdr2 activity increases and thus the frequency and duration of these Wee1 bursts, leading to Wee1 inhibition by the second Sad1 kinase Cdr1 associated with the nodes and promoting mitotic entry (Allard et al., 2018; Guzman-Vendrell et al., 2015).

Moreover, it has been recently shown that Pom1 forms very dynamic cortical clusters that bind more frequently at the cell tips than in the cell middle where they overlap with Cdr2 nodes. The density of Pom1 clusters in the cell middle decreases with cell growth, while the density of Cdr2 nodes doubles. This confirms that Pom1 can act as a tool to actively measure cell size and transmit this information to Cdr2 nodes to prevent short cells from dividing too soon (Allard et al., 2019; Gerganova et al., 2019). Additionally, the density of Pom1 gradient is regulated by nutrient availability. Under glucose deprivation Pom1 redistributes to the medial cortex, disrupting Wee1 bursting, and preventing Wee1 inhibition by Cdr2 (Allard et al., 2019). As a consequence, Pom1 buffers the length at which cells divide, balancing the mitosis-promoting effect of the MAPK pathway (Kelkar and Martin, 2015).

4.2 From early genetic screens to a detailed molecular understanding of cytokinesis

Fission yeast has emerged has a key model system to study cell division upon isolation in the 70s by Nurse and his collaborators (Nurse and Thuriaux, 1980; Nurse et al., 1976) of cell division cycle mutants (termed cdc) that kept elongating instead of dividing. This both allowed the discovery of the main components controlling the biochemical clock of the cell cycle such as the cyclin dependent kinase Cdc2 (Cdk1), the cyclin Cdc13 (cyclin B) or the Cdc25 phosphatase, and those of the cytokinetic apparatus, Cdc3 (profilin), Cdc4 (myosin light chain), Cdc8 (tropomyosin), Cdc12 (formin), Cdc15 (F-BAR protein) and of the Septation Initiation Network (SIN) that induces its constriction upon mitotic exit (Cdc7, Cdc11, Cdc14, Cdc16). Additional screens in the 90s have managed to identify total of about 130 genes involved in cytokinesis (Gould and Simanis, 1997; Guertin et al., 2002a).

Since then, a wealth of studies combining molecular genetics to live cell imaging have allowed an in-depth understanding of the network of molecular interactions leading to cytokinetic ring assembly and of the spatial and temporal regulatory mechanisms controlling fission yeast cytokinesis (Lee et al., 2012; Mangione and Gould, 2019; Pollard and O'Shaughnessy, 2019; Pollard and Wu, 2010; Rincon and Paoletti, 2012; Rincon and Paoletti, 2016).

Even if multiple works have revealed that basic cytokinetic players are conserved from yeast to humans, the regulation of their assembly into activated complexes shows species-specific peculiarities

(Balasubramanian et al., 2004). One of the main differences of *S. pombe* versus animal cells is the presence of a closed mitosis where the nuclear envelope does not break down before chromosome segregation: this event has effects in the mechanisms they adopt to establish the division plane within the cell (Yam et al., 2011). Moreover, while in metazoans the specification of the division plane occurs at anaphase onset, while chromosome segregate, and is dependent on the position of the spindle, in fission yeast this process starts in interphase during G2 with the organization of cytokinetic precursors in the cell middle around the nucleus that pre-establish the position of the division plane (Glotzer, 2017).

4.3 Definition of the division site

In fission yeast, a combination of negative and positive cues sets the position of the division plane in the cell middle to promote symmetrical division. Both mechanisms contribute to the distribution of the anillin-like protein Mid1 to the medial cortex (Almonacid and Paoletti, 2010; Rincon and Paoletti, 2012; Saha and Pollard, 2012). *mid1Δ* cells show strong defects in CR organization with disorganized actomyosin strands assembled in random locations within the cell, which results in the formation of aberrant and offset septa (Huang et al., 2008; Sohrmann et al., 1996).

The CGN predefines the division plane in interphase

Besides its role in regulating mitotic entry (see 4.1), the CGN has a pivotal role in the pre-definition of the division plane during interphase (Almonacid et al., 2009; Celton-Morizur et al., 2006; Moseley et al., 2009; Padte et al., 2006; Rincon et al., 2014; Rincon and Paoletti, 2012). The negative regulation exerted by the Pom1 gradient on the activity and localization of Cdr2 ensures the medial position of its nodes which function as precursors for the assembly of the CR. Indeed, Cdr2 acts as a receptor for Mid1, which, at mitotic entry, initiates CR assembly in the cell middle by the recruitment of essential CR components (Fig23). Defective Cdr2 position results in division plane positioning defects. Moreover, in the absence of Pom1, cells only grow in a monopolar fashion and Cdr2 cortical domain extends towards the non-growing tip, resulting in the asymmetric recruitment of CR precursors and eventual asymmetric cell division (Bahler and Pringle, 1998). Cdr2 has been shown to be the major protein responsible for node assembly (Moseley et al., 2009; Rincon and Paoletti, 2012). The molecular details of how Pom1 inhibits Cdr2 and therefore the mechanism underlying the initial assembly of medial cortical nodes have been uncovered: 1) Pom1 reduces Cdr2 affinity for the PM by phosphorylating its C-terminal region characterized by a KA-1 domain and a proximal basic fragment that establish electrostatic interactions with acidic phospholipids 2) it restrains Cdr2 clustering properties by diminishing the association between Cdr2 N-terminal region and Mid1, affecting at the same time the activation of Cdr2 kinase activity by the CaMKK Ssp1 (Deng et al., 2014; Rincon et al., 2014).

Of note, in the absence of Pom1, medial cortical nodes are still excluded from the growing cell tip by an unknown mechanism (Celton-Morizur et al., 2006). We can speculate that it may either involve factors associated with the cell polarity or growth or be linked to a specific lipid environment at growing cell tips that could restrict node assembly.

Positive signaling of the division plane by the nucleus is exerted by Mid1 export from the nucleus

A second mechanism links the position of the division site to the position of the nucleus at mitotic entry. In physiological conditions, the nucleus is actively maintained in the cell center by opposing pushing forces exerted by nuclear-anchored antiparallel MTs, whose plus ends grow towards the cell tips (Tran et al., 2001). However, mutants in MTs organization that present delocalized nuclei also display delocalized septa (Radcliffe et al., 1998; Toda et al., 1983). Additional experiments have confirmed that nuclear displacement in early mitosis in the absence of MTs or by micromanipulation results in the formation of CR and septa in the new position assumed by the nucleus (Daga and Chang, 2005; Tolic-Norrelykke et al., 2005).

This second mechanism for division plane positioning also involves Mid1: in interphase Mid1 mainly remains nuclear and associated to a small extent with Cdr2 cortical nodes at the cell equator surrounding the nucleus (Almonacid et al., 2009; Moseley et al., 2009; Paoletti and Chang, 2000; Sohrmann et al., 1996). At mitotic onset, a massive export of Mid1 from the nucleus induced by phosphorylation of Mid1 by the polo-like kinase Plo1, enriches its medial cortical pool (Fig23) (Almonacid et al., 2011; Almonacid et al., 2009; Bahler et al., 1998a). It was shown that the position of the nucleus at the time of mitosis entry dictates the region of the cortex where Mid1 will be delivered, and eventually, the position of CR assembly. Accordingly, Mid1 mutants defective for nuclear localization are not able to readjust the division plane to the new nuclear location, once it has been displaced by centrifugation (Almonacid et al., 2009). Altogether, this proves the positive influence of the nucleus in the specification of the division plane at mitosis onset and its dominance over the prepositioning of the division plane by the CGN during interphase.

Importantly, in mutants defective for nuclear shuttling (Mid1^{nsm}) the negative regulation exerted by the cell tips through the CGN restricts Mid1 position in the cell middle, leading to a symmetrical division. Similarly, in absence of Cdr2, cells are still able to achieve a medial division thanks to the nuclear positive signaling. In contrast, the combination of cdr2Δ and Mid1^{nsm} leads to an abnormal Mid1 spreading all over the cortex, resulting in division plane positioning defects or to the formation of multiple rings (Rincon and Paoletti, 2012).

To conclude, these two overlapping mechanisms ensure that cytokinesis takes place both at the cell geometrical center to produce cells of equal size and at the position where the genetic material sits before anaphase to ensure its equal segregation in daughter cells.

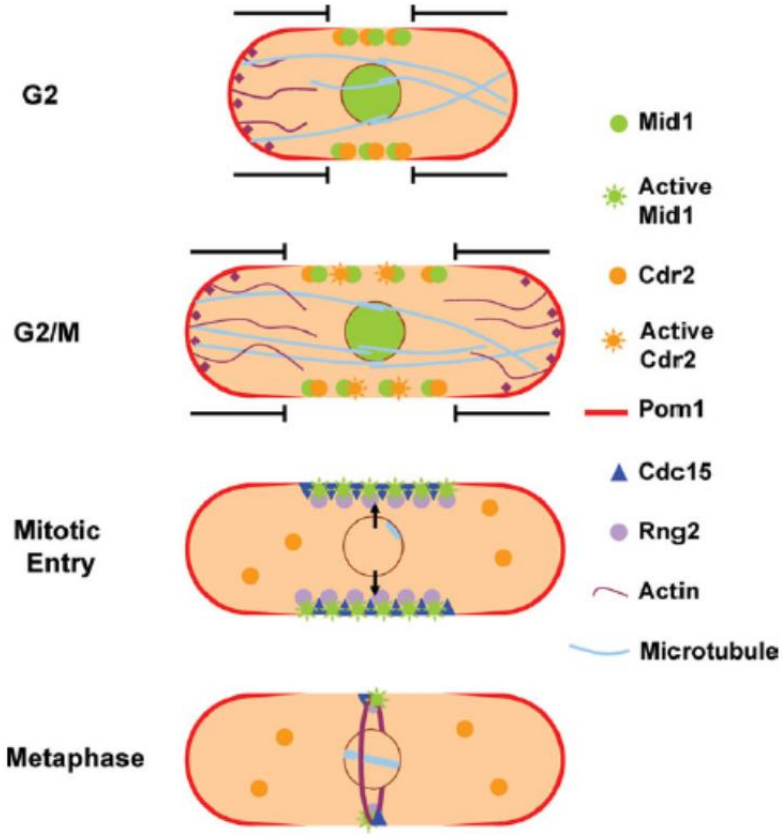

Figure 23 (From Rincon and Paoletti 2012) Major pathways regulating division plane position and mitotic entry. During interphase, negative signals emanating from the cell tips (Pom1 gradient and cell growth) exclude medial cortical nodes containing Cdr2 and Mid1 from the cell tips, predefining the position of the division plane in the cell middle. When cells grow in length, Pom1 inhibition is gradually relieved in the cell middle, allowing Cdr2 activation and mitotic entry. At this stage, positive signaling from the nucleus, mediated by Plo1-dependent nuclear export of Mid1, couples the position of the contractile ring to nuclear position. Concomitantly, Mid1 activation by Plo1 initiates the recruitment of contractile ring components such as Rng2 or Cdc15 to medial cortical nodes, leading to the assembly of a medially-placed contractile ring upon compaction of the cortical nodes. This double signaling mechanism favors an equal division of the cytoplasm as well as proper segregation of the chromosomes in the two daughter cells.

Additional elements influence Mid1 localization and therefore division plane positioning.

In addition to binding to Cdr2 cortical nodes, Mid1 is able on its own to interact with membrane lipids via an amphipathic helix and a basic cluster, which are part of a cryptic C2 domain, which by dimerization, strengthen Mid1 affinity for PIP2 (Celton-Morizur et al., 2004; Sun et al., 2015). This structural organization places the PH domain of Mid1 in an opposite orientation with respect to the C2 domain, excluding its involvement in PM binding. This might explains why the PH domain is not essential for Mid1 membrane association *in vivo* (Lee and Wu, 2012; Paoletti and Chang, 2000).

Besides, Cdr2 and Mid1 interact within medial cortical nodes with several non-essential CR components that remain associated with the CR until full constriction such as Blt1, the RhoGEF Gef2, the kinesin-like Klp8 and Nod1 (Allard et al., 2018; Guzman-Vendrell et al., 2013; Guzman-Vendrell et al., 2015; Jourdain et al., 2013; Martin and Berthelot-Grosjean, 2009; Morrell et al., 2004a; Moseley et al., 2009; Paoletti and Chang, 2000; Ye et al., 2012; Zhu et al., 2013). All of them could be involved in Mid1 stabilization at the cell cortex, although the precise contribution of each of them is difficult to identify since they form a complex with redundancy between interactions.

Among them, Blt1 possesses a C-terminus enriched in basic residues that preferentially binds to PIPs *in vitro* (Guzman-Vendrell et al., 2013). There are evidences showing that this protein can tetramerize (Goss et al., 2014) which could enhance its affinity for membrane lipids. Blt1 N-terminus interacts with Mid1N-terminus in a Gef2-dependent manner suggesting Blt1 and Mid1 play overlapping roles as scaffolds and PM cortical anchors. It was shown accordingly that these interactions are key to stabilize the cortical nodes in early stages of CR assembly. In fact, when membrane-anchoring of both Mid1 and Blt1 is impaired, the nodes detach from the cortex and abnormally placed cytokinetic rings are formed (Guzman-Vendrell et al., 2013). Additionally, Mid1 could also be influenced by the Rho GTPase Gef2 since it has been noticed that the combination of *plo1-18* ts mutant with *gef2Δ* or with its interacting partner, *nod1Δ*, show severe division plane positioning defects (Jourdain et al., 2013; Ye et al., 2012; Zhu et al., 2013).

In fact, live cell imaging of node proteins has recently led to the conclusion that two distinct type of nodes exist: type I, characterized by Cdr2, Cdr1 and Mid1 that form a broad band around the nucleus and type II with Blt1, Gef2, Klp8 and Nod1 deriving from the remnants of the disassembling CR at the end of cytokinesis. It has been proposed that type II nodes diffuse away from the division site toward the medial cell cortex where they may fuse with the type I nodes to form the cytokinetic nodes (Akamatsu et al., 2014; Akamatsu et al., 2017). However long range movements of type II nodes have not been documented. Therefore an alternative hypothesis is that the components of type II nodes may slowly dissociate from the CR remnants at the cell tips and reassociate with type I nodes.

Additionally, Cdr2 dissociates from the cortex at mitotic entry in a SIN-dependent fashion (Morrell et al., 2004a; Rincon et al., 2017). This event was shown to facilitate the repositioning of nodes in the middle of the new-born daughter cells in the next cell cycle.

Links between division plane positioning and ER organization

Besides *mid1* deletion, a second mutant background combining the deletion of three reticulon-like proteins can lead to random division plane positioning: these proteins are important for the formation of cortical endoplasmic reticulum (ER) tubules. Their absence leads to the transformation of cortical ER

in flat cisternae, which shield the plasma membrane, preventing contractile ring assembly from medial cortical nodes. The authors indeed showed that removing ER-PM interaction by deleting vesicle-associated membrane-protein-associated proteins (VAMPs) restored division plane positioning (Zhang et al., 2010; Zhang et al., 2012).

4.4 Assembly of the contractile ring

In *S. pombe* CR formation begins immediately at mitotic onset by maturation of the medial cortical nodes. Mid1 is the critical protein necessary for the hierarchical recruitment and scaffolding of CR components (Coffman et al., 2009; Laporte et al., 2011; Lee et al., 2012; Padmanabhan et al., 2011; Wu et al., 2003; Wu et al., 2006). Mid1 is activated at mitotic entry by the Polo kinase Plo1 in a dual manner: on the one hand, it phosphorylates Mid1 to drive its export from the nucleus at mitosis onset with impact on division plane position (see 4.3); on the other, it promotes the recruitment of other cytokinetic proteins, resulting in medial cortical node maturation (Almonacid et al., 2011; Lee and Wu, 2012; Padmanabhan et al., 2011). Plo1 effect is mediated by phosphorylation of several residues in the N-terminal region of Mid1 which activates its first nuclear export sequence (NES1) (Paoletti and Chang, 2000), and favors its interaction with the IQGAP protein Rng2 (Almonacid et al., 2011).

Additional time lapse microscopy and genetic analysis have revealed that Mid1 organizes two independent recruitment modules: the first one includes the IQGAP protein Rng2 and the myosin II light chain Cdc4, which cooperate to recruit the myosin II heavy chain Myo2 and the regulatory myosin II subunit Rlc1; the second one contains the F-BAR protein Cdc15. Together they recruit the formin Cdc12, which nucleates F-actin filaments for the organization of the CR (Laporte et al., 2011) (Fig24). Of note, the recruitment of all these components is actin independent (Takaine et al., 2014; Wu et al., 2003; Wu et al., 2006).

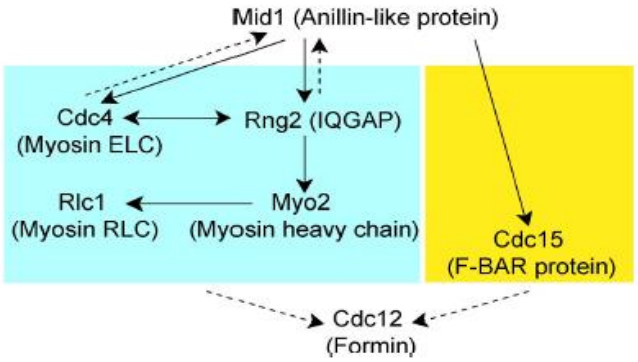

Figure 24 (From Laporte et al 2011): The localization hierarchy for cytokinesis node assembly. The complete and partial dependencies of node localization on a specific protein are depicted by solid and dashed lines, respectively. The two modules are colored differently.

Spindle pole bodies (SPBs) are the yeast orthologs of metazoan centrosomes. Their separation at mitotic entry is commonly used as a reference for mitotic entry, and has allowed defining a timeline for cytokinetic protein recruitment during cortical node maturation. Using this timer, Rng2 and Myo2 are

recruited by Mid1 around 10 minutes before SPB separation; while Cdc12 and Cd15 accumulate at time 0 (Willet et al., 2015b; Wu et al., 2003; Wu et al., 2006).

Recently, the importance of the hierarchical recruitment has been tested and it has been observed that, in absence of Mid1, an artificial targeting of Rng2, myosin II and Cdc12 to Cdr2 medial cortical nodes restores division plane specification in the cell middle. However, in this case CR assembly was strongly delayed and the cells lost their ability to relocalize the position of the division plane upon movement of the nucleus (Tao et al., 2014).

This highlights the importance of Mid1-dependent medial cortical nodes organization in functioning not only as spatial cues to predefine division plane positioning, but also as an efficient recruitment platform for the assembly of the CR.

Super-resolution analysis of live cells expressing cytokinetic fluorescent proteins has revealed novel quantitative data about their initial recruitment. At mitotic entry Mid1 distributes in a large cortical band of about 75 punctuate structures around the cell middle. A single node comprehends a cluster of about 20 Mid1 proteins that interact with approximately 20 dimers each of Rng2, Cdc15, and myosin-II Myo2 and with about 2 dimers of Cdc12 (Pollard and O'Shaughnessy, 2019; Wu et al., 2006).

Multiple studies have analyzed molecular interactions between CR components. Besides interacting with the Mid1 1-100 N-terminus upon Plo1-dependent phosphorylation (Almonacid et al., 2011; Padmanabhan et al., 2011), the IQ motifs of Rng2 interact with Cdc4, which in turn associates with Myo2 and Rlc1 and this is known to act as a positive feedback loop for Mid1 recruitment (Eng et al., 1998; Laporte et al., 2011; Le Goff et al., 2000). Interestingly, the recruitment of Cdc15 and Cdc12 are known to be interdependent and in absence of their interaction, defects in F-actin accumulation and delay in CR formation have been described (Willet et al., 2015a).

Besides, the activity of Cdc15 is regulated by phosphorylation/dephosphorylation. The Cdc14 family phosphatase Clp1, which is activated by the SIN during anaphase, dephosphorylates Cdc15 (Chen et al., 2008; Hachet and Simanis, 2008; Trautmann et al., 2001). Cdc15 modification guides a transition from a closed to an open state that promotes its oligomerization and scaffolding activity (Clifford et al., 2008; Roberts-Galbraith et al., 2010). Accordingly, a mutant of Cdc15 with reduced phosphorylation appears before mitotic entry at the division site in filamentous structures containing most of the CR components, except for Mid1, suggesting an important role for this protein in CR organization (Roberts-Galbraith et al., 2010).

The F-actin network of the CR is assembled by the formin Cdc12, an atypical formin, not regulated by Rho-type GTPases or by autoinhibitory domains interaction (Bohnert et al., 2013a; Yonetani et al., 2008).

Yet, Cdc12 hyperactivity is lethal (Kovar et al., 2003), indicating that its function needs to be strictly controlled. Indeed, Cdc12 is subject to SIN-dependent regulation: the kinase Sid2 phosphorylates a C-terminal oligomerization domain of Cdc12 that also participates in F-actin bundling, inhibiting Cdc12 multimerization, to render it active for CR assembly (Bohnert et al., 2013a; Willet et al., 2015b). Of note, a Cdc12 fragment carrying a C-terminal deletion and lacking sequences distal to the FH2 and the DAD domains, induces the formation of normal rings in interphase cells when overexpressed (Yonetani and Chang, 2010). This is suggestive of the existence of an intramolecular inhibitory mechanism in Cdc12 that remains to be characterized.

F-actin is nucleated *de novo* at the division site by the formin Cdc12, which is essential for cell survival (Wu et al., 2006), but transport of existing filaments to the medial region may also support CR formation (Huang et al., 2012). Interestingly, it has been shown that For3 becomes essential in cells expressing N-terminal truncations of Cdc12: these activated alleles retain the ability to nucleate actin filaments, but in the absence of For3 they cannot get properly localized to the division site (Coffman et al., 2013). This implies that both formins cooperate to orchestrate CR assembly at the cell equator, with Cdc12 being responsible for CR F-actin nucleation.

Genetic screens in *S. pombe* allowed the identification of genes involved in actin organization: mutants of profilin *cdc3* and of tropomyosin *cdc8* display strong aberrations in actin organization, with severe impacts both on the actin ring and on the interphase patches and cables, suggesting that they play essential roles in orchestrating actin organization in all phases of the cell cycle (Balasubramanian et al., 1992; Balasubramanian et al., 1994; Chang et al., 1996).

The ability of profilin to increase Cdc12-mediated F-actin assembly for the CR is essential in fission yeast (Bestul et al., 2015; Kovar et al., 2003). Indeed, profilin helps to regulate spatially and temporally the controlled growth of actin filaments by binding to G-actin and then to the proline-rich FH1 domains of formins. Profilin depletion leads to clumps of cytokinetic precursor nodes, suggesting that Cdc12 is not able to elongate F-actin fast enough to connect them successfully (Vavylonis et al., 2008). Interestingly, when present in excess, profilin acts as a G-actin sequestering protein: *in vivo* analysis of cdc3 overexpressing cells leads to elongated and abnormally shaped cells arrested at cytokinesis with no detectable F-actin structures (Balasubramanian et al., 1994).

Besides opposing the cofilin-mediated severing activity and controlling myosin II binding to F-actin (Nakano and Mabuchi, 2006; Skoumpla et al., 2007), tropomyosin Cdc8 plays key roles in actin organization at the division site: 1) it doubles the elongation rate of Cdc12-nucleated actin filaments by avoiding monomer dissociation 2) it cross-links actin filaments end-to-end 3) and it limits the time of

Cdc12-mediated elongation activity at the barbed ends, regulating the length of actin filaments (Skau et al., 2009).

Cdc15, the founding member of the Pombe Cdc15 Homology (PCH) family of proteins, which is able to bind membranes without deforming them via its Fes/CIP4 homology-Bin/Amphiphysin/Rvsp (F-BAR) domain, is also linked to actin assembly (Lippincott and Li, 2000; McDonald et al., 2015; Roberts-Galbraith et al., 2010). *cdc15* mutants show defects in actin ring formation and they are necessary for Cdc12 localization to the CR (Chang et al., 1997; Chang et al., 1996). In addition, overexpression of *cdc15* leads to the assembly of ectopic actin rings in interphase (Fankhauser et al., 1995), similarly to a *cdc12ΔC* truncation overexpression (Yonetani and Chang, 2010). Altogether, these results indicate that Cdc15 plays a key role in the establishment of the CR, in close association with Cdc12. Indeed, a direct interaction between their N-terminal regions has been discovered. In addition, a direct contact of the N-terminus of Cdc15 with the C-terminus of Myo1, activator of the Arp2/3 complex has been found (Carnahan and Gould, 2003). This places Cdc15 at a convergence point for the coordinated organization of different F-actin structures at the PM in *S. pombe*. Interestingly, the oligomeric state of Cdc15, regulated by phosphorylation, affects its function: when phosphorylated is it proficient for endocytosis, whereas when dephosphorylated it is proficient for cytokinesis (Arasada and Pollard, 2011; Roberts-Galbraith et al., 2010).

In addition, the IQGAP protein Rng2 has been proposed to contribute to CR organization: it participates both to the generation of F-actin and in its arrangement into a ring structure, while at the same time it bundles actin filaments and regulate their dynamics by antagonizing Adf1-dependent F-actin depolymerization (Takaine et al., 2009). Interestingly, by creating mutants of Rng2 domains, it has been discovered that IQ motifs are key for ring constriction and septum assembly, while the C-terminal of the protein is involved in its localization to the cortical nodes and in the formation of the ring (Tebbs and Pollard, 2013). Besides this, Rng2 is also involved in the assembly and maintenance of the F-actin independent ring fraction of myosin-II at the CR (Takaine et al., 2014). Indeed, *rng2* mutants show a reduced, uneven and unstable concentration of myosin II in the ring, often leading to cytokinesis failure.

4.5 Compaction of the contractile ring

Once all the CR components have been recruited to the medial nodes, cytokinesis nodes start to coalescence into a continuous ring about 10 minutes after SPBs separation. Live-cell imaging studies combined with mathematical simulations have led to the elaboration of a model for this compaction process called Search, Capture, Pull and Release (SCPR). It proposes that Cdc12-nucleated F-actin may be captured by myosin II associated with a neighboring node. The force generated by the myosin motor on the actin filament pulls the nodes together and then, filaments are released. Consecutive rounds of

this event lead to the compaction of the nodes into a thin band. The release of this interaction happens with a constant rate and it is critical for this interaction since a permanent association results in a series of clumps instead of a ring at the equator (Ojkic et al., 2011; Vavylonis et al., 2008).

Of note, two other factors are essential in this model. First, the activity of myosin II, regulated by the UCS chaperon Rng3, which ensures the activity of intrinsically unstable myosin II motors, thus supporting actin filament organization and cytokinesis (Lord and Pollard, 2004; Stark et al., 2013). Second, the presence of F-actin cross-linkers such as α-actinin Ain1 and fimbrin Fim1, which stabilize the actin cytoskeleton and contributes to compaction by aligning actin filaments (Laporte et al., 2012; Wu et al., 2001). Indeed, a double deletion of *ain1* and *fim1* leads to the formation of F-actin clumps instead of a contractile ring (Laporte et al., 2012).

Besides, an alternative way of CR assembly has been reported in *mid1Δ* cells where medial precursor nodes do not form. This backup pathway is entirely dependent on the Septation Initiation Network (SIN) (see chapter 4.7) and on the F-BAR protein Cdc15. The hyperactivation of the SIN leads to the formation of contractile acto-myosin structures in interphase cells (Fig25). In this case, the ring is formed by a leading cable-like process. Strands of CR proteins (including Myo2, actin, Cdc12 and Cdc15) are dispersed along the cortex and sometimes they can condense into a functional acto-myosin filament that organizes in random positions within the cell. These misplaced and mis-oriented rings have been shown to contract slower compared to the ring formed in wild type cells, indicating that they function less efficiently (Hachet and Simanis, 2008; Huang et al., 2008). Although CRs can form in single mutants of *mid1* and the SIN, analysis of ring formation in the double mutants shows that both pathways act in parallel, since no acto-myosin structure can be formed, and eventually cells die (Hachet and Simanis, 2008). This indicates that Mid1 and the SIN cooperate to orchestrate spatially and temporally CR assembly in fission yeast.

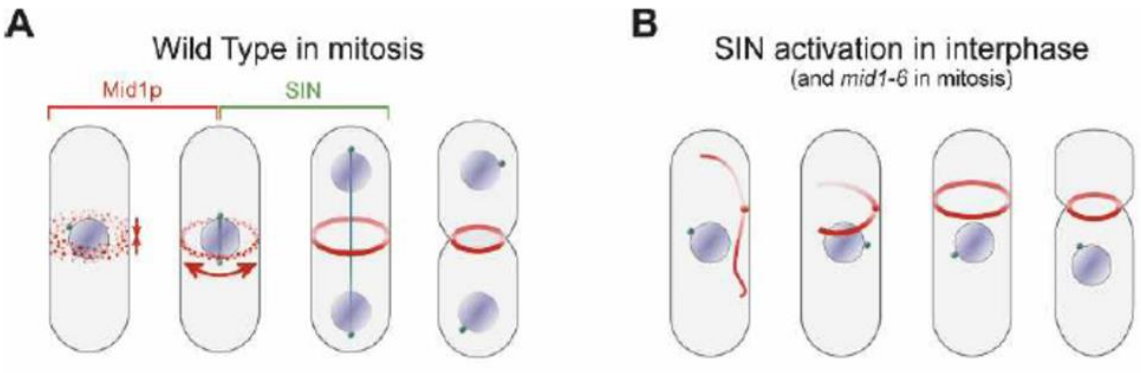

Figure 25 (Adapted from Hachet and Simanis 2008): Models for contractile ring assembly. (**A**) In wild-type mitosis, ring assembly is initiated by the formation of a cortical network of ring components that undergoes lateral condensation, giving rise to a nonhomogeneous ring precursor. This structure eventually matures by recruitment of additional factors such as Cdc15p, displaying the uniform distribution of ring components distribution that characterizes a functional ring. (**B**) When the SIN is activated in interphase, ring assembly is initiated by the formation of a Mid1p-independent filamentous actomyosin structure that eventually forms a ring structure. This structure is then competent for contraction, although it contracts more slowly. This mode of assembly is also observed in *mid1* mutants in mitosis.

In wild type cells, once Mid1 has left the ring, the maintenance of the ring is also dependent on the SIN and Cdc15: indeed in SIN and *cdc15* mutants the CR assembles normally, but after Mid1 leaves the ring, it collapses, showing clumps and gaps of ring components (Hachet and Simanis, 2008). Additionally, when high SIN activity persists far longer than normal in *cdc16-116* temperature sensitive mutants, contractile rings assemble and constrict normally, but disassemble slowly, delaying cell separation (Dey and Pollard, 2018). Altogether, this indicates that SIN activity is required to activate and recruit Cdc15 and to build a mechanically stable contractile ring capable of full constriction.

4.6 Maturation of the contractile ring

Once compaction has occurred, the CR maintains a constant diameter for a period of about 15-20 minutes before ring constriction begins (Rincon and Paoletti 2016). Meanwhile, it matures by the addition and removal of several factors, which altogether provide structural integrity to the contractile ring, in order to avoid its disruption at the time of its constriction. Among them, one major player in CR constriction that is recruited is the unconventional myosin II Myp2 (Laplante et al., 2015; Wu et al., 2003). Indeed, it has been found that in its absence the CR ring persisted longer in the contracting state, occasionally splitting into two separate rings (Mulvihill and Hyams, 2003). Conversely, Mid1 leaves the ring before its constriction in a SIN-dependent process. Indeed recent finding have shown that Mid1 phosphorylation by the SIN kinase Sid2 (see 4.7) contributes to the proper timing of CR assembly and constriction (Willet et al., 2019).

In parallel, it has been suggested that the SIN pathway (see 4.6) is also responsible of a 10 fold increase in Cdc15 amounts in the CR during maturation (Wu and Pollard, 2005). This protein contributes to ring stability and integrity during ring constriction by interacting with other factors that join the ring such as the F-BAR protein Imp2, the paxillin-like protein Pxl1 and the C2 domain protein Fic1 (Ge and Balasubramanian, 2008; Pinar et al., 2008; Roberts-Galbraith et al., 2009). Imp2 and Cdc15 bind to the PM via their F-BAR domains, while interacting with Fic1 and Pxl1 by their SH3 domains. Pxl1, in turn, recruits the phosphatase calcineurin, Ppb1, to control Cdc15 phosphorylation status and, possibly, other related proteins (Martın-Garcıa et al., 2018). Interestingly, it has been found that when Cdc15 is mutated or depleted or in *pxl1Δ* cells, defects in CR anchoring are observed with Myp2-dependent ring

sliding along the long axis of the cell, resulting in a mis-localization of the division site (Arasada and Pollard, 2014). Moreover, these proteins coordinate ring constriction with septum formation, two key steps which are necessary for the completion of cytokinesis in fission yeast (Fig26).

Imp2 and Cdc15 also recruit the RhoGEF Rgf3 (Ren et al., 2015), which activates specifically the GTPase Rho1 involved in the activation of the β-glucan synthases Bgs1 and Bgs4, enzymes that participate in septum formation (Tajadura et al., 2004). Further work has identified another F-BAR protein, Rga7, which is recruited to the CR during its maturation phase and associates with Cdc15 and Imp2 (Martin-Garcia et al., 2014). Rga7 contains a Rho GTPase activating domain and negatively regulates Rho2 (Martin-Garcia et al., 2014). Rga7 and Cdc15 support septum formation by targeting Bgs enzymes from late Golgi compartments to the site of cell division on the PM (Arasada and Pollard, 2014; Arasada and Pollard, 2015).

Finally, septins and subsequently the anillin-like protein Mid2 start to accumulate in proximity of the CR, while it undergoes maturation (An et al., 2004; Berlin et al., 2003; Wu et al., 2003) (see chapter 4.8 for details).

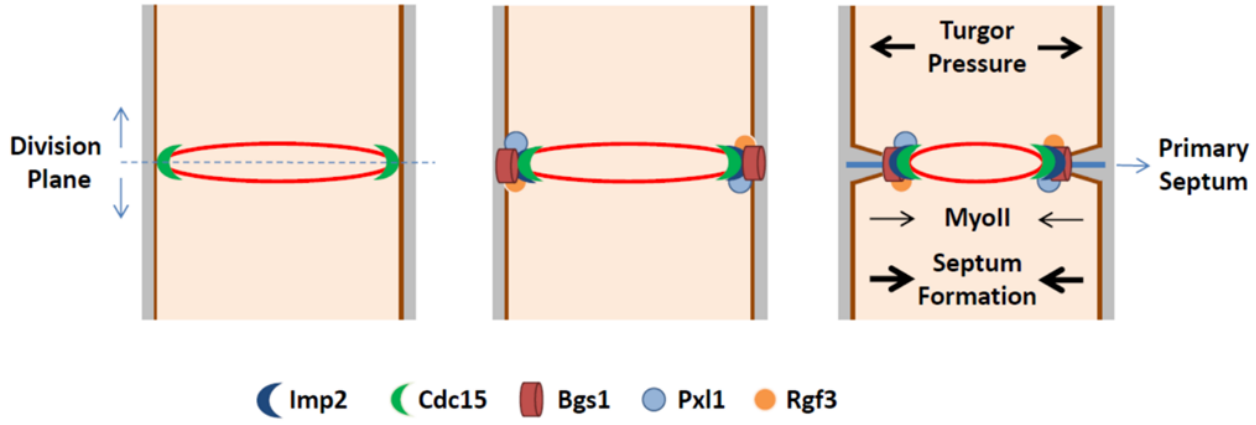

Figure 26 (From Rincon and Paoletti 2016): Regulation of contractile ring constriction and septum synthesis. After its assembly, the ring undergoes a maturation process during which the F-BAR protein Cdc15 accumulates to higher levels in the ring. At this stage, the contractile ring can still slide laterally in a Myp2-dependent manner. The F-BAR protein Cdc15 promotes the transfer of the β-glucan synthase Bgs1 responsible for primary septum formation from late Golgi compartments to the plasma membrane underneath the contractile ring. In conjunction with the F-bar protein Imp2, Cdc15 recruits the paxillin Pxl1 that also contributes to Bgs1 accumulation, as well as the RhoGef Rgf3 which activates Bgs1 through Rho1. Furrow ingression requires to overcome the strong turgor pressure of fission yeast cells. The tension exerted by the contractile ring may be a very minor force contributor compared to septum formation to counter-act turgor pressure. Contractile ring tension may act as a local guide regulating septum synthesis to allow its circular synthesis.

4.7 Constriction of the contractile ring and septum formation

CR constriction

CR constriction has been reported to start approximately 35 minutes after SPBs separation and lasts about 30 minutes (Wu et al 2003). It was classically thought to start at the end of anaphase in concert with the initiation of septum synthesis in order to maintain cell integrity during cell division. However, a recent electron microscopy study revealed that septum assembly may start slowly in early anaphase B and then speeds up in telophase (Cortes et al., 2018). This suggests that CR constriction and cleavage furrow formation may in fact be initiated during spindle elongation, while the CR undergoes maturation. Two phases of cytokinesis, maturation and constriction would then overlap.

In vitro experiments in permeabilized spheroplasts produced by digestion of the cell wall, have demonstrated that ring constriction proceeds in an ATP and myosin-II-dependent manner in the absence of other cytoplasmic constituents. Surprisingly, neither actin polymerization nor its disassembly are required for contraction, while the addition of actin cross-linkers can block it (Mishra et al., 2013).

A combination of *in vivo* and *in vitro* studies have also revealed that three myosins are implicated in this process where Myp2 plays the leading role while Myo2, which is critical for CR assembly, has a redundant role with Myp2 during constriction and can partially compensate its absence. In addition, the myosin V Myo51, even if it is not sufficient to drive ring constriction by itself, also contributes to ring constriction if either Myp2 or Myo2 are lacking (Laplante et al., 2015).

Additionally, it has been recently shown that Myp2 is immobile during cytokinesis whereas Myo2 is highly dynamic and that both myosins II play essential roles in guiding septum formation (Okada et al., 2019).

Of note, myosin II function is regulated by phosphorylation that targets both Myo2 and Rlc1 with impacts on the velocity of ring constriction (Loo and Balasubramanian, 2008; Sladewski et al., 2009). In particular, Pak-related protein Pak1 kinase phosphorylates Rlc1 to inhibit ring constriction until completion of chromosome segregation.

Further studies in yeast protoplasts have led to the development of a mathematical model proposing that actin filaments and myosin II clusters are able to self-assemble into a ring that produces tension and their fast turnover progressively reshape the ring during its constriction. A remarkable conclusion is that the CR constricting rate has to be set up by other cellular process, like, for instance, the septum synthesis pushing force (Stachowiak et al., 2014).

Septum synthesis

The fission yeast septum, like its cell wall, is composed of polysaccharides mainly represented by glucans and mannoproteins (Garcia Cortes et al., 2016; Perez et al., 2016). EM studies revealed that it is a three-layered structure with a central primary septum flanked at both sides by a secondary septa, which are synthetized in concert in a centripetal manner (Johnson et al., 1973). All the three layers contain branched β(1,3) glucans and linear α(1,3)glucans. Additionally, the primary septum comprehends a small portion of linear β(1,3) glucans, while the secondary septa contain branched β(1,6) glucans that could have a role in cross-linking the different sugar components of the cell wall (Garcia Cortes et al., 2016; Perez et al., 2016).

The enzymes responsible for the biosynthesis of these polymers have been characterized. The Bgs enzymes (β-glucan synthase) are transmembrane proteins which localize to the growing poles, to the division area and at the sites of wall synthesis (Roncero and Sanchez, 2010). Among them, Bgs1 produces linear β(1,3) glucans and Bgs4 generates branched β(1,3) glucans (Cortes et al., 2005; Cortes et al., 2007). In parallel, Ags1 is responsible for the synthesis of α(1,3)glucans (Cortes et al., 2012). It is a large membrane protein which also localizes to the growing poles and around the septum (Cortes et al., 2016; Katayama et al., 1999).

Rho GTPases are known regulators of glucan synthases: in *S. pombe* Bgs1 and Bgs4 are activated by Rho1 (Arellano et al., 1996), while Ags1 activation is triggered by Rho2 (Calonge et al., 2000).

Since the CR is not needed for the resolution of the septum, once septum synthesis has advanced to a certain extent, the CR becomes dispensable. Therefore, it has been suggested that the role of the CR is mainly to target and organize the septum machinery at the cleavage site, which in turn will produce the forces required to oppose the high turgor pressure of yeast cells (Proctor et al., 2012). Accordingly, two studies have detected that septum formation is mechanosensitive and linked to the tension exerted by the CR. Indeed, they show that septum growth is increased in the zone of higher curvature of the cleavage furrow controlled by ring tension, resulting in the creation of circular septum edges when the structure closes. If CR integrity is affected, the septum completion cannot occur normally and its shape is also compromised (Thiyagarajan et al., 2015; Zhou et al., 2015b).

Conversely, it has been shown that the loss of Bgs1 and Bgs4 result in CR sliding and instability, further supporting the idea that septum ensures the forces to complete the last steps of cytokinesis (Cortes et al., 2015; Munoz et al., 2013).

Signalling of CR constriction and septum synthesis by the SIN pathway

The temporal coordination of mitosis and cytokinesis is mediated by the SIN, a signaling pathway related to the budding yeast mitotic exit network (MEN) and the metazoan Hippo pathway (Hergovich et al., 2006).

The SIN pathway is a GTPase induced kinase cascade that culminates with the activation of the Sid2 kinase (Fig27). Genetic screens have identified that this signaling network is composed of 13 elements. Two scaffold proteins (Sid4 and Cdc11) mediate its anchorage to the SPB, a coordinator hub for cell cycle regulation (Hagan and Grallert, 2013). All two proteins have extensive regions of coiled structure that mediate their interactions with one another. The other SIN components are signaling proteins that bind to the N-terminus of Cdc11 (Krapp et al., 2004b).

SIN activation is regulated by the GTPase Spg1, whose nucleotide status is in turn modulated by the balance of spontaneous nucleotide exchange, a putative GEF, Etd1p and the bipartite GAP containing a catalytic subunit Cdc16 and a scaffold protein Byr4. At the time of SPBs separation, Spg1 activation triggers the recruitment to the SPB of the STE-20 family kinase Cdc7. The signal is then transduced to the downstream PAK-GC kinase Sid1 associated with its activator Cdc14 and finally to the NDR-family kinase Sid2 associated with its activator Mob1. The kinase Sid2, the final effector of the SIN pathway, moves from the SPB to the cell division site, initiating medial ring constriction and septation (Simanis, 2015).

In interphase, only the Spg1-GAP complex and the scaffolding elements localize to the SPBs, while the kinases associate with the SPB only during mitosis. Interestingly, once cells undergo the anaphase transition the SIN components interact asymmetrically with the SPBs: Cdc7p and Sid1-Cdc14 associate preferentially with the new SPB, while the Cdc16-Byr4 GAP reorganize on the old one (Krapp and Simanis, 2008). Failure in the asymmetric distribution of SIN components results in defective SIN signaling and silencing at the end of cytokinesis (Johnson et al., 2012).

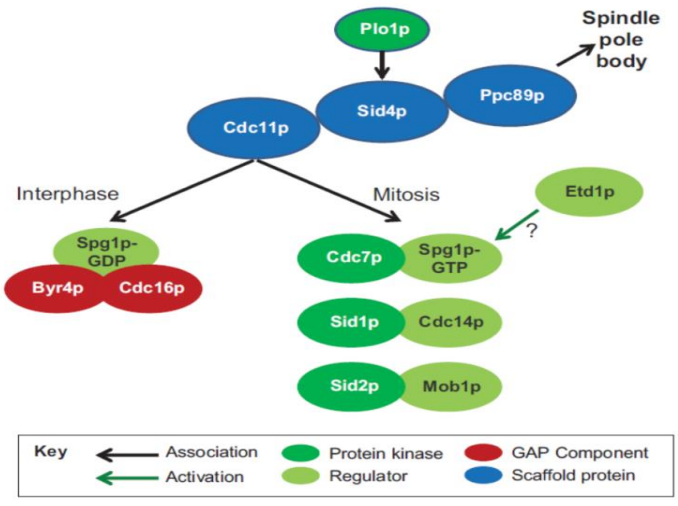

Figure 27 (Adapted from Simanis 2015): The essential components of the SIN. Schematic representation of the key components of the SIN. Protein kinases required for signaling are shown in dark green and their regulatory subunits in light green. Scaffold proteins are shown in blue. Ppc89p (a SPB component) links the other scaffold proteins to the SPB. All of these proteins, as well as Etd1p, are required for signal transmission and loss of function of any of them produces a SIN phenotype. Byr4p and Cdc16p are shown in red to represent their inhibitory activity towards SIN signaling.

Multiple evidences have shown that SIN signaling is essential for CR maintenance and constriction and septum formation during cytokinesis (Cortes et al., 2002; Hachet and Simanis, 2008; Jin et al., 2006; Krapp et al., 2004b; Liu et al., 2002; Simanis, 2003).

Mutants in core elements of the SIN display two different phenotypes (Krapp and Simanis, 2008; McCollum and Gould, 2001). Loss of function mutations in activator components including Cdc7, Cdc11, Cdc14, Etd1, Mob1, Sid2, Sid1, Sid4 and Spg1 lead to multiple rounds of nuclear division without septation, resulting in long and multinucleated cells that will eventually lyse (Balasubramanian et al., 1998; Fankhauser and Simanis, 1994; Guertin et al., 2000; Jimenez and Oballe, 1994; Nurse et al., 1976; Salimova et al., 2000; Schmidt et al., 1997; Sparks et al., 1999). Conversely, mutations in one of the GAP components, Cdc16 and Byr4, promote continuous rounds of septation in absence of nuclear division cycle and cell cleavage, leading to multiseptated cells (Fankhauser et al., 1993; Minet et al., 1979; Song et al., 1996).

Recent works have started to identify targets of the SIN, which include cytoskeletal regulators and signaling proteins. Among them, Cdc2 and many CR component have been identified such as Mid1, Cdc15 and Cdc12 (Bohnert et al., 2013a; Chen et al., 2008; Rincon et al., 2017; Willet et al., 2019). This indicates that the SIN is key to remodel the CR organization to ensure the success of cytokinesis.

An important SIN-regulated factor is the Cdc14-like phosphatase Clp1/Flp1 (Le Goff et al., 1999; McCollum and Gould, 2001; Mishra et al., 2004; Trautmann et al., 2001). In interphase, Clp1 is sequestered in the nucleolus. At mitotic entry, Clp1 moves from the nucleolus to SPBs and to the division site, where it is recruited by Mid1 (Clifford et al., 2008). The SIN is required to avoid Clp1 re-confinement in the nucleolus until the end of cytokinesis. In return, Clp1 transduces SIN activation by dephosphorylating Cdk1 targets, ensuring that cytokinesis is completed before a new cell cycle starts (Trautmann et al., 2001).

Several SPB-associated kinases and phosphatases have been identified as SIN regulators: besides its role as Mid1 activator, Plo1 kinase is an upstream regulator of the SIN. Indeed *plo1* mutants do not form a septum (Tanaka et al., 2001), while an increased *plo1* expression causes septation in interphase cells (Ohkura et al., 1995). In particular, Plo1 binds to Sid4 and it is known to be involved in the phosphorylation of Cdc11 during anaphase at the time of septum formation (Krapp et al., 2004a; Morrell et al., 2004b).

In addition, Cdk1 activity can impact SIN signaling both positively and negatively. Once the cell enters mitosis, Cdk1 cooperates with Plo1 to promote the removal of the SIN inhibitor Byr4 from the SPBs and the inhibition of the GAP Byr4-Cdc16, inducing SIN activation and cytokinesis induction in anaphase (Rachfall et al., 2014). On the other side, in early anaphase full activation of the SIN requires Cdk1

inactivation, delaying cytokinesis until the chromosomes have been properly segregated (Bohnert and Gould, 2011). This is in agreement with the identification of two separable SIN states during mitosis: an early state with a reduced activity and a late state where SIN becomes fully active (Wachowicz et al., 2015).

Conversely, several phosphatases have been shown to negatively regulate the SIN by dephosphorylating Cdc11 at the end of mitosis including the aforementioned Clp1, PP2A and the PP2A-related SIN-inhibitory phosphatase (SIP) complex. Mutants in PP2A and in its regulators as well as SIP mutants lead to a cytokinesis failure due to a symmetrical distribution of the SIN components (Chen et al., 2013; Goyal and Simanis, 2012; Singh et al., 2011).

The ubiquitin ligase Dma1 has a role in inhibiting SIN activity in mitotically arrested cells, operating in a cytokinetic checkpoint that works in parallel to the spindle checkpoint. By ubiquitinating Sid4, Dma1 prevents Plo1 localization to the SPBs and therefore SIN activation, preventing Cdk1 inactivation, mitotic exit and cytokinesis in absence of chromosome segregation (Guertin et al., 2002b).

Additionally, a role has been proposed for the medial node component Blt1 in regulating the SIN: Blt1 controls the recruitment of the complex Sid2-Mob1, which, in turn, regulates the accumulation of the Clp1 phosphatase and of Bgs1, enzyme necessary for septum synthesis (Goss et al., 2014).

Altogether this indicates that a finely tuned regulation of this signaling network is critical to ensure that each step of cytokinesis occurs accurately.

4.8 Cell separation

Inner cell wall digestion by glucanases

Cell separation is a critical moment of the cell cycle for cell integrity. It requires the precise and controlled digestion of the primary septum by the β(1,3)glucanase Eng1 and the degradation of the lateral cell wall surrounding the septum by the α(1,3)glucanases Agn1 and Agn2, which together result in the physical separation of the two daughter cells (Dekker et al., 2004; Martin-Cuadrado et al., 2003).

Moreover, it has been demonstrated that both Bgs4 and Ags1 are essential for cell integrity and to ensure a proper cell-cell division since their depletion leads to cell lysis upon cell separation (Cortes et al., 2012; Munoz et al., 2013).

The molecular machinery responsible for the delivery of the glucanases enzymes to the division site is complex and involves several genes, including some involved in the cell wall organization such as Agn1

or Cfh4 and others with still uncharacterized function (adg1-3 genes), whose expression is regulated by the transcription factor cascade Sep1-Ace2 (Alonso-Nunez et al., 2005).

Besides, one of the major factor involved is the exocyst complex, an octameric complex that is localized to zones of active exocytosis and has the role to tether secretory vesicles to the PM. Compromised exocyst function leads to defects in the localization of Agn1 and Eng1 (Martin-Cuadrado et al., 2005; Wang et al., 2002).

Septins and the anillin-like protein Mid2

Septins and the anillin-like protein Mid2 are also involved in cell separation (see chapters 2.2 and 2.3 for a general introduction on septins and anillins). They assemble into ring structures that delineate the boundaries of the cleavage furrow and the recruitment site of the inner septum hydrolytic enzymes: in their absence the localization of Eng1 and Agn1 is disorganized and more dispersed (Martin-Cuadrado et al., 2005) and cell separation is delayed inducing the formation of cell chains.

S. pombe genome contains seven genes encoding septins (Kinoshita, 2003b; Longtine et al., 1996; Pan et al., 2007; Wu et al., 2010). Spn1-4 are expressed in vegetatively growing cells, whereas Spn5-7 are exclusively expressed during sporulation where they are important for the formation of the forespore membrane (Onishi et al., 2010). Fission yeast mitotic septins mutants are viable, but show defects in cell-cell separation, resulting in the formation of multiseptated chains of cells (Longtine et al., 1996).

By combining proteomic and genetic approaches, it has been revealed that the structure of the septin complex organizes similarly to the one discovered in budding yeast. Two copies of a Spn3–Spn4–Spn1–Spn2 subunit are proposed to array in a linear order to form an octameric complex, in which Spn1 and Spn4 appear to be the core members, with Spn2 and Spn3 as auxiliary subunits (Fig28). Since Spn1 and 4 localize to the center of the complex, it is not surprising that their deletion leads to much more severe cell division defects compared to deletion of the other two septins (An et al., 2004).

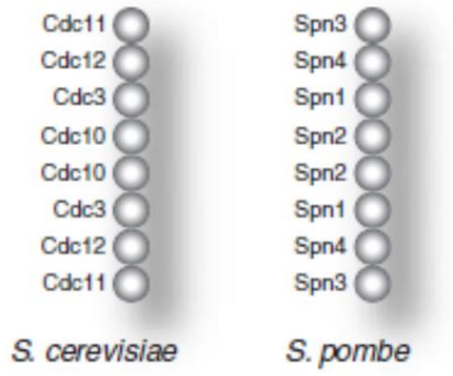

Figure 28 (Adapted from Hall, Russell and Pringle 2008): Comparison of the septins heteroligomeric complexes in the indicated species. In both cases they assemble in linear and apolar octameric rods made of two tetramers with a mirror symmetry.

Unlike in *S. cerevisiae* where septins are necessary for CR formation, fission yeast septins are recruited after the CR has been fully assembled. Septins organize late in mitosis and form first a single ring which splits in two during CR constriction and septum formation (Fig29). This double ring does not contract together with the contractile ring, but it remains on the cell surface to delineate the boundaries of the cleavage furrow and it dissociates after cell separation. So, conversely to septins in budding yeast, fission yeast septins are not essential for cell viability and may work mainly in the late stages of cytokinesis (An et al., 2004; Berlin et al., 2003; Juanes and Piatti, 2016; Wu et al., 2003).

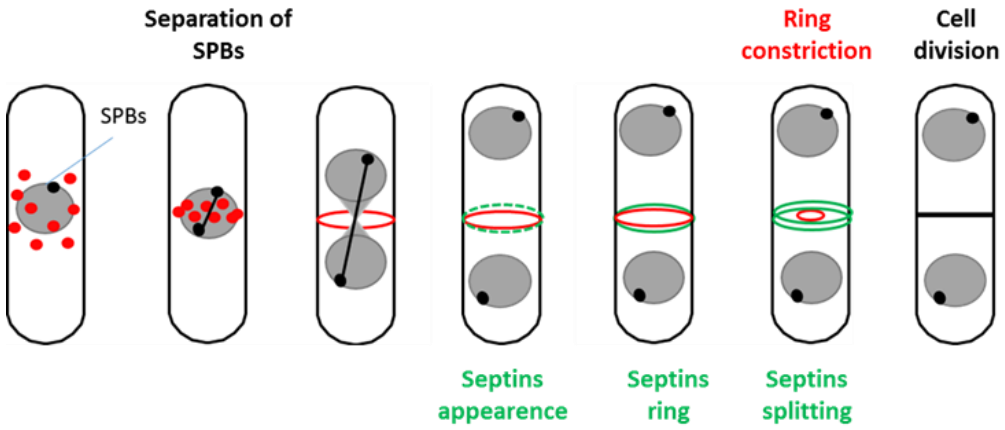

Figure 29: Schematic representation of septin behaviour in the main steps of fission yeast cytokinesis. See text for details.

Indeed, it has been shown that septin mutants have defects in cell-cell separation since they have a key role, in concert with the exocyst complex and Mid2, in delivering the two hydrolytic enzymes (Agn1 and Eng1) in the area around the septum, regulating the step that finishes cytokinesis (Alonso-Nunez et al., 2005; Martin-Cuadrado et al., 2005).

Interestingly, a recent work has highlighted that septins may play a role in earlier cytokinetic events: they appear to regulate CR assembly and constriction by controlling the equatorial dynamics of the SIN kinase Sid2 and glucan synthases Bgs1 and Ags1 in the septum region (Zheng et al., 2018).

One important factor for septin ring organization is the conserved protein anillin whose disruption leads to defects in cytokinesis in animal cells (see chapter 2.3). *S. pombe* genome codes two anillin-related proteins: Mid1 (described in 4.3), and Mid2. Genetic tests have excluded any overlapping functions between them, thus they work independently in separate phases of the cell cycle (Berlin et al., 2003).

The anillin-like protein Mid2 was identified in a genome-wide analysis for its sequence homology with Mid1. Mid2 shows a moderate sequence similarity with Mid1 (24.3%), human anillin (19.5%), *S. cerevisiae* Bud4 (14.9%) and *Candida albicans* Int1 (12.8%): they share a C-terminus fragment that

contains a PH domain and an upstream common region. This overall portion is known to mediate interaction with septins, suggesting that all these proteins have in common this function (Berlin et al., 2003; Paoletti and Chang, 2005; Tasto et al., 2003) (Fig30).

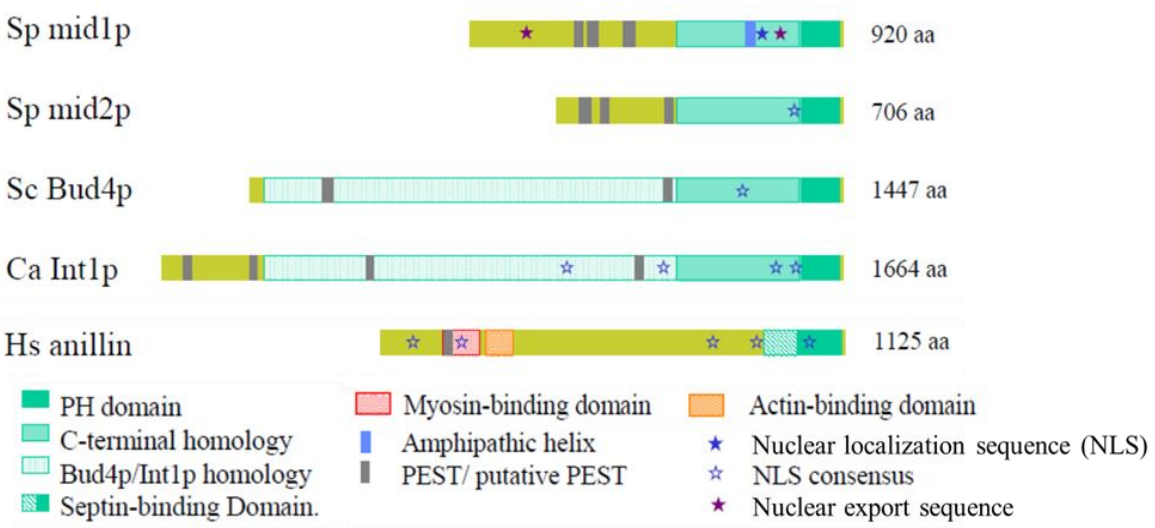

Figure 30 (Adapted from Paoletti and Chang 2005): Domain structure of human Anillin and anilin-like proteins in different Fungi.

In an attempt to identify Mid2 functional domains, a structure-function study was performed, concluding that the PH domain is necessary but not sufficient to drive Mid2 localization and function, suggesting that it might not mediate PM interaction, but rather interaction with other proteins (Tasto et al., 2003). *mid2Δ* cells display the same phenotype as septin-deleted cells. Moreover, Mid2 co-localizes with septins, probably arriving just after septin ring formation since its localization is not only F-actin but also septin-dependent. Similar to septins, Mid2 appears as a single ring, then splits into two in concomitance with septum formation and disassemble when cells divide (Berlin et al., 2003; Tasto et al., 2003) (Fig31). These observations suggest that Mid2 interacts with septins.

Additionally, FRAP analysis has revealed that in absence of Mid2 septins are much more dynamic (30-fold more) in comparison with wild type cells and are largely misorganized, invading the cleavage furrow (Berlin et al., 2003).

Mid2 protein levels are tightly controlled during the cell cycle, peaking during septation. Two layers of regulation control Mid2 levels: Mid2 expression is under the control of the late cytokinesis transcription wave regulated by Sep1-Ace2; additionally Mid2 is degraded through ubiquitination by SCF–dependent proteolysis. Indeed, Mid2 contains three PEST sequences, one in a medial region and two at the N-terminus, that could act as signal for protein degradation (Alonso-Nunez et al., 2005; Petit et al., 2005; Tasto et al., 2003).

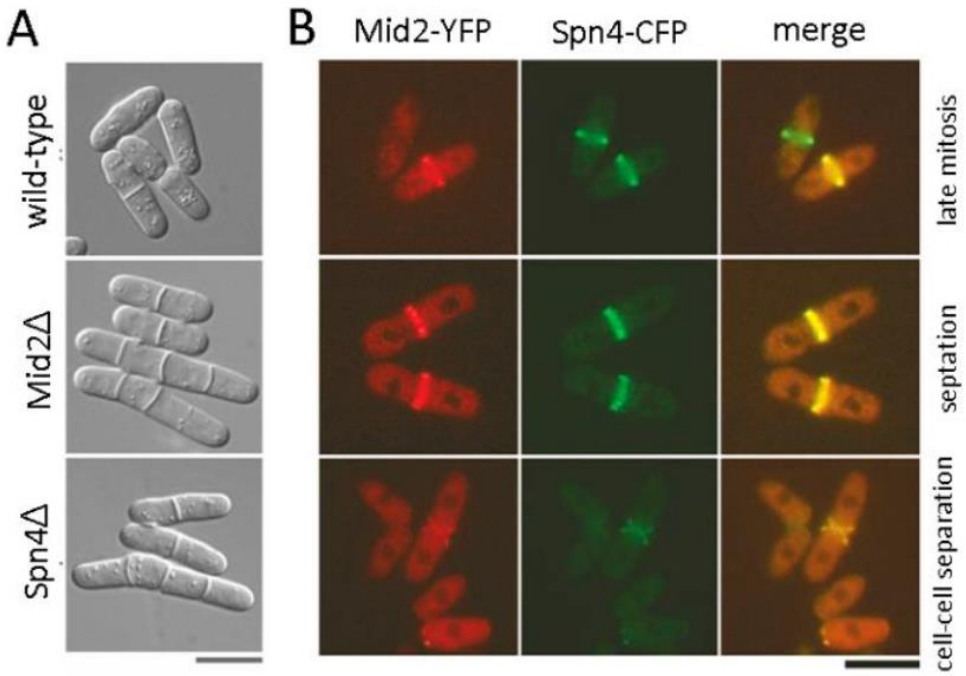

Figure 31 (Adapted from Berlin et al 2003): Potential functional interaction between anillin Mid2 and septins Spn4. (**A**) **mid2Δ and spn4Δ cells have similar cell–cell separation defects.** DIC images of representative wild-type, mid2Δ, and spn4Δ mutant cells grown in rich medium at 30° C to the exponential phase of growth. (**B**) **Mid2p colocalizes with Spn4p.** Cells expressing Mid2p-YFP (green) and Spn4p-CFP (red) were imaged by fluorescence microscopy. (Top) Cells in late mitosis just after initial assembly of the single septin ring. Some of these cells exhibit septin but not Mid2p staining (left cell). (Middle) Cells during septation with double septin rings. (Bottom) Cells during cell–cell separation and during interphase. Scale bars, 5µm.

Overexpression of a non-degradable form of Mid2 let septin filaments persist in the next cell cycle, indicating that the degradation of Mid2 is required for the proper disassembly of septins rings (An et al., 2004; Tasto et al., 2003).

Interestingly, by using a temperature sensitive mutant strain (*cdc16-116*) where septation can occur before mitosis (Minet et al., 1979), septin and Mid2 rings were not detected in interphase cells except in the ones which underwent mitosis before septation. A mild overproduction of Mid2 under a constitutive promoter to allow its presence during interphase rescued septin ring organization in this context (An et al., 2004). This suggests that septin ring organization during interphase requires the presence of Mid2.

Altogether these data imply that Mid2 impacts on septin ring organization and stability: septins alone are able to accumulate at the cell middle, but then Mid2 directly or indirectly seems to be necessary to form a compact and stable septin ring in late mitosis (Berlin et al., 2003; Tasto et al., 2003).

Role of Rho GTPases

Rho GTPases are also involved in the regulation of these final events of cell division. In particular, the RhoGEF Gef3 is recruited by septins to the division site, where it regulates the RhoGTPase Rho3 and

Rho4, for a precise delivery of the glucanases at the cytokinetic furrow through the exocyst (Munoz et al., 2014; Perez et al., 2015; Santos et al., 2005; Wang et al., 2003; Wang et al., 2014).

During this process, a gradual curvature of the secondary septa occurs, which will represent the new ends of the two daughter cells (Fig32). The combination of laser cut experiments of fully septated cells and mathematical simulations unraveled that this remodeling process is not dependent on actin or new cell wall synthesis, but it is driven by mechanical forces. The turgor pressure inflates the elastic cell wall, creating the round shape of the new edges and it may also support the separation and detachment of the daughter cells (Atilgan et al., 2015).

When septum synthesis is completed, the CR remnants needs to be removed to permit polarized growth at the new daughter cell ends (Bohnert and Gould, 2012). Indeed, the closure of CR constriction and the conclusion of septum formation induce SIN inactivation, allowing the Morphogenesis Orb6 Network (MOR) to become active and initiate cell separation and establish interphase polarity (Garcia-Cortes and McCollum, 2009). The MOR signaling pathway is hindered during cytokinesis by SIN-dependent phosphorylation since an improper MOR activation would cause cell lysis in the septum region due to an early initiation of cell separation (Gupta et al., 2014; Ray et al., 2010). This antagonistic balance between the SIN and MOR is key to orchestrate cytoskeleton remodeling between mitosis and interphase thus avoiding polar growth until the end of cytokinesis and cytokinesis events occurring in interphase.

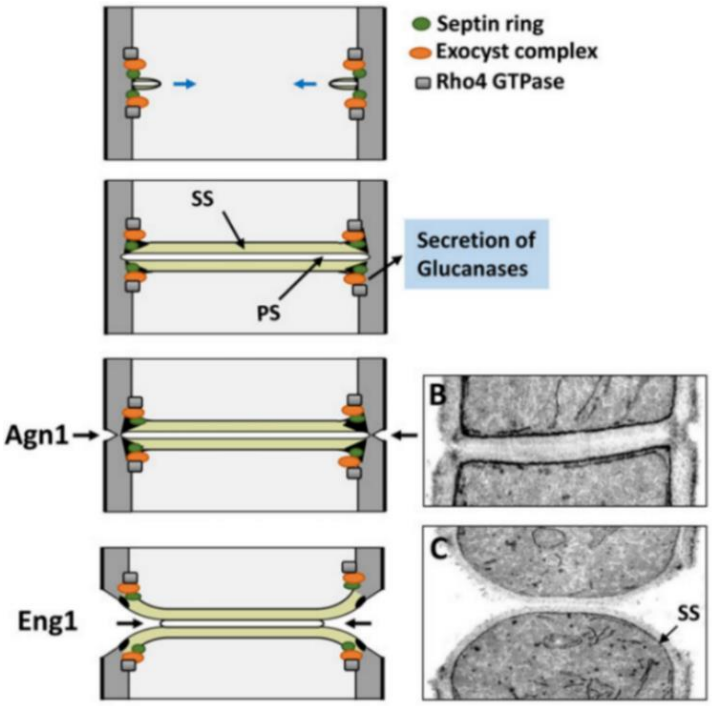

Figure 32 (adapted from Perez et al 2016): Model of cell separation at the end of cytokinesis. Transmission electron micrograph showing how degradation of the lateral cell wall (**B**) and primary septum (**C**) leaves the secondary septum that, upon separation, changes from flat to round shape.

Interplay between the end of cytokinesis and cell repolarization

When septum cleavage is completed, polarized growth at the new daughter cell ends resumes.

In addition, division site signaling by Fic1 was shown to impact on CR remnants clearance from the division site and on the re-establishment of bipolar cell growth in the following cell cycle (Bohnert and Gould, 2012). Interestingly, other genes involved in cell separation like septins or Mid2 display a similar phenotype as well as genes encoding ESCRT-III components Vps2 and Vps24 or ESCRT-III-associated Sst2. Since ESCRT-III are key proteins for abscission in animal cells, this opens the question on whether PM membrane remodeling and scission upon full constriction of the ring is actively controlled in fission yeast like in animal cells and participates in the signaling events controlling growth resumption at the division site.

4.9 Role of membrane lipids in fission yeast cytokinesis

Lipids act as essential structural and regulatory components of cellular membranes dynamic reorganization during cytokinesis, but a comprehensive understanding of the specific roles that lipids may play to regulate this multistep process has not yet been obtained in fission yeast. Only sparse data are available, based on the analysis of a limited series of mutants in lipid biosynthetic pathways identified in various genetic screens.

To date, the major part of the studies in this field has focused on phosphoinositides, which play key roles in membrane and cytoskeleton remodeling, although representing less than 1% of the total cellular lipids (Cauvin and Echard, 2015; Echard, 2012). By using specific probes to detect PIP2, it has been observed that this PI, together with Ptn1, the homologue of the phosphatase PTEN, which dephosphorylates PIP3 to PIP2, and the functional homologue of the PI4P5-kinase, Its3, which catalyzes PIP2 production, are localized to the division plane in the cell middle (Mitra et al., 2004; Zhang et al., 2000). In addition, a temperature sensitive mutant of *its3*, at the restrictive temperature was no longer present at the cell equator and resulted in late cytokinetic defects with an increased number of septated cells and mis-localization of Bgs1 (Deng et al., 2005; Zhang et al., 2000). One possible explanation for this phenotype is that PIP2 has a role in recruiting proteins responsible for septation. Indeed, PIP2 has been found to interact *in vitro* with two of the exocyst subunits (Sec3 and Exo70) in *S. cerevisiae* (He et al., 2007) and with septins. In fission yeast the exocyst is essential for cell division (Martin-Cuadrado et al., 2005) and PIP2 lipid domains may be key for the completion of this process.

In *S. pombe*, as in other yeasts, specific cortical compartments, known as eisosomes, organized as membrane invaginations, have been linked to PIP2 turnover. Pil1, a BAR-protein which is the core

component of eisosomes, binds and tubulates preferentially PIP-enriched membranes and when overexpressed leads to the formation of long cytoplasmic filamentous invaginations that cause defects in cell polarity and cytokinesis (Douglas and Konopka, 2014; Kabeche et al., 2011; Kabeche et al., 2014).

Interestingly, the PI4-kinase PIK1, involved in the generation of the PI4-phosphate, which acts as precursor of other important PIs, is also necessary for septation and cell separation (Park et al., 2009) and an association with the myosin II-light chain Cdc4 has been described (Desautels et al., 2001). When the interaction between them is prevented, cytokinesis was severely impaired, suggesting that PIK1 may be critical for the ring assembly and function.

Recently, it has been demonstrated that the PM lipid composition determines the proper anchoring of the CR, and it is critical for the success of cell division and the equal distribution of the genetic material into the two daughter cells (Snider et al., 2017). The authors discovered that in absence of a correct localization of the phosphatidylinositol-4 kinase Stt4, due to the deletion of its scaffold subunit Efr3, the CR, first organized in the middle of the cell, slides toward one cell tip during anaphase (Baird et al., 2008). A similar phenotype is obtained in the *its3-1* temperature sensitive mutant, where the decrease in PIP2 amount leads to the generation of large vacuoles that prevent the nucleus from localizing around the cell center, leading to CR defects in anchoring and positioning (Snider et al., 2018) (Fig33). These evidences support the fact that PIP2, the kinases that catalyze its production and its precursor PI4-Phosphate are important for securing CR attachment at the PM, its stability and proper septa organization in the cell middle.

Besides, PIPs, also other types of lipids have been reported to play functional roles in cytokinesis.

Mutants in the fission yeast Pps1, which encodes a predicted phosphatidylserine (PS) synthase, exhibit defects in cell morphology, cell wall organization and cytokinesis (Matsuo et al., 2007). Recent findings have revealed that PS is localized to the sites of active growth and cell division in an actin-dependent endocytosis manner, creating a polarized gradient of negative charges throughout the PM with key impacts on cell polarity and morphogenesis (Haupt and Minc, 2016).

Moreover, Css1 (can`t stop synthesizing cell wall), an essential protein related to mammals neutral sphingomyelinases, when mutated, presented defects in cell wall formation, due to the accumulation of α- and β-glucans in the periplasmic space, with cell division arrest and a lethal outcome (Feoktistova et al., 2001). Css1 mutants are defective in the hydrolysis of sphingolipids that produces ceramide, which has been proposed to act as signal transducer in cell growth and death, senescence and in many stress responses pathways (Matmati and Hannun, 2008).

Additionally, sterol-rich domains (SRDs) have been shown to be distributed in a cell-cycle dependent manner at growing tips in interphase cells and at the cell middle during cytokinesis and a functional secretory pathway is required for their localization, since it was disrupted in presence of brefeldin A (Wachtler et al., 2003). Interestingly, it has also been demonstrated that they act as scaffolds for the localization of the growth machinery and polarity factors in establishing *de novo* cell polarity during starvation exit (Makushok et al., 2016).

Ergosterols, the equivalent of cholesterol in Fungi, form liquid-ordered domains by interacting preferentially with sphingolipids with recognized roles in signal transduction, vesicular sorting and polarity (Rajendran and Simons, 2005; Wachtler and Balasubramanian, 2006).

Key elements for the formation of SRDs have been identified in *S. pombe*: the F-BAR protein Cdc15 and type I myosin Myo1. It has been described that *cdc15* mutants form SRDs with spiral configuration in the PM, whereas its over-expression leads to abnormal lipid rafts domains organization (Takeda et al., 2004). Similarly, a *myo1* mutant without the TH1 domain, which includes a putative binding site for phospholipids, displays a uniform spreading of SRDs domains and its overproduction produces the formation of ectopic SRDs (Takeda and Chang, 2005). Cdc15 and Myo1 are known to interact (Carnahan and Gould, 2003) and it has been proposed that, by binding preferentially with acidic phospholipids, these proteins could shape the lipid composition of the PM, creating, directly or indirectly, functional and structural frameworks to facilitate connections between proteins involved in cell polarity, endocytosis and cytokinesis (Alvarez et al., 2007).

Finally, it has been found that the overexpression of Erg25, a C-4 sterol methyl oxidase of the ergosterol synthesis pathway alters ergosterol distribution within the cell and disrupts contractile ring positioning, leading to random septum assembly (Wachtler et al., 2003) (Fig33). This phenotype recapitulates that of *mid1Δ* cells, although a possible connection between both is missing (Almonacid et al., 2009; Celton-Morizur et al., 2006; Daga and Chang, 2005; Paoletti and Chang, 2000; Sohrmann et al., 1996).

Altogether, these evidences indicate that lipid composition may be key to regulate the assembly, distribution and/or function of several elements that control and orchestrate cytokinesis.

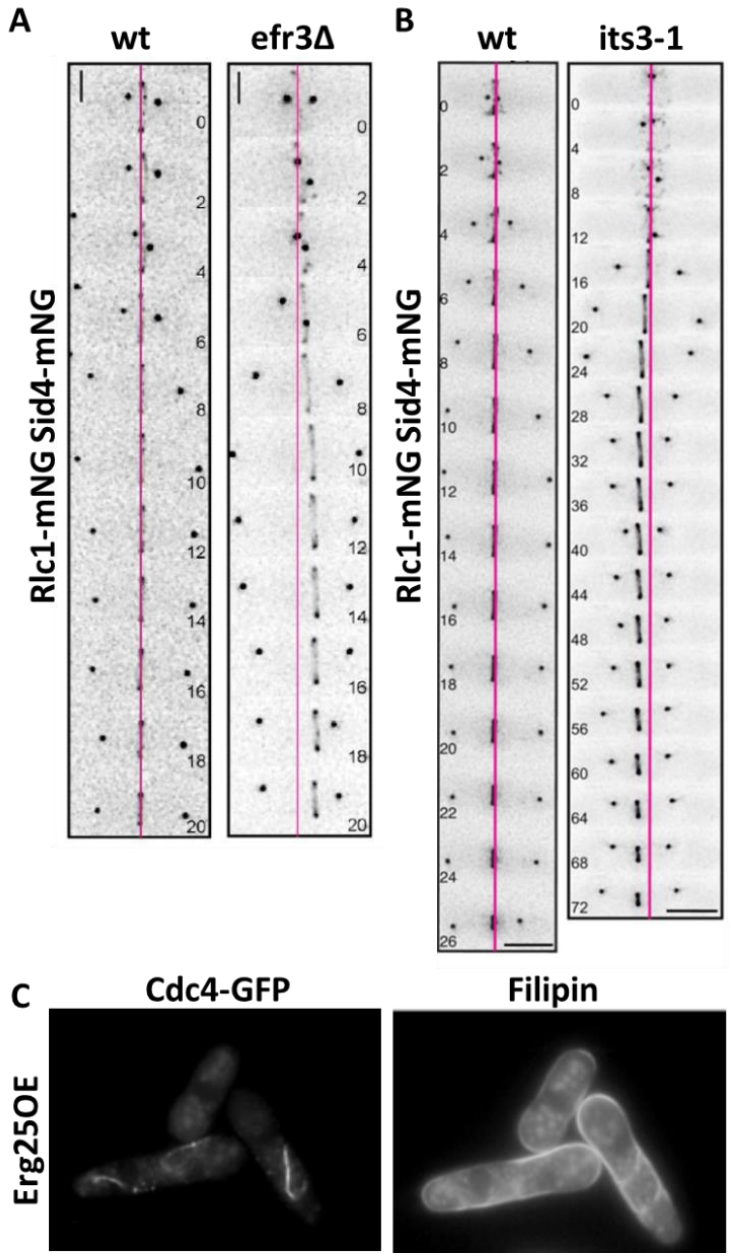

Figure 33 (Adapted from Snider et al 2017; Snider et al 2018 and Wachtler et al 2003): CRs form off-center in mutants of PIP2 and ergosterol phenotypes. (**A**) Live-cell imaging comparison of wild type and efr3Δ grown at 25°C. Bars, 2 µm. Numbers indicate minutes elapsed; magenta line indicates the cell center. (**B**) Montages of time-lapse imaging of wild type and *its3-1* grown at 25°C and shifted to 32°C for 2 h before imaging. Bars, 2 µm. Numbers indicate minutes elapsed; magenta line indicates the cell center. (**C**) Defects in cdc4-GFP organization in cells overexpressing Erg25 under the nmt1-promoter (upper panel) and incubated with filipin for 1 minutes (bottom panel).

II. THESIS OUTLINE

The “leitmotiv” of my PhD project has been cytokinesis, which has been studied in the fission yeast model system, from two different perspectives. My work has first focused on the first step of cytokinesis, division plane positioning, and has addressed the role of a membrane lipid in this process. The second part of my project has been devoted to late cytokinesis, analyzing septin ring assembly at the division site.

In the first part, the aim of my work was to understand the role of ergosterol levels in division plane positioning. Overexpression of a protein involved in ergosterol biosynthesis resulted in random positioning of the contractile ring (CR). Combining fission yeast genetics and live-cell imaging of CR components, I have found that increased ergosterol levels do not disrupt the cytokinetic precursor nodes that define the position of the division plane, but specifically inhibits F-actin assembly from cytokinetic precursor nodes by the formin Cdc12, preventing their compaction into a medially placed CR. This suggests that ergosterol may negatively regulate Cdc12 activity in a direct or indirect manner.

In the second part of my PhD, my project focused on the dynamic behavior of septins during cytokinesis and the regulatory mechanisms that control their assembly into rings defining the borders of the cleavage furrow. This part was approached in three ways: 1) Description of the recruitment, assembly and disassembly of septins and the anillin-like protein Mid2 by live cell imaging using precise cell cycle timers 2) Determining how Mid2 impacts on septin ring assembly using a combination of molecular genetics and biochemistry approaches 3) Identification of the key regulators controlling the major transitions observed in septins and Mid2 organization. I have found first that septins are initially recruited as a diffuse meshwork to a 1.5 µm wide region of the cortex surrounding the CR in anaphase, at time of maximum spindle elongation, before compacting into rings when constriction of the CR is initiated. Second, my work provides evidence that the anillin-like protein Mid2 may act as a bundler for septins that promotes this new compaction step as well as further accumulation of septins at the division site. Third, looking at cell cycle regulators, I found that high Cdk activity allows for septins and Mid2 recruitment but not for their compaction, whereas the SIN pathway is crucial for septin and Mid2 accumulation at the division site and compaction. Finally, PIP2 levels were found to be critical to initiate septin recruitment to the plasma membrane, before Mid2 becomes available at the initiation of CR constriction, with impact on the maximum amount of septins at the division site. This work highlights the complex regulations that allow the coordination between septin ring assembly and cell cycle progression.

These results are presented in two manuscripts. The first one was published in July 2019 in the Journal of Cell Science, while the second on septins and mid2 is currently in preparation.

III. RESULTS

Article 1: Increasing ergosterol levels delays formin-dependent assembly of F-actin cables and disrupts division plane positioning in fission yeast

Federica Arbizzani[1], Sergio A. Rincon[1, 2] and Anne Paoletti[1]

[1] Institut Curie, PSL University, CNRS UMR 144, F-75005, Paris, France.

[2] Instituto de Biología Funcional y Genómica and Departamento de Microbiología y Genética, Consejo Superior de Investigaciones Científicas (CSIC) / Universidad de Salamanca, Salamanca, 37007 Spain.

© 2019. Published by The Company of Biologists Ltd | Journal of Cell Science (2019) 132, jcs227447. doi:10.1242/jcs.227447

RESEARCH ARTICLE

Increasing ergosterol levels delays formin-dependent assembly of F-actin cables and disrupts division plane positioning in fission yeast

Federica Arbizzani[1], Sergio A. Rincon[1,2,*,‡] and Anne Paoletti[1,*,‡]

ABSTRACT

In most eukaryotes, cytokinesis is mediated by the constriction of a contractile acto-myosin ring (CR), which promotes the ingression of the cleavage furrow. Many components of the CR interact with plasma membrane lipids suggesting that lipids may regulate CR assembly and function. Although there is clear evidence that phosphoinositides play an important role in cytokinesis, much less is known about the role of sterols in this process. Here, we studied how sterols influence division plane positioning and CR assembly in fission yeast. We show that increasing ergosterol levels in the plasma membrane blocks the assembly of F-actin cables from cytokinetic precursor nodes, preventing their compaction into a ring. Abnormal F-actin cables form after a delay, leading to randomly placed septa. Since the formin Cdc12 was detected on cytokinetic precursors and the phenotype can be partially rescued by inhibiting the Arp2/3 complex, which competes with formins for F-actin nucleation, we propose that ergosterol may inhibit formin dependent assembly of F-actin cables from cytokinetic precursors.

KEY WORDS: Actin, Contractile ring, Cytokinesis, Fission yeast, Formin, Sterol-rich domain

INTRODUCTION

Cell division is an essential process required for the proliferation of unicellular organisms as well as for the development of multicellular organisms and cell renewal within tissues. Its final step, cytokinesis, ensures the physical separation of the two daughter cells. Defective control of this step can either lead to cell death or to aneuploidy, and can contribute to cancer progression (Fujiwara et al., 2005; Lacroix and Maddox, 2012; Storchova and Pellman, 2004). Cytokinesis is therefore under the control of very tight spatial and temporal regulatory mechanisms.

In most eukaryotes, cytokinesis relies on an acto-myosin based contractile ring (CR), which assembles at the division site and constricts to cause the invagination of the plasma membrane and promote the ingression of the cleavage furrow between the two sets of segregating chromosomes. Fission yeast (*Schizosaccharomyces pombe*) has provided crucial insights into the molecular mechanisms of CR assembly. In this model organism, CR assembly is initiated by cytokinetic precursors organized since interphase on the medial cortex of the cell by the SAD kinase Cdr2 (Akamatsu et al., 2017; Moseley et al., 2009; Pollard and Wu, 2010; Rincon and Paoletti, 2016; Willet et al., 2015b; Wu et al., 2006). Medial positioning of these nodes contributes to division plane positioning and is ensured by negative signalling by the gradient of the DYRK kinase Pom1 emanating from the cell tips (Celton-Morizur et al., 2006; Martin and Berthelot-Grosjean, 2009; Moseley et al., 2009; Padte et al., 2006; Rincon et al., 2014). These cytokinetic precursors contain several non-essential cytokinetic ring components, such as the anillin-like protein Mid1, Blt1, Gef2, Klp8 and Nod1 (Goss et al., 2014; Guzman-Vendrell et al., 2013; Jourdain et al., 2013; Martin and Berthelot-Grosjean, 2009; Moseley et al., 2009; Ye et al., 2012; Zhu et al., 2013). Upon mitotic entry, positive signalling from the medially placed nucleus, mediated by the polo-like kinase Plo1-induced export from the nucleus of the anillin-like protein Mid1, reinforces division plane positioning in the cell middle (Almonacid et al., 2009), while Cdr2 dissociates from the cytokinetic precursors in a septation initiation network (SIN)-dependent manner (Akamatsu et al., 2014; Rincon et al., 2017). Plo1 also activates Mid1, which becomes competent for the sequential recruitment of essential ring components (Almonacid et al., 2011): Mid1 first engages the IQGAP protein Rng2 and myosin II light chain Cdc4, heavy chain Myo2 and regulatory light chain Rlc1. Mid1 also contributes directly to the recruitment of the F-BAR protein Cdc15 (Laporte et al., 2011). Rng2 and myosin II, together with Cdc15 collaborate in the recruitment of the formin Cdc12, which nucleates F-actin cables required for CR assembly (Coffman et al., 2009, 2013; Laporte et al., 2011; Padmanabhan et al., 2011; Willet et al., 2015a; Wu et al., 2003, 2006). This step is necessary for myosin II-dependent node compaction into a tight acto-myosin ring in a mechanism modeled under the name of search-capture-pull-release (Ojkic et al., 2011; Vavylonis et al., 2008).

In parallel to CR assembly, modifications in the lipid composition of the plasma membrane take place at the division site with a functional impact on cytokinesis (Atilla-Gokcumen et al., 2014; Echard and Burgess, 2014). So far, major studies have focused on phosphoinositides, which play key roles in membrane trafficking and cytoskeleton rearrangements. In particular, in human cells, phosphatidylinositol 4,5-bisphosphate [PI(4,5)P_2] enrichment at the cytokinesis furrow and early intercellular bridges is crucial for F-actin remodeling by RhoA, anillin and septins, whereas its hydrolysis by the PIP_2 phosphatase OCRL is necessary for abscission, avoiding abnormal F-actin accumulation at cytokinesis bridges (Cauvin and Echard, 2015; Dambournet et al., 2011; Echard, 2012).

In fission yeast, only sparse data are available on the role of membrane lipids in cytokinesis. First, the correct localization of the PI4 kinase Stt4 by its scaffolding subunit Efr3 (Baird et al., 2008) was recently shown to play a role in the spatial regulation of

[1]Institut Curie, PSL University, CNRS UMR 144, 75005 Paris, France. [2]Instituto de Biología Funcional y Genómica and Departamento de Microbiología y Genética, Consejo Superior de Investigaciones Científicas (CSIC)/Universidad de Salamanca, Salamanca 37007, Spain.
*These authors contributed equally to this work

‡Authors for correspondence (anne.paoletti@curie.fr; sarpadilla@usal.es)

S.A.R., 0000-0002-7169-2097; A.P., 0000-0002-9004-559X

Received 2 November 2018; Accepted 31 May 2019

Journal of Cell Science (2019) 132, jcs227447. doi:10.1242/jcs.227447

cytokinesis by preventing the CR sliding toward one cell tip during anaphase (Snider et al., 2017). Similarly, defects in the spatial regulation of cytokinesis at the beginning of mitosis have been reported in the PI-5 kinase *its3-1* mutant, characterized by reduced levels of phosphatidylinositol 3,5-bisphosphate [$PI(3,5)P_2$] (Snider et al., 2018). Second, defects in cytokinesis as well as cell morphology and cell wall organization were observed in a mutant of Pps1, involved in phosphatidylserine (PS) synthesis (Matsuo et al., 2007). Third, defects in sphingolipid hydrolysis into ceramide in *css1* mutant were shown to induce defects in cell wall and septum formation, due to the accumulation of α- and β-glucans in the periplasmic space, with cell division arrest and a lethal outcome (Feoktistova et al., 2001).

Some data also point out a role for sterols in the regulation of cytokinesis (Wachtler et al., 2003). Sterols are synthesized and mature in the ER by a cascade of coupled enzymatic reactions. The final metabolic product, cholesterol in the case of animal cells and ergosterol in fungi, is then transported to the plasma membrane where it forms liquid-ordered domains by interacting preferentially with sphingolipids, which have recognized roles in signal transduction, vesicular sorting and polarity (Rajendran and Simons, 2005). Key factors for the formation of sterol-rich domains (SRDs) are the F-BAR protein Cdc15 and the type I myosin Myo1, which interact with one another, binding preferentially to acidic phospholipids (Alvarez et al., 2007; Carnahan and Gould, 2003; Takeda and Chang, 2005; Takeda et al., 2004). Besides, SRDs redistribute from growing cell tips in interphase, where they act as scaffolds for polarity factors and the growth machinery (Makushok et al., 2016), to the division site in mitosis (Wachtler et al., 2003).

Interestingly, Wachtler et al. (2003) found that the overexpression of Erg25, a C-4 sterol-methyl-oxidase of the ergosterol synthesis pathway, could alter ergosterol distribution within the cell and disrupt CR positioning, leading to the formation of random positioned and misshapen septa (Wachtler et al., 2003). This phenotype is strikingly similar to the phenotype produced by the deletion of the main division plane position factor Mid1, which is associated with the cytokinetic precursors described above.

Here, by combining fission yeast genetics with live-cell imaging of CR assembly from cytokinetic precursors, we show that increasing ergosterol levels does not affect the assembly or distribution of cytokinetic precursors, nor the recruitment of the IQGAP protein Rng2, myosin II or the F-BAR protein Cdc15, at mitotic entry. Instead, it inhibits the assembly of medial F-actin cables from cytokinetic precursors preventing node compaction into a tight ring. Randomly positioned F-actin cables finally emerge, with a long delay compared to the wild-type situation, leading to abnormally placed septa. Analysis of the formin Cdc12 that nucleates F-actin cables from cytokinetic precursors revealed that its recruitment to the medial cortex is not abolished in these circumstances, although we cannot exclude the possibility that its amount is reduced. Since the stability of F-actin cables was not altered altogether and the phenotype could be partially rescued by inhibition of Arp2/3, which competes with formins, we propose that increasing ergosterol levels in the plasma membrane may inhibit the activity of the formin Cdc12.

RESULTS

To understand how ergosterol homeostasis may influence division plane positioning, we decided to reproduce Erg25 overexpression (denoted Erg25 OE) from a multicopy plasmid under the control of the thiamine-repressible *nmt1* promoter (Maundrell, 1993). Septum organization was analysed by staining cells with the cell wall dye Calcofluor after thiamine removal to induce Erg25 OE (Fig. 1A). We found that 85.6±4.3% (mean±s.d.) of cells overexpressing Erg25 had abnormal septa compared to 1.9±0.2% of control cells (Fig. 1B).

To determine the ergosterol distribution pattern in this context, cells were stained with the ergosterol-specific dye filipin. As expected, an altered pattern of distribution of ergosterol was observed upon Erg25 OE, with increased levels of ergosterol not only at the cell tips where it normally accumulates (Takeda et al., 2004; Wachtler et al., 2003), but also around the whole-cell periphery, including at the medial cell cortex (Fig. 1C). Accordingly, the intensity of filipin staining in late G2 cells, ranging from 11.5 to 13.5 µm, in length showed a 1.7-fold increase of sterols at the cell tips, and a 1.5-fold increase of sterols in the cell middle, compared to the wild-type situation (n=15 for both control and Erg25 OE cells; Fig. 1D). Finally, in dividing cells, filipin was concentrated at the division site, which was abnormally shaped upon Erg25 OE. These data confirms that ergosterol levels are increased in the plasma membrane upon Erg25 OE, including in the medial region of the cell where CR assembly takes place at mitotic entry.

Next, in order to verify whether the defects in division plane position were due to ergosterol enrichment, we treated control and Erg25 overexpressing cells with miconazole. This drug inhibits Erg11, a lanosterol 14-α demethylase that functions immediately upstream of Erg25 in the ergosterol synthesis pathway (Fig. S1A) (Löffler et al., 1997; Marichal et al., 1999; Rippon and Fromtling, 1993; Sanglard et al., 1998; Sheehan et al., 1999). Miconazole induced a reduction of ∼80% in the number of abnormally shaped septa upon Erg25 OE (Fig. 1E; Fig. S1B). In parallel, we also overexpressed Erg25 in cells lacking *erg6* (*erg6*Δ), which encodes a protein acting immediately downstream of Erg25 in the ergosterol synthesis pathway (Fig. S1A) (Bard et al., 1996; Iwaki et al., 2008). The number of abnormally shaped septa was reduced from ∼85% in Erg25 OE cells to less than 40% in the *erg6*Δ mutant (Fig. S1C), consistent with the suppression of the phenotype induced by miconazole. The partial suppression seen in the *erg6*Δ mutant might be due to alternative biosynthetic pathway allowing ergosterol production from zymosterol independently of *erg6*. From these experiments, we conclude that ring positioning defects produced by Erg25 OE require an active sterol synthesis pathway and are effectively related to sterol overproduction, excluding other unrelated functional defects that Erg25 OE might have caused.

We next determined the localization of Erg25 by fusing it to the green fluorescent tag ENVY (Slubowski et al., 2015) at its C-terminus. Fluorescence microscopy revealed that Erg25 has both a perinuclear and a peripheral distribution around the cell (Fig. S1D), reminiscent of the endoplasmic reticulum (ER) distribution. Accordingly, when Erg25–ENVY was expressed together with the ER marker Elo2, a fatty acid elongase (labelled as ER-mCherry in Fig. S1D), we found that the two proteins perfectly colocalized. This result is in agreement with the fact that sterol metabolism takes place in this organelle (Jacquier and Schneiter, 2012).

We next wanted to determine whether the distribution of Erg25 was altered upon its overexpression. To do so, we ectopically overexpressed Erg25 in the endogenously producing Erg25–ENVY strain. In interphase cells, the protein lost its strong enrichment around the nucleus and the cell surface, and formed irregular patterns in a medial cytoplasmic zone (Fig. S1E). Quantification of this phenotype showed that 82.6±3.3% of interphase cells overexpressing Erg25 displayed an abnormal distribution of Erg25 in comparison to none in the control (Fig. S1F). This result indicates that Erg25 OE alters the organization of the ER.

Journal of Cell Science (2019) 132, jcs227447. doi:10.1242/jcs.227447

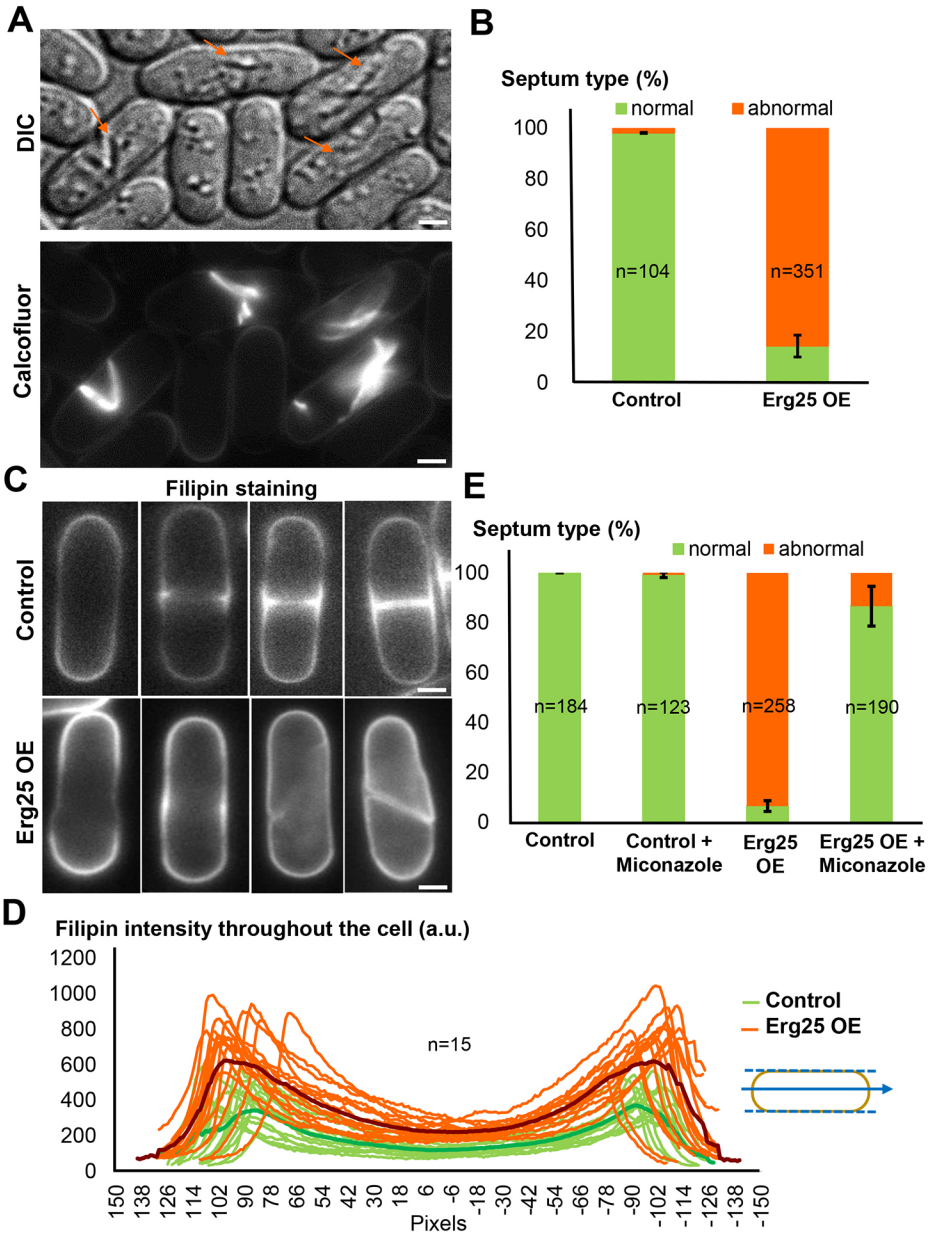

Fig. 1. Erg25 OE induces cytokinesis defect by increasing ergosterol levels. (A) DIC image (top) and Calcofluor staining of septa (bottom) in Erg25 OE cells. Orange arrows indicate cells with abnormal septa. Scale bars: 5 µm. (B) Quantification of the percentage of defective septa in Erg25 OE (n=351) and control cells (n=104). Error bars: s.d. (C) Filipin staining of ergosterol in control (top panel) and Erg25 OE cells (bottom panel). Scale bars: 5 µm. (D) Analysis of filipin intensity along linescans for control (green, n=15) and Erg25 OE cells (orange, n=15). The average curves are displayed in dark green for the control and in dark red for Erg25 OE cells. (E) Quantification of the percentage of defective septa in control or Erg25 OE cells grown in the presence or absence of 1 µM miconazole. Error bars: s.d.

This phenotype was reminiscent of the triple deletion mutant of the reticulon-like proteins Tts1, Rtn1, and Yop1 (hereafter called tryΔ), which displays alteration of the subcortical reticular ER into abnormal cisternae, associated with severe defects in division plane positioning (Zhang et al., 2010). This phenotype has been shown to be suppressed by the deletion of the two vesicle-associated membrane protein-associated proteins (VAPs) genes *scs2* and *scs22*, which link the cortical ER to the plasma membrane. This led to the proposal that abnormal ER cisternae could shield the plasma membrane, preventing normal CR assembly (Zhang et al., 2012). Since Erg25 OE alters ER organization, we wondered if the septum positioning defects it generates could result from the same phenomenon. To test this, Erg25 OE was induced in the VAP single and double deletion mutants. Septum staining with Calcofluor showed that deletion of VAPs only had a minor impact on the effect of Erg25 OE on division plane positioning (~10% reduction in abnormal positioning; Fig. S1G). From this experiment, we conclude that membrane shielding by the ER only has a minor role in the division plane positioning defects produced by Erg25 OE. This result points toward a more direct effect of ergosterol on CR positioning and assembly mechanisms.

To determine how Erg25 OE affects CR assembly, we performed live imaging of Cdr2, the main organizer of cytokinetic precursors, and of Blt1, a component of cytokinetic precursors that remains in the CR until its full constriction (Moseley et al., 2009). These proteins were visualized after fusion to EGFP and mEGFP, respectively, in cells expressing the regulatory light chain of myosin II fused to mCherry (Rlc1–mCherry) in order to follow CR assembly. These cells also expressed the spindle pole body (SPB) component Sid4, also fused to mCherry (Sid4-mCherry), to use SPB separation as a timer for mitosis onset.

Cdr2 was not affected by Erg25 OE (Fig. 2A,B): in cells ranging from 11 to 14 µm in length, neither the length of Cdr2 domain (Fig. S2A) nor the intensity of Cdr2–EGFP were modified (Fig. S2B). Similarly, Blt1 behaved normally during interphase, but at mitotic entry, it started spreading laterally along the cell cortex

Journal of Cell Science (2019) 132, jcs227447. doi:10.1242/jcs.227447

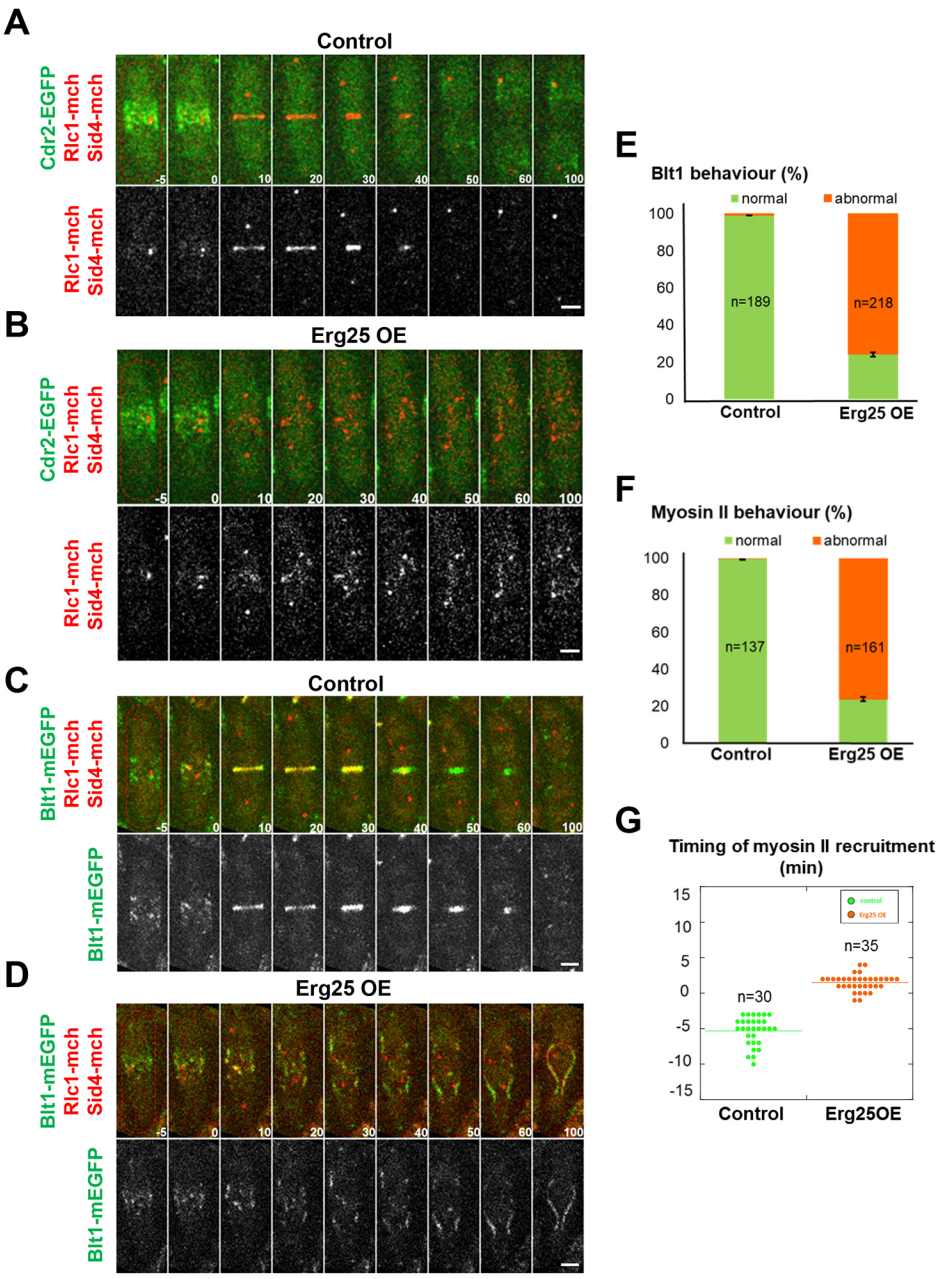

Fig. 2. Erg25 OE affects ring assembly, but not the assembly of cytokinetic precursor nodes in interphase. (A,B) Time-lapse analysis (min) of Cdr2–EGFP, Rlc1–mCherry (mch) and Sid4–mCherry in control (A) and Erg25 OE cells (B) incubated at 25°C for 2 h. Medial plane confocal images are shown. Time 0 corresponds to mitotic entry. (C,D) Time-lapse analysis of Blt1–mEGFP, Rlc1–mCherry and Sid4–mCherry in control (C) and Erg25 OE cells (D) incubated at 25°C for 2 h. Medial plane confocal images are shown. Time 0 corresponds to mitotic entry. Scale bars: 5 µm. (E) Quantification of the percentage of cells where Blt1 showed a normal and abnormal pattern (behaviour) for control (*n*=189) and Erg25 OE cells (*n*=218). (F) Quantification of percentage of cells where myosin II (Rlc1) showed a normal and abnormal pattern (behaviour) for control (*n*=137) and Erg25 OE cells (*n*=161). (G) Timing of myosin II recruitment at cytokinetic precursors after SPB separation (Time 0) in control (*n*=30) and Erg25 OE cells (*n*=35). All error bars represent s.d.

rather than compacting into a ring (Fig. 2C,D). Quantitative analysis showed that 75.7±1.1% (mean±s.d.) of cells overexpressing Erg25 showed an abnormal behaviour of Blt1 in early mitosis compared to 1.0±0.04% in the control situation (Fig. 2E).

We then analysed the behaviour of the light chain of myosin II, Rlc1 in the movies. Although recruited to the medial cortex in early mitosis (Fig. 2A–D; Fig. S3A) to a domain of similar length to that in control cells (2.83±0.23 µm and 2.63±0.18 µm, respectively; Fig. S3B), myosin II was recruited to the cytokinetic precursors with a delay of ∼7 min upon Erg25 OE (Fig. 2G). This delay was confirmed by monitoring the intensity of myosin II in the cell middle (Fig. S3C). While in the control cells, Rlc1–mCherry intensity raised over 30 min before decreasing rapidly at the time of ring constriction, myosin II intensity stopped increasing 20 min after SPB separation in Erg25 OE cells. Intensity then fluctuated at intermediate levels for an extended period of time (Fig. S3C). Strikingly, and similar to Blt1, Rlc1 never compacted into a ring after its recruitment to cytokinetic precursors but spread laterally on the cortex instead (Fig. 2A–D; Fig. S3C, *t*=10 to 20 min). Some abnormal myosin II cables were observed at later time points (Fig. 2A–D; Fig. S3A, *t*=30–100 min). These cables, which ran sometimes along the long axis of the cell, were most often unable to constrict (Fig. 2A,B). Indeed, 76.2±1.1% cells displayed abnormal myosin II rings upon Erg25 OE compared to 0.3±0.4% in the control (Fig. 2F). We conclude that upon Erg25 OE, cytokinetic precursors are well assembled in interphase and competent for myosin II recruitment with a small delay, but they subsequently fail to compact into a ring.

Since the compaction of cytokinetic precursors depends on myosin II-dependent pulling on F-actin filaments nucleated by adjacent nodes (Ojkic et al., 2011; Vavylonis et al., 2008), we next analysed F-actin distribution with Lifeact–GFP (Huang et al., 2012; Riedl et al., 2008). During interphase, Erg25 OE did not alter F-actin patches at the cell tips nor F-actin cables running along the

Journal of Cell Science (2019) 132, jcs227447. doi:10.1242/jcs.227447

length of the cell (Fig. 3A,B). However, after SPB separation, cells failed to accumulate F-actin at the cell middle, indicating that the cytokinetic precursors were unable to promote F-actin assembly upon Erg25 OE (Fig. 3A,B; Fig. S4A,B). Delocalized F-actin dots were detected all over the cell instead, and, after a variable delay, cells started to form F-actin cables with irregular shapes and random orientations [37.0±10.2 min (mean±s.d.) after SPB separation as compared to the appearance of F-actin at the division site 7.3±1.8 min in normal cells; Fig. 3D; see also Movies 1–3]. Quantification revealed that 75.6±1.7% Erg25 OE cells displayed delayed and abnormal F-actin cable assembly compared to 0.6±0.9% in control conditions (Fig. 3C). We conclude that defects in division plane positioning in Erg25 OE cells result from defective F-actin nucleation from cytokinetic precursors.

To understand why F-actin assembly from cytokinetic precursors was abolished in presence of higher ergosterol levels at the medial cortex, we decided to carefully check the whole pathway of recruitment of cytokinetic ring components to cytokinetic precursors (Almonacid et al., 2011; Laporte et al., 2011; Padmanabhan et al., 2011). We started with the anillin-like protein Mid1, which triggers the recruitment of CR ring components to cytokinetic precursors at mitotic onset upon phosphorylation by the polo kinase Plo1 (Almonacid et al., 2011; Bahler et al., 1998a; Celton-Morizur et al., 2004; Paoletti and Chang, 2000; Sohrmann et al., 1996). Similar to Cdr2 and Blt1, and as expected from the fact that myosin II was recruited to medial nodes, Mid1 co-localized normally with Cdr2 at cytokinetic precursors during interphase in Erg25 OE cells (Fig. 4A; Fig. S2C–F). As cells entered mitosis, Mid1 started enriching at the normal timing on the medial cortex upon export from the nucleus (i.e. 2 to 10 min before SPB separation; Fig. 4D) and in a domain of similar length to that of normal cells (Fig. 4E). However, in absence of precursor node compaction, Mid1 then spread along the cell cortex as observed for Blt1 and Rlc1 (Fig. 4A; Fig. S5A).

We next analysed the localization of the IQGAP protein Rng2 (Laporte et al., 2011; Takaine et al., 2014) and of the F-BAR protein Cdc15 (Arasada and Pollard, 2014; Willet et al., 2015a) whose recruitments depend on Mid1. Rng2 and Cdc15 were recruited with

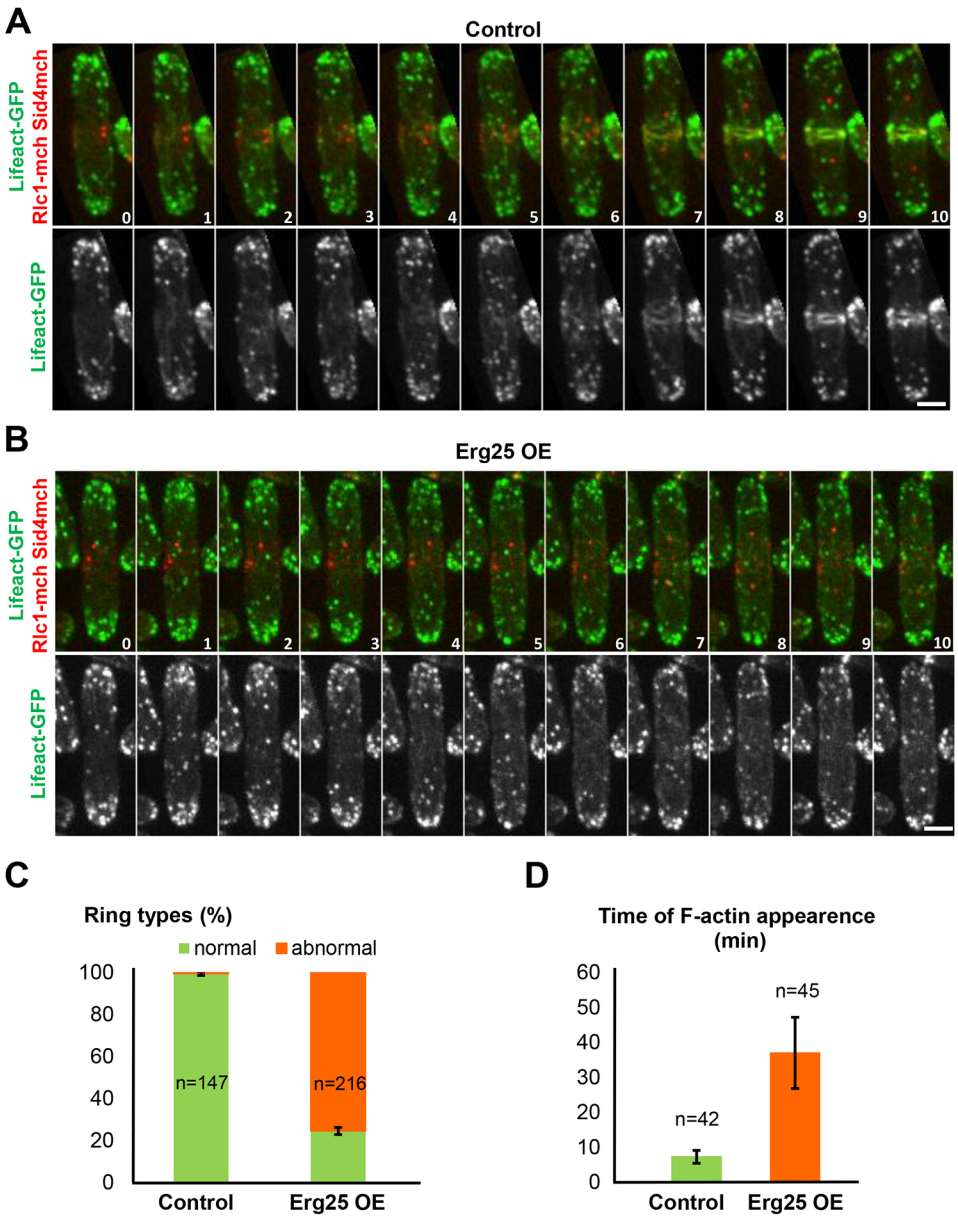

Fig. 3. Inhibition of F-actin nucleation from cytokinetic precursor nodes upon Erg25 OE. Time-lapse imaging (min) of Lifeact–GFP, Rlc1–mCherry (mch) and Sid4–mCherry in control (A) and Erg25 OE cells (B). Maximum projection confocal images are shown. Time 0 corresponds to mitotic entry. Scale bars: 5 µm. (C) Percentage of normal and abnormal contractile rings in control (n=147) and Erg25 OE cells (n=216). Error bars: s.d. (D) Timing of medial actin cable appearance after SPB separation (Time 0) in control (n=42) and Erg25 OE cells (n=45). Error bars: s.d.

Journal of Cell Science (2019) 132, jcs227447. doi:10.1242/jcs.227447

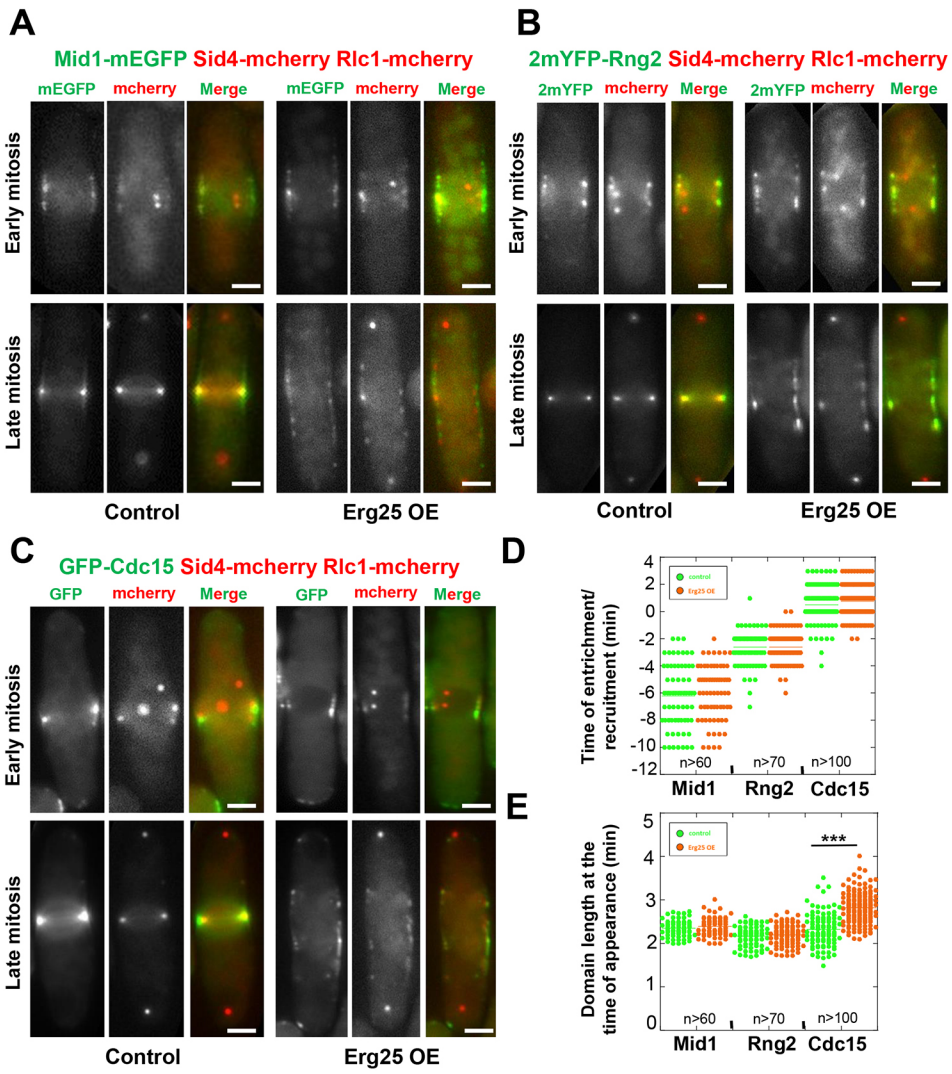

Fig. 4. Erg25 OE does not prevent the recruitment of Mid1, Rng2 and Cdc15 to cytokinetic precursor nodes. (A–C) Epifluorescence images of Mid1–mEGFP (A) or 2mYFP–Rng2 (B) or GFP–Cdc15 (C) and of Rlc1–mCherry and Sid4–mCherry in control and Erg25 OE cells in early mitosis (upper) and late mitosis (bottom). Scale bars: 2 µm. (D) Timing of Mid1 enrichment and Rng2 and Cdc15 recruitment to cytokinetic precursors after SPB separation (time 0) in control (green) and Erg25 OE cells (orange); n>50. (E) Length of Mid1, Rng2 and Cd15 domain at initial time of recruitment in control (green) and Erg25 OE cells (orange); n>50. ***P<0.001.

normal kinetics (Fig. 4B–D) but again, they did not compact into a medial ring and spread out after SPB separation (Fig. 4B,C; Fig. S5B,C). The domain of recruitment was of normal length for Rng2 but slightly enlarged by 0.5 µm for Cdc15 (2.32±0.38 µm in the control and 2.82±1.21 µm upon Erg25 OE, mean±s.d.; Fig. 4E). Since Cdc15 is recruited a few minutes later than Rlc1 or Rng2, the expansion of the domain of recruitment might be due to the spreading of cytokinetic precursors observed during the course of mitosis in Erg25 OE cells.

We finally examined the formin Cdc12, which is responsible for F-actin nucleation from cytokinetic precursors. Cdc12 recruitment depends on the recruitment of all other components of the CR mentioned above (Laporte et al., 2011). Although the Cdc12 signal in fusion to either three YFP tags or three GFP tags was very faint, we were able to detect its recruitment to cytokinetic precursors in all cells examined (Fig. 5A,D,E) and to establish that there was no alteration in the timing of its recruitment upon Erg25 OE (7.38±1.85 min in the control and 7.22±1.95 min upon Erg25 OE; Fig. 5B). But Cdc12 was recruited to a larger domain (2.19±0.19 µm in Erg25 OE cells compared to 0.96±0.12 µm in control cells; Fig. 5C). The enlargement of the domain could be due to precursor node spreading over the cortex upon Erg25 OE instead of compacting as soon as Cdc12 is recruited and promotes F-actin assembly.

Given the weak signals observed for Cdc12, we also designed a control experiment to ascertain that the faint signals observed were genuine: *cdc25-22* cells overexpressing Erg25 synchronized by block in G2 for 2 h at 36°C and released into mitosis at 25°C were compared to *cdc25-22* cells and to *mid1*Δ *cdc25-22* cells, which cannot recruit Cdc12 on medial cortex in mitosis (Laporte et al., 2011). While no signal was detected in *mid1*Δ cells, Erg25 OE cells showed faint Cdc12 nodes dispersed along the medial cell cortex upon Erg25 OE (Fig. 5F).

Unfortunately, the low signal of Cdc12, and its dispersion on the medial cortex upon Erg25 OE prevented us from quantifying the amounts of Cdc12 recruited to cytokinetic precursors. Therefore, although we can confirm that Cdc12 is still recruited to cytokinetic precursors upon Erg25 OE, we cannot exclude quantitative defects in Cdc12 recruitment in Erg25 OE cells at this stage. In any case, since F-actin assembly is fully abolished, we conclude that the molecules of Cdc12 recruited to cytokinetic precursors are unable to induce the assembly of stable F-actin cables.

We next wondered whether Erg25 OE could result in a general defect of F-actin cable stability or assembly by formins. To assess whether this was the case, we analysed F-actin distribution in interphase cells, in which F-actin cable formation depends exclusively on the formin For3 (Feierbach and Chang, 2001). Interphase cells overexpressing Erg25 presented normal For3-nucleated F-actin

Journal of Cell Science (2019) 132, jcs227447. doi:10.1242/jcs.227447

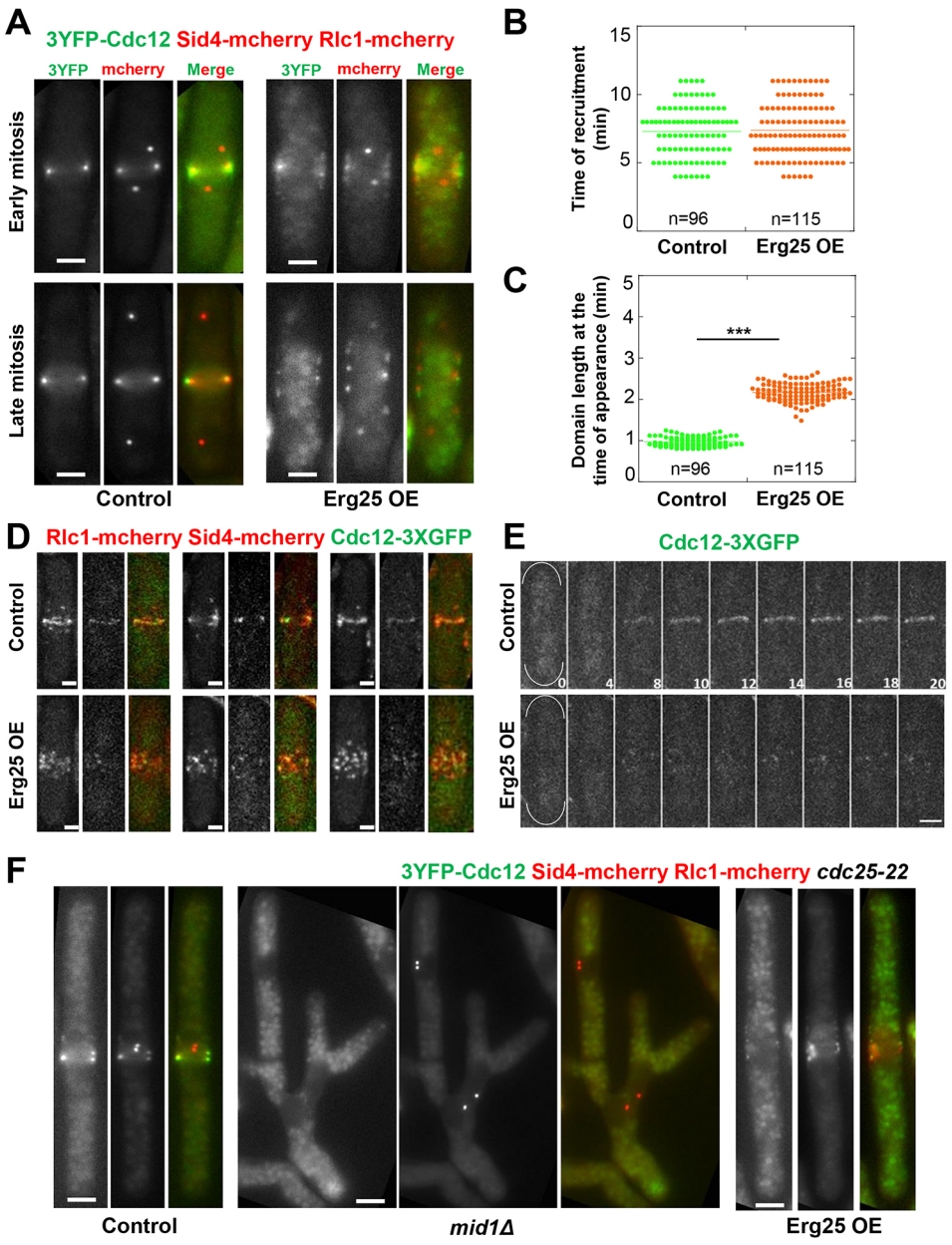

Fig. 5. Erg25 OE does not prevent the recruitment of the formin Cdc12 to cytokinetic precursor nodes. (A) Epifluorescence medial plane images of 3YFP–Cdc12, Rlc1–mCherry and Sid4–mCherry in control and Erg25 OE cells in early mitosis (upper) and late mitosis (bottom). Scale bars: 5 µm. (B) Timing of Cdc12–3×GFP recruitment to cytokinetic precursor nodes after SPB separation (time 0) in control (green, *n*=96) and Erg25 OE cells (orange, *n*=115). (C) Length of the Cdc12–3×GFP domain at initial time of recruitment in control (green, *n*=96) and Erg25 OE cells (orange, *n*=115). ***$P<10^{-10}$. (D) Maximum projections of confocal *z*-stacks showing the Cdc12–3×GFP, Rlc1–mCherry and Sid4–mCherry distribution in control (top) and Erg25 OE cells (bottom). Scale bars: 2 µm. (E) Time lapse images (min) of Cdc12–3×GFP in control (top) and Erg25 OE cells (bottom). Time 0 corresponds to the time of SPB separation. Scale bar: 5 µm. (F) Epifluorescence images of 3YFP–Cdc12, Rlc1–mCherry and Sid4–mCherry at the time of SPB separation in synchronized *cdc25-22* control (left), *mid1Δ* (center) and Erg25 OE cells (right). Scale bars: 5 µm.

cables, and quantitative analysis did not reveal a reduction in the mean number of F-actin cables per cell (Fig. 6A,B). This implies that F-actin cable assembly and stability are not impaired altogether in Erg25 OE cells, and that the formin For3 but also the profilin Cdc3 and the tropomyosin Cdc8, which are necessary for For3-dependent F-actin cable assembly (Balasubramanian et al., 1992, 1994), are not affected by increased ergosterol levels. This suggest that increased ergosterol levels may specifically inhibit the function of the mitotic formin Cdc12.

Since the assembly of F-actin cables by Cdc12 was shown to be in competition with the assembly of actin patches mediated by the Arp2/3 complex (Suarez et al., 2015), we further tested whether Cdc12 inhibition was responsible for Erg25 OE effects by blocking Arp2/3 function in Erg25 overexpressing cells with CK666, reasoning that it should rescue CR assembly. CK666 treatment was performed in cells expressing Lifeact–GFP as well as Rlc1–mCherry and Sid4–mCherry. In wild-type and Erg25 OE cells in interphase, we first observed as expected a fast disappearance of F-actin patches, and an accumulation of For3-dependent F-actin cables (Fig. 6A). Next, by looking at cells overexpressing Erg25 entering mitosis within 1 h of CK666 treatment, we observed an increase in the number of medially placed contractile rings as compared to what was seen in non-treated cells overexpressing Erg25 (Fig. 6C). This indicates that Arp2/3 inhibition can rescue the effect of Erg25 OE. Since Arp2/3 complex inhibition affects endocytosis, which may in turn alter membrane composition, we also verified ergosterol levels before and after CK666 treatment. While a mild reduction of ergosterol levels was detected in the control, high ergosterol levels were maintained 1 h after CK666 addition in Erg25 OE cells (Fig. S6). This rules out the possibility that the partial suppression of the Erg25 OE phenotype upon CK666 treatment is due to a reduction in the ergosterol amounts. Rather, by favouring actin availability for formin, due to the inhibition of Arp2/3, there is a partial rescue in the ability of Erg25 OE cells to assemble F-actin from cytokinetic precursors. Likewise, a small reduction in the number of abnormally placed contractile rings was

Journal of Cell Science (2019) 132, jcs227447. doi:10.1242/jcs.227447

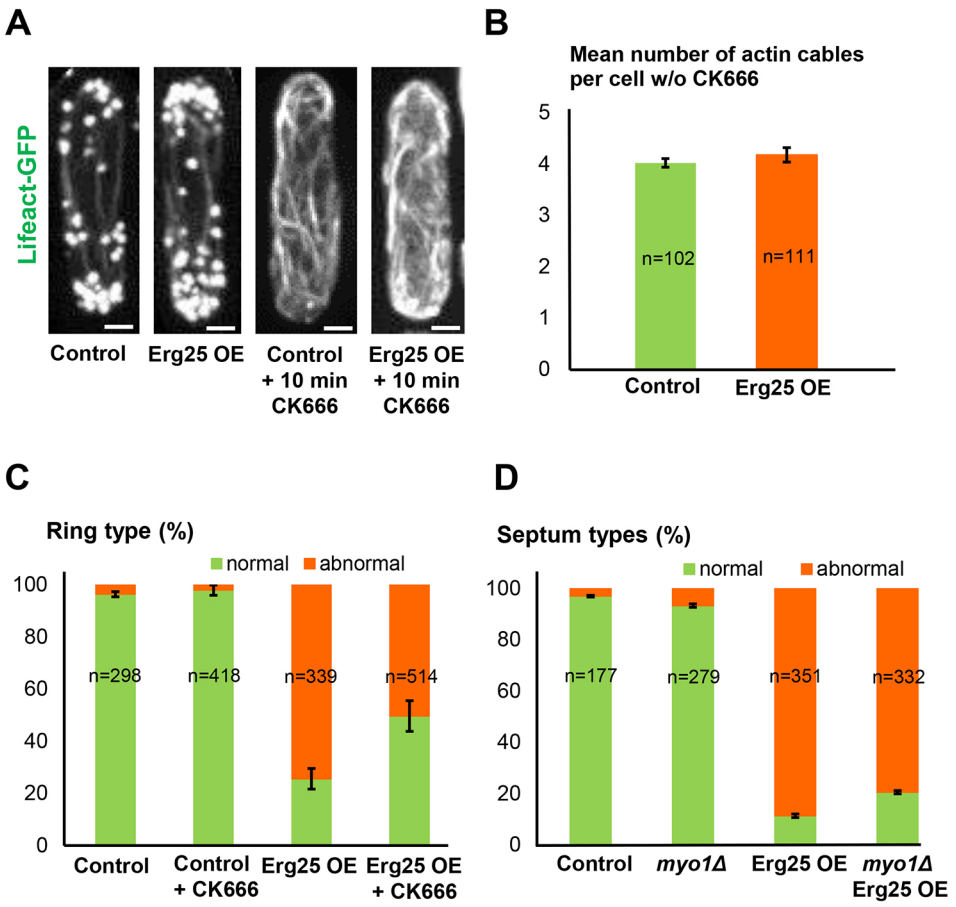

Fig. 6. Inhibition of the Arp2/3 complex by CK666 partially rescues the effects of Erg25 OE. (A) Lifeact–GFP fluorescence in control and Erg25 OE cells, 10 min after being treated or not with CK666. Maximum intensity projections of *z*-series acquired at 0.3 µm intervals. Scale bars: 5 µm. (B) Mean number of F-actin cables per interphase cell measured from maximum intensity projections in wild-type (*n*=102) and Erg25 OE cells (*n*=111). (C) Percentage of normal and abnormal rings assembled within 1 h after the addition or not of 100 µM CK666, as measured in time-lapse movies of control (*n*=298 w/o CK666 and *n*=418 with CK666) and Erg25 OE cells (*n*=339 w/o CK666 and *n*=514 with CK666). (D) Quantification of the percentage of normal and abnormal septum types as determined through Calcofluor staining in wild-type (*n*=177), Erg25 OE (*n*=279), *myo1Δ* (*n*=351) and Erg25 OE *myo1Δ* cells (*n*=332). All error bars represent s.d.

observed in the deletion mutant of Myo1 (Myo1 is known to act as an activator of Arp2/3 and also to organize sterol-rich domains) (Fig. 6D) (Lee et al., 2000; Sirotkin et al., 2005; Takeda and Chang, 2005). These experiments are in agreement with our hypothesis that increased ergosterol levels may inhibit the Cdc12-dependent assembly of F-actin cables from cytokinetic precursors.

DISCUSSION

Although Erg25 OE results in a similar phenotype to that seen upon the absence of the anillin-like protein Mid1, which blocks the recruitment of essential CR components to cytokinetic precursors, and that seen upon the deletion of reticulon-like proteins (tryΔ mutant), which transforms the subcortical reticular ER into cisternae, strikingly enough, neither of these pathways seems to be strongly affected by Erg25 OE.

Our results show that Erg25 OE results in a moderate delay in myosin II recruitment. Since neither Mid1 accumulation in medial nodes upon nuclear export, nor Rng2 recruitment were delayed, we can exclude that this results from a defect in Mid1 activation by Plo1 (Almonacid et al., 2011; Padmanabhan et al., 2011; Laporte et al., 2011). One hypothesis to explain this delay is that increasing ergosterol levels may create a lipid environment that alters the ability of myosin II to interact with Rng2.

Nevertheless, this short delay in myosin II recruitment cannot account for the strong division plane positioning defects. Accordingly, we observed another major phenotype upon Erg25 OE, consisting of an inhibition of Cdc12-dependent F-actin assembly from cytokinetic precursors in early mitosis. While we cannot exclude a reduction in the amounts recruited to cytokinetic precursors, the formin Cdc12 was always recruited to cytokinetic nodes at the proper time, i.e. ∼7 min after mitotic entry. However, cytokinetic precursors did not generate F-actin filaments. Importantly, analysing F-actin cables generated by the formin For3 during interphase ruled out a general effect of Erg25 OE on F-actin cable stability or on formins in general. Furthermore, the phenotype produced by increased ergosterol levels was partially rescued by inhibiting Arp2/3, which competes with the formin Cdc12 (Suarez et al., 2015). Taken together, these data suggest that high ergosterol levels may directly or indirectly affect the activity of the formin Cdc12.

In contrast to what is observed in *cdc12* mutants that only display randomly organized medial wisps of actin that are not able to condense into a ring structure (Chang et al., 1997, 1996), Erg25 overexpressing cells sometimes managed to assemble misshapen and mis-oriented contractile rings after a long delay, ranging from 20 to 40 min. This suggests that Erg25 OE may affect Cdc12 activity only transiently or partially, or that in late stages of cytokinesis, an activatory mechanism for Cdc12 can overcome the inhibition imposed on Cdc12 by increased ergosterol levels.

Cdc12 is an atypical formin that is not regulated by Rho-type GTPases or an auto-inhibitory domain (Yonetani et al., 2008; Bohnert et al., 2013). However, Cdc12 hyperactivity is lethal (Kovar et al., 2003), indicating that its function needs to be strictly controlled. Cdc12 is also subject to SIN-dependent regulation; the kinase Sid2 inhibits Cdc12 multimerization in order to properly assemble and maintain the CR (Bohnert et al., 2013; Willet et al., 2015b). Our results suggest that the lipid environment of Cdc12 at the plasma membrane could represent a novel mechanism to negatively regulate Cdc12 activity, and possibly also its level of recruitment.

How could the lipid composition of the plasma membrane regulate the activity of a formin? Previous work has revealed that the

localization and activity of the mammalian formin mDia1 is tuned by interactions with phospholipids (Ramalingam et al., 2010). This multidomain protein is able to bind to negatively charged phospholipids (PIP_2 and phosphatidylserine) through a basic domain located in the N-terminus of the protein, which mediates its recruitment at the plasma membrane, and an additional membrane-binding site in the C-terminal region has been shown to inhibit mDia1 F-actin polymerization activity (Ramalingam et al., 2010). This shows that the recruitment and the activation of formins are two distinct processes and that lipids can play an active role in both processes. Our results in fission yeast suggest that ergosterol levels may exert an inhibitory effect on Cdc12 by affecting its F-actin nucleation activity and possibly, its full recruitment to the cortex.

From the point of view of the PM composition homeostasis, it is legitimate to wonder whether increased levels of ergosterols have an impact in the composition or organization of other plasma membrane lipids. Indeed, ergosterols preferentially sort to the outer leaflet of the plasma membrane (Solanko et al., 2018), and their overproduction may affect the distribution of other membrane components on the inner leaflet of the plasma membrane. As mentioned above, PIP_2 plays important roles in cytokinesis. In our experiments using the PH domain of PLC1δ as a molecular probe for PIP_2, no major changes of this phospholipid could be detected upon Erg25 OE at the moment of ring assembly (our unpublished results). Although we cannot exclude the possibility that other lipids might affect cytokinesis, we favour the hypothesis that the defective ring assembly produced upon Erg25 OE is likely to be due to increased ergosterol levels per se.

Furthermore, tight-packed sphingolipid–sterol clusters prime lipid–lipid and lipid–protein interactions by sorting them according to their length and level of saturation (Simons and Ikonen, 1997; Simons and Toomre, 2000). In this way, SRDs organize the plasma membrane in dynamic microdomains that, by concentrating specific groups of proteins, can contribute to membrane and cytoskeleton changes. Strikingly, the F-BAR protein Cdc15 is both involved in the regulation of Cdc12 (Bohnert et al., 2013) and in the organization of a SRD at the division site in late cytokinesis (Takeda et al., 2004). This makes of Cdc15 a good candidate to link Cdc12 regulation to sterol concentration. Further work will then be necessary to determine whether and how Cdc15 could be involved in this process.

Finally, the physiological relevance of the negative regulation of cytokinetic F-actin cables assembly by ergosterol levels remains to be defined.

To conclude, we have shown that ergosterol levels at the plasma membrane can regulate Cdc12-dependent assembly of F-actin cables from cytokinetic precursors, a crucial step for the assembly of the cytokinetic ring. The molecular mechanisms by which ergosterol levels might regulate Cdc12 remain elusive at this stage. An interesting approach would be to turn to *in vitro* studies in presence of lipids to determine whether membrane lipids can directly influence Cdc12 activity. This would help us to understand the impact of membrane microenvironment on CR assembly. It will also be very interesting to determine whether our finding are relevant to animal cells, where formins play a key role in cytokinesis, and in other cellular processes where SRDs are also involved such as cell polarity or cell migration (Gomez-Mouton et al., 2001; Head et al., 2014; Mañes et al., 1999; Seveau et al., 2001).

MATERIALS AND METHODS

Strains and plasmids

Standard *S. pombe* media and genetic manipulations were used. All strains used in the study were isogenic to wild-type 972 and are described in Table S1. Strains from genetic crosses were selected by random spore germination and replica in plates with appropriate supplements or drugs.

For *erg25* overexpression, the plasmid pAF12, a derivative of pREP3x (Maundrell, 1993) was created by cloning the *erg25* open reading frame (ORF) between the SalI and BamHI sites of the vector polylinker. In parallel, we created pAF23, a modified pREP42X plasmid (Basi et al., 1993) in which the weaker *nmt1* promoter of pREP42X was replaced by the strongest *nmt1* promoter, by cloning it between SacI and PstI sites, upstream of the *erg25* ORF. All plasmids were checked by diagnostic PCR and restriction enzyme digestion, and the DNA fragments amplified by PCR were sequenced.

The *erg6*, *scs2* and *scs22* genes were deleted according to the method described in Bahler et al. (1998b). KanMX6- or NatMX6-resistant transformants were checked by PCR for correct DNA integration in the desired locus.

Transformations were performed by using the lithium-DTT method. 20 ml of exponentially growing cells [optical density at 600 nm (OD_{600}) of 0.5–0.8] were harvested by centrifugation (2500 ***g*** for 5 min) and washed with 10 mM Tris-HCl pH 7.4. After a second centrifugation (600 ***g*** for 1 min), they were re-suspended in 100 mM lithium acetate with 10 mM DTT and were incubated on an orbital wheel at room temperature for 40 min. 100 µl of these cells were mixed with 80 µl of 100 mM lithium acetate, 10 µl of single-stranded DNA from salmon testes (D9156-5ML, Sigma-Aldrich) and 2 µg of the desired plasmid or the purified PCR product. After 10 min of incubation on an orbital wheel, 300 µl of PEG 4000, previously diluted 1:1 in 100 mM lithium acetate, was added. After a second round of 10 min on the wheel, 15 µl of DMSO were added and the cells were subjected to heat shock at 42°C for 20 min in a water bath. Cells were then plated on selection plates. To induce Erg25 OE, cells were grown overnight at 25°C in EMM2S with 0.5 µg/ml thiamine. The following day, cells were washed three times with sterile water and were inoculated in EMM2S without thiamine for 24 h.

Live-cell imaging and microscopy

Epifluorescence images were taken on a DMRXA2 upright microscope (Leica Microsystems), equipped with a 100×1.4NA oil immersion PlanApo objective and a Coolsnap HQ CCD camera (Photometrics). Exposure times were 2 s for GFP, 1 s for mCherry and 10 ms for Calcofluor or filipin staining. To analyse Erg25–ENVY localization an exposure time of 500 ms for GFP was used.

To measure filipin intensity, a linescan throughout cells ranging from 11.5 to 13.5 µm in length was drawn according to the scheme shown in Fig. 1D.

For time-lapse imaging, 1 ml of exponentially growing cells were harvested by centrifugation (600 ***g*** for 1 min), the supernatant was discarded and 1 µl of the cells was deposited in a 2% YE5S agar pad at the center of PDMS slide chambers prepared as described in (Costa et al., 2013).

Time-lapse movies were acquired with an inverted Spinning Disc Confocal (Roper/Nikon), equipped with a Plan Apochromat 100×1.4 NA objective lens (Nikon), a PIFOC (perfect image focus) objective stepper, and a charge-coupled device camera (EMCCD 512×512 QuantEM; Photometrics). To analyse Cdr2–EGFP, Blt1–mEGFP, GFP–Cdc15 and F-actin, stacks of seven planes spaced at 1 µm apart were acquired every 1 min for 3 h (binning 1, 300 EM gain; 200 ms exposure with 6% laser power for GFP and 5.5% laser power for mCherry). For analysis of recruitment/enrichment of Mid1–mEGFP, 2mYFP–Rng2 and Cdc12–3XGFP similar movies of 1 h were acquired with a laser power of 8% for GFP.

All images were acquired and processed with MetaMorph 7.8 (Molecular Devices).

Analysis of the Cdr2–EGFP domain length was performed on single medial planes of images acquired with a spinning disc confocal microscope with 2 s exposure of 7% GFP laser power. The fluorescence intensity of Cdr2–EGFP was measured on maximal projections of *z*-stacks of seven planes spaced at 1 µm apart on a 40-pixel-long line along the medial cortex. Background fluorescence measured at the cell tips was then deduced.

To determine the Mid1–mEGFP and Cdr2–tagRFP cortical fluorescence intensity, stacks of seven planes spaced at 1µm apart were acquired (binning 1, 300 EM gain; 2 s exposure with 7% laser power for GFP and 7% laser power for mCherry). Intensity along a 100-pixel-long line on the medial cortex was measured on single medial focal planes taken with a spinning

disc confocal microscope. The percentage of Cdr2 nodes containing Mid1 was derived from linescans as the percentage of Cdr2 peaks corresponding to a Mid1 peak.

For myosin II intensity measurement, the strain containing Rlc1–mCherry and Sid4–GFP was imaged with a spinning disc confocal microscope, and stacks of seven planes spaced at 1 µm apart was acquired every 1 min for 3 h (binning 1, 300 EM gain; 100 ms exposure with 10% laser power for GFP and 5.5% laser power for mCherry). The Rlc1–mCherry signal was measured on maximal projection of 3D-stacks in a rectangle in the cell middle (scheme in Fig. S4C). Background measured at the cell tips was then deduced.

Calcofluor staining

Cell wall staining was performed by mixing 1 ml of early exponentially growing cells with 5 µl of 10 mg/ml Calcofluor (Fluorescent Brightener 28, F3543, Sigma). After washing the cells in 1 ml of PBS, 2 µl of the mix was deposited on slides for microscopy.

Miconazole treatment

Control and Erg25 OE cells were grown overnight in EMM2S with 15 µM thiamine to achieve exponential growth. Cells were washed three times with water and inoculated in EMM2S without thiamine to induce Erg25 OE for 22 h in the presence or absence of miconazole 1 µM before analysing septum morphology through Calcofluor staining.

Filipin staining

Filipin (F4767, Sigma-Aldrich) was dissolved in DMSO to create a stock at 5 mg/ml. Sterol staining was performed by adding 5 µl of the filipin stock to 1 ml of cell culture, and cells were observed immediately to avoid filipin internalization (Wachtler et al., 2003).

CK666 treatment

CK666 (SML0006, Sigma-Aldrich) was used at the final concentration of 100 µM from a 500× stock dissolved in DMSO. Cells with Lifeact–GFP marker were incubated with the drug and immediately imaged for 1 h with a spinning disc confocal microscopy (*z*-stacks of seven planes spaced by 1 µm were acquired every 1 min, binning 1, 300 EM gain; 200 ms exposure with 6% laser power for GFP and 5.5% laser power for mCherry).

The number of actin cables in interphase cells of 10.5 to 12.5 µm in length was measured 10 min after CK666 treatment from maximum intensity projections of confocal z-stack spanning the entire cell at 0.3 µm intervals (binning 1, 100 EM gain, 500 ms exposure with 25.5% laser power for GFP).

Statistical analysis

Sample size (*n*) is defined in each figure and is derived from three independent experiments. The error bars correspond to standard deviation (s.d.) between experiments and are specifically indicated in each figure. Throughout all figures, two-tailed *t*-test analysis on homoscedastic populations were applied: the significance of this statistical test is marked with asterisks, with $*P<0.05$, $**P<0.01$ and $***P<0.001$.

Acknowledgements

We thank Vincent Fraisier for maintenance of the microscope setups that were used in this study. Imaging was performed at PICT-IBISA (Institut Curie, Paris) which is part of France-Bioimaging national research infrastructure.

Competing interests

The authors declare no competing or financial interests.

Author contributions

Conceptualization: S.A.R., A.P.; Methodology: F.A., S.A.R., A.P.; Software: F.A.; Validation: F.A., S.A.R., A.P.; Formal analysis: F.A.; Investigation: F.A.; Resources: S.A.R., A.P.; Data curation: F.A.; Writing - original draft: F.A., S.A.R., A.P.; Writing - review & editing: S.A.R., A.P.; Visualization: F.A.; Supervision: S.A.R., A.P.; Project administration: S.A.R., A.P.; Funding acquisition: F.A.

Funding

This work was supported by a grant from Fondation ARC pour la Recherche sur le Cancer (PJA 20171206550) to A.P., which also provided a. received a fourth year PhD fellowship to F.A. A.P. is a member of the LabEx CelTisPhyBio.

Supplementary information

Supplementary information available online at
http://jcs.biologists.org/lookup/doi/10.1242/jcs.227447.supplemental

References

Akamatsu, M., Berro, J., Pu, K.-M., Tebbs, I. R. and Pollard, T. D. (2014). Cytokinetic nodes in fission yeast arise from two distinct types of nodes that merge during interphase. *J. Cell Biol.* **204**, 977-988. doi:10.1083/jcb.201307174

Akamatsu, M., Lin, Y., Bewersdorf, J. and Pollard, T. D. (2017). Analysis of interphase node proteins in fission yeast by quantitative and superresolution fluorescence microscopy. *Mol. Biol. Cell* **28**, 3203-3214. doi:10.1091/mbc.e16-07-0522

Almonacid, M., Moseley, J. B., Janvore, J., Mayeux, A., Fraisier, V., Nurse, P. and Paoletti, A. (2009). Spatial control of cytokinesis by Cdr2 kinase and Mid1/anillin nuclear export. *Curr. Biol.* **19**, 961-966. doi:10.1016/j.cub.2009.04.024

Almonacid, M., Celton-Morizur, S., Jakubowski, J. L., Dingli, F., Loew, D., Mayeux, A., Chen, J.-S., Gould, K. L., Clifford, D. M. and Paoletti, A. (2011). Temporal control of contractile ring assembly by Plo1 regulation of myosin II recruitment by Mid1/anillin. *Curr. Biol.* **21**, 473-479. doi:10.1016/j.cub.2011.02.003

Alvarez, F. J., Douglas, L. M. and Konopka, J. B. (2007). Sterol-rich plasma membrane domains in fungi. *Eukaryot. Cell* **6**, 755-763. doi:10.1128/EC.00008-07

Arasada, R. and Pollard, T. D. (2014). Contractile ring stability in S. pombe depends on F-BAR protein Cdc15p and Bgs1p transport from the Golgi complex. *Cell Rep* **8**, 1533-1544. doi:10.1016/j.celrep.2014.07.048

Atilla-Gokcumen, G. E., Muro, E., Relat-Goberna, J., Sasse, S., Bedigian, A., Coughlin, M. L., Garcia-Manyes, S. and Eggert, U. S. (2014). Dividing cells regulate their lipid composition and localization. *Cell* **156**, 428-439. doi:10.1016/j.cell.2013.12.015

Bahler, J., Steever, A. B., Wheatley, S., Wang, Y., Pringle, J. R., Gould, K. L. and McCollum, D. (1998a). Role of polo kinase and Mid1p in determining the site of cell division in fission yeast. *J. Cell Biol.* **143**, 1603-1616. doi:10.1083/jcb.143.6.1603

Bahler, J., Wu, J. Q., Longtine, M. S., Shah, N. G., McKenzie, A., III, Steever, A. B., Wach, A., Philippsen, P. and Pringle, J. R. (1998b). Heterologous modules for efficient and versatile PCR-based gene targeting in Schizosaccharomyces pombe. *Yeast* **14**, 943-951. doi:10.1002/(SICI)1097-0061(199807)14:10<943::AID-YEA292>3.0.CO;2-Y

Baird, D., Stefan, C., Audhya, A., Weys, S. and Emr, S. D. (2008). Assembly of the PtdIns 4-kinase Stt4 complex at the plasma membrane requires Ypp1 and Efr3. *J. Cell Biol.* **183**, 1061-1074. doi:10.1083/jcb.200804003

Balasubramanian, M. K., Helfman, D. M. and Hemmingsen, S. M. (1992). A new tropomyosin essential for cytokinesis in the fission yeast S. pombe. *Nature* **360**, 84-87. doi:10.1038/360084a0

Balasubramanian, M. K., Hirani, B. R., Burke, J. D. and Gould, K. L. (1994). The Schizosaccharomyces pombe cdc3+ gene encodes a profilin essential for cytokinesis. *J. Cell Biol.* **125**, 1289-1301. doi:10.1083/jcb.125.6.1289

Bard, M., Bruner, D. A., Pierson, C. A., Lees, N. D., Biermann, B., Frye, L., Koegel, C. and Barbuch, R. (1996). Cloning and characterization of ERG25, the Saccharomyces cerevisiae gene encoding C-4 sterol methyl oxidase. *Proc. Natl. Acad. Sci. USA* **93**, 186-190. doi:10.1073/pnas.93.1.186

Basi, G., Schmid, E. and Maundrell, K. (1993). TATA box mutations in the Schizosaccharomyces pombe nmt1 promoter affect transcription efficiency but not the transcription start point or thiamine repressibility. *Gene* **123**, 131-136. doi:10.1016/0378-1119(93)90552-E

Bohnert, K. A., Grzegorzewska, A. P., Willet, A. H., Vander Kooi, C. W., Kovar, D. R. and Gould, K. L. (2013). SIN-dependent phosphoinhibition of formin multimerization controls fission yeast cytokinesis. *Genes Dev.* **27**, 2164-2177. doi:10.1101/gad.224154.113

Carnahan, R. H. and Gould, K. L. (2003). The PCH family protein, Cdc15p, recruits two F-actin nucleation pathways to coordinate cytokinetic actin ring formation in Schizosaccharomyces pombe. *J. Cell Biol.* **162**, 851-862. doi:10.1083/jcb.200305012

Cauvin, C. and Echard, A. (2015). Phosphoinositides: lipids with informative heads and mastermind functions in cell division. *Biochim. Biophys. Acta* **1851**, 832-843. doi:10.1016/j.bbalip.2014.10.013

Celton-Morizur, S., Bordes, N., Fraisier, V., Tran, P. T. and Paoletti, A. (2004). C-terminal anchoring of mid1p to membranes stabilizes cytokinetic ring position in early mitosis in fission yeast. *Mol. Cell. Biol.* **24**, 10621-10635. doi:10.1128/MCB.24.24.10621-10635.2004

Celton-Morizur, S., Racine, V., Sibarita, J.-B. and Paoletti, A. (2006). Pom1 kinase links division plane position to cell polarity by regulating Mid1p cortical distribution. *J. Cell Sci.* **119**, 4710-4718. doi:10.1242/jcs.03261

Chang, F., Woollard, A. and Nurse, P. (1996). Isolation and characterization of fission yeast mutants defective in the assembly and placement of the contractile actin ring. *J. Cell Sci.* **109**, 131-142.

Chang, F., Drubin, D. and Nurse, P. (1997). cdc12p, a protein required for cytokinesis in fission yeast, is a component of the cell division ring and interacts with profilin. *J. Cell Biol.* **137**, 169-182. doi:10.1083/jcb.137.1.169

Coffman, V. C., Nile, A. H., Lee, I.-J., Liu, H. and Wu, J.-Q. (2009). Roles of formin nodes and myosin motor activity in Mid1p-dependent contractile-ring assembly during fission yeast cytokinesis. *Mol. Biol. Cell* **20**, 5195-5210. doi:10.1091/mbc.e09-05-0428

Coffman, V. C., Sees, J. A., Kovar, D. R. and Wu, J.-Q. (2013). The formins Cdc12 and For3 cooperate during contractile ring assembly in cytokinesis. *J. Cell Biol.* **203**, 101-114. doi:10.1083/jcb.201305022

Costa, J., Fu, C., Syrovatkina, V. and Tran, P. T. (2013). Imaging individual spindle microtubule dynamics in fission yeast. *Methods Cell Biol.* **115**, 385-394. doi:10.1016/B978-0-12-407757-7.00024-4

Dambournet, D., Machicoane, M., Chesneau, L., Sachse, M., Rocancourt, M., El Marjou, A., Formstecher, E., Salomon, R., Goud, B. and Echard, A. (2011). Rab35 GTPase and OCRL phosphatase remodel lipids and F-actin for successful cytokinesis. *Nat. Cell Biol.* **13**, 981-988. doi:10.1038/ncb2279

Echard, A. (2012). Phosphoinositides and cytokinesis: the "PIP" of the iceberg. *Cytoskeleton* **69**, 893-912. doi:10.1002/cm.21067

Echard, A. and Burgess, D. (2014). The changing lipidome during cell division. *Cell* **156**, 394-395. doi:10.1016/j.cell.2014.01.018

Feierbach, B. and Chang, F. (2001). Roles of the fission yeast formin for3p in cell polarity, actin cable formation and symmetric cell division. *Curr. Biol.* **11**, 1656-1665. doi:10.1016/S0960-9822(01)00525-5

Feoktistova, A., Magnelli, P., Abeijon, C., Perez, P., Lester, R. L., Dickson, R. C. and Gould, K. L. (2001). Coordination between fission yeast glucan formation and growth requires a sphingolipase activity. *Genetics* **158**, 1397-1411.

Fujiwara, T., Bandi, M., Nitta, M., Ivanova, E. V., Bronson, R. T. and Pellman, D. (2005). Cytokinesis failure generating tetraploids promotes tumorigenesis in p53-null cells. *Nature* **437**, 1043-1047. doi:10.1038/nature04217

Gomez-Mouton, C., Abad, J. L., Mira, E., Lacalle, R. A., Gallardo, E., Jimenez-Baranda, S., Illa, I., Bernad, A., Manes, S. and Martinez-A, C. (2001). Segregation of leading-edge and uropod components into specific lipid rafts during T cell polarization. *Proc. Natl. Acad. Sci. USA* **98**, 9642-9647. doi:10.1073/pnas.171160298

Goss, J. W., Kim, S., Bledsoe, H. and Pollard, T. D. (2014). Characterization of the roles of Blt1p in fission yeast cytokinesis. *Mol. Biol. Cell* **25**, 1946-1957. doi:10.1091/mbc.e13-06-0300

Guzman-Vendrell, M., Baldissard, S., Almonacid, M., Mayeux, A., Paoletti, A. and Moseley, J. B. (2013). Blt1 and Mid1 provide overlapping membrane anchors to position the division plane in fission yeast. *Mol. Cell. Biol.* **33**, 418-428. doi:10.1128/MCB.01286-12

Head, B. P., Patel, H. H. and Insel, P. A. (2014). Interaction of membrane/lipid rafts with the cytoskeleton: impact on signaling and function. *Biochim. Biophys. Acta* **1838**, 532-545. doi:10.1016/j.bbamem.2013.07.018

Huang, J., Huang, Y., Yu, H., Subramanian, D., Padmanabhan, A., Thadani, R., Tao, Y., Tang, X., Wedlich-Soldner, R. and Balasubramanian, M. K. (2012). Nonmedially assembled F-actin cables incorporate into the actomyosin ring in fission yeast. *J. Cell Biol.* **199**, 831-847. doi:10.1083/jcb.201209044

Iwaki, T., Iefuji, H., Hiraga, Y., Hosomi, A., Morita, T., Giga-Hama, Y. and Takegawa, K. (2008). Multiple functions of ergosterol in the fission yeast Schizosaccharomyces pombe. *Microbiology* **154**, 830-841. doi:10.1099/mic.0.2007/011155-0

Jacquier, N. and Schneiter, R. (2012). Mechanisms of sterol uptake and transport in yeast. *J. Steroid Biochem. Mol. Biol.* **129**, 70-78. doi:10.1016/j.jsbmb.2010.11.014

Jourdain, I., Brzezińska, E. A. and Toda, T. (2013). Fission yeast Nod1 is a component of cortical nodes involved in cell size control and division site placement. *PLoS ONE* **8**, e54142. doi:10.1371/journal.pone.0054142

Kovar, D. R., Kuhn, J. R., Tichy, A. L. and Pollard, T. D. (2003). The fission yeast cytokinesis formin Cdc12p is a barbed end actin filament capping protein gated by profilin. *J. Cell Biol.* **161**, 875-887. doi:10.1083/jcb.200211078

Lacroix, B. and Maddox, A. S. (2012). Cytokinesis, ploidy and aneuploidy. *J. Pathol.* **226**, 338-351. doi:10.1002/path.3013

Laporte, D., Coffman, V. C., Lee, I.-J. and Wu, J.-Q. (2011). Assembly and architecture of precursor nodes during fission yeast cytokinesis. *J. Cell Biol.* **192**, 1005-1021. doi:10.1083/jcb.201008171

Lee, W.-L., Bezanilla, M. and Pollard, T. D. (2000). Fission yeast myosin-I, Myo1p, stimulates actin assembly by Arp2/3 complex and shares functions with WASp. *J. Cell Biol.* **151**, 789-800. doi:10.1083/jcb.151.4.789

Löffler, J., Kelly, S. L., Hebart, H., Schumacher, U., Lass-Florl, C. and Einsele, H. (1997). Molecular analysis of cyp51 from fluconazole-resistant Candida albicans strains. *FEMS Microbiol. Lett.* **151**, 263-268. doi:10.1016/S0378-1097(97)00172-9

Makushok, T., Alves, P., Huisman, S. M., Kijowski, A. R. and Brunner, D. (2016). Sterol-rich membrane domains define fission yeast cell polarity. *Cell* **165**, 1182-1196. doi:10.1016/j.cell.2016.04.037

Mañes, S., Mira, E., Gómez-Moutón, C., Lacalle, R. A., Keller, P., Labrador, J. P. and Martinez, A. C. (1999). Membrane raft microdomains mediate front-rear polarity in migrating cells. *EMBO J.* **18**, 6211-6220. doi:10.1093/emboj/18.22.6211

Marichal, P., Gorrens, J., Laurijssens, L., Vermuyten, K., Van Hove, C., Le Jeune, L., Verhasselt, P., Sanglard, D., Borgers, M., Ramaekers, F. C. S. et al. (1999). Accumulation of 3-ketosteroids induced by itraconazole in azole-resistant clinical Candida albicans isolates. *Antimicrob. Agents Chemother.* **43**, 2663-2670. doi:10.1128/AAC.43.11.2663

Martin, S. G. and Berthelot-Grosjean, M. (2009). Polar gradients of the DYRK-family kinase Pom1 couple cell length with the cell cycle. *Nature* **459**, 852-856. doi:10.1038/nature08054

Matsuo, Y., Fisher, E., Patton-Vogt, J. and Marcus, S. (2007). Functional characterization of the fission yeast phosphatidylserine synthase gene, pps1, reveals novel cellular functions for phosphatidylserine. *Eukaryot. Cell* **6**, 2092-2101. doi:10.1128/EC.00300-07

Maundrell, K. (1993). Thiamine-repressible expression vectors pREP and pRIP for fission yeast. *Gene* **123**, 127-130. doi:10.1016/0378-1119(93)90551-D

Moseley, J. B., Mayeux, A., Paoletti, A. and Nurse, P. (2009). A spatial gradient coordinates cell size and mitotic entry in fission yeast. *Nature* **459**, 857-860. doi:10.1038/nature08074

Ojkic, N., Wu, J.-Q. and Vavylonis, D. (2011). Model of myosin node aggregation into a contractile ring: the effect of local alignment. *J. Phys. Condens Matter* **23**, 374103. doi:10.1088/0953-8984/23/37/374103

Padmanabhan, A., Bakka, K., Sevugan, M., Naqvi, N. I., D'Souza, V., Tang, X., Mishra, M. and Balasubramanian, M. K. (2011). IQGAP-related Rng2p organizes cortical nodes and ensures position of cell division in fission yeast. *Curr. Biol.* **21**, 467-472. doi:10.1016/j.cub.2011.01.059

Padte, N. N., Martin, S. G., Howard, M. and Chang, F. (2006). The cell-end factor pom1p inhibits mid1p in specification of the cell division plane in fission yeast. *Curr. Biol.* **16**, 2480-2487. doi:10.1016/j.cub.2006.11.024

Paoletti, A. and Chang, F. (2000). Analysis of mid1p, a protein required for placement of the cell division site, reveals a link between the nucleus and the cell surface in fission yeast. *Mol. Biol. Cell* **11**, 2757-2773. doi:10.1091/mbc.11.8.2757

Pollard, T. D. and Wu, J.-Q. (2010). Understanding cytokinesis: lessons from fission yeast. *Nat. Rev. Mol. Cell Biol.* **11**, 149-155. doi:10.1038/nrm2834

Rajendran, L. and Simons, K. (2005). Lipid rafts and membrane dynamics. *J. Cell Sci.* **118**, 1099-1102. doi:10.1242/jcs.01681

Ramalingam, N., Zhao, H., Breitsprecher, D., Lappalainen, P., Faix, J. and Schleicher, M. (2010). Phospholipids regulate localization and activity of mDia1 formin. *Eur. J. Cell Biol.* **89**, 723-732. doi:10.1016/j.ejcb.2010.06.001

Riedl, J., Crevenna, A. H., Kessenbrock, K., Yu, J. H., Neukirchen, D., Bista, M., Bradke, F., Jenne, D., Holak, T. A., Werb, Z. et al. (2008). Lifeact: a versatile marker to visualize F-actin. *Nat. Methods* **5**, 605-607. doi:10.1038/nmeth.1220

Rincon, S. A. and Paoletti, A. (2016). Molecular control of fission yeast cytokinesis. *Semin. Cell Dev. Biol.* **53**, 28-38. doi:10.1016/j.semcdb.2016.01.007

Rincon, S. A., Bhatia, P., Bicho, C., Guzman-Vendrell, M., Fraisier, V., Borek, W. E., Alves, F. L., Dingli, F., Loew, D., Rappsilber, J. et al. (2014). Pom1 regulates the assembly of Cdr2-Mid1 cortical nodes for robust spatial control of cytokinesis. *J. Cell Biol.* **206**, 61-77. doi:10.1083/jcb.201311097

Rincon, S. A., Estravis, M., Dingli, F., Loew, D., Tran, P. T. and Paoletti, A. (2017). SIN-Dependent Dissociation of the SAD Kinase Cdr2 from the Cell Cortex Resets the Division Plane. *Curr. Biol.* **27**, 534-542. doi:10.1016/j.cub.2016.12.050

Rippon, W. J. and Fromtling, A. R. (1993). *Cutaneous Antifungal Agents: Selected Compounds in Clinical Practice and Development*. New York: M. Dekker.

Sanglard, D., Ischer, F., Koymans, L. and Bille, J. (1998). Amino acid substitutions in the cytochrome P-450 lanosterol 14alpha-demethylase (CYP51A1) from azole-resistant Candida albicans clinical isolates contribute to resistance to azole antifungal agents. *Antimicrob. Agents Chemother.* **42**, 241-253.

Seveau, S., Eddy, R. J., Maxfield, F. R. and Pierini, L. M. (2001). Cytoskeleton-dependent membrane domain segregation during neutrophil polarization. *Mol. Biol. Cell* **12**, 3550-3562. doi:10.1091/mbc.12.11.3550

Sheehan, D. J., Hitchcock, C. A. and Sibley, C. M. (1999). Current and emerging azole antifungal agents. *Clin. Microbiol. Rev.* **12**, 40-79. doi:10.1128/CMR.12.1.40

Simons, K. and Ikonen, E. (1997). Functional rafts in cell membranes. *Nature* **387**, 569-572. doi:10.1038/42408

Simons, K. and Toomre, D. (2000). Lipid rafts and signal transduction. *Nat. Rev. Mol. Cell Biol.* **1**, 31-39. doi:10.1038/35036052

Sirotkin, V., Beltzner, C. C., Marchand, J.-B. and Pollard, T. D. (2005). Interactions of WASp, myosin-I, and verprolin with Arp2/3 complex during actin patch assembly in fission yeast. *J. Cell Biol.* **170**, 637-648. doi:10.1083/jcb.200502053

Slubowski, C. J., Funk, A. D., Roesner, J. M., Paulissen, S. M. and Huang, L. S. (2015). Plasmids for C-terminal tagging in Saccharomyces cerevisiae that contain improved GFP proteins, Envy and Ivy. *Yeast* **32**, 379-387. doi:10.1002/yea.3065

Snider, C. E., Willet, A. H., Chen, J.-S., Arpağ, G., Zanic, M. and Gould, K. L. (2017). Phosphoinositide-mediated ring anchoring resists perpendicular forces to promote medial cytokinesis. *J. Cell Biol.* **216**, 3041-3050. doi:10.1083/jcb.201705070

Snider, C. E., Willet, A. H., Brown, H. S. T. and Gould, K. L. (2018). Analysis of the contribution of phosphoinositides to medial septation in fission yeast highlights the importance of PI(4,5)P2 for medial contractile ring anchoring. *Mol. Biol. Cell* **29**, 2148-2155. doi:10.1091/mbc.E18-03-0179

Sohrmann, M., Fankhauser, C., Brodbeck, C. and Simanis, V. (1996). The dmf1/mid1 gene is essential for correct positioning of the division septum in fission yeast. *Genes Dev.* **10**, 2707-2719. doi:10.1101/gad.10.21.2707

Solanko, L. M., Sullivan, D. P., Sere, Y. Y., Szomek, M., Lunding, A., Solanko, K. A., Pizovic, A., Stanchev, L. D., Pomorski, T. G., Menon, A. K. et al. (2018). Ergosterol is mainly located in the cytoplasmic leaflet of the yeast plasma membrane. *Traffic* **19**, 198-214. doi:10.1111/tra.12545

Storchova, Z. and Pellman, D. (2004). From polyploidy to aneuploidy, genome instability and cancer. *Nat. Rev. Mol. Cell Biol.* **5**, 45-54. doi:10.1038/nrm1276

Suarez, C., Carroll, R. T., Burke, T. A., Christensen, J. R., Bestul, A. J., Sees, J. A., James, M. L., Sirotkin, V. and Kovar, D. R. (2015). Profilin regulates F-actin network homeostasis by favoring formin over Arp2/3 complex. *Dev. Cell* **32**, 43-53. doi:10.1016/j.devcel.2014.10.027

Takaine, M., Numata, O. and Nakano, K. (2014). Fission yeast IQGAP maintains F-actin-independent localization of myosin-II in the contractile ring. *Genes Cells* **19**, 161-176. doi:10.1111/gtc.12120

Takeda, T. and Chang, F. (2005). Role of fission yeast myosin I in organization of sterol-rich membrane domains. *Curr. Biol.* **15**, 1331-1336. doi:10.1016/j.cub.2005.07.009

Takeda, T., Kawate, T. and Chang, F. (2004). Organization of a sterol-rich membrane domain by cdc15p during cytokinesis in fission yeast. *Nat. Cell Biol.* **6**, 1142-1144. doi:10.1038/ncb1189

Vavylonis, D., Wu, J.-Q., Hao, S., O'Shaughnessy, B. and Pollard, T. D. (2008). Assembly mechanism of the contractile ring for cytokinesis by fission yeast. *Science* **319**, 97-100. doi:10.1126/science.1151086

Wachtler, V., Rajagopalan, S. and Balasubramanian, M. K. (2003). Sterol-rich plasma membrane domains in the fission yeast Schizosaccharomyces pombe. *J. Cell Sci.* **116**, 867-874. doi:10.1242/jcs.00299

Willet, A. H., McDonald, N. A., Bohnert, K. A., Baird, M. A., Allen, J. R., Davidson, M. W. and Gould, K. L. (2015a). The F-BAR Cdc15 promotes contractile ring formation through the direct recruitment of the formin Cdc12. *J. Cell Biol.* **208**, 391-399. doi:10.1083/jcb.201411097

Willet, A. H., McDonald, N. A. and Gould, K. L. (2015b). Regulation of contractile ring formation and septation in Schizosaccharomyces pombe. *Curr. Opin. Microbiol.* **28**, 46-52. doi:10.1016/j.mib.2015.08.001

Wu, J.-Q., Kuhn, J. R., Kovar, D. R. and Pollard, T. D. (2003). Spatial and temporal pathway for assembly and constriction of the contractile ring in fission yeast cytokinesis. *Dev. Cell* **5**, 723-734. doi:10.1016/S1534-5807(03)00324-1

Wu, J.-Q., Sirotkin, V., Kovar, D. R., Lord, M., Beltzner, C. C., Kuhn, J. R. and Pollard, T. D. (2006). Assembly of the cytokinetic contractile ring from a broad band of nodes in fission yeast. *J. Cell Biol.* **174**, 391-402. doi:10.1083/jcb.200602032

Ye, Y., Lee, I.-J., Runge, K. W. and Wu, J.-Q. (2012). Roles of putative Rho-GEF Gef2 in division-site positioning and contractile-ring function in fission yeast cytokinesis. *Mol. Biol. Cell* **23**, 1181-1195. doi:10.1091/mbc.e11-09-0800

Yonetani, A., Lustig, R. J., Moseley, J. B., Takeda, T., Goode, B. L. and Chang, F. (2008). Regulation and targeting of the fission yeast formin cdc12p in cytokinesis. *Mol. Biol. Cell* **19**, 2208-2219. doi:10.1091/mbc.e07-07-0731

Zhang, D., Vjestica, A. and Oliferenko, S. (2010). The cortical ER network limits the permissive zone for actomyosin ring assembly. *Curr. Biol.* **20**, 1029-1034. doi:10.1016/j.cub.2010.04.017

Zhang, D., Vjestica, A. and Oliferenko, S. (2012). Plasma membrane tethering of the cortical ER necessitates its finely reticulated architecture. *Curr. Biol.* **22**, 2048-2052. doi:10.1016/j.cub.2012.08.047

Zhu, Y.-H., Ye, Y., Wu, Z. and Wu, J.-Q. (2013). Cooperation between Rho-GEF Gef2 and its binding partner Nod1 in the regulation of fission yeast cytokinesis. *Mol. Biol. Cell* **24**, 3187-3204. doi:10.1091/mbc.e13-06-0301

Table S1. Table of strains used in this study.

Strain	Genotype	Source or reference
	Figure 1	
AP240	*ade6-M210 ura4-D18 leu1-32 h-*	Laboratory collection
AP5400	*AP240 + pAF12 (pREP3X-Erg25) ade6-M210 ura4-D18 leu1-32*	This study
	Figure 2	
AP5507	*cdr2-EGFP:kanMX6, rlc1-mcherry:natMX6, sid4-mcherry:hphMX6 ade6-M210 ura4-D18 leu1-32*	This study
AP5511	*cdr2-EGFP:kanMX6, rlc1-mcherry:natMX6, sid4-mcherry:hphMX6 + pAF12 (pREP3X-Erg25) ade6-M210 ura4-D18 leu1-32*	This study
AP5718	*blt1-mEGFP:kanMX6, rlc1-mcherry:natMX6, sid4-mcherry:hphMX6 ade6-M210 ura4-D18 leu1-32*	This study
AP5741	*blt1-mEGFP:kanMX6, rlc1-mcherry:natMX6, sid4-mcherry:hphMX6 + pAF12 (pREP3X- Erg25) ade6-M210 ura4-D18 leu1-32*	This study
	Figure 3	
AP5802	*Pact1-lifeact-GFP:leu1+, rlc1-mcherry:Nat, sid4-mcherry:hphMX6 ade6-M210 ura4-D18 leu1-32*	Laboratory collection
AP5806	*Pact1-lifeact-GFP:leu1+, rlc1-mcherry:natMX6, sid4-mcherry:hphMX6 + pAF23 (pREP42X- Erg25) ade6-M210 ura4-D18 leu1-32*	This study
	Figure 4 and Figure S5	
AP5595	*mid1-mEGFP:kanMX6, rlc1-mcherry:natMX6, sid4-mcherry:hphMX6 ade6- ura4-D18 leu1-32*	This study
AP5621	*mid1-mEGFP:kanMX6, rlc1-mcherry:natMX6, sid4-mcherry:hphMX6 + pAF12 (pREP3X- Erg25) ade6- ura4-D18 leu1-32*	This study
AP5629	*2mYFP-rng2:ura4+, rlc1-mcherry:natMX6, sid4-mcherry:hphMX6 ade6- ura4-D18 leu1-32*	This study
AP5665	*2mYFP-rng2:ura4+, rlc1-mcherry:natMX6, sid4-mcherry:hphMX6 + pAF12 (pREP3X- Erg25) ade6-ura4-D18 leu1-32*	This study

AP5598	*GFP-cdc15:kanMX6, rlc1-mcherry:natMX6, sid4-mcherry:hphMX6 ade6- ura4-D18 leu1-32*	This study
AP5640	*GFP-cdc15:kanMX6, rlc1-mcherry:natMX6, sid4-mcherry:hphMX6 + pAF12 (pREP3X- Erg25) ade6-ura4-D18 leu1-32*	This study
	Figure 5	
AP5601	*cdc12-3YFP:kanMX6, rlc1-mcherry:natMX6, sid4-mcherry:hphMX6 ade6-M210 ura4-D18 leu1-32*	This study
AP5635	*cdc12-3YFP:kanMX6, rlc1-mcherry:natMX6, sid4-mcherry:hphMX6 + pAF12 (pREP3X- Erg25) ade6-M210 ura4-D18 leu1-32*	This study
AP6183	*cdc12-3XGFP:kanMX6, rlc1-mcherry:kanMX6, sid4-mcherry:hphMX6 ade6-M210 ura4-D18 leu1-32*	From Bohnert et al., 2013 (KG15568)
AP6193	*cdc12-3XGFP:kanMX6, rlc1-mcherry:kanMX6, sid4-mcherry:hphMX6 + pAF12 (pREP3X-Erg25)ade6-M210 ura4-D18 leu1-32*	This study
AP6129	*cdc12-3YFP:kanMX6, rlc1-mcherry:natMX6, sid4-mcherry:hphMX6 cdc25-22 ade6-M210 ura4-D18 leu1-32*	This study
AP6145	*cdc12-3YFP:kanMX6, rlc1-mcherry:natMX6, sid4-mcherry:hphMX6 cdc25-22 + pAF12 (pREP3X-Erg25) ade6-M210 ura4-D18 leu1-32*	This study
AP6166	*cdc12-3YFP:kanMX6, rlc1-mcherry:natMX6, sid4-mcherry:hphMX6 cdc25-22 mid1::ura4^{+} ade6-M210 ura4-D18 leu1-32*	This study
	Figure 6	
AP5802	*Pact1-lifeact-GFP:leu1+, rlc1-mcherry:natMX6, sid4-mcherry:hphMX6 ade6-M210 ura4-D18 leu1-32*	Laboratory collection
AP5806	*Pact1-lifeact-GFP:leu1+, rlc1-mcherry:natMX6, sid4-mcherry:hphMX6 + pAF23 (pREP42X- Erg25) ade6-M210 ura4-D18 leu1-32*	This study
AP240	*ade6-M210 ura4-D18 leu1-32 h-*	Laboratory collection
AP5400	*AP240 + pAF12 (pREP3X- Erg25) ade6-M210 ura4-D18 leu1-32*	This study
TP1032	*myo1::kanMX6 h- ade6-M210 leu1-32*	from Riken Institute (FY13570)
AP5894	*myo1::kanMX6 + pAF12 (pREP3X-Erg25) ade6-M210 leu1-32*	This study
	Figure S1	

AP240	*ade6-M210 ura4-D18 leu1-32 h-*	Laboratory collection
AP5400	*AP240 + pAF12 (pREP3X-Erg25) ade6-M210 ura4-D18 leu1-32*	This study
AP5323	*erg6Δ::kanMX6 ade6-M210 ura4-D18 leu1-32*	This study
AP5724	*erg6Δ::kanMX6 + pAF12 (pREP3X-Erg25) ade6-M210 ura4-D18 leu1-32*	This study
AP5716	*erg25-ENVY:kanMX6 ade6-M210 ura4-D18 leu1-32*	This study
AP5770	*erg25-ENVY:kanMX6, (SPAC1B2.03c)ER-marker-mcherry:natMX6 ade6-M210 ura4-D18 leu1-32*	This study
AP5790	*erg25-ENVY:kanMX6, rlc1-mcherry:natMX6, sid4-mcherry:hphMX6 + pAF12 (pREP3X-Erg25) ade6-M210 ura4-D18 leu1-32*	This study
AP5808	*scs2Δ::kanMX6 ade6-M210 ura4-D18 leu1-32*	This study
AP5843	*scs2Δ::kanMX6 + pAF12 (pREP3X-Erg25) ade6-M210 ura4-D18 leu1-32*	This study
AP5785	*scs22Δ::kanMX6 ade6-M210 ura4-D18 leu1-32*	This study
AP5793	*scs22Δ::kanMX6 + pAF12 (pREP3X-Erg25) ade6-M210 ura4-D18 leu1-32*	This study
AP5837	*scs22Δ::kanMX6, scs2Δ::natMX6 ade6-M210 ura4-D18 leu1-32*	This study
AP5847	*scs22Δ::kanMx6, scs2Δ::natMX6 + pAF12 (pREP3X-Erg25) ade6-M210 ura4-D18 leu1-32*	This study
	Figure S2	
AP5507	*cdr2-EGFP:kanMX6, rlc1-mcherry:natMX6, sid4-mcherry:hphMX6 ade6-M210 ura4-D18 leu1-32*	This study
AP5511	*cdr2-EGFP:kanMX6, rlc1-mcherry:natMX6, sid4-mcherry:hphMX6 + pAF12 (pREP3X-Erg25) ade6-M210 ura4-D18 leu1-32*	This study
AP3788	*cdr2-tagRFP:natMX6 mid1-mEGFP:kanMX6 ade6-M210 ura4-D18 leu1-32*	Laboratory collection
AP6094	*cdr2-tagRFP:natMX6 mid1-mEGFP:kanMX6+ pAF12 (pREP3X-Erg25) ade6-M210 ura4-D18 leu1-32*	This study
	Figure S3	
AP6184	sid4-GFP:kanMX6, rlc1-mcherry:NatMX6 *ade6-M210 ura4-D18 leu1-32*	This study
AP6155	sid4-GFP:kanMX6, rlc1-mcherry:NatMX6 *+ pAF12 (pREP3X-Erg25) ade6-M210 ura4-D18 leu1-32*	This study
	Figure S4 and S6	

AP5802	*Pact1-lifeact-GFP:leu1+, rlc1-mcherry:natMX6, sid4-mcherry:hphMX6 ade6-M210 ura4-D18 leu1-32*	Laboratory collection
AP5806	*Pact1-lifeact-GFP:leu1+, rlc1-mcherry:natMX6, sid4-mcherry:hphMX6 + pAF23 (pREP42X- Erg25) ade6-M210 ura4-D18 leu1-32*	This study

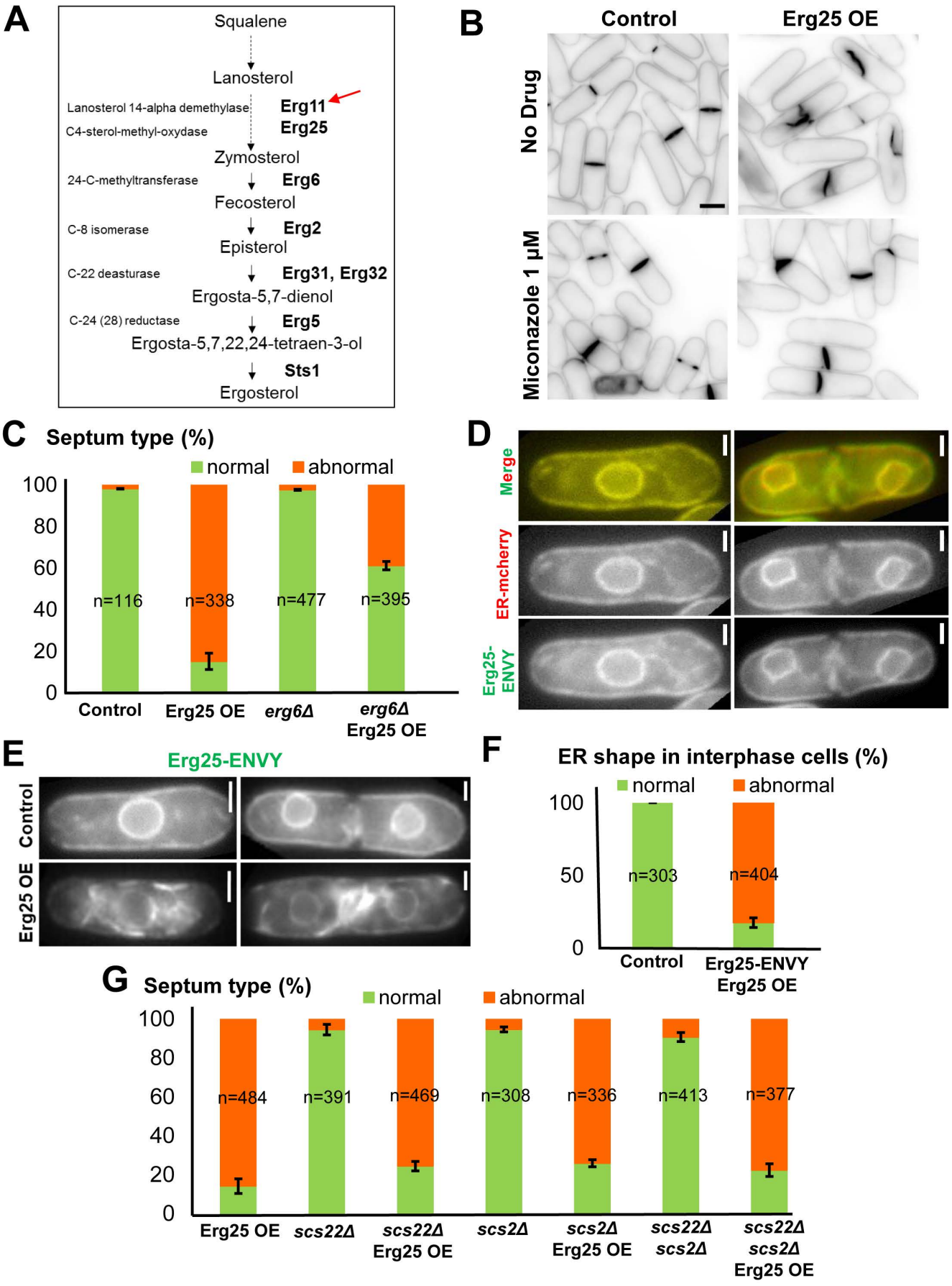

Figure S1. Cytokinetic defects induced by Erg25 OE require an active sterol biosynthetic pathway, while Erg25 affects ER organization with little impact on division plane positioning.

A: Schematic representation of the late stages of ergosterol biosynthetic pathway in *S. pombe* deduced from *S. cerevisiae* (adapted from Iwaki et al., 2008). The red arrow indicates at which level of the pathway miconazole acts. **B:** Calcofluor staining of control and Erg25 OE cells, treated and non-treated with 1µM miconazole. Scale bar, 5µm. **C:** Quantification of septum defects observed by calcofluor staining of control (n=116), Erg25 OE (n=338), *erg6Δ* (n=477) and Erg25 OE *erg6Δ* cells (n=395). Error bars: SD. **D**: Epifluorescence images of Erg25-ENVY and of the ER marker Elo2 fused to mcherry (ER-mcherry). Scale bars: 5µm. **E**: Epifluorescence images of Erg25-ENVY in control (top) and Erg25 OE cells (bottom) in interphase (left) and in late cytokinesis (right). Scale bars: 5µm. **F**: Quantification of ER shape in interphase in control (n=303) and Erg25 OE cells (n=404). Error bars: SD. **G**: Quantification of septum types in Erg25 OE (n=484), *scs22Δ* (n=391), *scs22Δ* Erg25 OE (n=469), *scs2Δ* cells (n=308), *scs2Δ* Erg25 OE (n=336), *scs22Δscs2Δ* (n=413) and *scs22Δscs2Δ* Erg25 OE cells (n=377). Error bars: SD.

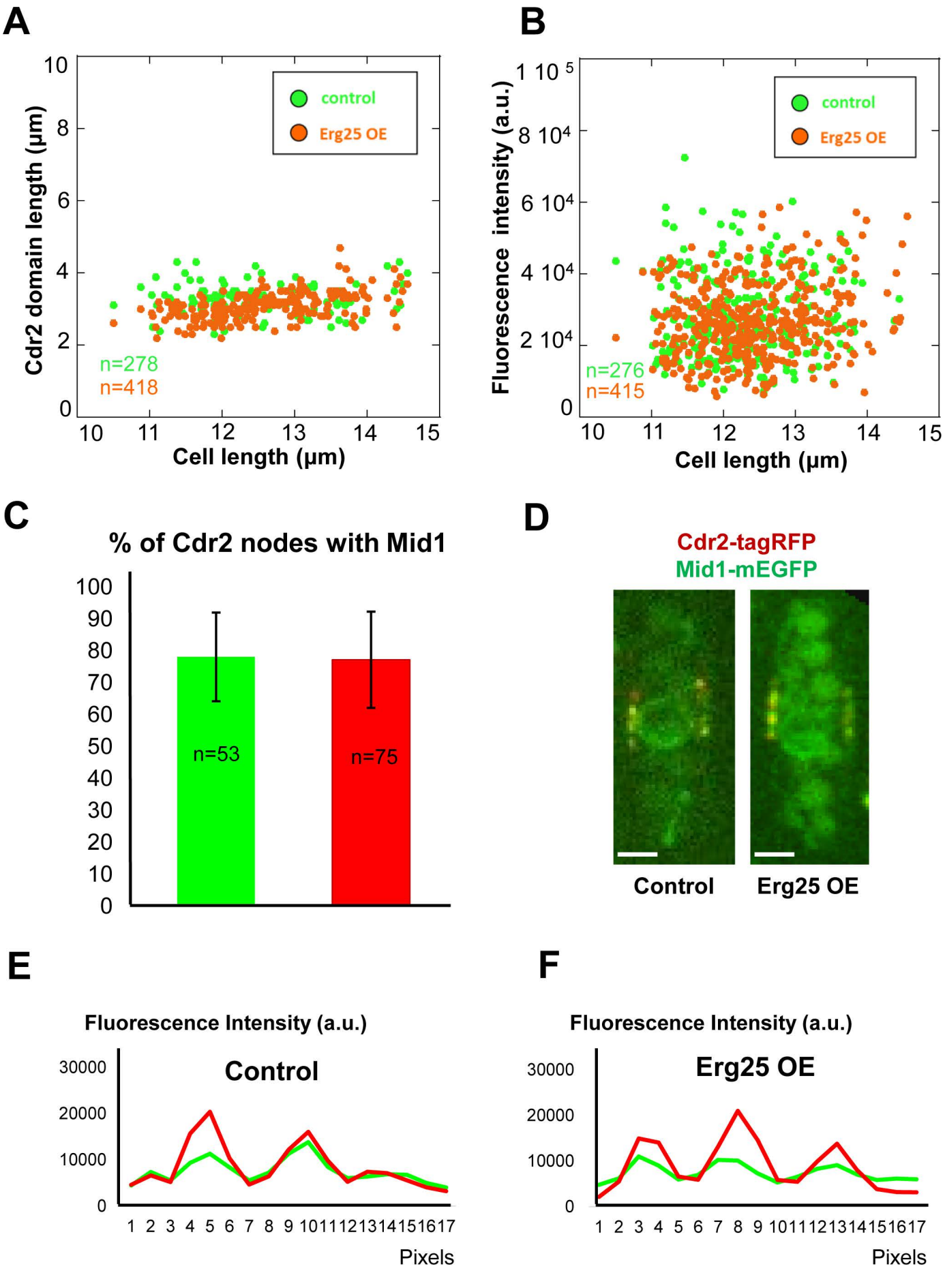

Figure S2. Characterization of Cdr2 and Mid1 domains upon Erg25OE.

A: Length of the Cdr2-EGFP domain relative to cell length in control (n=278) and Erg25 OE cells (n=418). **B:** Integrated fluorescence intensity (a.u.) of Cdr2-EGFP domain relative to cell length in control (n=278) and Erg25 OE cells (n=418). **C:** Percentage of Cdr2-tagRFP nodes containing Mid1-mEGFP in single cells. Error bars: SD (n>50 cells, top right). **D:** Medial planes confocal images of Mid1-mEGFP and Cdr2-tagRFP in control (left) and Erg25 OE cells (right). Scale bar, 5 µm. **E-F**: Linescan analyzing Mid1-mEGFP and Cdr2-tagRFP intensity along the medial cortex (bottom) along the cells shown at the top right.

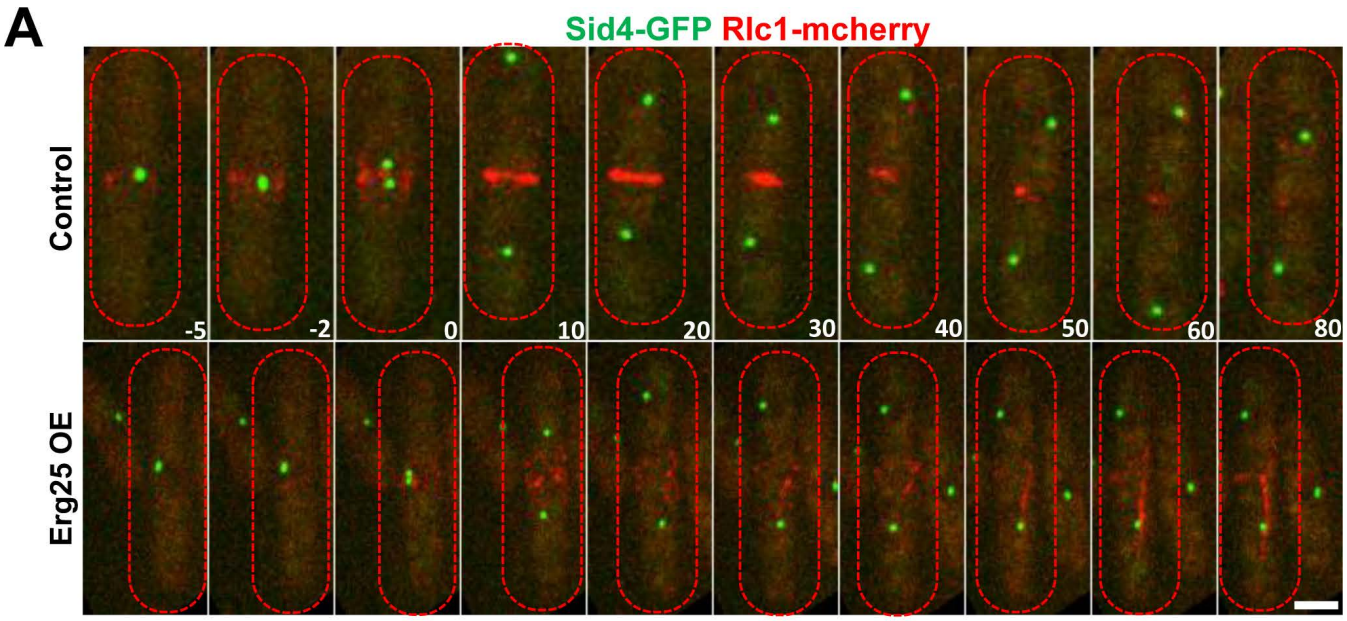

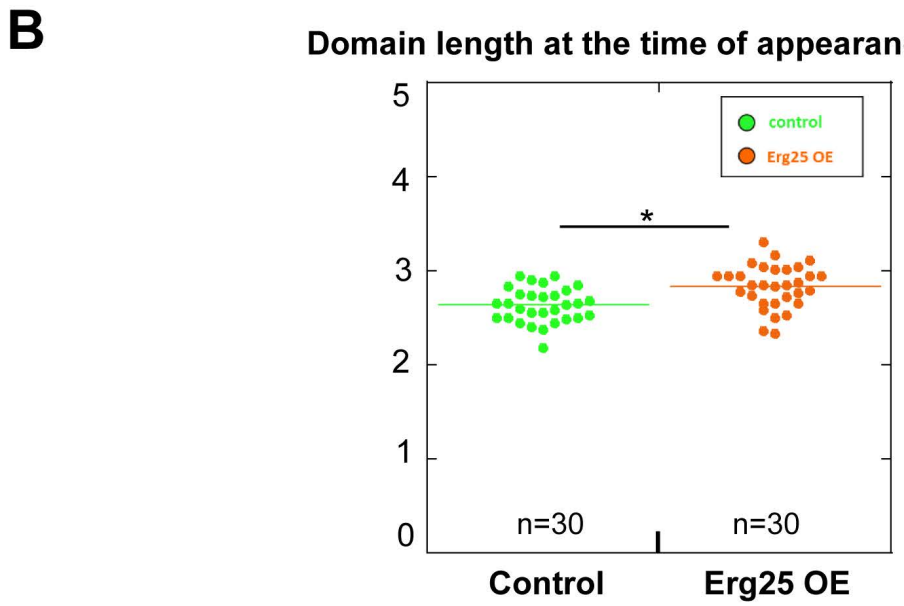

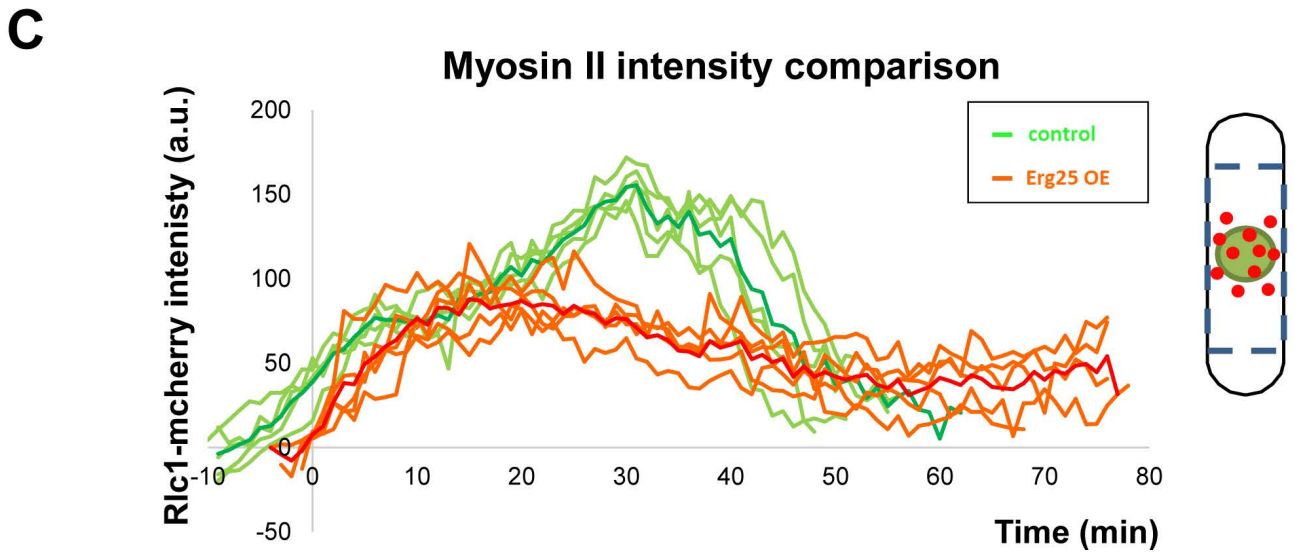

Figure S3. Analysis of myosin II behavior in Erg25 OE cells.

A: Time-lapse analysis of Sid4-GFP and Rlc1-mcherry in control (top) and Erg25 OE cells (bottom). Medial plane confocal images are shown. Time 0 corresponds to mitotic entry. Scale bars: 5 µm. **B:** Measurement of myosin II domain length at the time of its initial recruitment in control and Erg25 OE cells (n=30). **C:** Analysis of myosin II intensity (a.u.) in the central region in control and Erg25 OE cells (n=5). t=0 corresponds to SPB separation.

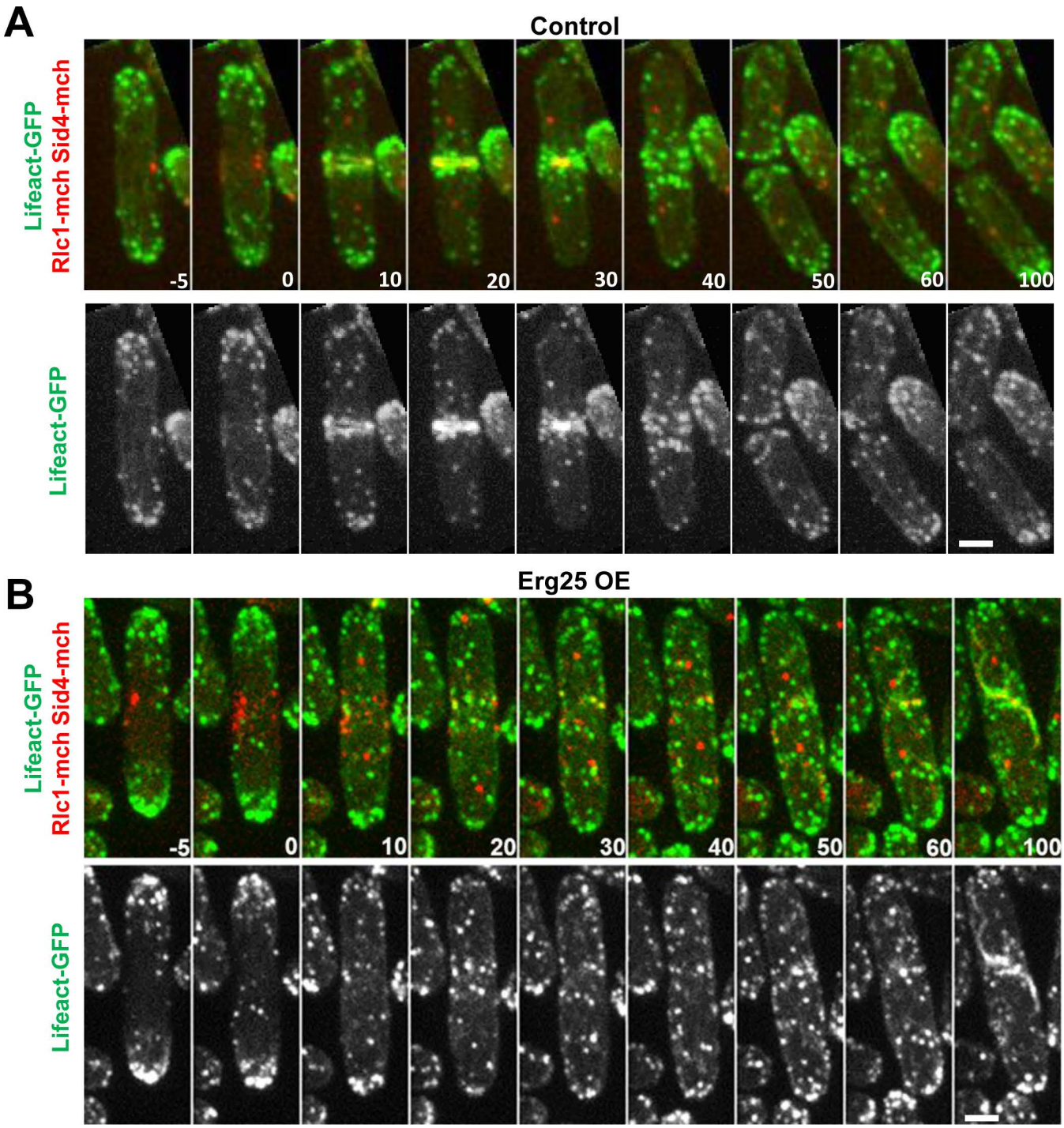

Figure S4: Inhibition of F-actin nucleation from cytokinetic precursor nodes upon Erg25 OE

Time-lapse images of control (**A**) and Erg25 OE cells (**B**) expressing lifeact-GFP, Rlc1-mcherry and Sid4-mcherry. Time 0 corresponds to mitotic entry. Scale bars: 5µm.

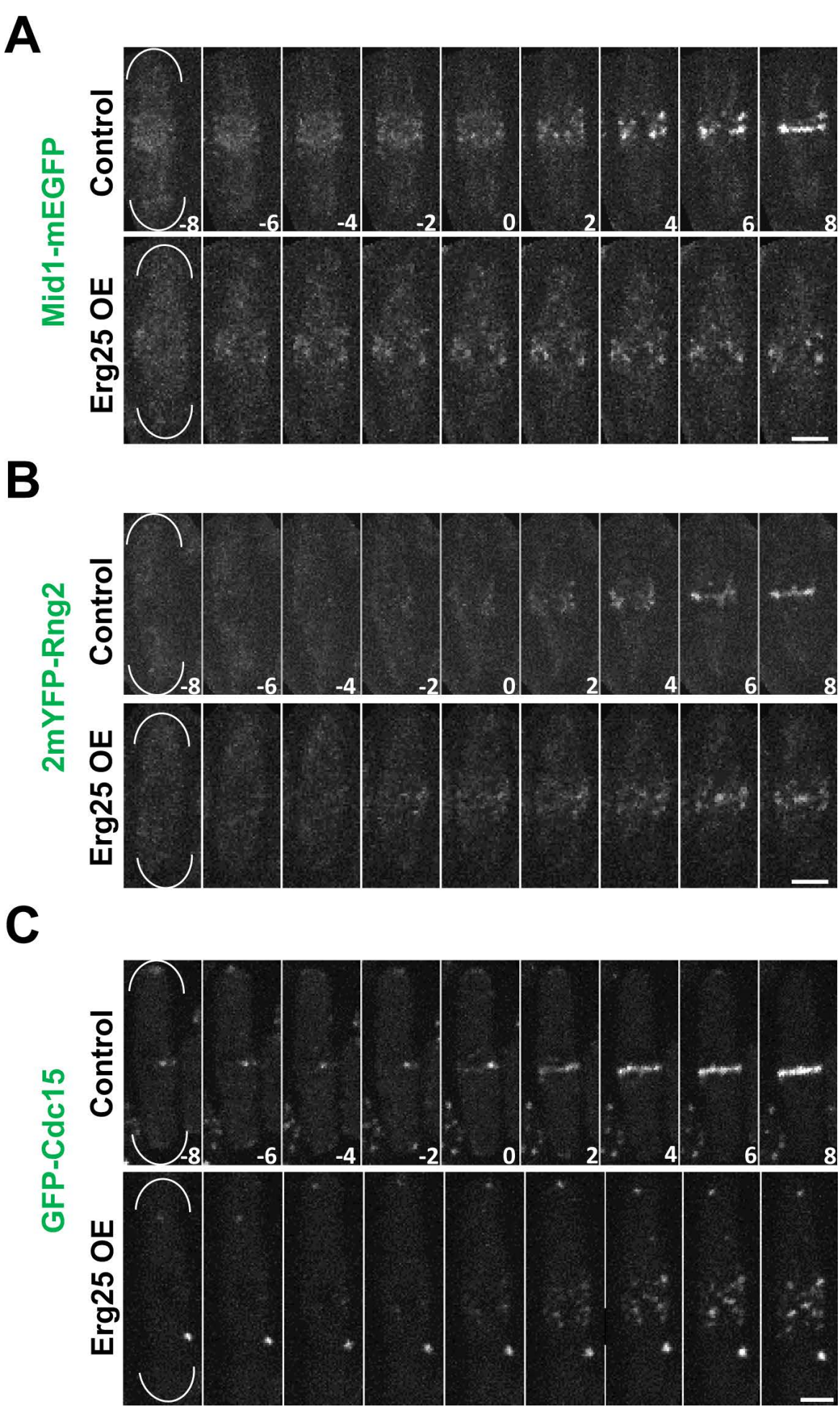

Figure S5. Analysis of Mid1, Rng2 and Cdc15 by time lapse imaging upon Erg25 OE.

Time lapse images of Mid1-mEGFP (**A**), 2mYFP-Rng2 (**B**) and GFP-Cdc15 (**C**) in control (top) and Erg25 OE cells (bottom). Time 0 corresponds to the time of SPB separation. Scale bar, 5 µm.

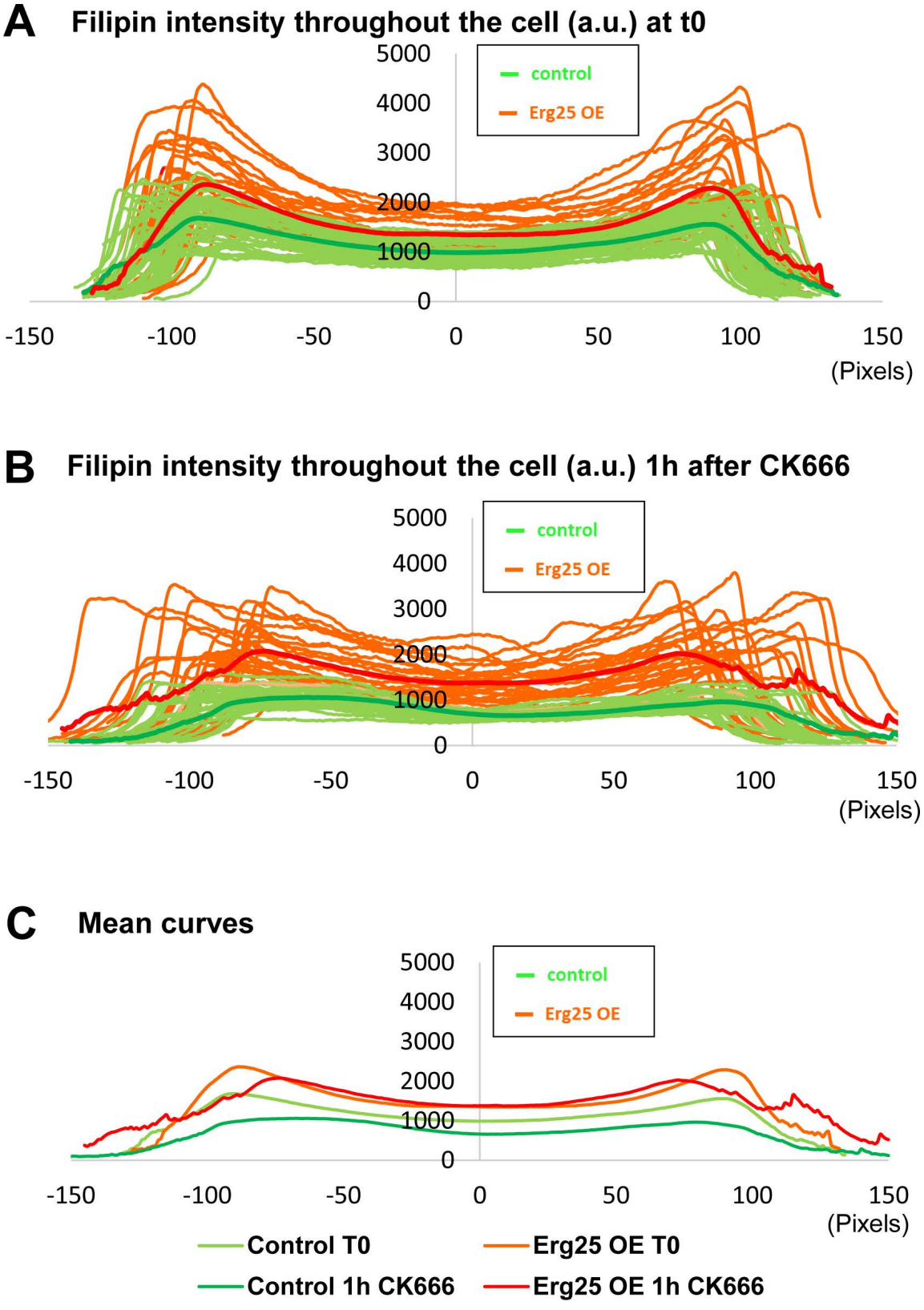

Figure S6. Measurement of Ergosterol levels after treatment with CK666

A-B: Filipin intensity expressed in a.u. was measured in control and Erg25 OE cells at time 0 (**A**) and after 1h of CK666 treatment (n=30 cells) (**B**). **C:** Graph showing the average curves of filipin intensity of control and Erg25 OE cells at time 0 and after 1h treatment with CK666.

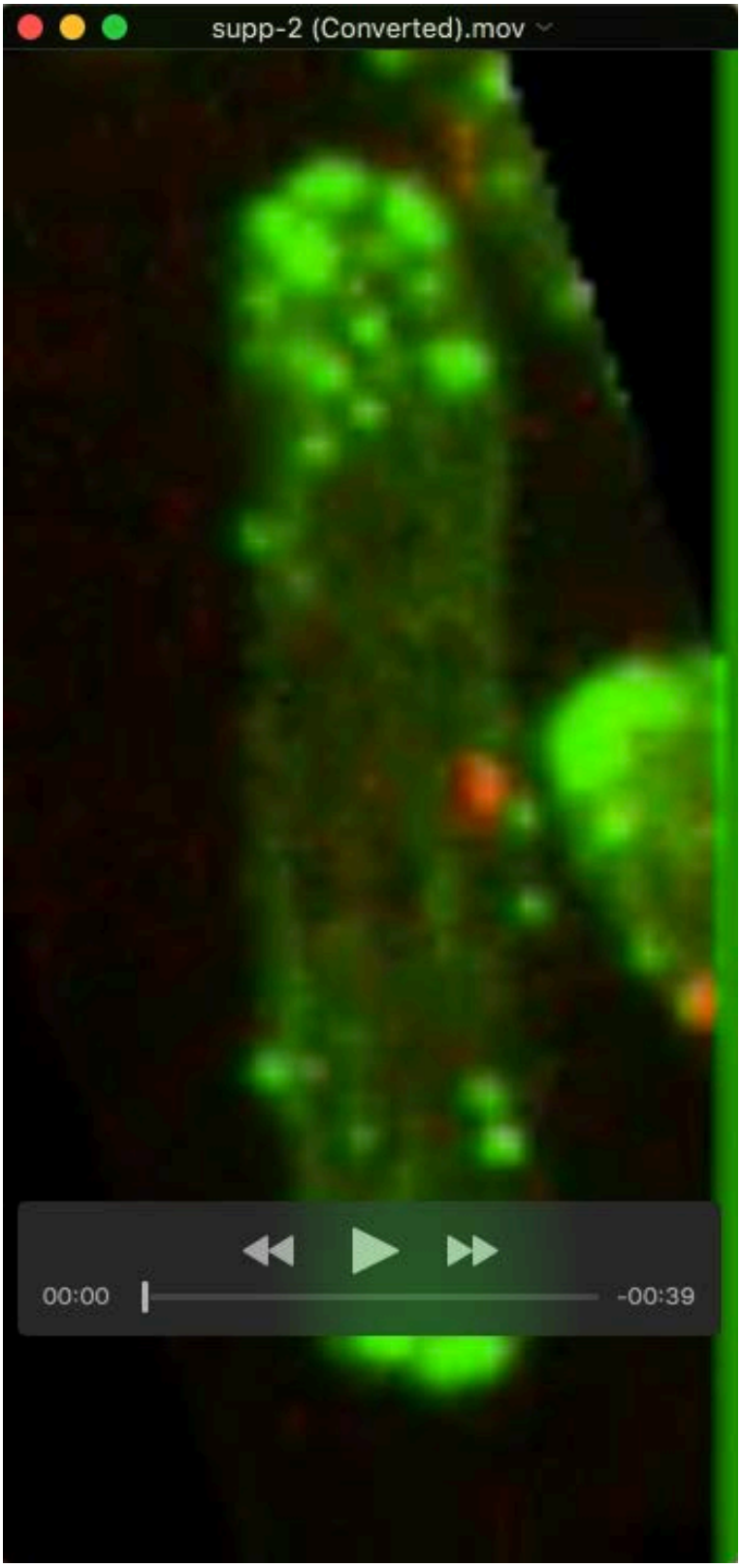

Movie 1. F-actin dynamic distribution in a representative dividing control cell.

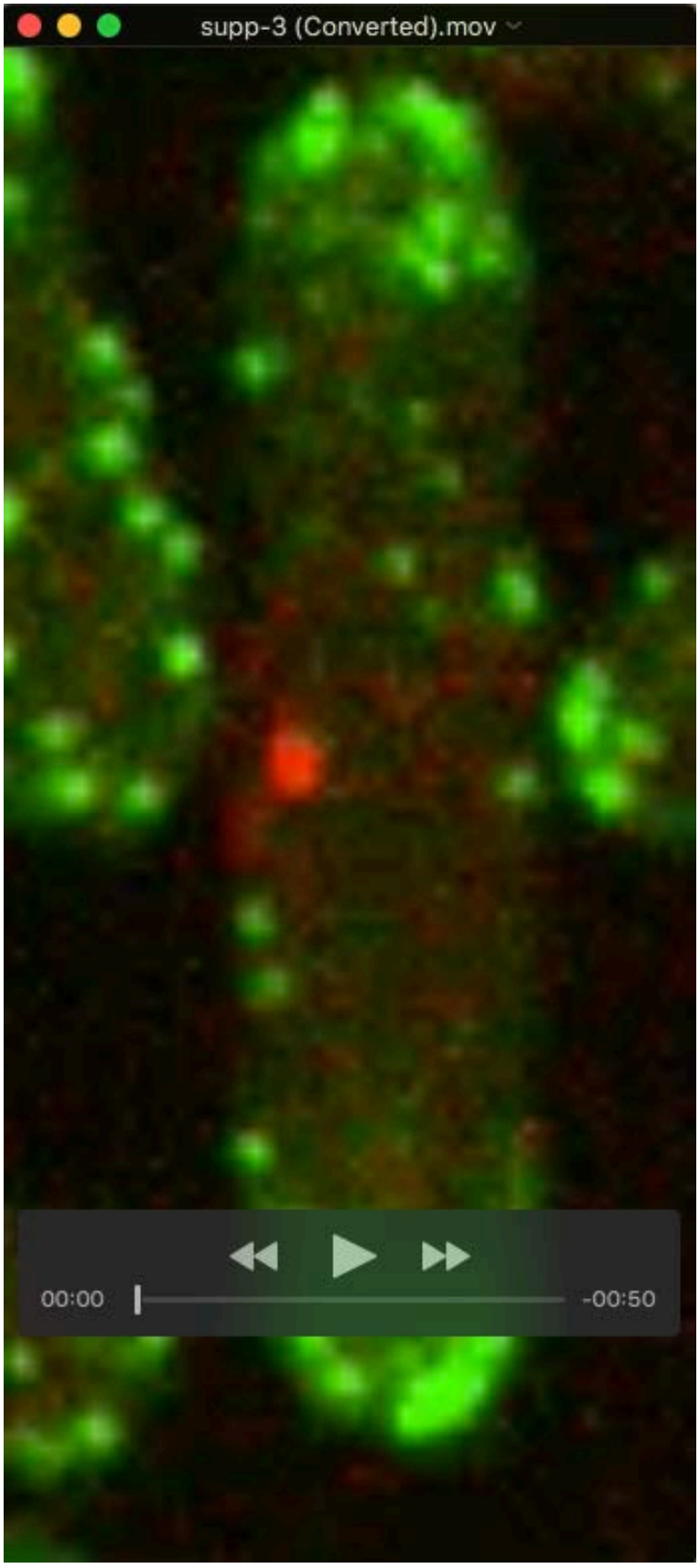

Movie 2. F-actin abnormal organization upon Erg25 OE.

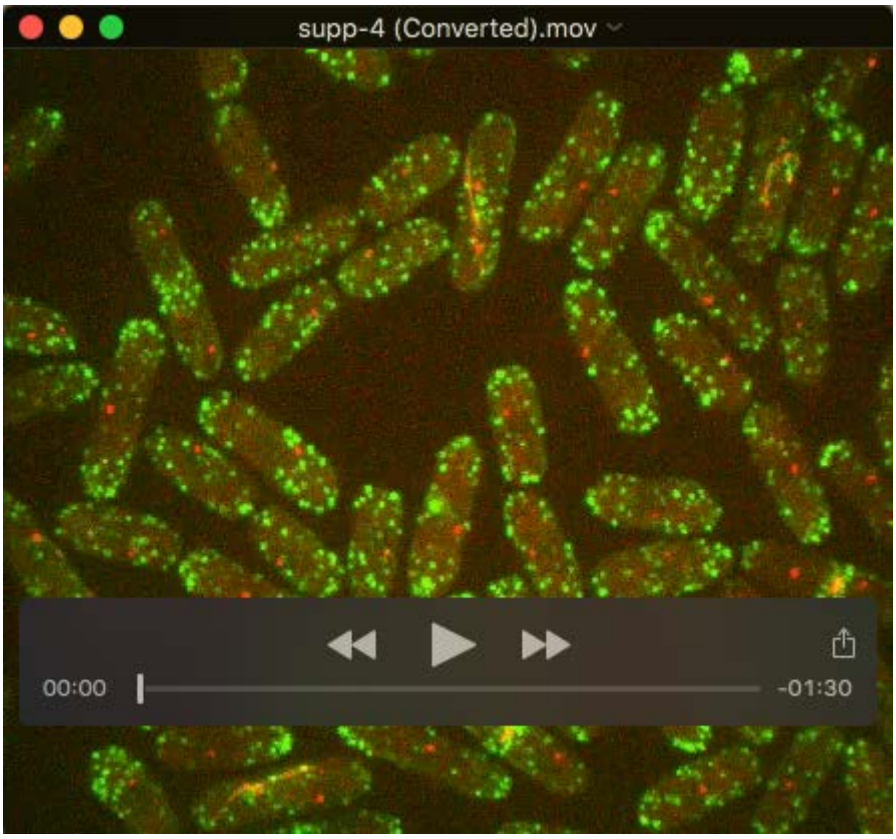

Movie 3. Multiple examples of F-actin aberrant organization upon Erg25 OE in comparison with control cells.

Article 2: Septin ring assembly by anillin-dependent compaction of a diffuse septin meshwork surrounding the acto-myosin contractile ring in fission yeast

Federica Arbizzani[1], Sergio A. Rincon[1, 2] and Anne Paoletti[1]

[1] Institut Curie, PSL University, CNRS UMR 144, F-75005, Paris, France.

[2] Instituto de Biología Funcional y Genómica and Departamento de Microbiología y Genética, Consejo Superior de Investigaciones Científicas (CSIC) / Universidad de Salamanca, Salamanca, 37007 Spain.

SUMMARY

Cell division is a fundamental process for cell proliferation and renewal, ending with cytokinesis that allows the physical separation of daughter cells. Besides the acto-myosin contractile ring, cytokinesis most often involves an additional component of the cytoskeleton, the septins, which form rings at the division site delineating the edges of the cleavage furrow. These conserved scaffold proteins act as macromolecular cortical organizers and are crucial for the success of cell division. Their dynamic behavior during cytokinesis progression is known to be regulated by post-translational modification and interactions with septin-associated regulators. However, how septins are finely tuned in space and time to properly perform their function during cytokinesis is still not well understood. In this study, we used fission yeast to explore septin organization throughout the cell cycle and decipher the key factors responsible for their regulation. Live-imaging analysis with precise timers to monitor the progression of cell division has uncovered that septins are initially recruited in a 1.5 µm-wide diffuse meshwork surrounding the CR in late anaphase. This meshwork then undergoes compaction into rings when CR constriction is initiated. We found evidence that the anillin-like protein Mid2 is necessary to promote this new compaction step and may function as a bundler for septin filaments. We also found that while Mid2-driven septin compaction requires mitotic exit, the SIN pathway is necessary for both septin meshwork assembly and compaction. Finally, PIP2 levels were found to be critical to initiate septin recruitment to the plasma membrane, before Mid2 becomes available at the initiation of CR constriction. This work highlights the complex regulations that allow the coordination between septin ring assembly and cell cycle progression.

INTRODUCTION

Cytokinesis is an irreversible process which must precisely partition an equal set of the replicated chromosomes and organelles to each daughter cell. Defects in this process can lead to chromosome mis-segregation or aneuploidy, a hallmark of cancer cells (Fujiwara et al., 2005; Lacroix and Maddox, 2012; Storchova and Pellman, 2004). Cytokinesis completion requires the participation of different components of the cytoskeleton, namely, the actin cytoskeleton at the basis of the contractile ring that pinches in the plasma membrane to create the cleavage furrow, microtubules involved in division plane signaling in animal cells, as well as septins which are present at the division site from yeast to mammals.

Septins are unique cytoskeletal components capable of assembling together to form intracellular structures of varied shapes such as filaments and rings. Their ability to interact with cellular membranes as well as actin filaments and microtubules allow them to participate in many biological processes, working as scaffolds for protein-protein interactions and/or as diffusion barriers for protein compartmentalization (Bridges and Gladfelter, 2015; Mostowy and Cossart, 2012; Saarikangas and Barral, 2011). These conserved GTP binding proteins were initially discovered in budding yeast, where they localize at the division site and are essential for cytokinesis (Cauvin and Echard, 2015; El Amine et al., 2013; Estey et al., 2010; Gladfelter et al., 2001; Hartwell, 1971; Kim et al., 2011; Kozubowski et al., 2005; McMurray and Thorner, 2009; Versele and Thorner, 2005; Wu et al., 2010). Septin organization undergoes multiple transitions during the cell cycle. In early G1, septins initially assemble as a patch-like structure at the presumptive bud site. Upon bud emergence, this patch narrows to form a single ring marking the future site of bud growth. Once the bud has formed, the septin ring extends into an hourglass-shaped collar present at the bud neck until mitotic entry. At cytokinesis onset, the septin hourglass splits into two distinct rings that sandwich the CR (Gladfelter et al., 2001). Finally, after cell division, the septin rings are disassembled and the septin subunits are partially replaced and recycled for a new cycle to begin (McMurray and Thorner, 2009). This dynamic behavior needs to be strictly controlled to ensure a proper cytokinesis, and several post-translational modifications of septins have been described. Phosphorylation regulates septins localization and high order rearrangements (Garcia et al., 2011; McQuilken et al., 2017); sumoylation seems to play a role in septin disassembly (Johnson and Blobel, 1999; Takahashi et al., 1999); and acetylation might control septin hourglass formation and stability (Marquardt et al., 2018; Mitchell et al., 2011; Ribet et al., 2017).

Importantly, septins are the first proteins recruited at the bud neck where they serve as a scaffold for the sequential and ordered assembly of the acto-myosin based contractile ring (Bhavsar-Jog and Bi, 2017; Juanes and Piatti, 2016; Meitinger and Palani, 2016). Among the several proteins that they help anchoring at the division site, septins are required for the localization and maintenance of Myo1, the

single myosin type II present in budding yeast. Disruption of the septin structure in a temperature sensitive mutant leads to the loss of previously formed Myo1 rings and inability to form new ones (Bi et al., 1998; Lippincott and Li, 1998).

Later on, when contractile ring constriction occurs, the septin double ring act as key cortical barriers to restrict exocyst components and the chitin synthase II (Chs2) enzyme at the division site (Dobbelaere and Barral, 2004). This is crucial to create specialized confined zones where membrane reorganization and septum formation at the cleavage furrow happen before cell division.

Septins are also present in animal cells and localized at the cleavage furrow during cytokinesis. They contribute to the recruitment of the cytokinetic apparatus to the site of cell division and to regulate its contraction (Kinoshita et al., 1997; Maddox et al., 2007; Mavrakis et al., 2014). Afterwards, septins are also important for the maturation of the intercellular bridge and the midbody formation and eventually for the abscission event (El Amine et al., 2013; Estey et al., 2010; Karasmanis et al., 2019; Renshaw et al., 2014).

In addition, in higher eukaryotes, septins localize at boundaries between cell compartments with pleiotropic roles (Caudron and Barral, 2009; Saarikangas and Barral, 2011): i.e. in the annulus separating the tail from the midbody in spermatozoa, which is key for spermiogenesis and reproduction (Ihara et al., 2005; Kuo et al., 2015); at the base of cilia where they are required for a correct cilium formation and function (Hu et al., 2010); in cage-like structures to respond to microbial infections in *Listeria monocytogenes* and *Shigella flexneri* (Krokowski et al., 2018; Mostowy et al., 2010) and at the base of dendritic protrusions in neurons where septins are key for spine and dendrite maturation (Ewers et al., 2014; Tada et al., 2007).

One important factor in the organization of septins is the conserved protein anillin, whose disruption leads to defects in cytokinesis (Echard et al., 2004; Field et al., 2005a; Kechad et al., 2012; Oegema et al., 2000; Somma et al., 2002; Straight et al., 2005; Zhao and Fang, 2005). *In vitro* studies have shown that anillin can bind septin and actin filaments. Indeed, an important function of anillin is the recruitment of septins to the AMR during cell division (Field et al., 2005a; Kinoshita et al., 2002; Oegema et al., 2000). It is well documented that anillin interacts with septins through a C-terminal region that comprehends the anillin homology (AH) domain upstream of the terminal PH domain (Piekny and Maddox, 2010). The C-terminal region of Bud4, the anillin-like protein in budding yeast, is important to direct septin organization during bud site selection and bud growth and to preserve the integrity of the septin ring during cytokinesis (Kang et al., 2013; Wu et al., 2015). Indeed, in *bud4Δ* mutants the septin double ring disassembles during cytokinesis (Eluere et al., 2012; Kang et al., 2013; Wloka et al., 2011), whereas the overexpression of Bud4 leads to the formation of extra septins structures (Kang et al., 2013). Recently,

polarized fluorescence microscopy studies have described a key role of Bud4 in the reorientation of septin filaments in the hourglass to double ring transition (McQuilken et al., 2017).

The fission yeast Schizosaccharomyces pombe, a model system for cell division studies, divides by the assembly and constriction of a medially placed actomyosin-based contractile ring (CR) (Lee et al., 2012; Pollard and Wu, 2010; Rincon and Paoletti, 2012; Rincon and Paoletti, 2016). This process is tightly regulated both in space and time and occurs in multiple stages: during interphase, contractile ring components are first recruited by the anillin-like protein Mid1 to precursor nodes on the medial cortex of the cell, before compacting into a tight medial CR. Upon mitotic exit, the Septation Initiation Network (SIN), related to the budding yeast mitotic exit network (MEN) and the metazoan Hippo pathway (Hergovich et al., 2006), promotes the next steps, represented by constriction of the CR and synthesis of an extracellular septum composed of polysaccharides (Krapp et al., 2004b; Simanis, 2003; Simanis, 2015). Eventually sister cell separation ensues, when the inner layer of the septum is digested by glucanases (Cortes et al., 2016; Perez et al., 2016). In contrast to budding yeast, in *S. pombe,* septins are mostly involved in late cytokinetic events.

The *S. pombe* genome contains seven genes encoding septins, identified by sequence homology with the *S. cerevisiae* counterparts: Spn1-4 are expressed in vegetatively growing cells, whereas Spn5-7 exclusively function during sporulation in the formation of the forespore membrane (Hall et al., 2008; Onishi et al., 2010). Differently from *S. cerevisiae,* where septins are necessary for CR formation, fission yeast septins are recruited after the contractile ring has been fully assembled. Septins form first a single ring in late mitosis which splits in two during CR constriction and septum formation. This double ring does not constrict together with the CR, but remains on the cell surface to delineate the boundaries of the cleavage furrow and dissociates after cell separation (An et al., 2004; Berlin et al., 2003; Juanes and Piatti, 2016; Wu et al., 2003). Septin mutants have defects in cell-cell separation since they have a key role, in concert with the exocyst complex, in the delivery of the two septum hydrolytic enzymes (Agn1 and Eng1) to the area around the septum, regulating thereby the step that finishes cytokinesis (Alonso-Nunez et al., 2005; Martin-Cuadrado et al., 2005). Recently, it has also been shown that septins play a role in driving the proper recruitment and maintenance in the septum region of the SIN effector kinase Sid2 and of the glucan synthase enzymes Bgs1 and Ags1, to guarantee a successful cytokinesis (Zheng et al., 2018).

S. pombe genome encodes two anillin related proteins: Mid1 and Mid2. Genetic tests have excluded any overlapping functions between them, indicating that they work independently in separate phases of the cell cycle (Berlin et al., 2003). Mid2 localizes at the division site in a septin-dependent manner (Berlin et al., 2003). Moreover, the fact that a *mid2Δ* strain displays the same phenotype than Spn4-deleted cells, where nuclear division and septum synthesis occur but cell separation is delayed (Berlin et al., 2003)

suggests that Mid2 and septins work together in the same process. Indeed, FRAP analysis has revealed that, in the absence of Mid2, septins are much more dynamic (30-fold more) compared to a wild type, indicating a role of Mid2 in septin organization (Berlin et al., 2003). Mid2 protein levels are tightly controlled during the cell cycle, peaking during septation and decreasing after cell separation. Although this might be controlled by phosphorylation, the candidate kinases have not been identified yet (Kim et al., 2017; Tasto et al., 2003). Moreover, Mid2 contains three PEST sequences, one in a medial region and two at the N-terminus, which could act as signals for protein degradation through ubiquitination and SCF-dependent proteolysis (Alonso-Nunez et al., 2005; Petit et al., 2005; Tasto et al., 2003). Overexpression of a non-degradable Mid2 mutant let septin filaments persist through the next cell cycle, indicating that Mid2 is involved in septin rings maintenance (An et al., 2004; Tasto et al., 2003). Altogether these evidences indicate that: 1) septin filaments can organize as a ring in a CR-dependent fashion, 2) Mid2 recruitment is septin-dependent and 3) Mid2 contributes to septin ring stability.

However, how septins and Mid2 are precisely regulated in space and time to properly perform their function and how Mid2 contributes to septin ring organization remains elusive. Here, by using live cell imaging and precise timers for mitotic progression we describe in details septins and Mid2 behavior in fission yeast. Our approach identified a new step in septin ring assembly: septin compaction from a loose meshwork surrounding the CR into a tight ring when CR constriction is initiated. We show that this step requires Mid2 that has the properties of a bundler for septin filaments promoting their compaction. Second, septin compaction is inhibited in cells blocked in mitosis in spite of Mid2 association with septins. Since Mid2 is hyperphosphorylated in mitosis, septin compaction may require Mid2 dephosphorylation at mitotic exit. Third, compaction is also strongly perturbed, together with septin accumulation at the division site when the SIN is inactivated. Finally, we show that another important regulator of septin ring assembly is PIP2 that acts both on the timing of septin meshwork assembly and amounts present at the division site but perturbs their compaction only slightly. We conclude that a combination of positive and negative inputs contribute to the precise regulation of septin ring assembly by Mid2 at mitotic exit in fission yeast.

RESULTS

Septins form a diffuse network in the vicinity of the contractile ring before compacting into a ring structure

Fission yeast septins have been localized to the division site where they form non-contractile rings defining the edge of the cleavage furrow while the acto-myosin based contractile ring constricts and the septum is built (Berlin et al., 2003; Tasto et al., 2003). However, relatively little is known on how septin rings assemble. We therefore decided to characterize by time-lapse imaging the dynamic organization of

septins with respect to spindle assembly and elongation, used as a proxy for mitosis progression, and contractile ring assembly and constriction.

To do so, we created a strain expressing the septin Spn1 C-terminally fused to GFP, as well as the regulatory light chain of myosin II Rlc1 fused to mCherry to monitor the contractile ring, and the spindle pole body (SPB) component Sid4 tagged with mCherry to monitor the mitotic spindle. Indeed, since septins interact strictly with each other, imaging Spn1 is sufficient to have an overview of the whole septin network (An et al., 2004). In these movies, SPB separation was defined as a timer for mitotic entry (t=0 in Fig1).

Septins appeared on the cortex as a band surrounding the CR about 18 minutes after SPB separation, when the SPBs were the further apart, corresponding to maximum spindle elongation in anaphase (Fig 1A and 1D, t=18.7 ± 2.3). 7 minutes later, septins compacted into a tight ring structure (t=25.6 ± 2.8), concomitant with the initiation of CR constriction (t=26.1 ± 2.9). This compaction phenomenon is best visualized on enlargements of the medial region of the cell recorded at 1 minute intervals (Fig1C, dark green asterisk). About 20 minutes later, by the end of CR constriction (t=48.5 ± 3.6, Fig1C), the septins were visualized as a double ring (t= 43.4 ± 6.5, Fig1C, red asterisk). Eventually, septins re-spread to the new cell tip generated when the two sister-cells separated from one-another by cleavage of the septum (Fig1C, yellow asterisk).

Quantitative analysis of the septin signal further revealed that septin intensity raised for a period of about 15 minutes after they appeared on the cortex. The intensity then stayed roughly constant for 30 minutes before decreasing rapidly over 10 minutes (Fig 1F). Furthermore, analyzing the width of the cortical region on which septins were distributed revealed a two-fold reduction in width, from 1.4 ± 0.1 µm at their appearance to 0.75 ± 0.1 µm after compaction (n=30, Fig1G light green dots).

To conclude, this detailed live analysis of septins using the mitotic spindle and the CR as cell cycle timers reveals a new step in the process of septin ring assembly that we have named compaction.

The anillin Mid2 is necessary for septin ring compaction

A similar imaging strategy was taken to define the dynamic organization of the anillin-like protein Mid2, known to colocalize with septins and modulate their dynamics (Berlin et al., 2003; Tasto et al., 2003). Using a strain expressing Mid2 C-terminally fused to Envy, as well as Rlc1-Cherry and Sid4-mCherry, we found that Mid2 appeared 8 minutes later than septins (t=26.9 ± 2.5) at time of septin compaction (Fig1C right, light green asterisk and Fig1C left, dark green asterisk, Fig1D-E) and CR constriction (t=25.2 ± 2.4, Fig1B-E). Later on, Mid2 compacted slightly (Fig1C right, dark green asterisk), appeared as two rings concomitantly to septins (Fig1C, red asterisk) and spread out on the newly formed cell tips upon daughter cell separation (Fig1C, yellow asterisk).

Quantitative analysis of Mid2 signal confirmed the late recruitment of Mid2 compared to septins and showed that its intensity raised for about 30 minutes, stayed constant for 10 minutes and decreased rapidly, similarly to septins (Fig1F). Moreover, we found that Mid2 was recruited in a narrower region than septins and its compaction was limited compared to septins with the width decreasing from 1.1 ± 0.1 µm at appearance to 0.8 ± 0.1 µm after compaction (Fig1G dark green dots).

The coincidence between CR constriction, septin compaction and Mid2 recruitment suggested us that these events may be coupled. To determine if this was the case, we first tested whether Mid2 was involved in septin compaction. To do so we analyzed septin ring assembly in a *mid2* deletion mutant (Berlin et al., 2003), using the same markers for mitosis and cytokinesis progression as before. Time-lapse movies showed that in *mid2Δ* cells, septin initial recruitment occurred normally (Fig2 B, C, E), but septin intensity stopped increasing prematurely, about 8 minutes after they appeared, ie at the time when Mid2 normally appears (Fig2F). As a consequence, septin maximum intensity was decreased by 3 fold in *mid2Δ* compared to control cells (n=6 for both samples) (Fig2F). Furthermore, septin compaction was completely abolished (Fig2C, 2G). Instead, septin retained a diffuse distribution around the CR (Fig2C and S1A). As a consequence, splitting into two rings did not occur. Finally, whereas the CR constriction took normally place (FigS1B), cell separation and Mid2 re-spreading were delayed to the next cell cycle, as reported in a *mid2* deletion mutant [Fig2 A-E, (Berlin et al., 2003; Tasto et al., 2003)].

Mid2 may function as bundler for septin filaments

The fact that Mid2 is necessary for septin compaction, suggested us that Mid2 may function as a bundling protein for septin filaments promoting their alignment and assembly into a ring structure. To perform this activity, Mid2 should be able not only to interact with septins, but also to dimerize or multimerize in order to bridge together two or more septin filaments.

To test this hypothesis, we verified that Mid2 could co-immunoprecipitate with septins (see FigS3C). We also designed co-immunoprecipitation assays between differentially tagged versions of Mid2 co-expressed in the same cells. These experiments were performed in the presence or in the absence of Spn1 to exclude bridging by septin filaments of differentially tagged versions of Mid2. Our experiments show that Mid2-mEGFP co-immunoprecipitates with Mid2-13Myc regardless of the presence of septin filaments (Fig3A-D).

In order to map the Mid2-Mid2 interaction site, we also performed immunoprecipitations with a truncated version of Mid2 lacking the PH domain (Mid2-ΔPH) or with the isolated PH domain (see Fig3E for mid2 domains organization). Mid2-ΔPH-mEGFP co-immunoprecipitated with Mid2-13Myc to the same extent as Mid2-mEGFP, in the presence or absence of septin filaments (Fig3A-B). Mid2 PH domain also showed the ability to self-interact in co-immunoprecipitation assays, even in the absence of septins

(Fig3C-D). This altogether indicates that Mid2 has the ability to form structures of higher molecular order. Since Mid2 arrival at the cortex also coincides with septin compaction and Mid2 is necessary for this step, this suggests that Mid2 may promote compaction by bundling septin filaments.

Septins and Mid2 form wide bands surrounding the CR when cells are blocked in mitosis

Our work shows that septin filaments appear at a very precise time in mitosis, when the anaphase spindle length is maximum, and compact into rings when Mid2 appears and the CR starts constricting. This provides evidence for a tight coupling between septin ring assembly and cell cycle progression. To get insights into how this coupling is achieved, we first analyzed the localization of Spn1 and Mid2 in mutants blocked in mitosis, with a high CDK activity. We first used the cold sensitive β-tubulin mutant *nda3-KM311* expressing Spn1-GFP or Mid2-Envy together with Sid4-mCherry and Rlc1-mCherry. Strikingly, upon cold treatment, cells blocked in mitosis, carrying a CR, formed a large band of septins or Mid2 surrounding the CR rather than septin rings in control cells (Fig4A left). Interestingly, Spn1-GFP and Rlc1-mCherry intensity measurements by linescan along the cell axis showed a decrease in Spn1-GFP signal at the exact position of the CR (Fig4A right and FigS2B-C). Furthermore, imaging these cells at one hour intervals after the temperature shift showed that the width of the septin and Mid2 domains gradually increased in *nda3-KM311* cells (from 1.2 µm ±0.03 after 1 hour at 18ºC to 2.4 µm ± 0.2 after 7 hours at 18°C), while narrow rings were always present in control cells (0.9 µm ± 0.03, FigS2A). A similar situation was observed for Mid2 domain with width increasing from 1.0 µm ± 0.1 after 1 hour at 18ºC to 2.0 µm ±0.1 after 7 hours in *nda3-KM311* cells compared to narrow rings in control cells (0.9 µm ± 0.4, FigS2A). Release from the mitotic block by transferring the cells back to 25ºC for 1 hour resulted in a compaction of both septin and Mid2 domains with domain width decreasing to 1.2 µm ± 0.1 and 1.3 µm ± 0.2, respectively (FigS2A).

We also used the thermo-sensitive kinesin-5 *cut7-24* mutant, which forms a monopolar mitotic spindle at 36ºC, producing a temporary cell cycle arrest in metaphase with a high Cdk activity (Fu et al., 2009; Hagan and Yanagida, 1990; Hagan and Yanagida, 1992). Live cell imaging of the Spn1-GFP Rlc1-mCherry Sid4-mCherry strain in the wild-type cells at 36ºC slightly accelerated mitosis progression compared to 25ºC (Fig4B-C compared to Fig1A, C and D), but septin appearance occurred at time of maximum spindle elongation and septin compaction coincided with the initiation of CR constriction, like at 25ºC. In the *cut7-24* mutant, since no SPB separation could be observed, the time of transfer to 36ºC was defined as time 0 for this experiment. In this background septins appeared 9 minutes after the temperature shift in a large band (1.7 ± 0.2 µm compared to 1.45 ± 0.1 µm in control cells, Fig4F) and were excluded from the CR as seen in *nda3-KM311* cells. Unlike in control cells where septin compacted to 0.9 ± 0.05 µm, these bands became slightly larger over time in *cut7-24* cells (2.0 ± 0.1 µm Fig4D-F), until they escaped

the cell cycle arrest 34.4 ± 9.7 min in mean after transfer to 36ºC, as visualized by the initiation of CR constriction. Septins compacted at the same time (t=34.1 ± 9.4). Later on, septins were observed as two rings at t=50.9 ± 11.9 and re-spread along the cell cortex at t=60.9 ± 13.7(Fig4D-E). Intensity analysis displayed that in the cut7-24 mutant the increase in the septin signal occurs before control cells, but then it remains rather fixed until the cells escape from the mitotic block, where a faster signal enhancement is detected (after the dotted line, Fig4G). However, it never reaches the values measured in the control showing a general reduction of about 1.3 fold (Fig4G).

Live cell imaging of the Mid2-Envy Rlc1-mCherry Sid4-mCherry strain in the wild-type cells at 36ºC showed that similar to septins, Mid2 dynamics were accelerated at 36ºC compared to 25ºC (FigS4A-B). In the *cut7-24* mutant, Mid2-Envy appeared at the same time as in control cells (t=18± 3.9 compared to t=17.5 ± 1.2) but formed a faint band surrounding the CR that enlarged slightly over time (FigS4C-E), until cells escaped mitosis and CR constriction was initiated (t=33.9 ± 8.5) as well as Mid2 compaction (t=33.7± 8.6, FigS4C-E). Ring splitting and re-spreading were strongly delayed (t=46.0 ± 9.8 and t=66.9 ± 17.0, respectively) (FigS4D).

Overall, these data suggest that high Cdk activity allows septin and Mid2 recruitment, but inhibits the following compaction phase, even if Mid2 is present, suggesting that Mid2 bundling activity is impaired in these conditions.

This prompted us to investigate if Mid2 had still the ability to self-interact in this context. To do so, we performed co-immunoprecipitations between Mid2-13Myc and Mid2-GFP, Mid2ΔPH-GFP or the single PH domain of Mid2 tagged with GFP in the control or *nda3-KM311* mutant cells, after 7 hours of incubation at 18°C to block cells into mitosis (FigS3A-B). This did not reveal any modification in the ability of Mid2 to self-interact.

We then tested if high Cdk activity could reduce the avidity of Mid2 for septins. To test this hypothesis, coimmunoprecipitation assays between Spn1-GFP and Mid2-13Myc were performed in control and *nda3-KM311* cells after 7 hours of incubation at 18°C or after 7 hours at 18°C followed by 1 hour at 25°C to release cells from the mitotic block (FigS3C). This did not reveal significant differences in the ability of Mid2 to interact with septins (FigS3D).

This suggests that although Mid2 is necessary for septin compaction, it is not proficient for this function when Cdk1 activity is high, independently from its ability to self-interact or to interact with septins. Since Mid2 is hyperphosphorylated during mitosis (Tasto et al., 2003), one hypothesis is that Mid2 phosphorylation prevents septin compaction. Or else, Mid2 is not sufficient to promote septin ring compaction on its own.

SIN activity is required for normal septin accumulation at the division site and compaction

Since septin compaction is coincident with CR constriction, an event known to be triggered by the SIN pathway (McCollum and Gould, 2001), we next wondered if septins and Mid2 were also under the control of this pathway.

To check this, we analyzed the behavior of septins in the temperature sensitive hypo-active SIN mutant *sid2-250* at the non-permissive temperature of 36º C (Balasubramanian et al., 1998; Sparks et al., 1999). Live cell imaging of cell expressing Spn1-GFP Rlc1-mCherry Sid4-mCherry *sid2-250* revealed that in the majority of cells septins appeared as a diffuse cortical band at the normal timing controlled to control cells (Fig 5A-C, D-E). However, the intensity of the septin signal was diminished by ~ 4.5 fold (Fig5F) and compaction failed in 75% cells, while a loose compaction was observed in the remaining 25% (Fig5B-C). Indeed, quantification of the extent of compaction showed that while in control cells the width of the septin recruitment domain decreased from 1.5 ± 0.1 µm to 0.9 ± 0.1 µm between appearance and compaction state, around 5 minutes later, in the majority of *sid-250* mutant cells (phenotype 1) the initial width of the septin domain went from 1.6 ± 0.1 µm to 1.9 ± 0.1 µm in a similar period of time, whereas few *sid2-250* cells (phenotype 2) went from 1.6 ± 0.1 µm to 1 ± 0.1 µm around 9 minutes from their appearance (Fig5G). Similar observations, except for the fact that only the no compaction phenotype was detected, were made for Mid2 in *sid2-250* cells at 36ºC (FigS5).

This data altogether suggests that the SIN pathway is not only required for septin and Mid2 compaction, but it is also involved in regulating their assembly and recruitment at the plasma membrane in the cell middle.

A role for PIP2 in controlling septin appearance and accumulation at the division site

Phosphatidylinositol 4,5-bisphosphate (PIP2), is strongly enriched at the division site during cytokinesis (Cauvin and Echard, 2015; Echard, 2012) and is known to promote septin filament assembly (Bertin et al., 2010; Tanaka-Takiguchi et al., 2009). We checked how PIP2 affects septin ring assembly in *S. pombe* using the temperature sensitive PI5-kinase mutant *its3-1*, which is characterized by strongly reduced levels of PIP2 (Snider et al., 2018; Zhang et al., 2000). Interestingly, live cell imaging of cells expressing Spn1-GFP Rlc1-mCherry Sid4-mCherry at 36º C in this mutant showed a delay of about 4 minutes in septins appearance at the medial cortex compared to control cells (t= 16.0 in *its3-1* mutant instead of t=12.5 in control cells; Fig6A-D), but before CR contraction which is strongly delayed in this mutant (t= 31.1 in *its3-1* mutant instead of 16.8 in control cells). Afterwards, septins did not accumulate as much at the division site (about 3 fold reduction, Fig6F) and did not compact properly in the *its3-1* mutant. Indeed, quantification of the extent of compaction showed that while in control cells the width of the septin recruitment domain decreased from 1.5 ± 0.1 µm to 0.9 ± 0.1 µm between appearance and

compaction state, around 5 minutes later, in the *its3-1* mutant, the initial width of the septin domain went from 1.4 ± 0.1 µm to 1.1 ± 0.1 µm only about 7 minutes later (Fig6E). Then, the septin ring split coincidently with the delayed initiation of ring constriction (t= 31.1± 5.8 and 30.1 ± 4.3 respectively; Fig6A-D). Finally, septins re-spreading was strongly delayed compared to the control cells (Fig6A-D), as expected in *its3-1* mutant known to bear defects in septum cleavage (Zhang et al., 2000).

Imaging Mid2-ENVY together with Rlc1-mCherry Sid4-mCherry in *its3-1* mutant further revealed that similarly to septins, Mid2 appeared with a slight delay of 2 minutes compared to control cells, and after the delayed initiation of ring constriction (FigS6A-D). Mid2 maximum intensity was reduced by 3-fold compared to control cells (FigS6F). Differently from septins though, Mid2 appeared to compact like in control cells (with domain width decreasing from 1.1 ± 0.1 µm at appearance to 0.8 ± 0.1 µm after compaction in control cells compared to 1.1 ± 0.05 µm to 0.9 ± 0.05 µm in *its3-1* mutant), but with a slight delay of about 4 minutes compared to the control (FigS6E). Mid2 ring splitting occurred 14 minutes after its appearance, with a delay of about 8 minutes compared to the control and Mid2 re-spreading was strongly delayed as observed for septins (FigS6A-D). Strikingly, the timing of septin appearance in *its3-1* mutant (t=16.1 ± 2.1) coincides with the initiation of CR constriction and Mid2 appearance in control cells (t=16.8 ± 1.4 and t=18.1 ± 2.04, Fig 6 B, D) (FigS6). Given that Mid2 contributes to septin recruitment to the division site, this might suggest that when the concentration of PIP2 is reduced, septin recruitment starts only when Mid2 becomes available.

Overall, these data indicate that PIP2 concentration represents an additional mechanism of control of septin ring assembly besides Mid2 and Cdk1 and SIN activities.

DISCUSSION

Septins are important cytoskeletal elements that form apolar hetero-oligomeric polymers and higher ordered structures, in particular at the site of cell division where they contribute to the success of cytokinesis. Despite recent advances, septins remain relatively poorly characterized compared to F-actin or microtubule cytoskeletons (Mostowy and Cossart, 2012; Spiliotis, 2018). This is particularly true in fission yeast where septins are involved in cytokinesis but are not essential for cell survival. In this organism, the assembly of septin rings at the division site was never analyzed in a quantitative manner by live cell imaging like the assembly of the mitotic spindle or the CR, limiting the chance to achieve a precise molecular understanding of this process.

In this study, we have used time lapse microscopy with precise cell cycle timers (ie a spindle pole body component to monitor mitotic spindle assembly and elongation and myosin II light chain to monitor CR

assembly and constriction) to define the spatiotemporal behavior of septins with respect to mitotic and cytokinesis progression.

Our data show for the first time that septins first appear as a diffuse meshwork in a 1.5 μm wide region surrounding the CR when spindle elongation is maximal. This meshwork then compacts into discrete rings when CR constriction is initiated (Fig1 A, C, D, F, G). This process of compaction may be related to the transition from the hourglass to split ring organization in budding yeast (Glomb and Gronemeyer, 2016; Iwase et al., 2006; McQuilken et al., 2017). Indeed septin compaction takes place when CR constriction is initiated, itself concomitant to the initiation of septum synthesis, which implies that, although spinning-disc confocal microscopy could not resolve them, septins form two rings after compaction, located on each side of the incipient septum. Accordingly, the early diffuse septin meshwork organized around the CR appears to be physically excluded from it, by a yet-to-define mechanism (Fig4A, 4D and FigS2). This suggests that septins are originally recruited in two different pools separated by the CR, which are eventually compacted into two rings at each side of it. The apparent septin ring splitting that we recorded later in our movies may correspond to the time when the two rings are resolved by spinning-disc confocal microscopy upon enlargement of the septum or initiation of its cleavage by hydrolytic enzymes.

Our results also provide new information on the function of the anillin-like protein Mid2 in septin ring assembly. We first show that its recruitment is coincident with septin compaction into a tight ring (Fig2A, B, C and F). Second, we find that Mid2 deletion limits septin accumulation at the division site at the precise time when Mid2 arrives at the division site in control cells. This reduced recruitment may result from the fact that Mid2 stabilizes septin filaments, as demonstrated by FRAP (Berlin et al., 2003), and is in agreement with the fact that Mid2 mild overproduction in the SIN hyperactive mutant *cdc16-116* can induce septin ring assembly at ectopic cytokinesis sites (An et al., 2004). Third, Mid2 deletion also abolishes septin compaction. Finally, we found evidence that Mid2 is able to self-interact through different domains, in addition to being able to interact with septins (Fig3A-D). This altogether suggests that Mid2 could promote septin compaction by orienting and bundling septin filaments together.

Such hypothesis would be in agreement with results from polarized fluorescence microscopy in *S. cerevisiae* that identified a differential orientation at 90° of septin filaments between the hourglass and split ring stages and showed a role for Mid2 ortholog Bud4 in septin organization at the split ring stage (McQuilken et al., 2017; Vrabioiu and Mitchison, 2006). A decrease in septin intensity at the cell cortex is observed at this transition though (McQuilken et al., 2017), in contrast to the sharp increase observed in *S. pombe* during compaction.

However, in cells blocked in mitosis (n*da3-KM311* cold sensitive or cut7-24 heat-sensitive mutants), septins and Mid2 colocalize in a diffuse network, but do not compact, while Mid2 retains its ability to interact with septins and to self-interact, pointing towards a more complex situation. Several hypothesis can be proposed at this stage to account for these results: 1) post-translational modifications of Mid2 may inhibit its bundling activity for septins when cells are blocked in mitosis, and/or post-translational modifications may be missing at this stage to activate Mid2; 2) Septin bundling by Mid2 may require an additional factor, which may not be available or functional when cells are blocked in mitosis; 3) absence of compaction in mitosis could result from a combination of the two hypothesis.

In support of the first hypothesis, it is known that septins are subject to complex phospho-regulations (Marquardt et al., 2018; Ribet et al., 2017; Tasto et al., 2003) and Mid2 ortholog in in *S. Cerevisiae* Bud4 was shown to be phosphorylated by Cdk1 *in vivo* with impact on cytokinesis outcome in combination with the deletion of the septin kinase Gin4 (Eluère et al, 2012). Mid2 was similarly shown to be hyperphosphorylated in mitosis (Tasto et al., 2003; see also Mid2 slow migration profile in nda3-KM311 blocked cells in FigS3C). We can speculate that this regulation might trigger conformational changes in Mid2 or prevent the formation of high order Mid2 oligomers beyond dimers. This might inhibit its bundling activity until anaphase is triggered, independently of its ability to interact with itself and septins.

By using temperature sensitive cell cycle mutants (Fig4 and 5 and FigS4 and S5), we started to discover the regulatory network controlling septin ring assembly. We found on the one hand that septin and Mid2 recruitment can occur in the presence of high Cdk1 activity, but their compaction is then blocked. On the other hand, the SIN pathway, which activity antagonizes Cdk1 through the Cdc14 phosphatase Clp1/Flp1 at mitotic exit (Cueille et al., 2001; Trautmann et al., 2001), also plays a very important role in septin accumulation and compaction.

These data confirm that septins and Mid2 undergo tightly regulated cell-cycle dependent reorganizations, similarly to what has been described in budding yeast (Glomb and Gronemeyer, 2016; Hernandez-Rodriguez and Momany, 2012). Mass spectrometry analysis of septins and Mid2 in cell cycle mutants led to the identification of a large number of phospho-sites both in Mid2 and septins in mitotic blocked and SIN hyperactive mutants (our unpublished results). The production of phospho-inhibitory and phospho-mimetic mutants may help elucidate the specific role of mitotic and SIN kinases in controlling septin and Mid2 behavior in the future.

Finally, we have uncovered the importance of a PIP2 in the timely recruitment of septins and proper accumulation at the cell division site (Fig6 and FigS6). Septins are known to bind membranes, particularly to negatively charged lipids such as PIP2 domains through a conserved polybasic region

(Bertin et al., 2010; Casamayor and Snyder, 2003; Tanaka-Takiguchi et al., 2009; Zhang et al., 1999). Septins ability to associate with lipid bilayers also appears to be influenced by the curvature of the membrane (Beber et al., 2019; Bridges et al., 2016; McMurray, 2019), suggesting that septins preferentially assemble on membrane surfaces of defined shape and charge. A recent study on *S. cerevisiae* septin Cdc12 demonstrates that this property relies on a C-terminal amphipathic helix, necessary and sufficient for micrometer-range curvature sensing, which also exhibits higher affinity for PIP2 than PI or PS (Cannon et al., 2019). In addition, anillins contain a C-terminal PH domain which may also bind to membrane lipids. In the case of Mid2, the PH domain, is essential for its recruitment at the division site and its function (Berlin et al., 2003; Tasto et al., 2003), but lipid binding or specificity was never tested.

In light of the delayed recruitment of septins in *its3-1* mutant, at the time of CR constriction and Mid2 recruitment to the division site, we can propose a model where septin recruitment is first initiated by PIP2 when the mitotic spindle reaches its maximum length, followed by a second phase of recruitment at time of initiation of CR constriction promoted by Mid2 when it becomes available or activated. In this model, Mid2 could partially compensate for defects in PIP2 in *its3-1* mutant and allow for septin delayed recruitment in limited amounts. An *in vitro* assessment of fission yeast septins and/or Mid2 association with lipid vesicles of different lipid composition or degrees of curvature, would provide additional insights about the impact of membrane lipids and curvature in the process of septin ring assembly.

One important question that remains to be solved is why septins start accumulating in a 1.5 μm wide region surrounding the CR in late anaphase when the spindle reaches maximum length. Since there is no change in membrane curvature at the division site at this stage that could influence septin assembly, but the initial phase of septin accumulation requires PIP2, one tempting hypothesis is that the CR may locally generate a pool of PIP2 in late anaphase that can diffuse to this 1.5 μm wide region to locally promote septin recruitment.

Our results allow us not only to better understand the molecular mechanisms that control the organization of the septin network during cytokinesis progression in fission yeast, but due to their evolutionary conservation (Nishihama et al., 2011; Pan et al., 2007), they may also help to clarify septin behavior in other organisms during cytokinesis or in the plethora of other processes they have been proven to participate in (Bridges and Gladfelter, 2015; Caudron and Barral, 2009; Mostowy and Cossart, 2012; Saarikangas and Barral, 2011). Indeed, mutations or deletions of septins have been reported to lead to several pathologies ranging from reproductive diseases and infections to neurodegenerative disorders and cancer (Angelis and Spiliotis, 2016; Dolat et al., 2014; Lhuillier et al., 2009; Li et al., 2019; Lin et al., 2009; Marttinen et al., 2015; Mostowy and Cossart, 2012; Pous et al., 2016). A better

understanding of the detailed regulations controlling the behavior of these multifunctional proteins may therefore enable new therapeutic approaches for the treatment of many pathologies in the future.

MATERIALS AND METHODS

Yeast genetics and culture

Standard *S. pombe* media and genetic manipulations were used (Moreno et al., 1991). All strains used in the study were isogenic to wild-type 972 and are described in Supplemental Table S1. Strains from genetic crosses were selected by random spore germination and replica in plates with appropriate supplements or drugs.

Transformations were performed by using the Lithium-DTT method. 20 ml of exponentially growing cells (optical density 0.5-0.8) were harvested by centrifugation and washed with 10 mM Tris HCl pH 7.4. After a second centrifugation, they were re-suspended in 100 mM lithium Acetate with 10 mM DTT and were incubated on an orbital wheel at room temperature for 40 minutes. 100 μl of these cells were mixed with 80ul of 100mM lithium acetate, 10 μl of single stranded DNA from salmon testes (D9156-5ML, Sigma) and 2 μg of the desired plasmid or the purified PCR product. After 10 minutes of incubation on an orbital wheel, 300 μl of PEG 4000, previously diluted 1:1 in 100mM Lithium acetate, were added. After a second round of 10 minutes on the wheel, 15 μl of DMSO were added and the cells were subjected to heat shock at 42°C for 20 minutes in a water bath. Cells were plated on selection plates.

Production of mutant and tagged strains.

A mid2 construct tagged with the green fluorescent tag Envy (Slubowski et al., 2015) at its C-terminus was created by PCR from the plasmid pFA6a-Envy-kanMX6 as described (Bahler et al., 1998b).

A mid2 construct fused to the 13XMyc tag at its C-terminus was built by PCR from the plasmid pFA6a-13Xmyc-natMX6 according to Bahler et al. 1998.

An integration plasmid for Mid2 constructs was produced by insertion of 1 kb of the mid2 promoter (*pmid2*) and terminator (*tmid2*) into pFA6a-mEGFP-kanMX6 (Bahler et al 1998) between *SalI* and *BamHI* sites and *PmeI* and *SacII* sites, respectively. The mid2 open reading frame (ORF) was then inserted upstream of mEGFP between *BamHI* and *XmaI*. Full lenght mid2 was replaced between *BamHI* and *XmaI* sites by the single PH domain of Mid2 (582–685aa). pFA6a-GFP-kanMX6-derived plasmid was digested with *Not*I before transformation.

Constructs expressing Mid2-mEGFP full length, Mid2ΔPH-mEGFP (1-581aa) and the C-terminal PH domain of Mid2 (aa 582-685) tagged with mEGFP were integrated at the *leu1* locus under the control of

their own promoter. Briefly, a fragment containing 1 kb of 5` UTR and the ORF of three different mid2 fragments was amplified from genomic DNA purified from a wild-type strain and cloned between *KpnI* and *NotI* sites of pSR2 (pJK148 - Pcdr2-cdr2-GFP-Tnmt1) (Keeney and Boeke, 1994). The plasmids obtained were circularized by *NruI* or *Tth111* digestion to allow integration in the leu1 locus of a wild-type strain.

A construct expressing the single PH domain of Mid2 (582-685aa) was integrated into the leu1 locus under the control of their own promoter. Briefly, a fragment containing 1 kb of 5` UTR and the ORF of the PH domain of Mid2 (582-685aa) was amplified from genomic DNA purified from a wild-type strain and cloned between *KpnI* and *NotI* sites of pSR98 (pJK148 Pcdr2-Cdr2-13xmyc). The plasmid obtained was circularized by *NruI* digestion to allow integration in the leu1 locus of a wild-type strain.

All plasmids were checked by diagnostic PCR and restriction enzyme digestion, and the DNA fragments amplified by PCR were sequenced.

Microscopy and image analysis

Cells were grown at 25°C in YE5S except for cell cycle temperature sensitive (ts) mutants (*cdc7-24, sid2-250, its3-1,*), which were grown for 3 hours at 36°C or *nda3-KM311* cold sensitive (cs) mutants, which were grown up to 7h at 18C.

Epifluorescence images were taken on a DMRXA2 upright microscope (Leica Microsystems), equipped with a 100×/1.4NA oil immersion PlanApo objective and a Coolsnap HQ CCD camera (Photometrics), exposure time: 2s for GFP, 1s for mCherry and 100 ms for DIC light. Quantification in the nda3-KM311 mutant of Spn1-GFP comparison with the red markers signal were realized by drawing a linescan throughout the all cell (Fig4A and FigS2A-B). The average values obtained were detracted of the background measured in the same way outside the cell. The curves obtained were then centered according to the position of the ring.

For time lapse imaging, 1 ml of exponentially growing cells were harvested after a centrifugation of 60s for 3000rpm in a Minispin Eppendorf centrifuge equipped with a F-45-12-11 rotor, the supernatant was discarded and 1 µl of the cells was deposited in a 2% YE5S agar pad at the center of PDMS slide chambers prepared as described in (Costa et al., 2013).

Timelapse movies were performed on an inverted Spinning Disk Confocal (Roper/Nikon), equipped with Plan Apochromat 100×/1.4 NA objective lens (Nikon), a PIFOC (perfect image focus) objective stepper, and a charge-coupled device camera (EMCCD 512x512 QuantEM; Photometrics). To analyze Spn1-GFP Rlc1-mCherry Sid4-mCherry wild type as well as Mid2-ENVY Rlc1-mCherry Sid4-mCherry together with

the respective cell cycle ts and cs mutants, stacks of 7 planes spaced by 1µm were acquired every 1 min for 3h (binning 1, 300 EM gain; 200ms exposure with 6% laser power for GFP and 5.5% laser power for mCherry).
All images were scaled the same to their respective control and analyzed using MetaMorph software 7.7.8.

Analysis of Spn1-GFP and Mid2-ENVY signals were quantified from the time of mitotic entry (SPBs separation) by measuring the average fluorescence intensity of the medial region through linescan (Metamorph software 7.7.8) of 5 µm in length and 13µm in width oriented perpendicular to the long axis of the cell on maximum projection images. Background values, measured as the average intensity of an equivalent region outside of the cell, were then subtracted.

To compare the width of septins and mid2 at the two different data point indicated in the text in control and mutant cells, the linescan tool (MetaMorph software 7.7.8.) was oriented parallel to the long axis of the cell. The values measured derive from the average of 3 measurements within septin or mid2 band.

Coimmunoprecipitation experiments

Coimmunoprecipations experiments were performed as described (Guzman-Vendrell et al., 2013). Briefly, 200 ml of cells were grown to an optical density at 600 nm of 1 at 25°C in YE5S medium concentrated 2 times compared to regular YE5S medium (YE5S2X) and were resuspended in 300 µl of NP40 buffer. Extracts were incubated with anti-mouse IgG magnetic beads (M-280 DYNAL, Invitrogen), coupled to 6 µg of anti-GFP mAb (Roche).
Western blots were probed with anti-GFP mAb (1/500, Roche) or anti-myc mAb 9E10 (1/666, Roche). Secondary antibodies were coupled to peroxydase (Jackson Immunoresearch). Signal quantification was performed with Image Lab 4.0.1 (BioRad). Signals of coimmunoprecipitated proteins were normalized relative to the amount of primarily immunoprecipitated protein.
For *nda3-KM311* synchronization experiments, 1 litre of cells was grown overnight to an optical density of 0.6. Cells were synchronized by 8 hours incubation at 18°C before being processed.

Statistical analysis

Sample size (n) is defined in each figure and derived from 3 independent experiments, except for the Coimmunoprecipitations analysis in Figure S3 that were repeated twice. The error bars correspond standard deviation (SD) between experiments and are specifically indicated in each figure.

REFERENCES

Alonso-Nunez, M. L., An, H., Martin-Cuadrado, A. B., Mehta, S., Petit, C., Sipiczki, M., del Rey, F., Gould, K. L. and de Aldana, C. R. (2005). Ace2p controls the expression of genes required for cell separation in Schizosaccharomyces pombe. *Mol Biol Cell* **16**, 2003-17.

An, H., Morrell, J. L., Jennings, J. L., Link, A. J. and Gould, K. L. (2004). Requirements of fission yeast septins for complex formation, localization, and function. *Mol Biol Cell* **15**, 5551-64.

Angelis, D. and Spiliotis, E. T. (2016). Septin Mutations in Human Cancers. *Front Cell Dev Biol* **4**, 122.

Bahler, J., Wu, J. Q., Longtine, M. S., Shah, N. G., McKenzie, A., 3rd, Steever, A. B., Wach, A., Philippsen, P. and Pringle, J. R. (1998). Heterologous modules for efficient and versatile PCR-based gene targeting in Schizosaccharomyces pombe. *Yeast* **14**, 943-51.

Balasubramanian, M. K., McCollum, D., Chang, L., Wong, K. C., Naqvi, N. I., He, X., Sazer, S. and Gould, K. L. (1998). Isolation and characterization of new fission yeast cytokinesis mutants. *Genetics* **149**, 1265-75.

Beber, A., Alqabandi, M., Prevost, C., Viars, F., Levy, D., Bassereau, P., Bertin, A. and Mangenot, S. (2019). Septin-based readout of PI(4,5)P2 incorporation into membranes of giant unilamellar vesicles. *Cytoskeleton (Hoboken)* **76**, 92-103.

Berlin, A., Paoletti, A. and Chang, F. (2003). Mid2 stabilizes septin rings during cytokinesis in fission yeast. *JCB* **160**, 1083-1092.

Bertin, A., McMurray, M. A., Thai, L., Garcia, G., 3rd, Votin, V., Grob, P., Allyn, T., Thorner, J. and Nogales, E. (2010). Phosphatidylinositol-4,5-bisphosphate promotes budding yeast septin filament assembly and organization. *J Mol Biol* **404**, 711-31.

Bhavsar-Jog, Y. P. and Bi, E. (2017). Mechanics and regulation of cytokinesis in budding yeast. *Semin Cell Dev Biol* **66**, 107-118.

Bi, E., Maddox, P., Lew, D. J., Salmon, E. D., McMillan, J. N., Yeh, E. and Pringle, J. R. (1998). Involvement of an actomyosin contractile ring in Saccharomyces cerevisiae cytokinesis. *J Cell Biol* **142**, 1301-12.

Bridges, A. A. and Gladfelter, A. S. (2015). Septin Form and Function at the Cell Cortex. *J Biol Chem* **290**, 17173-80.

Bridges, A. A., Jentzsch, M. S., Oakes, P. W., Occhipinti, P. and Gladfelter, A. S. (2016). Micron-scale plasma membrane curvature is recognized by the septin cytoskeleton. *J Cell Biol* **213**, 23-32.

Cannon, K. S., Woods, B. L., Crutchley, J. M. and Gladfelter, A. S. (2019). An amphipathic helix enables septins to sense micrometer-scale membrane curvature. *J Cell Biol* **218**, 1128-1137.

Casamayor, A. and Snyder, M. (2003). Molecular dissection of a yeast septin: distinct domains are required for septin interaction, localization, and function. *Mol Cell Biol* **23**, 2762-77.

Caudron, F. and Barral, Y. (2009). Septins and the lateral compartmentalization of eukaryotic membranes. *Dev Cell* **16**, 493-506.

Cauvin, C. and Echard, A. (2015). Phosphoinositides: Lipids with informative heads and mastermind functions in cell division. *Biochim Biophys Acta* **1851**, 832-43.

Cortes, J. C., Ramos, M., Osumi, M., Perez, P. and Ribas, J. C. (2016). Fission yeast septation. *Commun Integr Biol* **9**, e1189045.

Costa, J., Fu, C., Syrovatkina, V. and Tran, P. T. (2013). Imaging individual spindle microtubule dynamics in fission yeast. *Methods Cell Biol* **115**, 385-94.

Cueille, N., Salimova, E., Esteban, V., Blanco, M., Moreno, S., Bueno, A. and Simanis, V. (2001). Flp1, a fission yeast orthologue of the s. cerevisiae CDC14 gene, is not required for cyclin degradation or rum1p stabilisation at the end of mitosis. *J Cell Sci* **114**, 2649-64.

Dobbelaere, J. and Barral, Y. (2004). Spatial coordination of cytokinetic events by compartmentalization of the cell cortex. *Science* **305**, 393-6.

Dolat, L., Hu, Q. and Spiliotis, E. T. (2014). Septin functions in organ system physiology and pathology. *Biol Chem* **395**, 123-41.

Echard, A. (2012). Phosphoinositides and cytokinesis: the "PIP" of the iceberg. *Cytoskeleton (Hoboken)* **69**, 893-912.

Echard, A., Hickson, G. R., Foley, E. and O'Farrell, P. H. (2004). Terminal cytokinesis events uncovered after an RNAi screen. *Curr Biol* **14**, 1685-93.

El Amine, N., Kechad, A., Jananji, S. and Hickson, G. R. (2013). Opposing actions of septins and Sticky on Anillin promote the transition from contractile to midbody ring. *J Cell Biol* **203**, 487-504.

Eluere, R., Varlet, I., Bernadac, A. and Simon, M. N. (2012). Cdk and the anillin homolog Bud4 define a new pathway regulating septin organization in yeast. *Cell Cycle* **11**, 151-8.

Estey, M. P., Di Ciano-Oliveira, C., Froese, C. D., Bejide, M. T. and Trimble, W. S. (2010). Distinct roles of septins in cytokinesis: SEPT9 mediates midbody abscission. *J Cell Biol* **191**, 741-9.

Ewers, H., Tada, T., Petersen, J. D., Racz, B., Sheng, M. and Choquet, D. (2014). A Septin-Dependent Diffusion Barrier at Dendritic Spine Necks. *PLoS One* **9**, e113916.

Field, C. M., Coughlin, M., Doberstein, S., Marty, T. and Sullivan, W. (2005). Characterization of anillin mutants reveals essential roles in septin localization and plasma membrane integrity. *Development* **132**, 2849-60.

Fu, C., Ward, J. J., Loiodice, I., Velve-Casquillas, G., Nedelec, F. J. and Tran, P. T. (2009). Phospho-regulated interaction between kinesin-6 Klp9p and microtubule bundler Ase1p promotes spindle elongation. *Dev Cell* **17**, 257-67.

Fujiwara, T., Bandi, M., Nitta, M., Ivanova, E. V., Bronson, R. T. and Pellman, D. (2005). Cytokinesis failure generating tetraploids promotes tumorigenesis in p53-null cells. *Nature* **437**, 1043-7.

Garcia, G., 3rd, Bertin, A., Li, Z., Song, Y., McMurray, M. A., Thorner, J. and Nogales, E. (2011). Subunit-dependent modulation of septin assembly: budding yeast septin Shs1 promotes ring and gauze formation. *J Cell Biol* **195**, 993-1004.

Gladfelter, A. S., Pringle, J. R. and Lew, D. J. (2001). The septin cortex at the yeast mother–bud neck. *Current Opinion in Microbiology* **4**, 681–689.

Glomb, O. and Gronemeyer, T. (2016). Septin Organization and Functions in Budding Yeast. *Front Cell Dev Biol* **4**, 123.

Guzman-Vendrell, M., Baldissard, S., Almonacid, M., Mayeux, A., Paoletti, A. and Moseley, J. B. (2013). Blt1 and Mid1 provide overlapping membrane anchors to position the division plane in fission yeast. *Mol Cell Biol* **33**, 418-28.

Hagan, I. and Yanagida, M. (1990). Novel potential mitotic motor protein encoded by the fission yeast cut7+ gene. *Nature* **347**, 563-6.

Hagan, I. and Yanagida, M. (1992). Kinesin-related cut7 protein associates with mitotic and meiotic spindles in fission yeast. *Nature* **356**, 74-6.

Hall, P. A., Russell, H. S. E. and Pringle, J. R. (2008). The Septins.

Hartwell, L. H. (1971). Genetic control of the cell division cycle in yeast. IV. Genes controlling bud emergence and cytokinesis. *Exp Cell Res* **69**, 265-76.

Hergovich, A., Stegert, M. R., Schmitz, D. and Hemmings, B. A. (2006). NDR kinases regulate essential cell processes from yeast to humans. *Nat Rev Mol Cell Biol* **7**, 253-64.

Hernandez-Rodriguez, Y. and Momany, M. (2012). Posttranslational modifications and assembly of septin heteropolymers and higher-order structures. *Curr Opin Microbiol* **15**, 660-8.

Hu, Q., Milenkovic, L., Jin, H., Scott, M. P., Nachury, M. V., Spiliotis, E. T. and Nelson, W. J. (2010). A septin diffusion barrier at the base of the primary cilium maintains ciliary membrane protein distribution. *Science* **329**, 436-9.

Ihara, M., Kinoshita, A., Yamada, S., Tanaka, H., Tanigaki, A., Kitano, A., Goto, M., Okubo, K., Nishiyama, H., Ogawa, O. et al. (2005). Cortical organization by the septin cytoskeleton is essential for structural and mechanical integrity of mammalian spermatozoa. *Dev Cell* **8**, 343-52.

Iwase, M., Luo, J., Nagaraj, S., Longtine, M., Kim, H. B., Haarer, B. K., Caruso, C., Tong, Z., Pringle, J. R. and Bi, E. (2006). Role of a Cdc42p effector pathway in recruitment of the yeast septins to the presumptive bud site. *Mol Biol Cell* **17**, 1110-25.

Johnson, E. S. and Blobel, G. (1999). Cell cycle-regulated attachment of the ubiquitin-related protein SUMO to the yeast septins. *J Cell Biol* **147**, 981-94.

Juanes, M. A. and Piatti, S. (2016). The final cut: cell polarity meets cytokinesis at the bud neck in S. cerevisiae. *Cell Mol Life Sci* **73**, 3115-36.

Kang, P. J., Hood-DeGrenier, J. K. and Park, H. O. (2013). Coupling of septins to the axial landmark by Bud4 in budding yeast. *J Cell Sci* **126**, 1218-26.

Karasmanis, E. P., Hwang, D., Nakos, K., Bowen, J. R., Angelis, D. and Spiliotis, E. T. (2019). A Septin Double Ring Controls the Spatiotemporal Organization of the ESCRT Machinery in Cytokinetic Abscission. *Curr Biol* **29**, 2174-2182 e7.

Kechad, A., Jananji, S., Ruella, Y. and Hickson, G. R. (2012). Anillin acts as a bifunctional linker coordinating midbody ring biogenesis during cytokinesis. *Curr Biol* **22**, 197-203.

Keeney, J. B. and Boeke, J. D. (1994). Efficient targeted integration at leu1-32 and ura4-294 in Schizosaccharomyces pombe. *Genetics* **136**, 849-56.

Kim, H., Johnson, J. M., Lera, R. F., Brahma, S. and Burkard, M. E. (2017). Anillin Phosphorylation Controls Timely Membrane Association and Successful Cytokinesis. *PLoS Genet* **13**, e1006511.

Kim, M. S., Froese, C. D., Estey, M. P. and Trimble, W. S. (2011). SEPT9 occupies the terminal positions in septin octamers and mediates polymerization-dependent functions in abscission. *J Cell Biol* **195**, 815-26.

Kinoshita, M., Field, C. M., Coughlin, M. L., Straight, A. F. and Mitchison, T. J. (2002). Self- and actin-templated assembly of Mammalian septins. *Dev Cell* **3**, 791-802.

Kinoshita, M., Kumar, S., Mizoguchi, A., Ide, C., Kinoshita, A., Haraguchi, T., Hiraoka, Y. and Noda, M. (1997). Nedd5, a mammalian septin, is a novel cytoskeletal component interacting with actin-based structures. *Genes Dev* **11**, 1535-47.

Kozubowski, L., Larson, J. R. and Tatchell, K. (2005). Role of the septin ring in the asymmetric localization of proteins at the mother-bud neck in Saccharomyces cerevisiae. *Mol Biol Cell* **16**, 3455-66.

Krapp, A., Gulli, M. P. and Simanis, V. (2004). SIN and the art of splitting the fission yeast cell. *Curr Biol* **14**, R722-30.

Krokowski, S., Lobato-Marquez, D., Chastanet, A., Pereira, P. M., Angelis, D., Galea, D., Larrouy-Maumus, G., Henriques, R., Spiliotis, E. T., Carballido-Lopez, R. et al. (2018). Septins Recognize and Entrap Dividing Bacterial Cells for Delivery to Lysosomes. *Cell Host Microbe* **24**, 866-874 e4.

Kuo, Y. C., Shen, Y. R., Chen, H. I., Lin, Y. H., Wang, Y. Y., Chen, Y. R., Wang, C. Y. and Kuo, P. L. (2015). SEPT12 orchestrates the formation of mammalian sperm annulus by organizing core octameric complexes with other SEPT proteins. *J Cell Sci* **128**, 923-34.

Lacroix, B. and Maddox, A. S. (2012). Cytokinesis, ploidy and aneuploidy. *J Pathol* **226**, 338-51.

Lee, I. J., Coffman, V. C. and Wu, J. Q. (2012). Contractile-ring assembly in fission yeast cytokinesis: Recent advances and new perspectives. *Cytoskeleton (Hoboken)* **69**, 751-63.

Lhuillier, P., Rode, B., Escalier, D., Lores, P., Dirami, T., Bienvenu, T., Gacon, G., Dulioust, E. and Toure, A. (2009). Absence of annulus in human asthenozoospermia: case report. *Hum Reprod* **24**, 1296-303.

Li, H., Saucedo-Cuevas, L., Yuan, L., Ross, D., Johansen, A., Sands, D., Stanley, V., Guemez-Gamboa, A., Gregor, A., Evans, T. et al. (2019). Zika Virus Protease Cleavage of Host Protein Septin-2 Mediates Mitotic Defects in Neural Progenitors. *Neuron* **101**, 1089-1098 e4.

Lin, Y. H., Lin, Y. M., Wang, Y. Y., Yu, I. S., Lin, Y. W., Wang, Y. H., Wu, C. M., Pan, H. A., Chao, S. C., Yen, P. H. et al. (2009). The expression level of septin12 is critical for spermiogenesis. *Am J Pathol* **174**, 1857-68.

Lippincott, J. and Li, R. (1998). Sequential assembly of myosin II, an IQGAP-like protein, and filamentous actin to a ring structure involved in budding yeast cytokinesis. *J Cell Biol* **140**, 355-66.

Maddox, A. S., Lewellyn, L., Desai, A. and Oegema, K. (2007). Anillin and the septins promote asymmetric ingression of the cytokinetic furrow. *Dev Cell* **12**, 827-35.

Marquardt, J., Chen, X. and Bi, E. (2018). Architecture, remodeling, and functions of the septin cytoskeleton. *Cytoskeleton (Hoboken)* **76**, 7-14.

Martin-Cuadrado, A. B., Morrell, J. L., Konomi, M., An, H., Petit, C., Osumi, M., Balasubramanian, M., Gould, K. L., Del Rey, F. and de Aldana, C. R. (2005). Role of septins and the exocyst complex in the function of hydrolytic enzymes responsible for fission yeast cell separation. *Mol Biol Cell* **16**, 4867-81.

Marttinen, M., Kurkinen, K. M., Soininen, H., Haapasalo, A. and Hiltunen, M. (2015). Synaptic dysfunction and septin protein family members in neurodegenerative diseases. *Mol Neurodegener* **10**, 16.

Mavrakis, M., Azou-Gros, Y., Tsai, F. C., Alvarado, J., Bertin, A., Iv, F., Kress, A., Brasselet, S., Koenderink, G. H. and Lecuit, T. (2014). Septins promote F-actin ring formation by crosslinking actin filaments into curved bundles. *Nat Cell Biol* **16**, 322-34.

McCollum, D. and Gould, K. L. (2001). Timing is everything: regulation of mitotic exit and cytokinesis by the MEN and SIN. *Trends Cell Biol* **11**, 89-95.

McMurray, M. A. (2019). The long and short of membrane curvature sensing by septins. *J Cell Biol* **218**, 1083-1085.

McMurray, M. A. and Thorner, J. (2009). Septins: molecular partitioning and the generation of cellular asymmetry. *Cell Div* **4**, 18.

McQuilken, M., Jentzsch, M. S., Verma, A., Mehta, S. B., Oldenbourg, R. and Gladfelter, A. S. (2017). Analysis of Septin Reorganization at Cytokinesis Using Polarized Fluorescence Microscopy. *Front. Cell Dev. Biol.* **5**, 42.

Meitinger, F. and Palani, S. (2016). Actomyosin ring driven cytokinesis in budding yeast. *Semin Cell Dev Biol* **53**, 19-27.

Mitchell, L., Lau, A., Lambert, J. P., Zhou, H., Fong, Y., Couture, J. F., Figeys, D. and Baetz, K. (2011). Regulation of septin dynamics by the Saccharomyces cerevisiae lysine acetyltransferase NuA4. *PLoS One* **6**, e25336.

Moreno, S., Klar, A. and Nurse, P. (1991). Molecular genetic analysis of fission yeast Schizosaccharomyces pombe. *Methods Enzymol* **194**, 795-823.

Mostowy, S., Bonazzi, M., Hamon, M. A., Tham, T. N., Mallet, A., Lelek, M., Gouin, E., Demangel, C., Brosch, R., Zimmer, C. et al. (2010). Entrapment of intracytosolic bacteria by septin cage-like structures. *Cell Host Microbe* **8**, 433-44.

Mostowy, S. and Cossart, P. (2012). Septins: the fourth component of the cytoskeleton. *Nat Rev Mol Cell Biol* **13**, 183-94.

Nishihama, R., Onishi, M. and Pringle, J. R. (2011). New insights into the phylogenetic distribution and evolutionary origins of the septins. *Biol Chem* **392**, 681-7.

Oegema, K., Savoian, M. S., Mitchison, T. J. and Field, C. M. (2000). Functional analysis of a human homologue of the Drosophila actin binding protein anillin suggests a role in cytokinesis. *J Cell Biol* **150**, 539-52.

Onishi, M., Koga, T., Hirata, A., Nakamura, T., Asakawa, H., Shimoda, C., Bahler, J., Wu, J. Q., Takegawa, K., Tachikawa, H. et al. (2010). Role of septins in the orientation of forespore membrane extension during sporulation in fission yeast. *Mol Cell Biol* **30**, 2057-74.

Pan, F., Malmberg, R. L. and Momany, M. (2007). Analysis of septins across kingdoms reveals orthology and new motifs. *BMC Evol Biol* **7**, 103.

Perez, P., Cortes, J. C., Martin-Garcia, R. and Ribas, J. C. (2016). Overview of fission yeast septation. *Cell Microbiol* **18**, 1201-7.

Petit, C. S., Mehta, S., Roberts, R. H. and Gould, K. L. (2005). Ace2p contributes to fission yeast septin ring assembly by regulating mid2+ expression. *J Cell Sci* **118**, 5731-42.

Piekny, A. J. and Maddox, A. S. (2010). The myriad roles of Anillin during cytokinesis. *Semin Cell Dev Biol* **21**, 881-91.

Pollard, T. D. and Wu, J. Q. (2010). Understanding cytokinesis: lessons from fission yeast. *Nat Rev Mol Cell Biol* **11**, 149-55.

Pous, C., Klipfel, L. and Baillet, A. (2016). Cancer-Related Functions and Subcellular Localizations of Septins. *Front Cell Dev Biol* **4**, 126.

Renshaw, M. J., Liu, J., Lavoie, B. D. and Wilde, A. (2014). Anillin-dependent organization of septin filaments promotes intercellular bridge elongation and Chmp4B targeting to the abscission site. *Open Biol* **4**, 130190.

Ribet, D., Boscaini, S., Cauvin, C., Siguier, M., Mostowy, S., Echard, A. and Cossart, P. (2017). SUMOylation of human septins is critical for septin filament bundling and cytokinesis. *J Cell Biol* **216**, 4041-4052.

Rincon, S. A. and Paoletti, A. (2012). Mid1/anillin and the spatial regulation of cytokinesis in fission yeast. *Cytoskeleton (Hoboken)* **69**, 764-77.

Rincon, S. A. and Paoletti, A. (2016). Molecular control of fission yeast cytokinesis. *Semin Cell Dev Biol* **53**, 28-38.

Saarikangas, J. and Barral, Y. (2011). The emerging functions of septins in metazoans. *EMBO Rep* **12**, 1118-26.

Simanis, V. (2003). Events at the end of mitosis in the budding and fission yeasts. *J Cell Sci* **116**, 4263-75.

Simanis, V. (2015). Pombe's thirteen - control of fission yeast cell division by the septation initiation network. *J Cell Sci* **128**, 1465-74.

Slubowski, C. J., Funk, A. D., Roesner, J. M., Paulissen, S. M. and Huang, L. S. (2015). Plasmids for C-terminal tagging in Saccharomyces cerevisiae that contain improved GFP proteins, Envy and Ivy. *Yeast* **32**, 379-87.

Snider, C. E., Willet, A. H., Brown, H. T. and Gould, K. L. (2018). Analysis of the contribution of phosphoinositides to medial septation in fission yeast highlights the importance of PI(4,5)P2 for medial contractile ring anchoring. *Mol Biol Cell* **29**, 2148-2155.

Somma, M. P., Fasulo, B., Cenci, G., Cundari, E. and Gatti, M. (2002). Molecular dissection of cytokinesis by RNA interference in Drosophila cultured cells. *Mol Biol Cell* **13**, 2448-60.

Sparks, C. A., Morphew, M. and McCollum, D. (1999). Sid2p, a spindle pole body kinase that regulates the onset of cytokinesis. *J Cell Biol* **146**, 777-90.

Spiliotis, E. T. (2018). Spatial effects - site-specific regulation of actin and microtubule organization by septin GTPases. *J Cell Sci* **131**.

Storchova, Z. and Pellman, D. (2004). From polyploidy to aneuploidy, genome instability and cancer. *Nat Rev Mol Cell Biol* **5**, 45-54.

Straight, A. F., Field, C. M. and Mitchison, T. J. (2005). Anillin binds nonmuscle myosin II and regulates the contractile ring. *Mol Biol Cell* **16**, 193-201.

Tada, T., Simonetta, A., Batterton, M., Kinoshita, M., Edbauer, D. and Sheng, M. (2007). Role of Septin cytoskeleton in spine morphogenesis and dendrite development in neurons. *Curr Biol* **17**, 1752-8.

Takahashi, Y., Iwase, M., Konishi, M., Tanaka, M., Toh-e, A. and Kikuchi, Y. (1999). Smt3, a SUMO-1 homolog, is conjugated to Cdc3, a component of septin rings at the mother-bud neck in budding yeast. *Biochem Biophys Res Commun* **259**, 582-7.

Tanaka-Takiguchi, Y., Kinoshita, M. and Takiguchi, K. (2009). Septin-mediated uniform bracing of phospholipid membranes. *Curr Biol* **19**, 140-5.

Tasto, J. J., Morrell, J. L. and Gould, K. L. (2003). An anillin homologue, Mid2p, acts during fission yeast cytokinesis to organize the septin ring and promote cell separation. *J Cell Biol* **160**, 1093-103.

Trautmann, S., Wolfe, B. A., Jorgensen, P., Tyers, M., Gould, K. L. and McCollum, D. (2001). Fission yeast Clp1p phosphatase regulates G2/M transition and coordination of cytokinesis with cell cycle progression. *Curr Biol* **11**, 931-40.

Versele, M. and Thorner, J. (2005). Some assembly required: yeast septins provide the instruction manual. *Trends Cell Biol* **15**, 414-24.

Vrabioiu, A. M. and Mitchison, J. M. (2006). Structural insights into yeast septin organization from polarized fluorescence microscopy. *Nature* **443**, 466-469.

Wloka, C., Nishihama, R., Onishi, M., Oh, Y., Hanna, J., Pringle, J. R., Krauss, M. and Bi, E. (2011). Evidence that a septin diffusion barrier is dispensable for cytokinesis in budding yeast. *Biol Chem* **392**, 813-29.

Wu, H., Guo, J., Zhou, Y. T. and Gao, X. D. (2015). The anillin-related region of Bud4 is the major functional determinant for Bud4's function in septin organization during bud growth and axial bud site selection in budding yeast. *Eukaryot Cell* **14**, 241-51.

Wu, J. Q., Kuhn, J. R., Kovar, D. R. and Pollard, T. D. (2003). Spatial and temporal pathway for assembly and constriction of the contractile ring in fission yeast cytokinesis. *Dev Cell* **5**, 723-34.

Wu, J. Q., Ye, Y., Wang, N., Pollard, T. D. and Pringle, J. R. (2010). Cooperation between the septins and the actomyosin ring and role of a cell-integrity pathway during cell division in fission yeast. *Genetics* **186**, 897-915.

Zhang, J., Kong, C., Xie, H., McPherson, P. S., Grinstein, S. and Trimble, W. S. (1999). Phosphatidylinositol polyphosphate binding to the mammalian septin H5 is modulated by GTP. *Curr Biol* **9**, 1458-67.

Zhang, Y., Sugiura, R., Lu, Y., Asami, M., Maeda, T., Itoh, T., Takenawa, T., Shuntoh, H. and Kuno, T. (2000). Phosphatidylinositol 4-phosphate 5-kinase Its3 and calcineurin Ppb1 coordinately regulate cytokinesis in fission yeast. *J Biol Chem* **275**, 35600-6.

Zhao, W. M. and Fang, G. (2005). Anillin is a substrate of anaphase-promoting complex/cyclosome (APC/C) that controls spatial contractility of myosin during late cytokinesis. *J Biol Chem* **280**, 33516-24.

Zheng, S., Dong, F., Rasul, F., Yao, X., Jin, Q. W., Zheng, F. and Fu, C. (2018). Septins regulate the equatorial dynamics of the separation initiation network kinase Sid2p and glucan synthases to ensure proper cytokinesis. *FEBS J* **285**, 2468-2480.

FIGURE LEGENDS

Figure 1: Dynamics of septins and Mid2 during cell division.

Time lapse imaging of wild type cells expressing Spn1-GFP, Rlc1-mCherry and Sid4-mCherry (**A**) or Mid2-ENVY, Rlc1-mCherry and Sid4-mCherry (**B**) grown at 25°C. Max projections of confocal images are shown. Time 0 corresponds to mitotic entry. Scale bars: 2 µm. **C:** Kymographs showing the medial region of the cell expressing Spn1-GFP Rlc1-mCherry (left) or Mid2-ENVY Rlc1-mCherry (right). Every image corresponds to 1-minute interval. The major transitions in their behavior are highlighted at the far right, in bigger panels and indicated with a star. **D:** Plot depicting the timing of Spn1-GFP transitions throughout cell division. Mean ± sd are shown. N=51 cells. **E:** Plot showing the dynamics of Mid2-ENVY throughout cell division. Mean ± sd are shown. N=51 cells. **F:** Analysis of Spn1-GFP (light green) and Mid2-ENVY (dark green) intensities from mitotic onset throughout cell division. The average curves ± sd are displayed. N=6 cells. **G:** Quantification of the extent of Spn1-GFP (light green) and Mid2-ENVY (dark green) width compaction over the time. N=30 cells

Figure 2: Defects in septins behavior in the absence of Mid2.

Time lapse imaging of wild type (**A**) and *mid2Δ* cells (**B**) expressing Spn1-GFP, Rlc1-mCherry and Sid4-mCherry grown at 25°C. Max projections of confocal images are shown. Time 0 corresponds to mitotic entry. Scale bars: 2 µm. **C:** Kymographs showing the medial region of wild type (left) or *mid2Δ* cells (right) expressing Spn1-GFP, Rlc1-mCherry and Sid4-mCherry. Each frame corresponds to 1 min interval. The major transitions in Spn1-GFP dynamics and the defects observed in absence of *mid2* are highlighted in bigger panels at the far right and indicated with a star. **D:** Plot displaying the dynamics of Spn1-GFP throughout cell division. Mean ± sd are shown. N=52 cells. **E:** Plot showing the dynamics of Spn1-GFP in *mid2Δ* cells during cytokinesis. Mean ± sd are shown. N=52 cells. **F:** Analysis of Spn1-GFP intensity in wild type (green) and in *mid2Δ* cells (orange) from mitotic onset throughout cell division. The average curves ± sd are displayed. N=6 cells. **G:** Quantification of the extent of Spn1-GFP width compaction over the time in wild type (green) and in *mid2Δ* cells (orange). N=20 cells

Figure 3: Mid2 interacts with other Mid2 molecule from different regions of the protein.

A: Coimmunoprecipitation assay between Mid2-13XMyc and Mid2_FL-GFP (full length) or Mid2_ΔPH-GFP in the presence (*spn1⁺*) or absence of Spn1 (*spn1Δ*). **B:** Quantification of western blot signals from three independent experiments. Error bars, SD. **C:** Coimmunoprecipitation assay between the PH domain of Mid2 tagged with 13XMyc and the PH domain of Mid2 tagged with GFP in the presence (*spn1⁺*) or absence of Spn1 (*spn1Δ*). **D:** Quantification of western blot signals from three independent experiments. Error bars, SD. **E:** Diagram showing the structure of the anillin-like protein Mid2 with the main domains highlighted.

Figure 4: Septins accumulate as a broad band at the cell middle under high Cdk1 activity.

A: Epifluorescence images of cells expressing Spn1-GFP Rlc1-mCherry Sid4-mCherry (left panels) or Mid2-ENVY Rlc1-mCherry Sid4-mCherry (right panels) in wild type or *nda3-KM311* cells growing at 18C during 4 hours. Fluorescence intensity analysis of Spn1-GFP, Rlc1-mCherry and Sid4-mCherry signals along the entire cell length of *nda3-KM311* cells incubated for 7 hours at 18°C. N=10 cells (far right panel). Time lapse imaging of wild type (**B**) or *cut7-24* cells (**D**) expressing Spn1-GFP, Rlc1-mCherry and Sid4-mCherry grown at 36°C. Max projections of confocal images are shown. Time 0 corresponds to mitotic entry. Scale bars: 2 µm. Plot showing Spn1-GFP transitions throughout cell division in the wild type (**C**) or the *cut7-24* mutant (**E**). Mean ± sd are shown. N=45 cells in each case. **F:** Quantification of the extent of Spn1-GFP width compaction over the time in wild type (green) and in *cut7-24* cells (orange). N=20 cells **G:** Analysis of Spn1-GFP intensity from mitotic onset throughout cell division in control (light green) and *cut7-24* cells (orange). The average curves ± sd are displayed. N=6 cells

Figure 5: Septins show defects in compaction and recruitment under low SIN activity.

Time lapse imaging of wild type (**A**) and *sid2-250* cells showing no compaction (**B**) or a loose compaction (**C**), expressing Spn1-GFP, Rlc1-mCherry and Sid4-mCherry incubated at 36ºC. Max projections of confocal images are shown. Time 0 corresponds to mitotic entry. Scale bars: 2 µm. Plot showing Spn1-GFP transitions throughout cell division in wild type (**D**) or *sid2-250* cells (**E**). Mean ± sd are shown. Wild type N=58 cells. *sid2-250* N=70 cells. **F:** Analysis of Spn1-GFP intensity from mitotic onset throughout cell division in control (light green) and *sid2-250* cells (orange). The average curves ± sd are displayed. N=6 cells. **G:** Quantification of the extent of Spn1-GFP width compaction over the time in wild type (green) and *sid2-250* cells displaying the phenotype 1 (orange) or the phenotype 2 (dark yellow). N=20 cells

Figure 6: Septin appearance and accumulation at the division site are impaired upon reduced PIP2 levels.

Time lapse imaging at 36°C of wild type (**A**) and *its3-1* cells (**C**) expressing Spn1-GFP, Rlc1-mCherry and Sid4-mCherry incubated at 36ºC. Max projections of confocal images are shown. Time 0 corresponds to mitotic entry. Scale bars: 2 µm. Plot displaying Spn1-GFP dynamics throughout cell division in control (**B**) and *its3-1* cells (**D**) cells. Mean ± sd are shown. Wild type N=58 cells. *its3-1* N=83 cells. **E:** Quantification of the extent of Spn1-GFP width compaction over the time in wild type (green) and in *its3-1* cells. N=20 cells. **F:** Analysis of Spn1-GFP intensity from mitotic onset throughout cell division in control (light green) and *its3-1* mutant cells (orange). The average curves ± sd are displayed. N=6 cells. The red arrow highlights the delay in Spn1-GFP appearance in the *its3-1* mutant.

SUPPLEMENTAL INFORMATION

Table S1. Table of strains used in this study.

Strain	Genotype	Source or reference
	Figure 1	
AP5501	*spn1-GFP:kanMX6, rlc1-mcherry:natMX6, sid4-mcherry:hphMX6 ade6-M210 ura4-D18 leu1-32*	This study
AP5678	*mid2-Envy:kanMX6, rlc1-mcherry:natMX6, sid4-mcherry:hphMX6 ade6-M210 ura4-D18 leu1-32*	This study
	Figure 2 and Figure S1	
AP5501	*spn1-GFP:kanMX6, rlc1-mcherry:natMX6, sid4-mcherry:hphMX6 ade6-M210 ura4-D18 leu1-32*	This study
AP5582	*spn1-GFP:kanMX6, mid2::kanMX6, rlc1-mcherry:natMX6, sid4-mcherry:hphMX6 ade6-M210 ura4-D18 leu1-32*	This study
	Figure 3	
AP5501	*spn1-GFP:kanMX6, rlc1-mcherry:natMX6, sid4-mcherry:hphMX6 ade6-M210 ura4-D18 leu1-32*	This study
AP5582	*mid2::kanMX6, spn1-GFP:kanMX6, rlc1-mcherry:natMX6, sid4-mcherry:hphMX6 ade6-M210 ura4-D18 leu1-32*	This study
AP5823	*mid2-13xmyc:Nat ade6-M210 ura4-D18 leu1-32*	This study
AP5831	*leu1^{+}:Pmid1-mid2-GFP mid2-13xmyc:Nat ade6-M210 ura4-D18 leu1-32*	This study
AP5829	*leu1^{+}:Pmid1-mid2ΔPH-GFP mid2-13xmyc:Nat ade6-M210 ura4-D18 leu1-32*	This study
AP5918	*spn1Δ::ura4+ mid2-13xmyc:Nat ade6-M210 ura4-D18 leu1-32*	This study
AP5920	*spn1Δ::ura4+ leu1^{+}:Pmid1-mid2-GFP mid2-13xmyc:Nat ade6-M210 ura4-D18 leu1-32*	This study
AP5927	*spn1Δ::ura4+ leu1^{+}:Pmid1-mid2ΔPH-GFP mid2-13xmyc:Nat ade6-M210 ura4-D18 leu1-32*	This study
AP5814	*leu1^{+}:Pmid1-PHmid2-13xmyc ade6-M210 ura4-D18 leu1-32*	This study
AP5932	*PHmid2-GFP:kanMX6, leu1^{+}:Pmid1-PHmid2-13xmyc ade6-M210 ura4-D18 leu1-32*	This study
AP5930	*spn1Δ::ura4+ leu1^{+}:Pmid1-PHmid2-13xmyc ade6-M210 ura4-D18 leu1-32*	This study

AP5943	*spn1Δ::ura4+PHmid2-GFP:kanMX6, leu1⁺:Pmid1-PHmid2-13xmyc ade6-M210 ura4-D18 leu1-32*	This study
	Figure 4	
AP5501	*spn1-GFP:kanMX6, rlc1-mcherry:natMX6, sid4-mcherry:hphMX6 ade6-M210 ura4-D18 leu1-32*	This study
AP5515	*spn1-GFP:kanMX6, rlc1-mcherry:natMX6, sid4-mcherry:hphMX6 nda3-KM311 ade6-M210 ura4-D18 leu1-32*	This study
AP6268	*spn1-GFP:kanMX6, rlc1-mcherry:natMX6, sid4-mcherry:hphMX6 cut7-24 ade6-M210 ura4-D18 leu1-32*	This study
AP5678	*mid2-Envy:kanMX6, rlc1-mcherry:natMX6, sid4-mcherry:hphMX6 ade6-M210 ura4-D18 leu1-32*	This study
AP5514	*mid2-Envy:kanMX6, rlc1-mcherry:natMX6, sid4-mcherry:hphMX6 nda3-KM311 ade6-M210 ura4-D18 leu1-32*	This study
	Figure 5	
AP5501	*spn1-GFP:kanMX6, rlc1-mcherry:natMX6, sid4-mcherry:hphMX6 ade6-M210 ura4-D18 leu1-32*	This study
AP5585	*spn1-GFP:kanMX6, rlc1-mcherry:natMX6, sid4-mcherry:hphMX6 sid2-250 ade6-M210 ura4-D18 leu1-32*	This study
	Figure 6	
AP5501	*spn1-GFP:kanMX6, rlc1-mcherry:natMX6, sid4-mcherry:hphMX6 ade6-M210 ura4-D18 leu1-32*	This study
AP5876	*spn1-GFP:kanMX6, rlc1-mcherry:natMX6, sid4-mcherry:hphMX6 its3-1 ade6-M210 ura4-D18 leu1-32*	This study
	Figure S2	
AP5501	*spn1-GFP:kanMX6, rlc1-mcherry:natMX6, sid4-mcherry:hphMX6 ade6-M210 ura4-D18 leu1-32*	This study
AP5515	*spn1-GFP:kanMX6, rlc1-mcherry:natMX6, sid4-mcherry:hphMX6 nda3-KM311 ade6-M210 ura4-D18 leu1-32*	This study
AP5678	*mid2-Envy:kanMX6, rlc1-mcherry:natMX6, sid4-mcherry:hphMX6 ade6-M210 ura4-D18 leu1-32*	This study
AP5514	*mid2-Envy:kanMX6, rlc1-mcherry:natMX6, sid4-mcherry:hphMX6 nda3-KM311 ade6-M210 ura4-D18 leu1-32*	This study
	Figure S3	

AP6274	*Mid2-13xmyc:natMX6 nda3-KM311 ade6-M210 ura4-D18 leu1-32*	This study
AP6069	*Mid2FL-GFP:leu1+ Mid2-13xmyc:natMX6 nda3-KM311 ade6-M210 ura4-D18 leu1-32*	This study
AP6073	*Mid2ΔPH-GFP:leu1+ Mid2-13xmyc:natMX6 nda3-KM311 ade6-M210 ura4-D18 leu1-32*	This study
AP6074	*PHmid2-GFP:leu1+ Mid2-13myc:NatMX6 nda3-KM311 ade6-M210 ura4-D18 leu1-32*	This study
AP5823	*mid2-13xmyc:Nat ade6-M210 ura4-D18 leu1-32*	This study
AP6276	*Spn1-GFP:KanMX6 Mid2-13XMyc:natMX6 ura4-D18 leu1-32*	This study
AP6280	*Spn1-GFP:KanMX6 Mid2-13XMyc:natMX6 nda3-KM311 ura4-D18 leu1-32*	This study
	Figure S4	
AP5678	*mid2-Envy:kanMX6, rlc1-mcherry:natMX6, sid4-mcherry:hphMX6 ade6-M210 ura4-D18 leu1-32*	This study
AP6271	*mid2-Envy:kanMX6, rlc1-mcherry:natMX6, sid4-mcherry:hphMX6 cut7-24 ade6-M210 ura4-D18 leu1-32*	This study
	Figure S5	
AP5678	*mid2-Envy:kanMX6, rlc1-mcherry:natMX6, sid4-mcherry:hphMX6 ade6-M210 ura4-D18 leu1-32*	This study
AP5564	*mid2-Envy:kanMX6, rlc1-mcherry:natMX6, sid4-mcherry:hphMX6 sid2-250 ade6-M210 ura4-D18 leu1-32*	This study
	Figure S6	
AP5678	*mid2-Envy:kanMX6, rlc1-mcherry:natMX6, sid4-mcherry:hphMX6 ade6-M210 ura4-D18 leu1-32*	This study
AP5878	*mid2-Envy:kanMX6, rlc1-mcherry:natMX6, sid4-mcherry:hphMX6 its3-1 ade6-M210 ura4-D18 leu1-32*	This study

Supplemental figure legend

Figure S1: In the absence of Mid2, septins localization is altered, but no effects on acto-myosin ring constriction are detected

A: Kymographs of the side region of the medial cortex of wild type (left) or *mid2Δ* cells (right) expressing Spn1-GFP, Rlc1-mCherry and Sid4-mCherry. Each frame corresponds to 1 min interval. The major transitions in their behavior from mitosis onset and the defects observed in absence of Mid2 are highlighted in bigger panels at the far right and indicated with a star. **B:** Plot showing total ring constriction duration in wild type and *mid2Δ* cells expressing Spn1-GFP, Rlc1-mCherry and Sid4-mCherry. Mean ± sd are shown. N=52 cells.

Figure S2: Under high Cdk1 activity, septins appear as a broad band separated by the acto-myosin ring.

A: Quantification of Spn1-GFP and Mid2-ENVY width over the time inwild type (light green for Spn1-GFP and dark green for mid2-ENVY) and *nda3-KM311* mutant cells (orange for Spn1-GFP and red for mid2-ENVY) incubated at 18°C during 7 hours. The last data point has been taken after switching the cells to 25°C for 1 hour. The average curves ± sd are displayed. N>500 cells. Fluorescence intensity analysis of Spn1-GFP, Rlc1-mCherry and Sid4-mCherry signal measured along the entire cell in epifluorescence images of the *nda3-KM311* cold sensitive mutant in a representative cell where the SPBs are aligned (**B**) or not (**C**) with the ring position.

Figure S3: Mid2 is able to self-interact and to bind septins in the presence of high Cdk1 activity.

A: Co-immunoprecipitation assay between Mid2-13XMyc and Mid2_FL-GFP (full length), Mid2_ΔPH-GFP or PH_Mid2-GFP in *nda3-KM311* cells incubated at 18°C for 7 hours. **B:** Quantification of western blot signals from two independent experiments. Error bars, SD. **C:** Co-immunoprecipitation assay between Mid2-13XMyc and Spn1-GFP in control and *nda3-KM311* cells incubated at 18°C for 7 hours (lanes 5, 6, 7 and 8) and released for 1 hour at 25°C (lanes 1, 2, 3 and 4). **D:** Quantification of western blot signals from two independent experiments. Error bars, SD.

Figure S4: Mid2 appears as a broad band at the cell middle under high Cdk1 activity.

Time lapse imaging of cells wild type (**A**) or cut7-24 cells (**C**) expressing Mid2-ENVY, Rlc1-mCherry and Sid4-mCherry incubated at 36ºC. Max projections of confocal images are shown. Time 0 corresponds to mitotic entry. Scale bars: 2 µm. Plot displaying Mid2-ENVY dynamics throughout cell division in control (**B**) and *cut7-24* cells (**D**). Mean ± sd are shown. N=45 cells in each case. **E:** Quantification of the extent of Mid2-ENVY width compaction over the time in wild type (dark green) and *cut7-24* cells (red). N=20 cells

Figure S5: Mid2 shows an aberrant behavior in presence of low SIN activity.

Time lapse imaging of wild type (**A**) and *sid2-250* cells (**C**) expressing Mid2-ENVY, Rlc1-mCherry and Sid4-mCherry incubated at 36ºC. Max projections of confocal images are shown. Time 0 corresponds to mitotic entry. Scale bars: 2 µm. Plot showing Mid2-ENVY transitions throughout cell division in control (**B**) or *sid2-250* cells (**D**). Mean ± sd are shown. Wild type N=57 cells. *sid2-250* N=70 cells. **E:** Analysis of Mid2-ENVY intensity from mitotic onset throughout cell division in control (dark green) and *sid2-250* cells (red). The average curves ± sd are displayed. N=6 cells

Figure S6: Low PIP2 levels influence the timing and amounts of Mid2 recruitment to the division site.

Time lapse imaging of wild type (**A**) and *its3-1* cells (**C**) expressing Mid2-ENVY, Rlc1-mCherry and Sid4-mCherry incubated at 36ºC. Max projections of confocal images are shown. Time 0 corresponds to mitotic entry. Scale bars: 2 µm. Plot showing Mid2-ENVY behavior throughout cell division in control (**B**) and *its3-1* cells (**D**). Mean ± sd are shown. Wild type N=57 cells. *its3-1* N=64 cells. **E:** Quantification of the extent of Mid2-ENVY width compaction over the time in wild type (dark green) and *its3-1* cells (red). N=20 cells **F:** Analysis of Mid2-ENVY intensity from mitotic onset throughout cell division in control (dark green) and *its3-1* mutant cells (red). The average curves ± sd are displayed. N=6 cells.

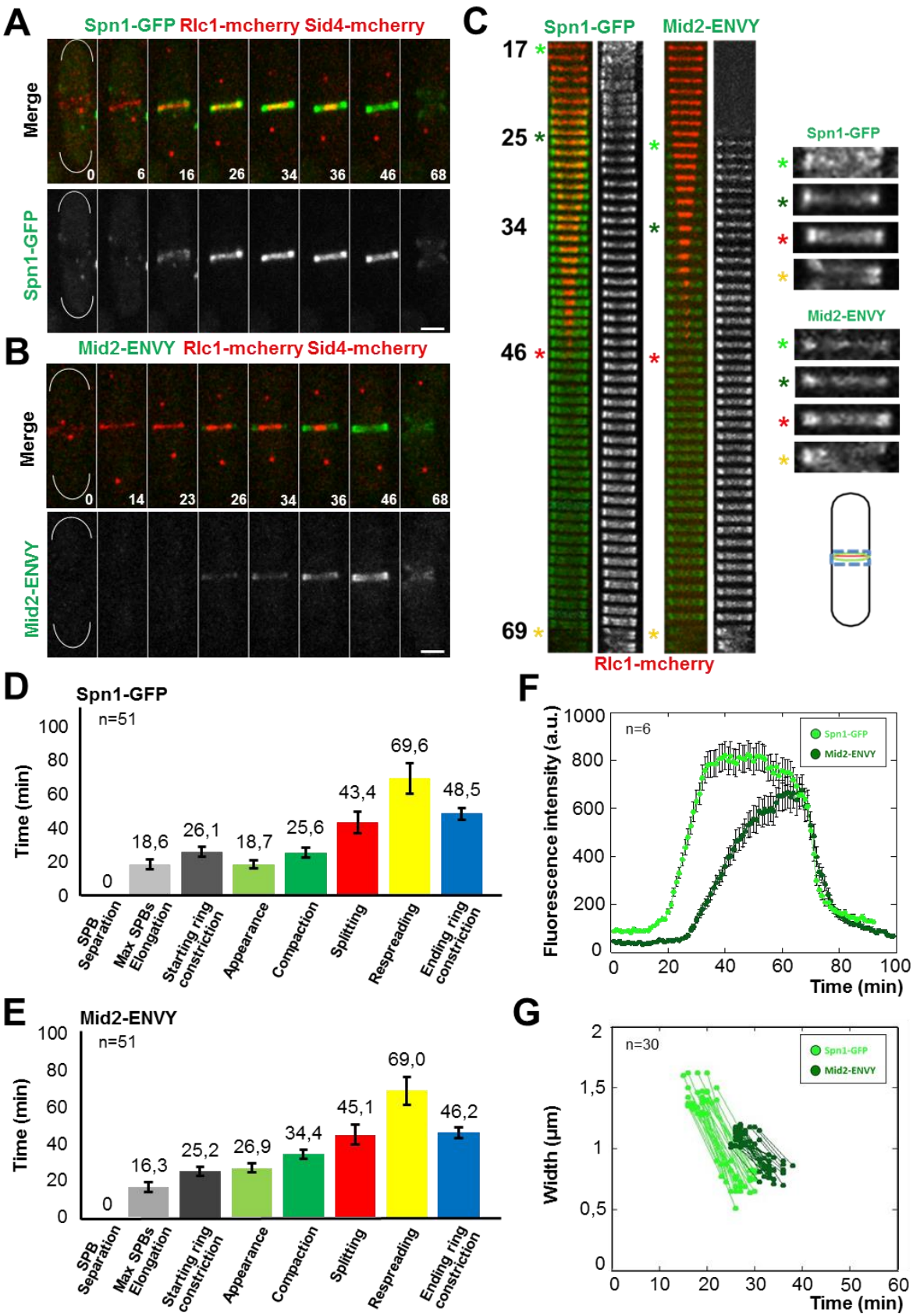
A
Spn1-GFP Rlc1-mcherry Sid4-mcherry
Merge
Spn1-GFP
0
6
16
26
34
36
46
68
B
Mid2-ENVY Rlc1-mcherry Sid4-mcherry
Merge
Mid2-ENVY
0
14
23
26
34
36
46
68
C
Spn1-GFP
Mid2-ENVY
17
25
34
46
69
Rlc1-mcherry
Spn1-GFP
Mid2-ENVY
D
Spn1-GFP
n=51
Time (min)
0
18,6
26,1
18,7
25,6
43,4
69,6
48,5
SPB Separation
Max SPBs Elongation
Starting ring constriction
Appearance
Compaction
Splitting
Respreading
Ending ring constriction
E
Mid2-ENVY
n=51
Time (min)
0
16,3
25,2
26,9
34,4
45,1
69,0
46,2
SPB Separation
Max SPBs Elongation
Starting ring constriction
Appearance
Compaction
Splitting
Respreading
Ending ring constriction
F
n=6
Spn1-GFP
Mid2-ENVY
Fluorescence intensity (a.u.)
Time (min)
G
n=30
Spn1-GFP
Mid2-ENVY
Width (µm)
Time (min)

Figure 1

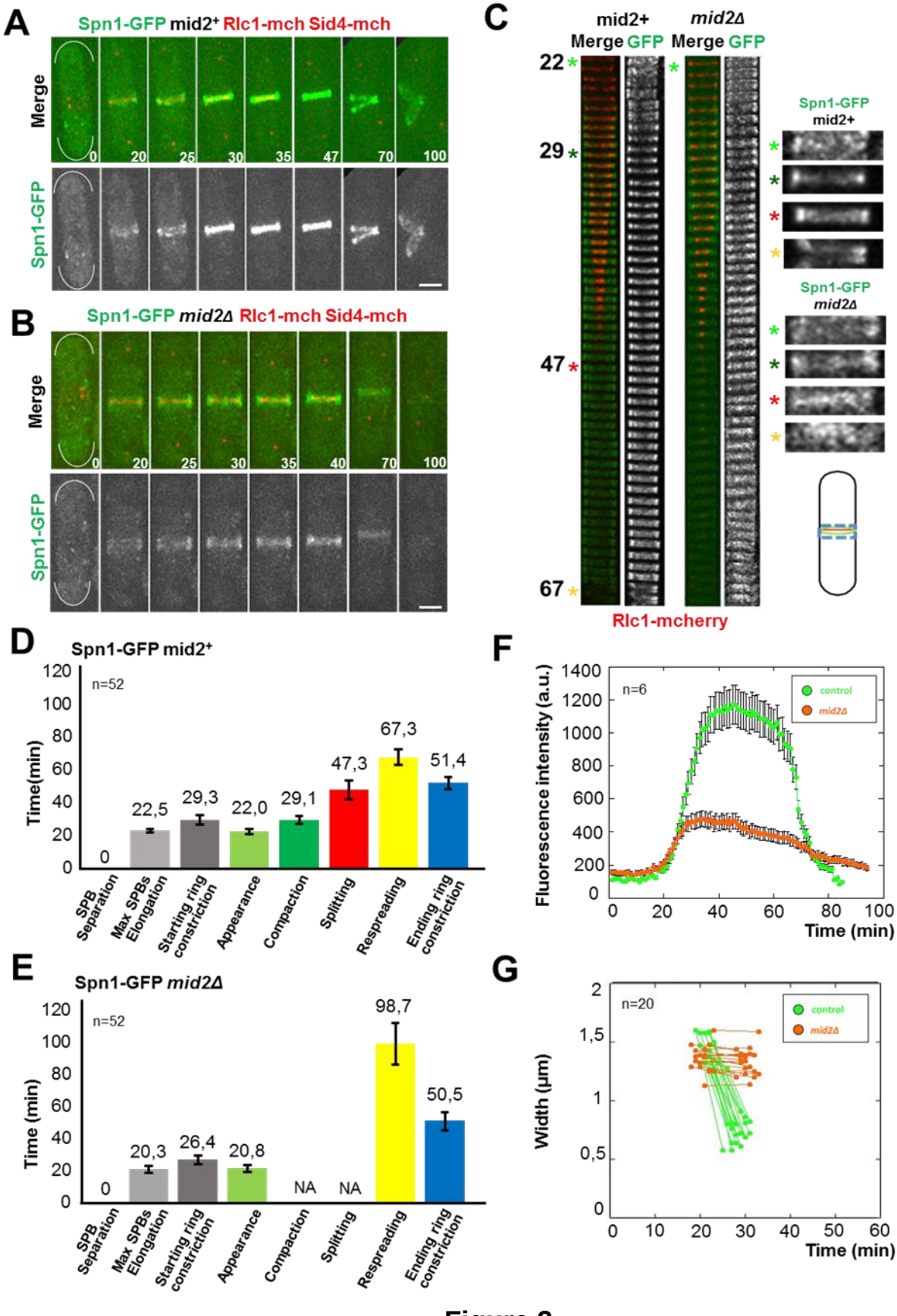
A
Spn1-GFP mid2+ Rlc1-mch Sid4-mch
Merge
Spn1-GFP
0 20 25 30 35 47 70 100
B
Spn1-GFP mid2Δ Rlc1-mch Sid4-mch
Merge
Spn1-GFP
0 20 25 30 35 40 70 100
C
mid2+
Merge GFP
mid2Δ
Merge GFP
22
29
47
67
Rlc1-mcherry
Spn1-GFP
mid2+
Spn1-GFP
mid2Δ
D
Spn1-GFP mid2+
n=52
Time(min)
0
22,5
29,3
22,0
29,1
47,3
67,3
51,4
SPB Separation
Max SPBs Elongation
Starting ring constriction
Appearance
Compaction
Splitting
Respreading
Ending ring constriction
E
Spn1-GFP mid2Δ
n=52
Time (min)
0
20,3
26,4
20,8
NA
NA
98,7
50,5
F
n=6
control
mid2Δ
Fluorescence intensity (a.u.)
Time (min)
G
n=20
control
mid2Δ
Width (µm)
Time (min)

Figure 2

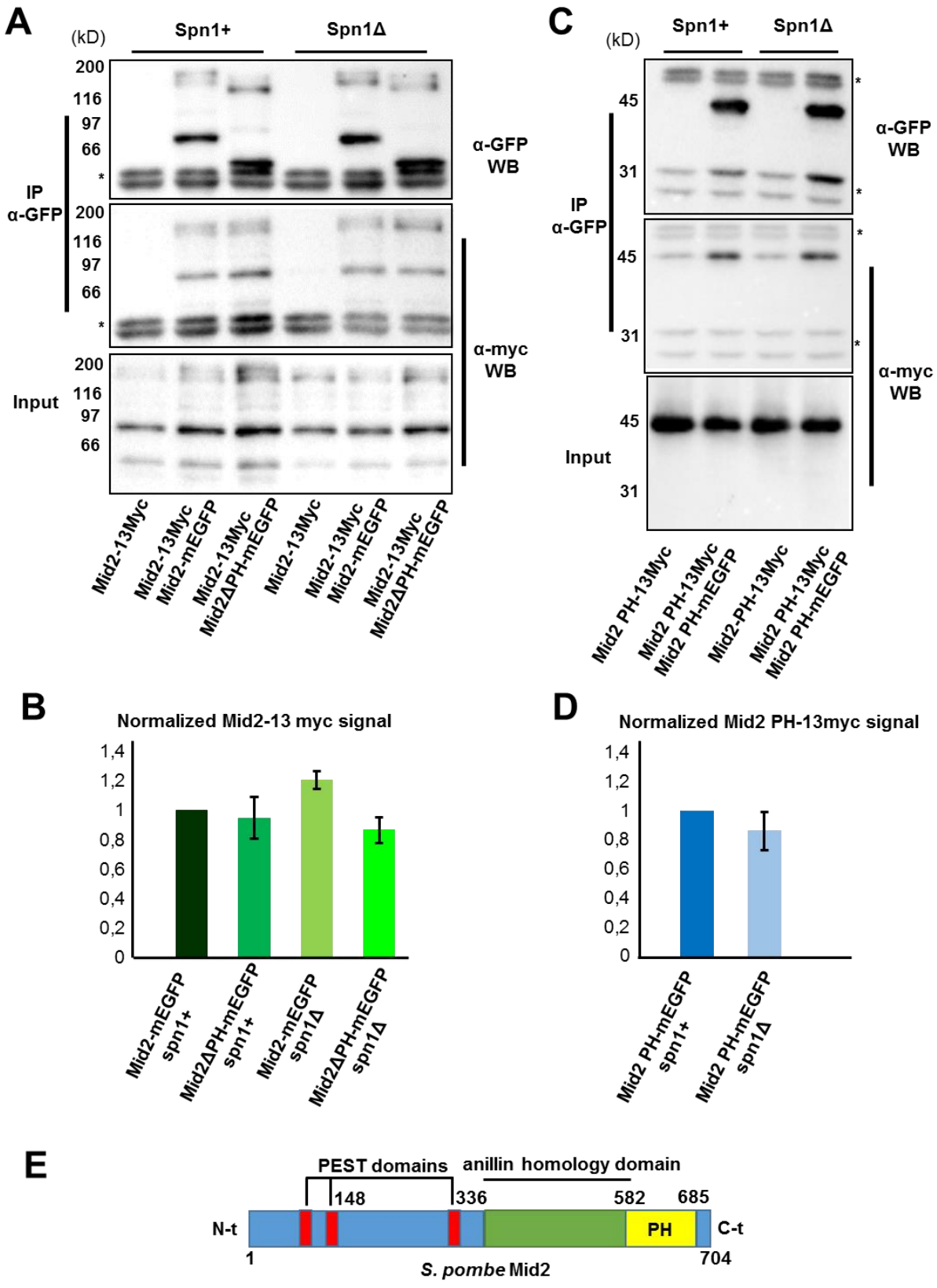
A
(kD)
Spn1+
Spn1Δ
200
116
97
66
*
IP
α-GFP
α-GFP
WB
α-myc
WB
Input
Mid2-13Myc
Mid2-13Myc
Mid2-mEGFP
Mid2-13Myc
Mid2ΔPH-mEGFP
Mid2-13Myc
Mid2-13Myc
Mid2-mEGFP
Mid2-13Myc
Mid2ΔPH-mEGFP
C
(kD)
Spn1+
Spn1Δ
45
31
*
IP
α-GFP
α-GFP
WB
α-myc
WB
Input
Mid2 PH-13Myc
Mid2 PH-13Myc
Mid2 PH-mEGFP
Mid2-PH-13Myc
Mid2 PH-13Myc
Mid2 PH-mEGFP
B
Normalized Mid2-13 myc signal
1,4
1,2
1
0,8
0,6
0,4
0,2
0
Mid2-mEGFP spn1+
Mid2ΔPH-mEGFP spn1+
Mid2-mEGFP spn1Δ
Mid2ΔPH-mEGFP spn1Δ
D
Normalized Mid2 PH-13myc signal
1,4
1,2
1
0,8
0,6
0,4
0,2
0
Mid2 PH-mEGFP spn1+
Mid2 PH-mEGFP spn1Δ
E
PEST domains
anillin homology domain
148
336
582
685
N-t
PH
C-t
1
704
S. pombe Mid2

Figure 3

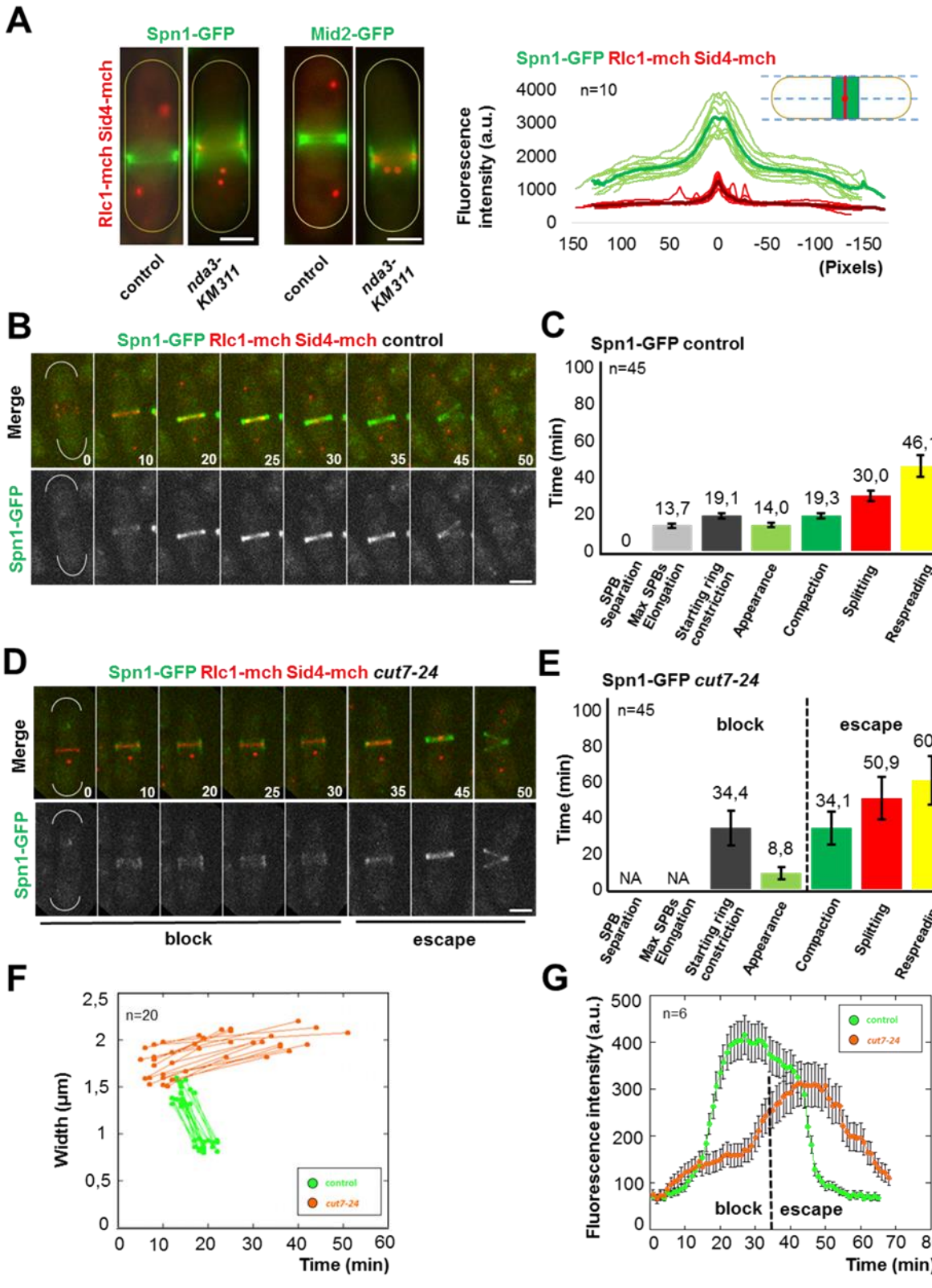
A
Spn1-GFP
Mid2-GFP
Rlc1-mch Sid4-mch
control
nda3-KM311
control
nda3-KM311
Spn1-GFP Rlc1-mch Sid4-mch
n=10
Fluorescence intensity (a.u.)
4000
3000
2000
1000
0
150 100 50 0 -50 -100 -150
(Pixels)
B
Spn1-GFP Rlc1-mch Sid4-mch control
Merge
Spn1-GFP
0 10 20 25 30 35 45 50
C
Spn1-GFP control
n=45
Time (min)
100 80 60 40 20 0
0
13,7
19,1
14,0
19,3
30,0
46,1
SPB Separation
Max SPBs Elongation
Starting ring constriction
Appearance
Compaction
Splitting
Respreading
D
Spn1-GFP Rlc1-mch Sid4-mch cut7-24
Merge
Spn1-GFP
0 10 20 25 30 35 45 50
block
escape
E
Spn1-GFP cut7-24
n=45
block
escape
Time (min)
100 80 60 40 20 0
NA
NA
34,4
8,8
34,1
50,9
60,9
SPB Separation
Max SPBs Elongation
Starting ring constriction
Appearance
Compaction
Splitting
Respreading
F
n=20
Width (µm)
2,5 2 1,5 1 0,5 0
0 10 20 30 40 50 60
Time (min)
control
cut7-24
G
n=6
Fluorescence intensity (a.u.)
500 400 300 200 100 0
block
escape
0 10 20 30 40 50 60 70 80
Time (min)
control
cut7-24

Figure 4

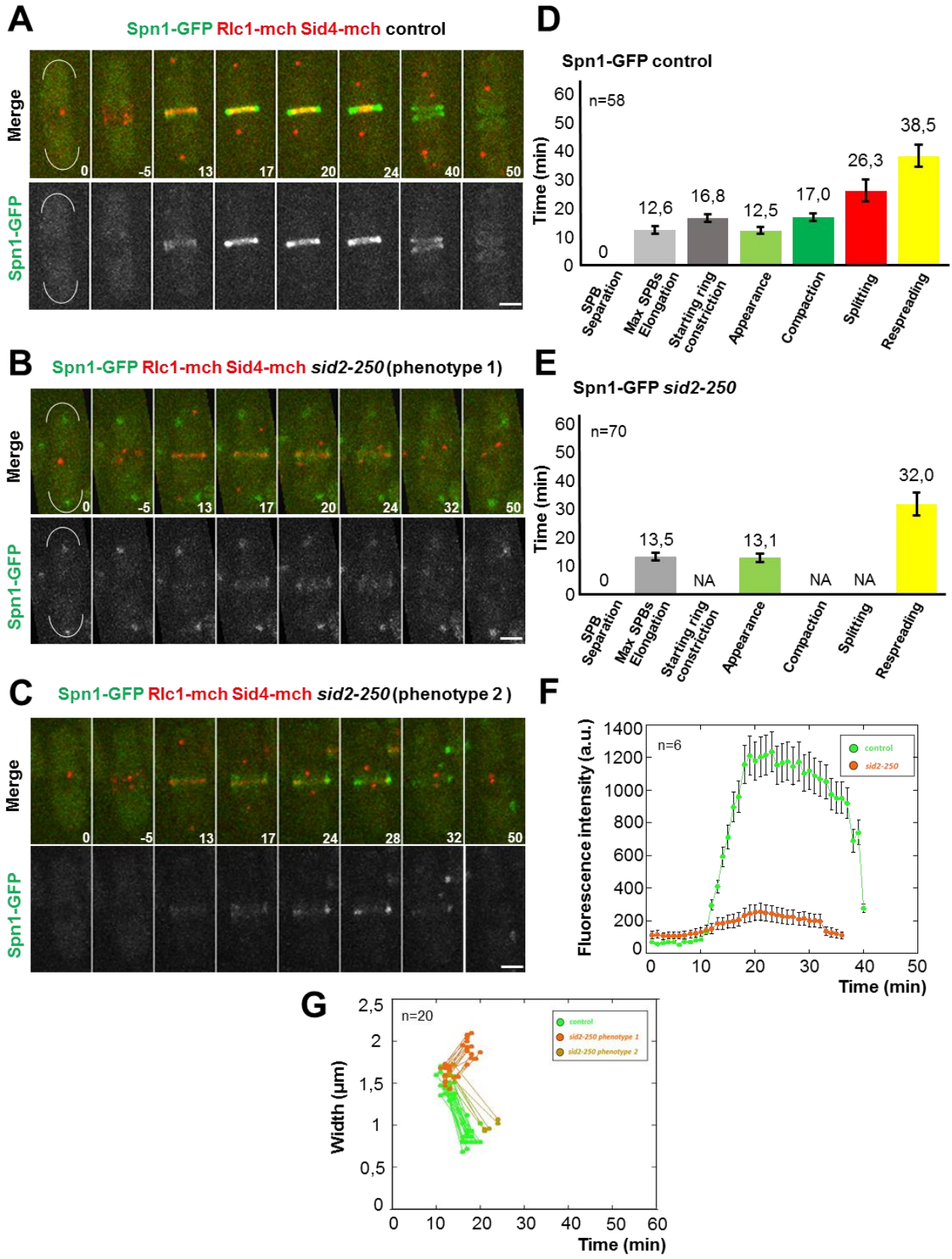
A
Spn1-GFP Rlc1-mch Sid4-mch control
Merge
Spn1-GFP
0
-5
13
17
20
24
40
50
B
Spn1-GFP Rlc1-mch Sid4-mch sid2-250 (phenotype 1)
Merge
Spn1-GFP
0
-5
13
17
20
24
32
50
C
Spn1-GFP Rlc1-mch Sid4-mch sid2-250 (phenotype 2)
Merge
Spn1-GFP
0
-5
13
17
24
28
32
50
D
Spn1-GFP control
n=58
Time (min)
0
12,6
16,8
12,5
17,0
26,3
38,5
SPB Separation
Max SPBs Elongation
Starting ring constriction
Appearance
Compaction
Splitting
Respreading
E
Spn1-GFP sid2-250
n=70
Time (min)
0
13,5
NA
13,1
NA
NA
32,0
SPB Separation
Max SPBs Elongation
Starting ring constriction
Appearance
Compaction
Splitting
Respreading
F
n=6
control
sid2-250
Fluorescence intensity (a.u.)
Time (min)
G
n=20
control
sid2-250 phenotype 1
sid2-250 phenotype 2
Width (µm)
Time (min)

Figure 5

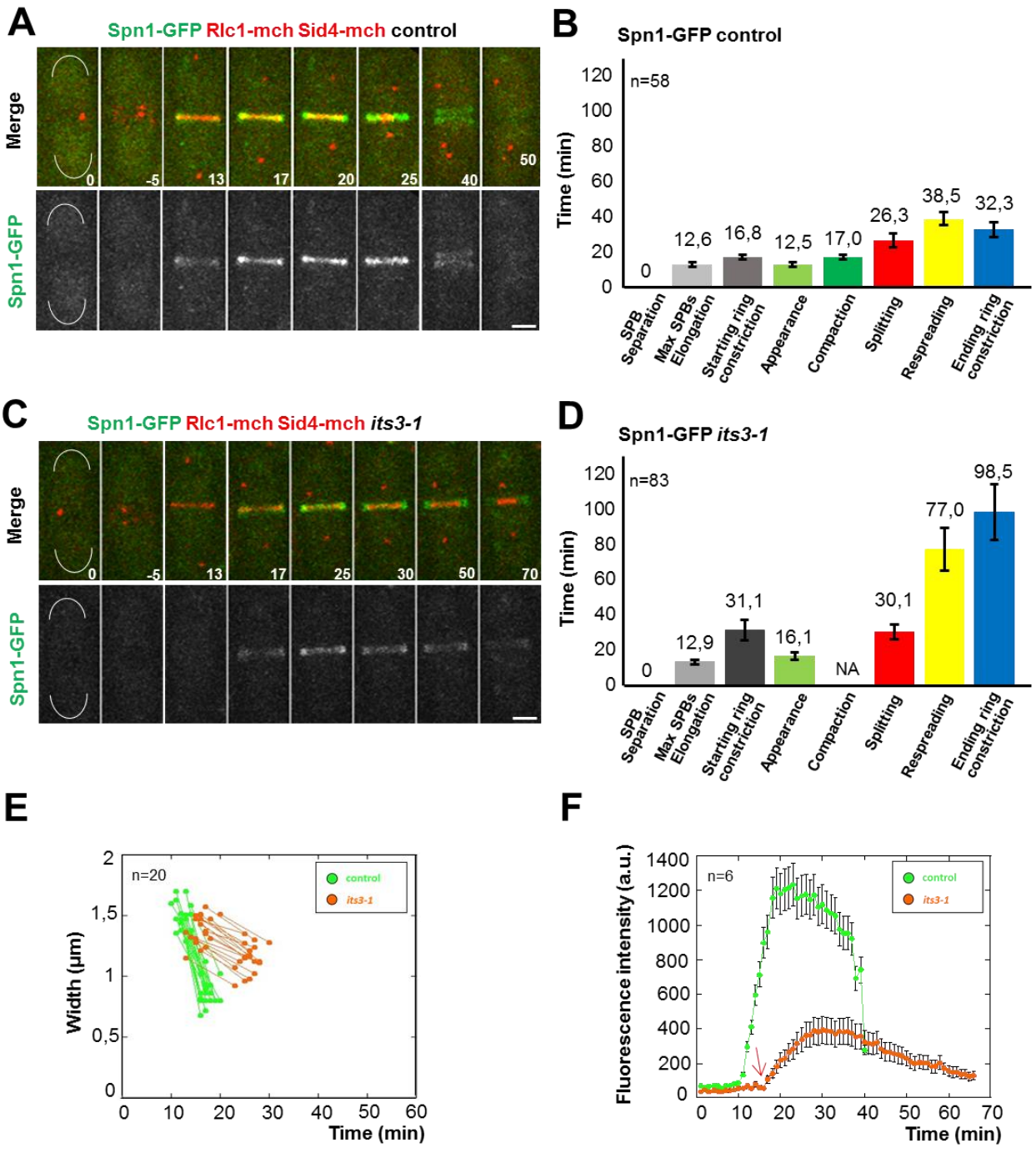
A
Spn1-GFP Rlc1-mch Sid4-mch control
Merge
Spn1-GFP
0
-5
13
17
20
25
40
50
B
Spn1-GFP control
n=58
Time (min)
0
12,6
16,8
12,5
17,0
26,3
38,5
32,3
SPB Separation
Max SPBs Elongation
Starting ring constriction
Appearance
Compaction
Splitting
Respreading
Ending ring constriction
C
Spn1-GFP Rlc1-mch Sid4-mch its3-1
Merge
Spn1-GFP
0
-5
13
17
25
30
50
70
D
Spn1-GFP its3-1
n=83
Time (min)
0
12,9
31,1
16,1
NA
30,1
77,0
98,5
SPB Separation
Max SPBs Elongation
Starting ring constriction
Appearance
Compaction
Splitting
Respreading
Ending ring constriction
E
n=20
control
its3-1
Width (µm)
Time (min)
F
n=6
control
its3-1
Fluorescence intensity (a.u.)
Time (min)

Figure 6

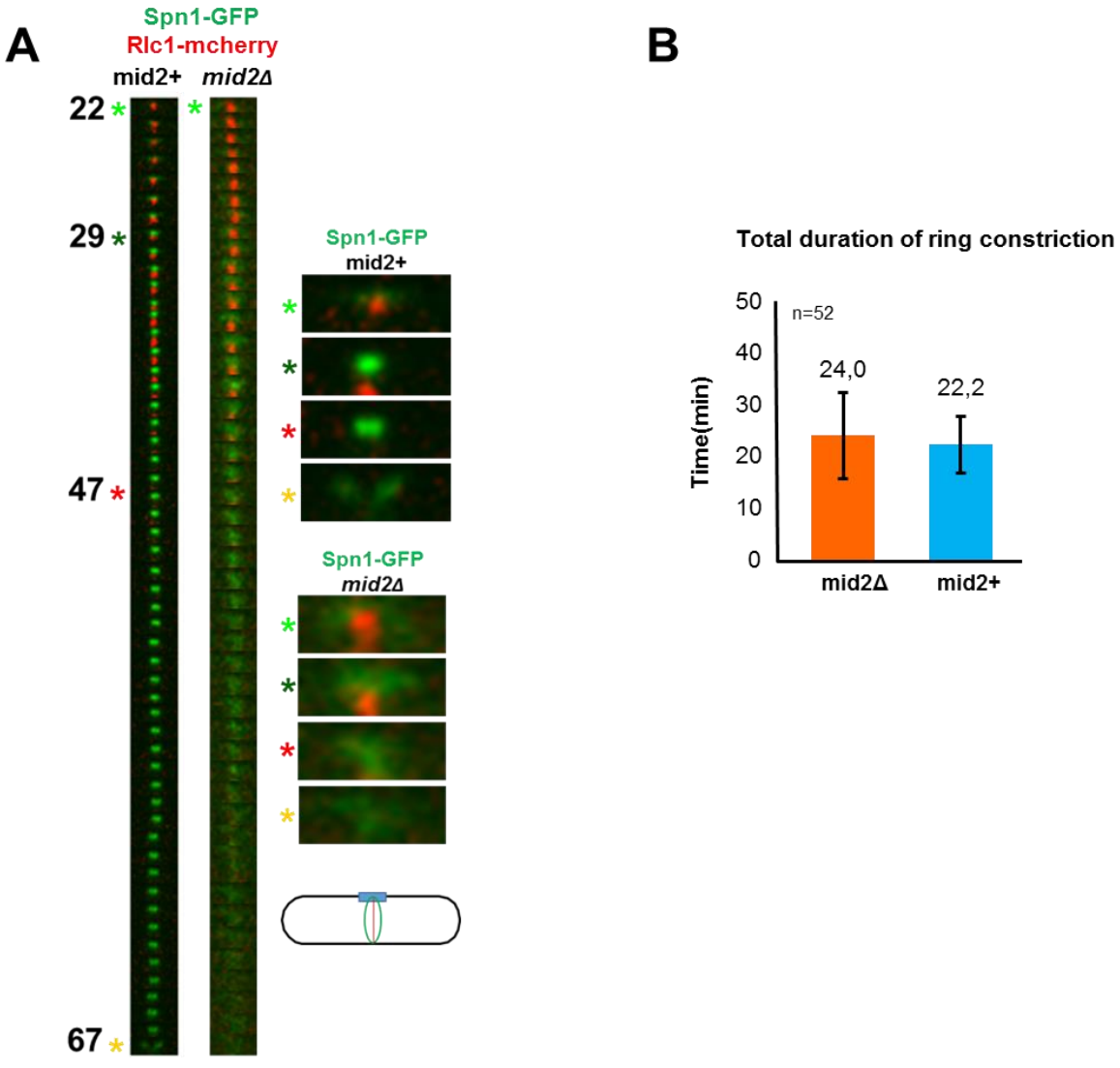
A
Spn1-GFP
Rlc1-mcherry
mid2+
mid2Δ
22
29
47
67
Spn1-GFP
mid2+
Spn1-GFP
mid2Δ
B
Total duration of ring constriction
n=52
Time(min)
50
40
30
20
10
0
24,0
22,2
mid2Δ
mid2+

Figure S1

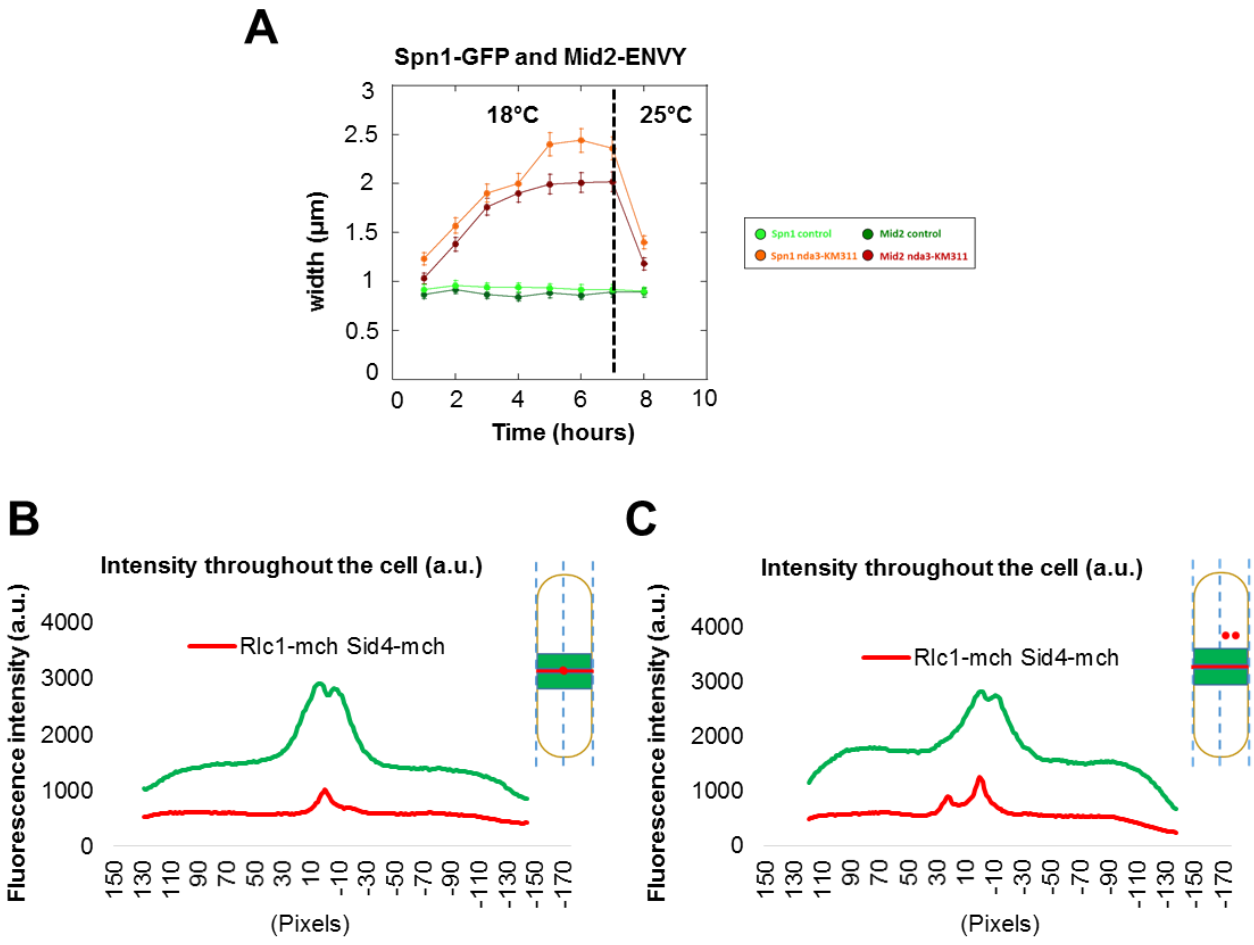
A
Spn1-GFP and Mid2-ENVY
18°C
25°C
width (µm)
Time (hours)
Spn1 control
Mid2 control
Spn1 nda3-KM311
Mid2 nda3-KM311
B
Intensity throughout the cell (a.u.)
Fluorescence intensity (a.u.)
Rlc1-mch Sid4-mch
(Pixels)
C
Intensity throughout the cell (a.u.)
Fluorescence intensity (a.u.)
Rlc1-mch Sid4-mch
(Pixels)

Figure S2

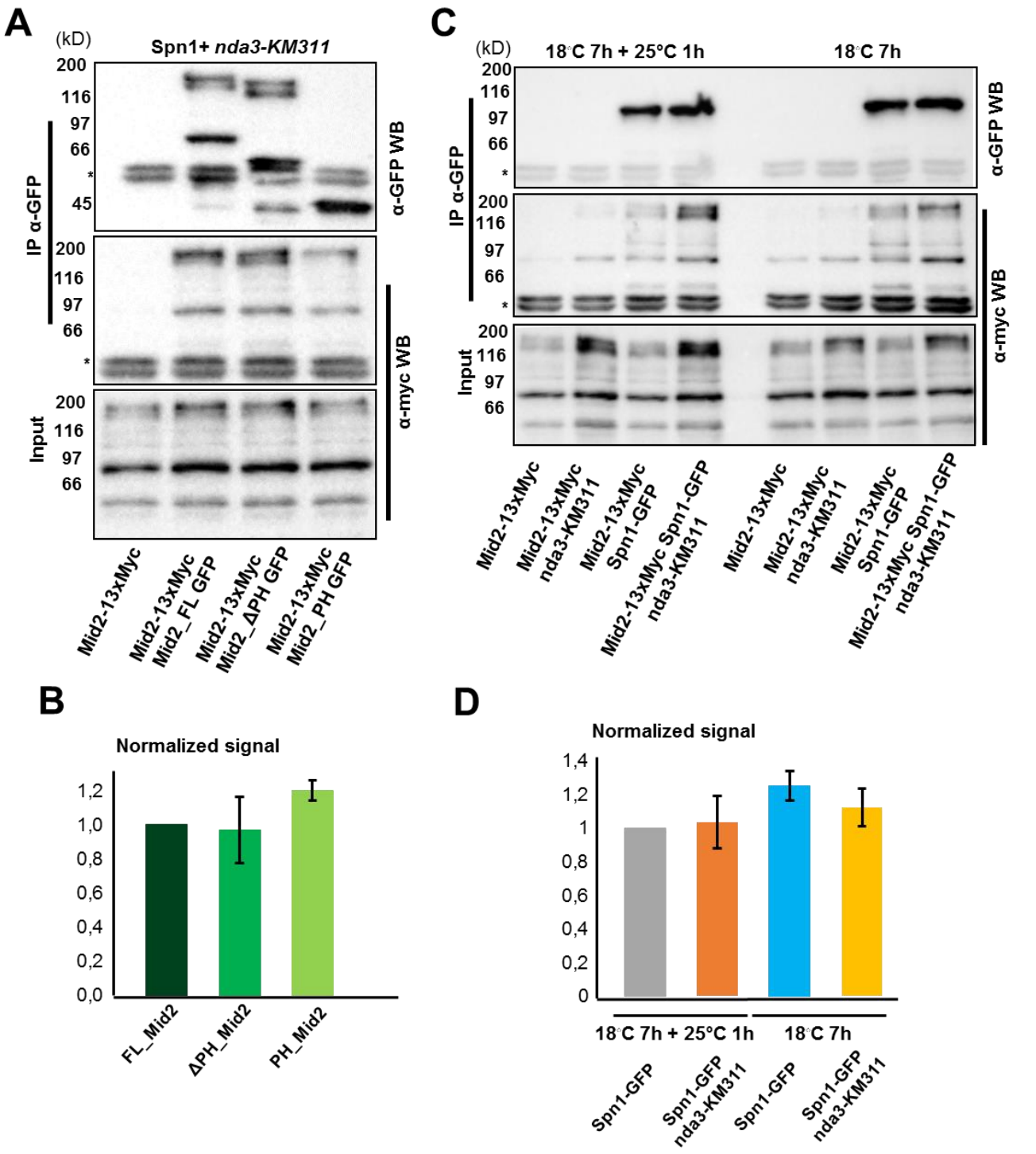
A
(kD)
Spn1+ nda3-KM311
200
116
97
66
45
IP α-GFP
α-GFP WB
α-myc WB
Input
Mid2-13xMyc
Mid2-13xMyc Mid2_FL GFP
Mid2-13xMyc Mid2_ΔPH GFP
Mid2-13xMyc Mid2_PH GFP
C
(kD)
18°C 7h + 25°C 1h
18°C 7h
Mid2-13xMyc
Mid2-13xMyc nda3-KM311
Mid2-13xMyc Spn1-GFP
Mid2-13xMyc Spn1-GFP nda3-KM311
B
Normalized signal
1,2
1,0
0,8
0,6
0,4
0,2
0,0
FL_Mid2
ΔPH_Mid2
PH_Mid2
D
Normalized signal
1,4
1,2
1
0,8
0,6
0,4
0,2
0
18°C 7h + 25°C 1h
18°C 7h
Spn1-GFP
Spn1-GFP nda3-KM311

Figure S3

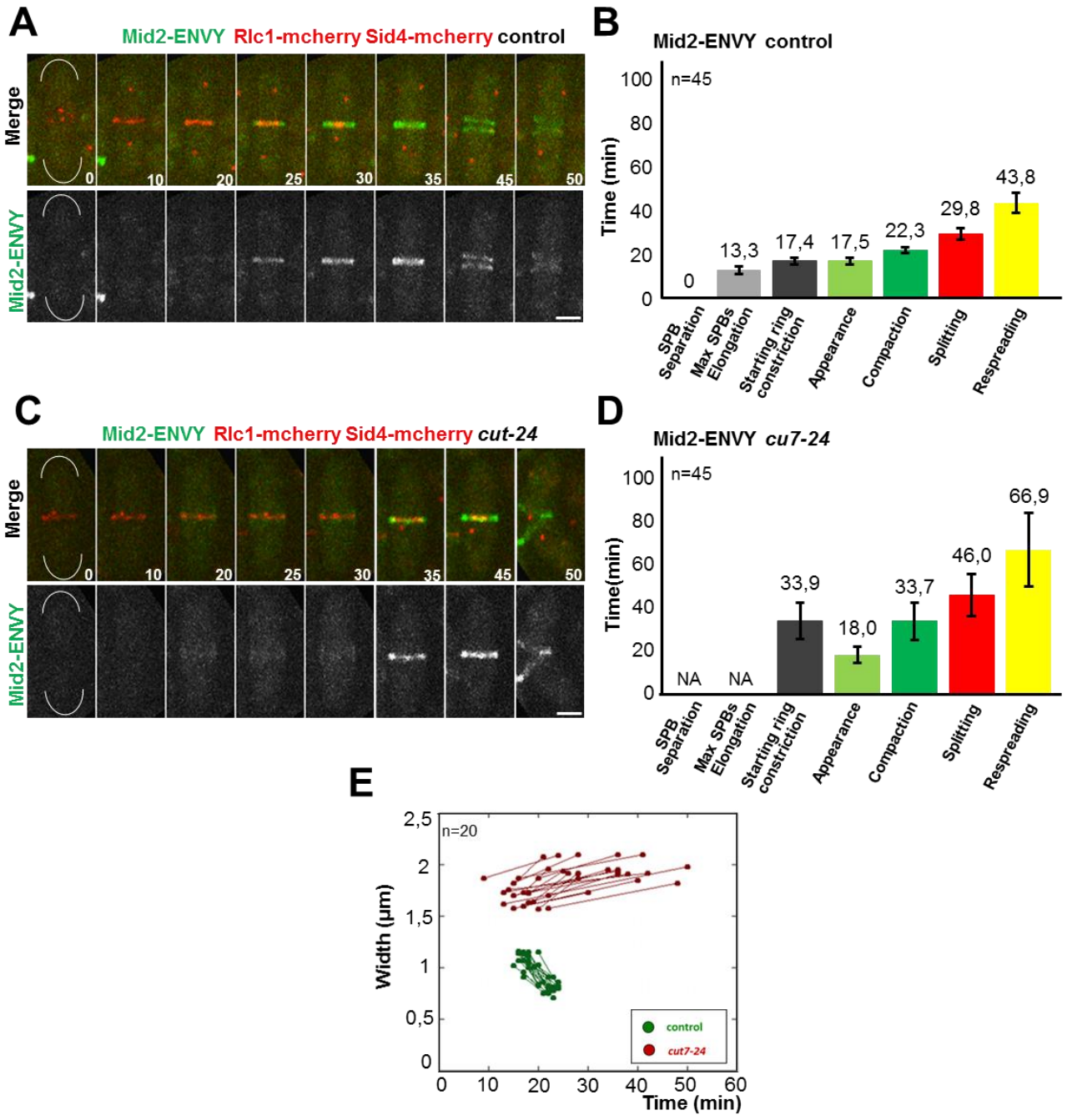
A
Mid2-ENVY Rlc1-mcherry Sid4-mcherry control
Merge
Mid2-ENVY
0
10
20
25
30
35
45
50
B
Mid2-ENVY control
n=45
Time (min)
100
80
60
40
20
0
0
13,3
17,4
17,5
22,3
29,8
43,8
SPB Separation
Max SPBs Elongation
Starting ring constriction
Appearance
Compaction
Splitting
Respreading
C
Mid2-ENVY Rlc1-mcherry Sid4-mcherry cut-24
Merge
Mid2-ENVY
0
10
20
25
30
35
45
50
D
Mid2-ENVY cu7-24
n=45
Time(min)
100
80
60
40
20
0
NA
NA
33,9
18,0
33,7
46,0
66,9
SPB Separation
Max SPBs Elongation
Starting ring constriction
Appearance
Compaction
Splitting
Respreading
E
n=20
Width (µm)
2,5
2
1,5
1
0,5
0
0
10
20
30
40
50
60
Time (min)
control
cut7-24

Figure S4

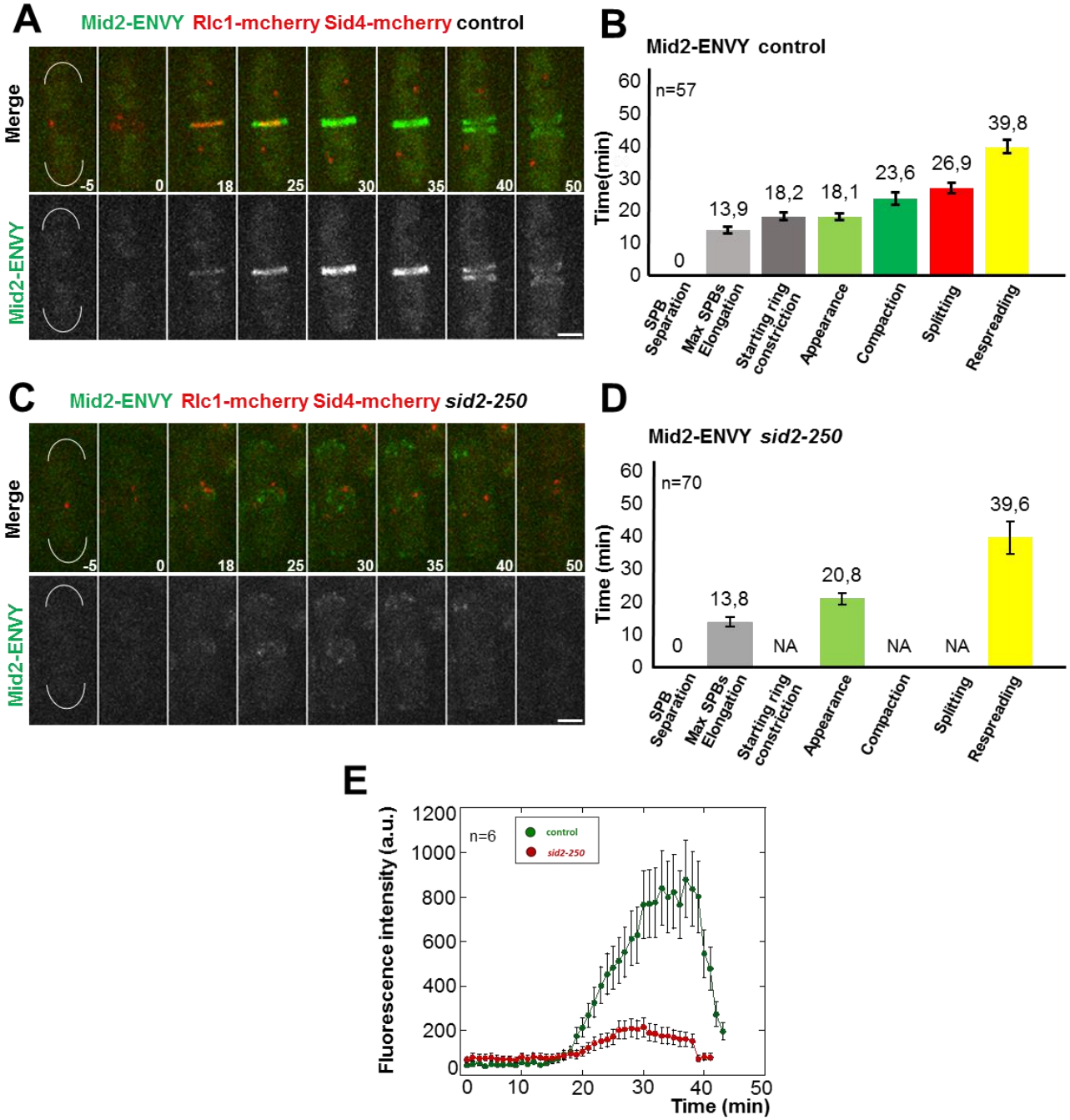
A
Mid2-ENVY Rlc1-mcherry Sid4-mcherry control
Merge
Mid2-ENVY
-5
0
18
25
30
35
40
50
B
Mid2-ENVY control
n=57
Time(min)
60
50
40
30
20
10
0
0
13,9
18,2
18,1
23,6
26,9
39,8
SPB Separation
Max SPBs Elongation
Starting ring constriction
Appearance
Compaction
Splitting
Respreading
C
Mid2-ENVY Rlc1-mcherry Sid4-mcherry sid2-250
Merge
Mid2-ENVY
-5
0
18
25
30
35
40
50
D
Mid2-ENVY sid2-250
n=70
Time (min)
60
50
40
30
20
10
0
0
13,8
NA
20,8
NA
NA
39,6
SPB Separation
Max SPBs Elongation
Starting ring constriction
Appearance
Compaction
Splitting
Respreading
E
n=6
control
sid2-250
Fluorescence intensity (a.u.)
1200
1000
800
600
400
200
0
0
10
20
30
40
50
Time (min)

Figure S5

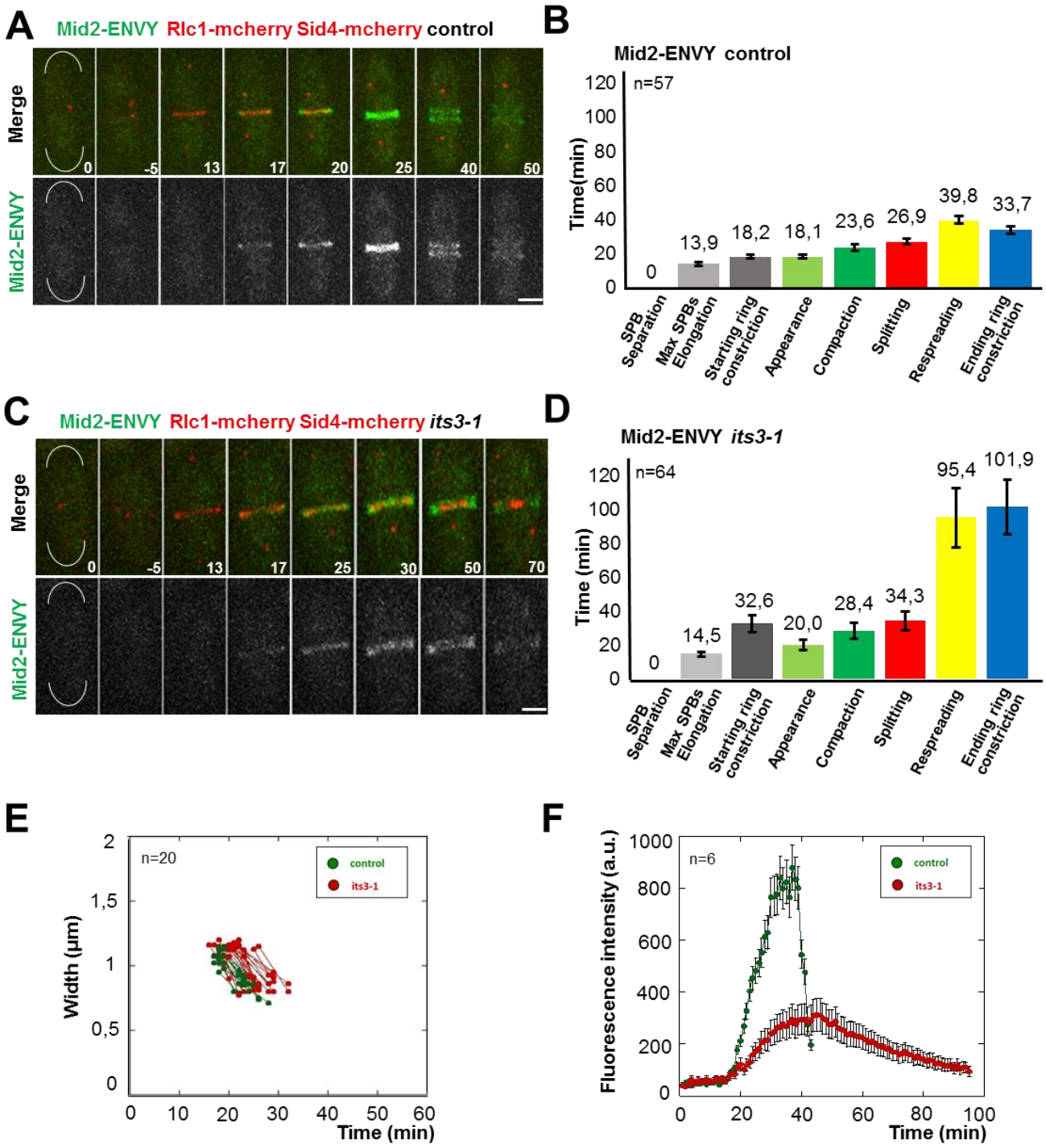
A
Mid2-ENVY Rlc1-mcherry Sid4-mcherry control
Merge
Mid2-ENVY
0
-5
13
17
20
25
40
50
B
Mid2-ENVY control
n=57
Time(min)
120
100
80
60
40
20
0
0
13,9
18,2
18,1
23,6
26,9
39,8
33,7
SPB Separation
Max SPBs Elongation
Starting ring constriction
Appearance
Compaction
Splitting
Respreading
Ending ring constriction
C
Mid2-ENVY Rlc1-mcherry Sid4-mcherry its3-1
Merge
Mid2-ENVY
0
-5
13
17
25
30
50
70
D
Mid2-ENVY its3-1
n=64
Time (min)
120
100
80
60
40
20
0
0
14,5
32,6
20,0
28,4
34,3
95,4
101,9
SPB Separation
Max SPBs Elongation
Starting ring constriction
Appearance
Compaction
Splitting
Respreading
Ending ring constriction
E
n=20
control
its3-1
Width (µm)
2
1,5
1
0,5
0
0
10
20
30
40
50
60
Time (min)
F
n=6
control
its3-1
Fluorescence intensity (a.u.)
1000
800
600
400
200
0
0
20
40
60
80
100
Time (min)

Figure S6

IV. DISCUSSION AND PERSPECTIVES

1. Increasing ergosterol levels delays formin-dependent assembly of F-actin cables and disrupts division plane positioning in fission yeast

Cytokinesis represents the final act of the cell cycle that physically separates one cell into two distinct entities. Both fission yeast and animal cells divide in the middle of the cell through the assembly of an acto-myosin contractile structure (CR). When the CR constricts inward from the cell cortex, it pinches in the plasma membrane leading to the ingression of the cleavage furrow. Defects in the spatio-temporal organization of the CR can alter the correct transmission of the genetic and cytoplasmic material, impacting several key processes such as cell proliferation, differentiation and morphogenesis. Understanding the mechanisms underlying cytokinesis is therefore crucial for our understanding of this basic process both in physiological and pathological conditions.

For successful completion of cell division, the CR must be intimately associated to the plasma membrane to allow plasma membrane pinching and furrow ingression while the CR undergoes constriction. It is therefore reasonable to imagine that lipid composition at the division site may represent an important regulator of cytokinesis. Accordingly, this cortical region requires remarkable remodeling to host the division site. Indeed, variations in its lipid composition and membrane trafficking dynamics strongly affect this process (Fremont and Echard, 2018; Gerien and Wu, 2018; Neto et al., 2011). Besides, yeasts are cell-walled organisms, whose cell wall biosynthetic enzymes are highly associated to the plasma membrane. In these systems, the formation of the septum, a specialized cell wall assembled during cytokinesis in the cleavage furrow while the CR constricts, represents an essential step for cell division. Therefore, the lipid environment at the division site might be utterly important in fission yeast. Accordingly, recent studies have shown that a correct phospholipid composition at the middle cortex cooperate with Cdc15-, Pxl1-, and cell wall–dependent PM anchoring to promote stable CR placement and successful cell division (Snider et al 2017; Snider et al 2018).

An important category of membrane lipids are sterols. Of note, fission yeast sterol, ergosterol, accumulates at the division site (Wachtler et al., 2003), pointing towards a function of those compounds in cytokinesis. Interestingly, overexpression of Erg25, an enzyme involved in the sterol biosynthetic pathway, leads to a general increased amount of ergosterols with defective positioning of the AMR and consequently of the division septum. This phenotype is highly reminiscent to that produced by the absence of the anillin-like protein Mid1, which can itself bind to the plasma membrane. However, detailed analysis of Mid1 localization by time lapse microscopy ruled out such possibility. Indeed, we found that different molecular mechanisms are involved: while in the mid1Δ mutant the division plane positioning defects are due to a faulty recruitment of several ring components including myosin II and the formin Cdc12 that nucleates the CR F-actin network, upon Erg25 OE the phenotype is the result of a

specific inhibition in F-actin assembly from well positioned and properly assembled cytokinetic precursor nodes. In parallel, we have excluded, in the observed phenotype, a contribution of an abnormal ER organization in presence of high ergosterol levels, suggesting a direct impact of these lipids in contractile ring positioning and assembly mechanisms.

In fission yeast, Mid1 promotes the assembly of the CR through the ordered recruitment of ring components to cytokinetic precursor nodes (Almonacid et al., 2011; Laporte et al., 2011; Padmanabhan et al., 2011; Wu et al., 2003; Wu et al., 2006). Altered lipid environment might affect Mid1-mediated recruitment of CR components. However, our analysis of cytokinetic precursors upon Erg25OE by live-cell time lapse imaging and quantitative analysis in interphase and mitosis allowed us to conclude that early reinforcement or accumulation of these proteins at the medial cortex is not globally affected. The only abnormality that we detected was a delay of 7 minutes in myosin II recruitment. Since myosin II levels are similar in control cells and Erg25 overexpressing cells during the period of ring assembly and no defects in the accumulation of CR precursors nodes were observed, we do not have at the moment a clear explanation for this event. It is possible that increasing levels of ergosterols affects myosin II capability to associate with Rng2. Nevertheless, this short delay in myosin II recruitment is not sufficient to explain the strong defects occurring in division plane position. Indeed, a Mid1 phospho-inhibitory mutants in Plo1-dependent sites produced in the laboratory, exhibited a longer delay in Myosin II recruitment (10 minutes), but the phenotype was milder compared to Erg25 OE (Almonacid et al 2011).

Our analysis rather indicates that the major defect produced by Erg25 overexpression is a strong delay in the assembly of F-actin cables from cytokinetic precursors. As a consequence, this results in a failure in cytokinetic node compaction that disrupts division plane positioning. Cdc12 is timely recruited at the cell middle, although to a broader region that makes challenging to conclude if there is a mild defect in the total amount of protein to the division site. Given the fact that F-actin cables assembly by the formin For3 and their stability are not altered, we propose that increased ergosterol levels may negatively regulate the nucleation activity of the formin Cdc12 (and possibly also its recruitment at the cell middle). Supporting this hypothesis, the phenotype generated by Erg25OE is partially rescued by using CK666, an inhibitor of the Arp2/3 complex, which competes with formins for the free pool of actin monomers (Burke et al., 2014; Moseley, 2014), in agreement with a compromised function of Cdc12 under this condition.

In *S. pombe* a functional secretory pathway is known to be involved in the formation of sterol rich domains at the cell equator since brefeldin A treated cells showed a limited filipin staining at the cell middle (Wachtler et al., 2003). Thus we have evaluated whether the rescue of Erg25OE phenotype seen in presence of CK666 was not due to an indirect effect mediated by endocytosis since CK666 treatment

can have effects on membrane composition and trafficking by the inhibition of Arp2/3 complex. By checking ergosterol levels through the measure of filipin intensity after CK666 application, we found that ergosterols start to decrease after 1 hour of treatment so we performed our analysis during the first hour of treatment. Therefore, we could exclude that the partial rescue we detect in presence of CK666 is linked to endocytosis.

In our study we have used filipin to stain sterols. Long exposure to sterol being toxic, we have analyzed ergosterols distribution in the external leaflet of the plasma membrane on still pictures of cells exposed to filipin few minutes only before imaging but we could not perform movies in presence of filipin. Recently, the Martin team has developed a new tool to follow ergosterols in vivo: it is a sterol biosensor (D4H) based on *Clostridium perfringens* theta toxin expressed inside cells and accessing ergosterol pools from the inner leaflet of the plasma membrane (abstract by Marek and Martin, 10th International Fission yeast Meeting 2019). They identified that the anterograde movement of sterols from internal compartments to the PM requires vesicular trafficking components, while retrograde transport is mediated by a nonvescicular process dependent on Ltc1 (Lipid transfer on contact site), a stARkin-domain protein that localizes at the ER-PM contact sites (Gatta et al., 2015; Horenkamp et al., 2018; Murley et al., 2015; Tong et al., 2018). In *ltc1Δ* cells sterols internalization is blocked so they remain at the plasma membrane forming extensive invaginations. It could be envisaged to use their probe to analyze *in vivo* the pattern of ergosterol distribution in Erg25 overexpressing cells to better understand the effects of sterols during CR assembly and division plane positioning. Moreover, it would be intriguing to test the role of *ltc1* deletion in combination with Erg25OE and CK666 treatment to check if we would still observe a partial rescue effect. Additionally, at the physiological level, it will give a key contribution in understanding how the regulation of this transport system controls the accumulation of ergosterol to the division site. Understanding this regulation might help unveiling novel roles of these lipids in cytokinesis.

At this stage a detailed understanding of the molecular mechanism underlying Erg25OE phenotype is missing. The development of *in vitro* experiments testing Cdc12 interactions with model membranes characterized by different lipid mixtures would permit to obtain important clues on the regulation and function of Cdc12 by membrane lipids. For instance, recent *in vitro* experiments with myosin-II and a formin fragment containing formin homology (FH) 2 and FH1 domains led to the confirmation of the SPCR model to explain contractile ring assembly in fission yeast (Zimmermann et al., 2017). Interestingly, this approach has also revealed that the FH1 domain of Cdc12 is mechano-sensitive and, when subjected to the pulling forces applied by myosin II, inhibits Cdc12 elongation activity. This is key to provide a proper contractile ring assembly, avoiding the formation of abnormal precursor node clumps that would delay this process (Zimmermann et al., 2017). Increased ergosterol levels certainly affect the

membrane biophysical parameters, and might inhibit Cdc12 activity in this way. Indeed, sterols behave as essential regulatory and structural components of cell membranes, thus affecting their fluidity and permeability. In parallel, it is known that different types of stress, including temperature and osmotic changes, can have effects on membrane organization (Klose et al., 2012; Leach and Cowen, 2014; Los and Murata, 2004). For instance, an abrupt increase in temperature triggers a rapid decrease in the molecular order of cellular membranes since the fatty acid tails of the phospholipids become less rigid and allow more movement of proteins and other molecules in and through the membrane. It would be interesting to test the effect of a high temperature on the Erg25OE phenotype to clarify the role of membrane properties in the process of contractile ring assembly and division plane positioning.

Additionally, to have a comprehensive understanding of the impact of the membrane environment on CR assembly, it would be interesting to test the impact of membrane lipids on precursor nodes organization and function, considering that many of them possess membrane binding domains and may be influenced by lipid composition. Super resolution microscopy studies to image CR components in presence of different lipid mixtures could help further understand how these dynamic molecular complexes interact with lipid domains**.** Indeed, the use of super-resolution microscopy in fixed cells combined with FRET technique has recently permitted to make exciting progress in understanding the organization of the CR. By measuring the distance of CR components with respect to the plasma membrane in fixed fission yeast cells just before the beginning of constriction, it has been found that the CR is organized in 3 layers (McDonald et al., 2017). Membrane-binding proteins, including Mid1 and F-bar proteins, but also Cdc12 and Rng2 and the tail of the essential myosin-II have been detected closest to the plasma membrane (0–80 nm). The intermediate layer (80–160 nm) is composed by multiple signaling components and cytokinesis accessory proteins that are key to maintain ring integrity. The most distal zone from the membrane (160–350 nm) contains F-actin, the motor domains of myosins, and F-actin crosslinkers. In parallel, another study which has also exploited an high speed single-molecule super-resolution technique in live cells has revealed that cytokinetic node components are organized in clusters in the CR where the C-terminus of Myo2, Mid1, Rng2, Cdc15 and Cdc12 co-localize in a compact structure at the plasma membrane, while the head of Myo2 extend in the cytoplasm where they can associate with actin filaments to drive AMR formation and constriction (Laplante et al., 2016). Both these studies provide important insights on the role of functional subdomains crucial for CR function. Considering the evolutionary conservation of the main organizers of CR structures, analyzing whether any of the features identified in the *S. pombe* contractile ring are in common with other model organisms is another subsequent area of future investigation.

Additionally, we need to consider whether the defects that we saw after Erg25OE could be linked to the accumulation of other downstream intermediates of the ergosterol biosynthetic pathway. This seems

unlikely considering that a treatment with the drug miconazole, that blocks the ergosterol pathway right upstream of Erg25, blocks almost completely the production of abnormal septa upon Erg25OE. However, the deletion of Erg6, a gene located immediately downstream of Erg25 in the ergosterol pathway, led to a ~50 % rescue in the number of abnormal septa. The partial suppression seen in the latter case could be due to the existence of additional branches in the metabolic pathway for ergosterol production that would form sterols independently from Erg6. In fact, lipid biosynthesis presents many interconnected feedback loops and this process is poorly understood in fission yeast. Lipidomic analysis would be crucial to better define the profile of lipids involved in cytokinesis (Atilla-Gokcumen et al., 2014; Echard and Burgess, 2014), but also to gather more informations on their spatio-temporal activity during fission yeast cell cycle.

Finally, the physiological relevance of the negative regulation of cytokinetic F-actin cables assembly by ergosterol levels remains to be defined. In fission yeast, ergosterol distribution is modified in a cell-cycle dependent manner (Makushok et al., 2016; Takeda and Chang, 2005; Takeda et al., 2004; Wachtler et al., 2003). This suggests that Cdc12 inhibition by ergosterol levels could be active at other cellular locations where sterols are enriched, preventing in particular the assembly of Cdc12-mediated F-actin cables at the cell tips. This mechanism could potentially be involved in the tip-occlusion pathway that prevents assembly of contractile rings at the very cell tip in the absence of Mid1 (Huang et al., 2007; Martin, 2009). The observation that a fusion construct of Tea1 with the N-terminal portion of Cdc12 localizes to the cell tips where it generates actin cables during interphase in presence of sterol rich domains (Johnson et al., 2014) could question the previous hypothesis. However, we have to consider that the fusion construct used contains only a N-terminal portion of the protein, excluding the membrane-association domain, and could have lost the ability to be regulated by specific lipids or with by other membrane binding protein sensitive to such lipids, with crucial effects on Cdc12 activity. Producing a full length Cdc12 protein for in vitro studies may be necessary to evidence sterol-dependent regulation of Cdc12.

2. Septin ring assembly by anillin-dependent compaction of a diffuse septin meshwork surrounding the acto-myosin contractile ring in fission yeast

Septins are GTP-binding proteins with the ability to form hetero-oligomeric complexes that can assemble into non polar filaments. They are considered as an element of the cytoskeleton, connected with both the actin and MT cytoskeletons. Septin filaments are also tightly connected to membranes. These properties allow septins to accomplish important biological functions such as serving as platforms for the recruitment of proteins dedicated to a specific task and/or diffusion barriers to create distinct cellular compartments. In particular, septins play key roles during cytokinesis, especially in budding yeast where they are involved in the recruitment of components of the CR and contribute to the mother-daughter cell asymmetry. In fission yeast, the initial stages of cytokinesis take place independently of septins though. Instead, septins are implicated in late stages of this process, ensuring cell-cell separation. Therefore, the spatio-temporal control of septins must be significantly different in these two evolutionarily distant yeasts.

A crucial family of factors impacting the properties of septin network is represented by anillin-like proteins, highly conserved multidomain proteins that are fundamental for the fidelity of cytokinesis. Indeed, in absence of these scaffold proteins, septins are mislocalized and disorganized in both animal and fungal cells (Berlin et al., 2003; Field et al., 2005a; Golbach et al., 2010; Maddox et al., 2005; Tasto et al., 2003). However, how these structural determinants accomplish this function is not well characterized. Given that septins are not essential in fission yeast cytokinesis and are poorly studied, we decided to study in details the dynamics and regulation of septins and of the fission yeast anillin-like protein Mid2 during cytokinesis.

Confocal live cell imaging has established the sequence of transitions that septins follow during cytokinesis: 1) accumulation of a 1.5 µm wide septin meshwork adjacent to, but excluded from the CR in anaphase when the mitotic spindle elongation is maximal; 2) compaction into a ring structure when CR constriction is initiated; 3) apparent splitting into a double ring when CR constriction terminates; and 4) disassembly of the septin ring and respreading of the meshwork over the new cell pole upon daughter cell separation. This dynamic behavior is interesting to compare to the transitions in budding yeast septin organization during cell cycle progression: at the time of bud emergence, the incipient septin structure appears first as a patch or cap, highly dynamic and unorganized, which transitions during S phase into a more stabilized septin ring/collar; this ring extends into an hourglass-shaped collar at the bud neck, which splits into two rings during CR constriction and eventually disassembles (Gladfelter et al., 2001). Given its timing when CR constriction is initiated, and similarity, we propose that the new septin compaction step that we have identified may correspond to the hourglass to split ring transition

in *S. cerevisiae*. In light of this comparison, the major difference between the two yeasts would be the much early recruitment of septins to the incipient bud site, associated with its early function in CR assembly.

The regulation of septin remodeling in *S. cerevisiae* is performed by complex network of posttranslational modifications and through the interaction with the anillin-like protein Bud4. Indeed, Bud4, in association with Bud3, another protein involved in the establishment of the axial landmark and bud site selection in haploid budding yeast cells, mediates and stabilizes septins at the bud neck during bud formation (Kang et al., 2013; Wu et al., 2015). Moreover, Bud4, regulated by Cdk1 phosphorylation, participates, together with Cla4 and Gin4 kinases, in the formation and disassembly of the septin double ring (Eluere et al., 2012). This suggests that similar molecular mechanisms may orchestrate septin dynamic organization in fission yeast.

Analyzing Mid2 dynamics in *S. pombe* revealed a delayed recruitment of this protein to the division site compared to septins, at the time of the initiation of CR constriction. This indicates that, contrary to Bud4 in *S. cerevisiae*, Mid2 does not play a role in septin initial recruitment to the division site. Reciprocally, the lack of Mid2 has no effect in the timing of septin recruitment. This data point to the existence of an anillin-independent mechanism for septin intial recruitment at the division site, in the 1.5 um wide region surrounding the CR. Our results in the *its3-1* mutant deficient for PIP2 production suggests that this initial recruitment could be triggered by PIP2. Indeed, septin organization is known to be influenced by specific membrane lipids (Bertin et al., 2010; Zhang et al., 1999).
It would be interesting to further test *in vitro* the role of PIP2 in supported lipid bilayers of different lipid compositions and degree of curvature on fission yeast septin organization, either alone or in presence of Mid2. Another open question is whether PIP2 distribution plays a role in defining the 1.5 um wide region where septin filaments accumulate by the end of anaphase. One hypothesis is that PIP2 may be produced at the CR and diffuse laterally on the 1.5 um domain. Demonstrating this would require tracking of PIP2 itself or PIP2 biosynthesis enzymes in living cells by time-lapse imaging. Use of the PH domain of Tubby as a biomarker or PIP2 in the laboratory lead to the identification of the medial domain that forms at the division site before septin appearance (Paoletti G and Paoletti A unpublished results), but the PH domain of Plc1δdid not identify such a domain, raising the question of the specificity of these living dyes.

Interestingly, Mid2 recruitment is coincident with septin filament compaction into a tight ring, and *mid2Δ* cells are not capable of septin ring compaction suggesting that Mid2 may bridge together septin filaments, acting as a bundler. For a bundler to work, it requires the ability to form dimers/oligomers, so that, on the one hand, each monomer binds a filament and, on the other, the interaction between the

monomers links the septin filaments together. By using a combination of molecular genetics and biochemistry approaches, we have shown that Mid2 is able to self-interact, and by doing so it could cross-link several septin filaments and possibly act as a septin bundler. However, the analysis of septins and Mid2 dynamics in cells blocked in mitosis, identified a situation where the septin meshwork does not compact although Mid2 retained the ability to interact with septins and with itself. This suggests that an additional mechanisms of regulation control septin compaction.

Mass Spectrometry analysis of Mid2 and septins partners in the mitotic-blocked mutant did not provide any hints of additional proteins promoting septin compaction in combination with Mid2 (our unpublished results), favoring the hypothesis that Mid2 bundling activity may be regulated by post-translational modifications independently of its ability to interact with septins and to self-interact.

Given that the major transitions detected in septins and Mid2 dynamics take place in anaphase and telophase, while cells switch from Cdk1 to SIN activation, an obvious approach was to check their behavior in mutants affected in those signaling pathways whereas septins and Mid2 can be recruited to the division site in presence of high Cdk1 activity but cannot compact, as previously mentioned, the SIN pathway is required for the recruitment as well as for the compaction of septins.

Since Mid2 is hyperphosphorylated in mitosis (Tasto et al., 2003), septin compaction might be driven by Mid2 dephosphorylation in anaphase. Interestingly, the mass spectrometry assay provided valuable information on the phosphorylation state of septins and Mid2, both in *nda3-KM11* mitotic-blocked cells, and in the *cdc16-116* SIN mutant where septation is uncoupled from mitosis, and several rounds of cytokinesis happen during the cell cycle (our unpublished results). Many of the detected sites are present in both mutants as well as specific phospho-sites for each mutant. One explanation for this is that although Cdk1 activity peaks before the SIN, *nda3-KM11* cells do carry some SIN activity, as proved by the SIN-dependent dissociation of Cdr2 from the cytokinetic precursor nodes (Rincon et al., 2017).

The creation of different combination of phospho-inhibitory and phospho-mimetic mutants should provide precious hints to elucidate the role of specific kinases in controlling Mid2 bundling activity and in clarifying the interplay between septins and Mid2.

More direct analysis of the role of Mid2 on septin organization could also be provided by *in vitro* reconstitution assays with purified fission yeast septins and full length or truncated forms of wild type or phospho-mutants of Mid2. These experiments would permit to study the organization of septin filaments in presence or absence of Mid2 and could permit to demonstrate its role as a septin filament bundler.

Last, we would need to decipher the impact of these phosphorylations in Mid2 oligomerization state or on its conformation, as well as to dig into the nanoscale structure of fission yeast septins filaments, which is still completely obscure. In *S. cerevisiae* single-molecule analysis by EM led to the discovery of the basic organization of the four essential septins and how these apolar rods associate end-to-end into long parallel filaments at low ionic strength (Bertin et al., 2008). The substitution in the octameric rod of the terminal subunit with the nonessential fifth septin, Shs1, has been shown to be sufficient to induce a different higher-order septin ultrastructure that can be further regulated by phosphorylation (Garcia et al., 2011). Additionally, Cryo-EM techniques permitted to visualize septin filaments at the mother/bud neck and their abnormal organization in septin mutants (Bertin et al., 2012). Furthermore, platinum-replica EM on budding yeast cells deprived of their cell wall revealed that septins filaments undergo a 90° reorientation during the hourglass-to- double ring transition (Ong et al., 2014). In collaboration with Aurelie Bertin, attempts of using EM have been made to gain insights into the dynamic organization of septins at different stages of the cell cycle, both in the presence and absence of Mid2, but although some filamentous structures were present at the cell division site, we cannot exclude that these were other proteins involved in the cytokinetic process. Correlative light and EM (CLEM), which preserves the fluorescence of labeled structures to facilitate the identification of septin filaments at the cleavage furrow was also tried. However, the experiments were not successful technically so far. This may be due to the fact that EM requires extensive manipulations to fix and section the samples, which may result in artifacts in cellular and protein morphology. Additionally, in fission yeast, the cytoplasm is really protein-dense which makes it difficult to recognize univocally specific protein complexes.

Another approach to gain information about septin organization through the cell cycle in live cells is polarized fluorescence microscopy, a technique that permits to gather data about the amount of order and the average orientation of proteins of interest tightly linked to fluorescent tags (Vrabioiu and Mitchison, 2006). By analyzing septins structures across diverse species, it has been shown that septins form paired filaments within higher order structures from yeast to mammals (DeMay et al 2011). Additionally, it was confirmed that these ordered ensembles experience a dramatic change in their direction at the onset of cytokinesis in budding yeast (Vrabioiu and Mitchison, 2006; Vrabioiu and Mitchison, 2007). Furthermore, polarized fluorescence microscopy has been instrumental in a screen to identify the Gin4 kinase, Bud4 and phosphorylation on Shs1 as key factors implicated in this structural reorientation (McQuilken et al., 2017). In collaboration with Manos Mavrakis and Sophie Brasselet (Aix-Marseille Université, Centre National de la Recherche Scientifique, Centrale Marseille, Institut Fresnel, MOSAIC team, Marseille, France), we have started to explore the configuration adopted by fission yeast septins filaments in wild type and *mid2Δ* cells by polarized fluorescence microscopy to better characterize the role of the anillin-like protein as a potential septin bundler. Moreover, to improve our

knowledge about the cell-cycle regulation of septin structural rearrangements, we are also assessing septins configuration in the *nda3-KM311* cold sensitive mutant blocked in mitosis in polarized fluorescence microscopy.

Altogether, these advanced microscopy approaches would be fundamental to understand how septins are assembled into higher order structures such as rings at a molecular and filament levels and how these structures are remodeled in time and space to perform specific functions during fission yeast cytokinesis.

A better molecular knowledge of septins regulation is crucial to advance our understanding of cell division and of anomalies in this process leading to cancer. Indeed, multiple evidences have reported that septins are deregulated in a variety of tumors, and septins dysfunctions have been also linked to a broad number of different pathologies, including male sterility and neurodegenerative diseases or zika-virus induced microcephaly (Angelis and Spiliotis, 2016; Dolat et al., 2014; Lhuillier et al., 2009; Li et al., 2019; Lin et al., 2009; Marttinen et al., 2015; Mostowy and Cossart, 2012; Pous et al., 2016). Thus, studying how these scaffold proteins function during cytokinesis may also provide hints to understand their roles in normal and pathological situations in higher eukaryotes.

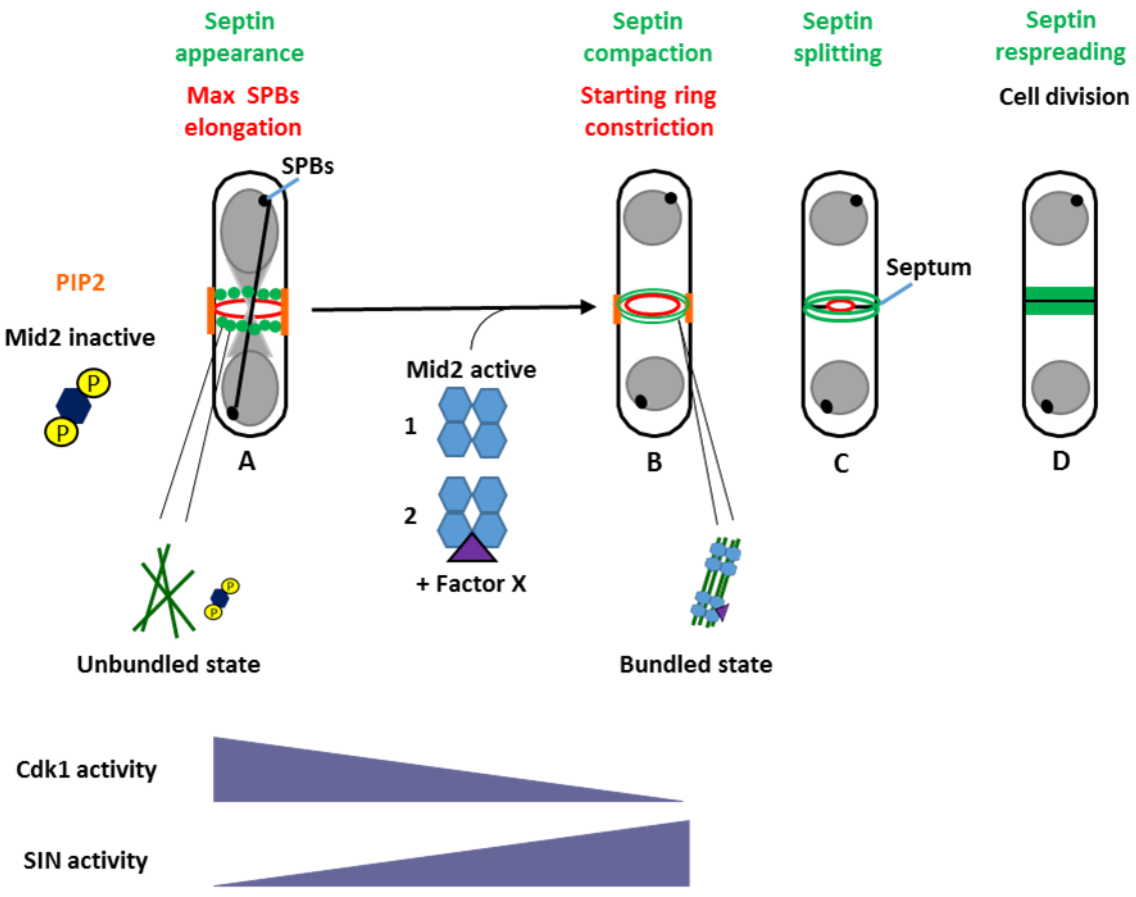

Model highlighting the sequence of septin filaments transitions during fission yeast cytokinesis and the role of Mid2, PIP2 and the cell-cycle in their regulation. (**A**) At the time of maximum SPBs elongation, when Cdk1 activity is high, the initial recruitment of septins to the division site is triggered by PIP2. At this stage, when Mid2 is inactive, probably due to hyperphosphorylation, the septin meshwork is disorganized and forms a wide band in a region surrounding the contractile acto-myosin ring. (**B**) When the SIN pathway becomes active, acto-myosin ring constriction begins and, septin filaments compact to form a ring, in a process mediated by Mid2, which may act as a bundler contributing to septin filaments alignment. This process may involve Mid2 activation upon dephosphorylation (1), or the participation of an additional factor (2). (**C**) Later on, once the acto-myosin ring constriction ends, septin are detected as a double ring due to the formation of the septum in between.
(**D**) Eventually septins respread over the new cell tip upon daughter cell separation.

V. SYNTHÈSE EN FRANÇAIS

Le cycle cellulaire est un processus clé utilisé par toutes les formes vivantes pour proliférer ou se renouveler. Il consiste en un ensemble d'événements ordonnés, aboutissant à la division de la cellule mère en deux cellules filles. Le cycle cellulaire comprend deux étapes principales: l'interphase composée des phases G1, S et G2, où les cellules font l'objet de croissance et reproduisent leur matériel génétique, et la mitose, au cours de laquelle la ségrégation des chromosomes est régie par le fuseau mitotique. La cytocinèse est la dernière étape du cycle cellulaire. Elle conduit à la séparation physique des deux cellules filles. Il s'agit d'un événement critique et irréversible, étroitement coordonné avec la sortie de la mitose et la séparation des chromosomes, afin de garantir une répartition égale du matériel génétique dans les cellules filles. Un contrôle défectueux de ce processus peut conduire à la mort cellulaire ou à l'aneuploïdie et peut contribuer au processus du cancerisation. Cet événement est donc sous le contrôle de mécanismes de régulation spatiaux et temporels très stricts.

Quatre événements majeurs peuvent être distingués au cours de la cytocinèse (Balasubramanian et al., 2004; Pollard and Wu, 2010). Tout d'abord, la position du plan de division est définie. Dans la plupart des organismes, cette étape implique la signalisation par la zone centrale du fuseau mitotique pour permettre à la division cellulaire de se produire entre les deux ensembles de chromosomes ségrégés. Deuxièmement, un anneau contractile (AC) à base d'actomyosine est assemblé au site de division sur la face interne de la membrane plasmique. La troisième étape est représentée par la contraction de cette structure qui conduit à la formation du sillon de division qui sépare la cellule en deux. La fermeture de l'AC est bien synchronisée avec les voies de trafic membranaire, de sorte que de nouvelles membranes sont synthétisées pour assurer l'extension de surface des deux cellules filles. Celles-ci sont physiquement séparées en deux entités distinctes lors de la dernière étape de la cytocinèse appelée abscission.

La cytocinèse s'accompagne d'un réarrangement massif de la forme des cellules avec des modifications de la composition membranaire et de la dynamique du trafic membranaire intracellulaire (Fremont and Echard, 2018; Gerien and Wu, 2018; Neto et al., 2011). Récemment, des techniques innovantes d'analyse et de quantification des lipides ont montré que la composition lipidique change à la fois dans l'espace et dans le temps au cours du cycle cellulaire (Muro et al., 2014; Shevchenko and Simons, 2010). Elles ont révélé en particulier que les cellules sont capables de contrôler et de modifier la composition et la répartition des lipides au cours de la division cellulaire, avec des rôles de signalisation et de rôles mécaniques (Atilla-Gokcumen et al., 2014; Echard and Burgess, 2014; Storck et al., 2018). En effet, de nombreuses évidences ont montré que certaines espèces lipidiques forment des plateformes de signalisation en interagissant avec d'autres lipides ou protéines pour réguler le transport de protéines clés, tandis que d'autres apportent un soutien structurel au remodelage de la courbure de la membrane (Albertson et al., 2005; Montagnac et al., 2008; van Meer et al., 2008).

Différentes catégories de lipides, notamment le cholestérol, les sphingolipides et les phosphoinositides, jouent un rôle important dans le succès de la cytocinèse (Brill et al., 2011; Cauvin and Echard, 2015; Storck et al., 2018). Ainsi, les lipides ne sont pas des constituants passifs des membranes cellulaires mais, grâce à leur géométrie, leur hydrophobicité et leur charge particulière, ils jouent un rôle actif dans la régulation de la forme et de la fonction de la membrane. Une structure membranaire unique avec une composition lipidique spécifique est assemblée de manière dynamique tout au long du cycle cellulaire et contribue aux fonctions clés pour la fidélité de la cytocinèse, notamment le trafic membranaire, l'insertion membranaire, le remodelage dynamique du cytosquelette et la signalisation.

En outre, l'achèvement de la cytocinèse nécessite la participation de différents composants du cytosquelette, à savoir le cytosquelette d'actine à la base de l'AC qui se contracte en tirant sur la membrane plasmique pour créer le sillon de clivage ; les microtubules impliqués dans la signalisation du plan de division dans les cellules animales ; ainsi que les septines, présentes sur le site de division des levures aux mammifères.

Les septines sont des composants du cytosquelette uniques capables de s'assembler pour former des structures intracellulaires de formes variées telles que des filaments et des anneaux (Bertin et al., 2008; DeMay et al., 2011; Garcia et al., 2011; Sirajuddin et al., 2007) en association avec des membranes cellulaires, ainsi que des filaments et des microtubules d'actine. Ceci leur permet de participer à de nombreux processus biologiques, où elles fonctionnent comme des échafaudages pour les interactions protéine-protéine et/ou comme des barrières de diffusion pour la compartimentalisation des protéines (Bridges and Gladfelter, 2015; Caudron and Barral, 2009; Mostowy and Cossart, 2012; Spiliotis, 2018). Ces protéines de liaison au GTP conservées ont été découvertes initialement chez la levure, où elles se localisent au site de division et sont essentielles pour la cytocinèse (Cauvin and Echard, 2015; El Amine et al., 2013; Estey et al., 2010; Gladfelter et al., 2001; Hartwell, 1971; Kozubowski et al., 2005; McMurray and Thorner, 2009; Versele and Thorner, 2005; Wu et al., 2010).

Les septines sont également présentes dans les cellules animales et localisées au niveau du sillon de division au cours de la cytocinèse. Elles contribuent au recrutement de l'anneau contractile sur le site de la division cellulaire et à la régulation de sa contraction (Kinoshita et al., 1997; Maddox et al., 2007; Mavrakis et al., 2014). Par la suite, les septines jouent également un rôle important dans la maturation du pont intercellulaire et de la formation du « mid-body », puis dans l'abscission (El Amine et al., 2013; Estey et al., 2010; Karasmanis et al., 2019; Renshaw et al., 2014).

On sait que leur comportement dynamique au cours de la progression de la cytocinèse est régulé par des modifications post-traductionnelles et des interactions avec des protéines régulatrices qui s'associent aux septines (Eluere et al., 2012; Kang et al., 2013; Marquardt et al., 2018; Wu et al., 2015).

Un facteur important pour l'organisation des septines est l'anilline, protéine conservée, dont la perturbation conduit à des défauts de cytocinèse (Echard et al., 2004; Field et al., 2005a; Kechad et al., 2012; Oegema et al., 2000; Somma et al., 2002; Straight et al., 2005; Zhao and Fang, 2005). Des études *in vitro* ont montré que l'anilline peut se lier aux filaments de septines et d'actine. En effet, une fonction importante de l'anilline est le recrutement des septines lors de la division cellulaire (Field et al., 2005a; Kinoshita et al., 2002; Oegema et al., 2000). Il est bien établi que l'anilline interagit avec les septines via une région C-terminale comprenant le domaine d'homologie de l'anilline (AH) en amont du domaine PH terminal (Piekny and Maddox, 2010). La région C-terminale de Bud4, la protéine analogue à l'anilline chez la levure *S. Cerevisiae*, joue un rôle important dans l'organisation des septines lors de la sélection du site de bourgeonnement et de la croissance des bourgeons ainsi que dans la préservation de l'intégrité des anneaux de septines lors de la cytocinèse (Kang et al., 2013; Wu et al., 2015). En effet, chez les mutants bud4Δ, le double anneau de septines se désassemble au cours de la cytocinèse (Eluere et al., 2012; Kang et al., 2013; Wloka et al., 2011), alors que la surexpression de Bud4 conduit à la formation de structures additionnelles de septines (Kang et al., 2013). Récemment, des études de microscopie à lumière polarisée ont décrit le rôle clé de Bud4 dans la réorientation des filaments de septines présents dans le cou joignant la cellule fille à la cellule mère, au moment de la transition à un double anneau (McQuilken et al., 2017).

La levure à fission est un organisme eucaryote simple unicellulaire qui a été largement utilisé pour étudier la division cellulaire en raison de sa forme stéréotypée, de sa génétique facile et de son temps de génération court (Hayles and Nurse, 2001; Hayles and Nurse, 2018). En particulier, ce système modèle s'est révélé très puissant pour la dissection moléculaire de l'AC (Almonacid and Paoletti, 2010; Lee et al., 2012; Pollard and Wu, 2010; Rincon and Paoletti, 2012; Rincon and Paoletti, 2016; Wu et al., 2003; Wu et al., 2006). C'est un organisme en forme de bâtonnet, qui se divise par l'assemblage et la constriction d'un AC à base d'acto-myosine placé en position médiane. Ce processus est étroitement régulé dans l'espace et dans le temps et se déroule en plusieurs étapes.

Une combinaison de signaux négatifs et positifs définit la position du plan de division au milieu de la cellule afin de promouvoir une division symétrique. L'assemblage de l'AC est initié par des précurseurs cytocinétiques assemblés dès l'interphase sur le cortex médian de la cellule par la SAD kinase Cdr2 (Akamatsu et al., 2017; Moseley et al., 2009; Pollard and Wu, 2010; Rincon and Paoletti, 2016; Willet et al., 2015b; Wu et al., 2006). Ces précurseurs cytocinétiques contiennent plusieurs composants non essentiels de l'AC, tels que la protéine analogue à l'anilline Mid1, Blt1, Gef2, Klp8 et Nod1 (Goss et al., 2014; Guzman-Vendrell et al., 2013; Jourdain et al., 2013; Martin and Berthelot-Grosjean, 2009; Moseley et al., 2009; Ye et al., 2012; Zhu et al., 2013). Le positionnement médial de ces nœuds est assuré par signalisation négative de la DYRK kinase Pom1 qui forme un gradient émanant des extrémités

des cellules (Celton-Morizur et al., 2006; Martin and Berthelot-Grosjean, 2009; Moseley et al., 2009; Padte et al., 2006; Rincon et al., 2014). Lors de l'entrée en mitose, l'exportation du noyau de la protéine de type anilline Mid1 induite par la kinase Plo1 de la famille Polo permet la signalisation positive du plan de division par le noyau placé médialement et renforce le positionnement du plan de division au centre de la cellule (Almonacid et al., 2009), tandis que Cdr2 se dissocie des précurseurs cytocinétiques d'une manière dépendante du SIN (Akamatsu et al., 2014; Rincon et al., 2017). Plo1 active également Mid1, qui devient compétent pour le recrutement séquentiel de composants essentiels de l'AC (Almonacid et al., 2011): Mid1 commence par recruter la protéine IQGAP Rng2 et Cdc4 la chaîne légère de la myosine II, puis sa chaîne lourde Myo2 et sa chaîne légère régulatrice Rlc1. Mid1 contribue également directement au recrutement de la protéine F-BAR Cdc15 (Laporte et al., 2011). Enfin, Rng2 et la myosin II, ainsi que Cdc15, collaborent au recrutement de la formine Cdc12, qui nuclée les câbles d'actine-F nécessaires à l'assemblage de l'AC (Coffman et al., 2009; Coffman et al., 2013; Laporte et al., 2011; Padmanabhan et al., 2011; Willet et al., 2015a; Wu et al., 2003; Wu et al., 2006). Cette étape est nécessaire à la compaction des nœuds précurseurs cytocinétiques en un anneau fin, par un mécanisme modélisé sous le nom de recherche-capture-traction (Ojkic et al., 2011; Vavylonis et al., 2008). Lors de la sortie de la mitose, le SIN, relié évolutivement au réseau de sortie de mitose de la levure bourgeonnante (MEN) et à la voie hippo des métazoaires (Hergovich et al., 2006), contrôle les étapes suivantes, représentées par la constriction de l'AC et la synthèse d'un septum extracellulaire composé de polysaccharides (Krapp et al., 2004b; Simanis, 2003; Simanis, 2015). Finalement, la séparation des cellules sœurs s'ensuit lorsque la couche interne du septum est digérée par des glucanases (Cortes et al., 2016; Perez et al., 2016).

Parallèlement à l'assemblage de l'AC, des modifications de la composition lipidique de la membrane plasmique ont lieu au site de division, avec un impact fonctionnel sur la cytocinèse. Cependant, dans la levure à fission, on ne dispose que de peu de données sur le rôle des lipides membranaires dans la cytocinèse. On sait cependant que la localisation correcte de la PI4 kinase Stt4 par sa sous-unité d'échafaudage Efr3 joue un rôle dans la régulation spatiale de la cytocinèse en empêchant l'AC de glisser vers l'extrémité de la cellule pendant l'anaphase (Snider et al., 2017). De même, des anomalies de la régulation spatiale de la cytocinèse ont été rapportées dans le mutant de la PI-5 kinase its3-1, caractérisé par des taux réduits de PI(3,5)P2 (Snider et al., 2018). Deuxièmement, des défauts de cytocinèse ainsi que de la morphologie cellulaire et de l'organisation de la paroi cellulaire ont été observés dans un mutant de Pps1 impliqué dans la synthèse de la phosphatidylsérine (PS) (Matsuo et al., 2007). Troisièmement, il a été démontré que les défauts d'hydrolyse des sphingolipides en céramide dans le mutant css1 induisent des défauts de formation de la paroi cellulaire et du septum, dus à l'accumulation de glucanes α et β dans l'espace périplasmique, avec arrêt de la division cellulaire et

issue fatale (Feoktistova et al., 2001). Certaines données indiquent également un rôle des stérols dans la régulation de la cytocinèse (Wachtler et al., 2003). Les stérols sont synthétisés et subissent leur maturation dans le reticulum endoplasmique par une cascade de réactions enzymatiques couplées. Le produit métabolique final, le cholestérol dans le cas des cellules animales et l'ergostérol chez les champignons, est ensuite transporté vers la membrane plasmique où il forme des domaines ordonnés liquides en interagissant préférentiellement avec les sphingolipides, qui jouent un rôle reconnu dans la transduction du signal, le tri vésiculaire et la polarité (Rajendran and Simons, 2005). Les facteurs clés pour la formation de domaines riches en stérols (SRD) sont la protéine F-BAR Cdc15 et la myosine Myo1 de type I, qui interagissent ensemble, et se lient préférentiellement aux phospholipides acides (Alvarez et al., 2007; Carnahan and Gould, 2003; Takeda and Chang, 2005; Takeda et al., 2004). De plus, les SRD se redistribuent des extrémités de cellules en croissance en interphase, où ils agissent comme des échafaudages pour les facteurs de polarité et le mécanisme de croissance (Makushok et al., 2016), vers le site de division en mitose (Wachtler et al., 2003). Fait intéressant, Wachtler et al. (2003) ont découvert que la surexpression de Erg25, une stérol-méthyl-oxydase C-4 de la voie de synthèse de l'ergostérol, pouvait altérer la distribution de l'ergostérol au sein de la cellule et perturber le positionnement du CR, conduisant à la formation de septa positionnés aléatoirement et déformés (Wachtler et al., 2003).

En plus de l'AC, la cytocinèse implique les anneaux de septines. Chez la levure de fission, ces protéines d'échafaudage interviennent aux derniers stades de la cytocinèse pour favoriser la séparation des cellules filles. En effet, contrairement à *S. cerevisiae*, où les septines sont nécessaires à la formation de l'AC, les septines sont recrutées une fois que l'anneau contractile a été complètement assemblé chez *S. pombe*. Les septines forment d'abord un anneau unique à la fin de la mitose, qui se sépare en deux lors de la constriction de l'AC et de la formation du septum. Ce double anneau ne se contracte pas avec l'AC, mais reste à la surface de la cellule pour délimiter les bords du sillon de division. Puis il se dissocie après la séparation des cellules filles (An et al., 2004; Berlin et al., 2003; Juanes and Piatti, 2016; Wu et al., 2003). Les mutants de septines présentent des défauts de séparation des cellules filles car les septines jouent un rôle clé, de concert avec le complexe exocyste, dans la sécrétion des deux enzymes hydrolytiques du septum (Agn1 et Eng1) dans la zone autour du septum, régulant ainsi l'étape terminale de la cytocinèse (Alonso-Nunez et al., 2005; Martin-Cuadrado et al., 2005). Récemment, il a également été démontré que les septines jouent un rôle dans le recrutement et le maintien correct dans la région du septum de la kinase Sid2 et des glucan-synthases Bgs1 et Ags1 afin de garantir le succès de la cytocinèse (Zheng et al., 2018).

Le génome de *S. pombe* code pour deux protéines apparentées à l'anilline: Mid1 et Mid2. Les tests génétiques ont exclu tout chevauchement de fonctions entre elles, indiquant qu'elles travaillent

indépendamment dans des phases distinctes du cycle cellulaire (Berlin et al., 2003). Mid2 se localise sur le site de la division de manière dépendante des septines (Berlin et al., 2003). De plus, le fait qu'une souche mid2Δ présente le même phénotype que le mutant Spn4Δ où la division nucléaire et la synthèse du septum se produisent mais la séparation cellulaire est retardée (Berlin et al., 2003) suggère que Mid2 et les septines participent au même processus. En effet, l'analyse par FRAP a révélé qu'en l'absence de Mid2, les septines sont beaucoup plus dynamiques (30 fois plus) que dans des cellules de type sauvage, ce qui indique un rôle de Mid2 dans l'organisation des septines (Berlin et al., 2003). Les niveaux de protéine Mid2 sont étroitement contrôlés pendant le cycle cellulaire, atteignant leur maximum pendant la septation et diminuant après la séparation cellulaire. Bien que cela puisse être contrôlé par phosphorylation, les kinases candidates n'ont pas encore été identifiées (Kim et al., 2017; Tasto et al., 2003). En outre, Mid2 contient trois séquences PEST, une dans une région médiale et deux au niveau de l'extrémité N-terminale, qui pourraient servir de signaux pour la dégradation des protéines par l'ubiquitination et la protéolyse dépendante du SCF (Alonso-Nunez et al., 2005; Petit et al., 2005; Tasto et al., 2003). La surexpression d'un mutant Mid2 non dégradable induit la persistance des filaments de septines tout au long du cycle cellulaire suivant, indiquant que Mid2 est impliqué dans la maintenance des anneaux de septine (An et al., 2004; Tasto et al., 2003). Globalement, ces évidences indiquent que: 1) les filaments de septines peuvent s'organiser en anneau de manière dépendante de l'AC, 2) le recrutement de Mid2 est dépendant des septines et 3) Mid2 contribue à la stabilité de cet anneau.
Cependant, la manière dont les septines et Mid2 sont régulées avec précision dans l'espace et dans le temps pour s'acquitter correctement de leur fonction et la manière dont Mid2 contribue à l'organisation des anneaux de septines reste incomprise.

J'ai étudié la cytocinèse dans le système modèle de levure à fission sous deux angles différents. Mon travail a d'abord porté sur la première étape de la cytocinèse, le positionnement du plan de division, et a abordé le rôle d'un lipide membranaire dans ce processus. La deuxième partie de mon projet a été consacré à la cytocinèse tardive, en analysant l'assemblage des anneaux de septine sur le site de la division.

La première partie de mon travail visait à comprendre l'impact du niveau d'ergostérol sur le positionnement du plan de division. En effet, la surexpression d'Erg25, une protéine impliquée dans la biosynthèse de l'ergostérol, entraîne un positionnement aléatoire de l'AC et par conséquent du septum. En combinant la génétique de la levure *S. pombe* et l'imagerie sur cellules vivantes des composants de l'AC, j'ai constaté qu'une augmentation du niveau d'ergostérol ne perturbe pas les noeuds précurseurs cytocinétiques qui définissent la position du plan de division, mais inhibe spécifiquement l'assemblage de l'actine-F à partir des noeuds précurseurs cytocinétiques par la formine Cdc12, empêchant leur

compaction en un AC placé en position médiane. Puisque la stabilité des câbles d'actine-F n'est pas complètement modifiée et que le phénotype peut être partiellement sauvé par l'inhibition du complexe Arp2/3 qui entre en compétition avec les formines, nous proposons que l'augmentation des niveaux d'ergostérol dans la membrane plasmique inhibe l'activité de la formine Cdc12 de manière directe ou indirecte.

Dans la deuxième partie de ma thèse, mon projet portait sur le comportement dynamique des septines au cours de la cytocinèse et les mécanismes de régulation qui contrôlent leur assemblage en anneaux définissant les limites du sillon de clivage. Cette partie a été abordée de trois manières: 1) Description du recrutement, de l'assemblage et du désassemblage des septines et de la protéine de type anilline Mid2 par imagerie sur cellules vivantes à l'aide de minuteurs précis de cycle cellulaire 2) Détermination de l'impact de Mid2 sur l'assemblage des anneaux de septines en combinant approches de génétique moléculaire et de biochimie 3) Identification des principaux régulateurs contrôlant les principales transitions d'organisation des septines et de Mid2. J'ai tout d'abord constaté que les septines sont initialement recrutées en tant que réseau diffus dans une région du cortex de 1,5 µm de large entourant l'AC, au moment de l'élongation maximale du fuseau, avant de se compacter en anneaux lors du déclenchement de la constriction de l'AC. Deuxièmement, mes travaux démontrent que la protéine Mid2, semblable à l'anilline, pourrait agir comme un « bundler » pour les septines favorisant cette nouvelle étape de compaction ainsi que l'accumulation supplémentaire de septines au niveau du site de division. Troisièmement, en regardant les régulateurs du cycle cellulaire, j'ai trouvé qu'une activité élevée de Cdk1 permettait le recrutement de septines et Mid2 mais pas leur compaction, alors que la voie SIN est cruciale pour l'accumulation de septines et Mid2 au site de division et leur compaction. Enfin, les niveaux de PIP2 se sont révélés essentiels pour déclencher le recrutement de septines sur la membrane plasmique, avant que Mid2 ne soit disponible au début de la constriction de l'AC, et ont un impact sur la quantité maximale de septines au site de division. Ce travail met donc en évidence les régulations complexes qui permettent la coordination entre l'assemblage des anneaux de septines et la progression du cycle cellulaire.

VI. BIBLIOGRAPHY

Abe, M., Makino, A., Hullin-Matsuda, F., Kamijo, K., Ohno-Iwashita, Y., Hanada, K., Mizuno, H., Miyawaki, A. and Kobayashi, T. (2012). A role for sphingomyelin-rich lipid domains in the accumulation of phosphatidylinositol-4,5-bisphosphate to the cleavage furrow during cytokinesis. *Mol Cell Biol* **32**, 1396-407.

Akamatsu, M., Berro, J., Pu, K. M., Tebbs, I. R. and Pollard, T. D. (2014). Cytokinetic nodes in fission yeast arise from two distinct types of nodes that merge during interphase. *J Cell Biol* **204**, 977-88.

Akamatsu, M., Lin, Y., Bewersdorf, J. and Pollard, T. D. (2017). Analysis of interphase node proteins in fission yeast by quantitative and superresolution fluorescence microscopy. *Mol Biol Cell* **28**, 3203-3214.

Alberts, A. S. (2001). Identification of a carboxyl-terminal diaphanous-related formin homology protein autoregulatory domain. *J Biol Chem* **276**, 2824-30.

Albertson, R., Riggs, B. and Sullivan, W. (2005). Membrane traffic: a driving force in cytokinesis. *Trends Cell Biol* **15**, 92-101.

Allard, C. A. H., Opalko, H. E., Liu, K. W., Medoh, U. and Moseley, J. B. (2018). Cell size-dependent regulation of Wee1 localization by Cdr2 cortical nodes. *J Cell Biol* **217**, 1589-1599.

Allard, C. A. H., Opalko, H. E. and Moseley, J. B. (2019). Stable Pom1 clusters form a glucose-modulated concentration gradient that regulates mitotic entry. *Elife* **8**.

Almonacid, M., Celton-Morizur, S., Jakubowski, J. L., Dingli, F., Loew, D., Mayeux, A., Chen, J. S., Gould, K. L., Clifford, D. M. and Paoletti, A. (2011). Temporal control of contractile ring assembly by Plo1 regulation of myosin II recruitment by Mid1/anillin. *Curr Biol* **21**, 473-9.

Almonacid, M., Moseley, J. B., Janvore, J., Mayeux, A., Fraisier, V., Nurse, P. and Paoletti, A. (2009). Spatial control of cytokinesis by Cdr2 kinase and Mid1/anillin nuclear export. *Curr Biol* **19**, 961-6.

Almonacid, M. and Paoletti, A. (2010). Mechanisms controlling division-plane positioning. *Semin Cell Dev Biol* **21**, 874-80.

Alonso-Nunez, M. L., An, H., Martin-Cuadrado, A. B., Mehta, S., Petit, C., Sipiczki, M., del Rey, F., Gould, K. L. and de Aldana, C. R. (2005). Ace2p controls the expression of genes required for cell separation in Schizosaccharomyces pombe. *Mol Biol Cell* **16**, 2003-17.

Alonso, A., Greenlee, M., Matts, J., Kline, J., Davis, K. J. and Miller, R. K. (2015). Emerging roles of sumoylation in the regulation of actin, microtubules, intermediate filaments, and septins. *Cytoskeleton (Hoboken)* **72**, 305-39.

Alvarez, F. J., Douglas, L. M. and Konopka, J. B. (2007). Sterol-rich plasma membrane domains in fungi. *Eukaryot Cell* **6**, 755-63.

An, H., Morrell, J. L., Jennings, J. L., Link, A. J. and Gould, K. L. (2004). Requirements of fission yeast septins for complex formation, localization, and function. *Mol Biol Cell* **15**, 5551-64.

Andrianantoandro, E. and Pollard, T. D. (2006). Mechanism of actin filament turnover by severing and nucleation at different concentrations of ADF/cofilin. *Mol Cell* **24**, 13-23.

Angelis, D. and Spiliotis, E. T. (2016). Septin Mutations in Human Cancers. *Front Cell Dev Biol* **4**, 122.

Arasada, R. and Pollard, T. D. (2011). Distinct roles for F-BAR proteins Cdc15p and Bzz1p in actin polymerization at sites of endocytosis in fission yeast. *Curr Biol* **21**, 1450-9.

Arasada, R. and Pollard, T. D. (2014). Contractile ring stability in S. pombe depends on F-BAR protein Cdc15p and Bgs1p transport from the Golgi complex. *Cell Rep* **8**, 1533-44.

Arasada, R. and Pollard, T. D. (2015). A role for F-BAR protein Rga7p during cytokinesis in S. pombe. *J Cell Sci* **128**, 2259-68.

Arellano, M., Duran, A. and Perez, P. (1996). Rho 1 GTPase activates the (1-3)beta-D-glucan synthase and is involved in Schizosaccharomyces pombe morphogenesis. *EMBO J* **15**, 4584-91.

Atilgan, E., Magidson, V., Khodjakov, A. and Chang, F. (2015). Morphogenesis of the Fission Yeast Cell through Cell Wall Expansion. *Curr Biol* **25**, 2150-7.

Atilla-Gokcumen, G. E., Bedigian, A. V., Sasse, S. and Eggert, U. S. (2011). Inhibition of glycosphingolipid biosynthesis induces cytokinesis failure. *J Am Chem Soc* **133**, 10010-3.

Atilla-Gokcumen, G. E., Muro, E., Relat-Goberna, J., Sasse, S., Bedigian, A., Coughlin, M. L., Garcia-Manyes, S. and Eggert, U. S. (2014). Dividing cells regulate their lipid composition and localization. *Cell* **156**, 428-39.

Bahler, J. and Pringle, J. R. (1998). Pom1p, a fission yeast protein kinase that provides positional information for both polarized growth and cytokinesis. *Genes Dev* **12**, 1356-70.

Bahler, J., Steever, A. B., Wheatley, S., Wang, Y., Pringle, J. R., Gould, K. L. and McCollum, D. (1998a). Role of polo kinase and Mid1p in determining the site of cell division in fission yeast. *J Cell Biol* **143**, 1603-16.

Bahler, J., Wu, J. Q., Longtine, M. S., Shah, N. G., McKenzie, A., 3rd, Steever, A. B., Wach, A., Philippsen, P. and Pringle, J. R. (1998b). Heterologous modules for efficient and versatile PCR-based gene targeting in Schizosaccharomyces pombe. *Yeast* **14**, 943-51.

Baird, D., Stefan, C., Audhya, A., Weys, S. and Emr, S. D. (2008). Assembly of the PtdIns 4-kinase Stt4 complex at the plasma membrane requires Ypp1 and Efr3. *J Cell Biol* **183**, 1061-74.

Balasubramanian, M. K., Bi, E. and Glotzer, M. (2004). Comparative analysis of cytokinesis in budding yeast, fission yeast and animal cells. *Curr Biol* **14**, R806-18.

Balasubramanian, M. K., Helfman, D. M. and Hemmingsen, S. M. (1992). A new tropomyosin essential for cytokinesis in the fission yeast S. pombe. *Nature* **360**, 84-7.

Balasubramanian, M. K., Hirani, B. R., Burke, J. D. and Gould, K. L. (1994). The Schizosaccharomyces pombe cdc3+ gene encodes a profilin essential for cytokinesis. *J Cell Biol* **125**, 1289-301.

Balasubramanian, M. K., McCollum, D., Chang, L., Wong, K. C., Naqvi, N. I., He, X., Sazer, S. and Gould, K. L. (1998). Isolation and characterization of new fission yeast cytokinesis mutants. *Genetics* **149**, 1265-75.

Barnum, K. J. and O'Connell, M. J. (2014). Cell cycle regulation by checkpoints. *Methods Mol Biol* **1170**, 29-40.

Beber, A., Alqabandi, M., Prevost, C., Viars, F., Levy, D., Bassereau, P., Bertin, A. and Mangenot, S. (2019). Septin-based readout of PI(4,5)P2 incorporation into membranes of giant unilamellar vesicles. *Cytoskeleton (Hoboken)* **76**, 92-103.

Beloribi-Djefaflia, S., Vasseur, S. and Guillaumond, F. (2016). Lipid metabolic reprogramming in cancer cells. *Oncogenesis* **5**, e189.

Berlin, A., Paoletti, A. and Chang, F. (2003). Mid2 stabilizes septin rings during cytokinesis in fission yeast. *JCB* **160**, 1083-1092.

Bertin, A., McMurray, M. A., Grob, P., Park, S. S., Garcia, G., 3rd, Patanwala, I., Ng, H. L., Alber, T., Thorner, J. and Nogales, E. (2008). Saccharomyces cerevisiae septins: supramolecular organization of heterooligomers and the mechanism of filament assembly. *Proc Natl Acad Sci U S A* **105**, 8274-9.

Bertin, A., McMurray, M. A., Pierson, J., Thai, L., McDonald, K. L., Zehr, E. A., García, G., Peters, P., Thorner, J. and Nogales, E. (2012). Three-dimensional ultrastructure of the septin filament network in Saccharomyces cerevisiae. *Molecular Biology of the Cell* **23**, 423-432.

Bertin, A., McMurray, M. A., Thai, L., Garcia, G., 3rd, Votin, V., Grob, P., Allyn, T., Thorner, J. and Nogales, E. (2010). Phosphatidylinositol-4,5-bisphosphate promotes budding yeast septin filament assembly and organization. *J Mol Biol* **404**, 711-31.

Bestul, A. J., Christensen, J. R., Grzegorzewska, A. P., Burke, T. A., Sees, J. A., Carroll, R. T., Sirotkin, V., Keenan, R. J. and Kovar, D. R. (2015). Fission yeast profilin is tailored to facilitate actin assembly by the cytokinesis formin Cdc12. *Mol Biol Cell* **26**, 283-93.

Bhatia, P., Hachet, O., Hersch, M., Rincon, S. A., Berthelot-Grosjean, M., Dalessi, S., Basterra, L., Bergmann, S., Paoletti, A. and Martin, S. G. (2014). Distinct levels in Pom1 gradients limit Cdr2 activity and localization to time and position division. *Cell Cycle* **13**, 538-52.

Bhavsar-Jog, Y. P. and Bi, E. (2017). Mechanics and regulation of cytokinesis in budding yeast. *Semin Cell Dev Biol* **66**, 107-118.

Bi, E., Maddox, P., Lew, D. J., Salmon, E. D., McMillan, J. N., Yeh, E. and Pringle, J. R. (1998). Involvement of an actomyosin contractile ring in Saccharomyces cerevisiae cytokinesis. *J Cell Biol* **142**, 1301-12.

Blank, H. M., Perez, R., He, C., Maitra, N., Metz, R., Hill, J., Lin, Y., Johnson, C. D., Bankaitis, V. A., Kennedy, B. K. et al. (2017). Translational control of lipogenic enzymes in the cell cycle of synchronous, growing yeast cells. *EMBO J* **36**, 487-502.

Bohnert, K. A. and Gould, K. L. (2011). On the cutting edge: post-translational modifications in cytokinesis. *Trends Cell Biol* **21**, 283-92.

Bohnert, K. A. and Gould, K. L. (2012). Cytokinesis-based constraints on polarized cell growth in fission yeast. *PLoS Genet* **8**, e1003004.

Bohnert, K. A., Grzegorzewska, A. P., Willet, A. H., Vander Kooi, C. W., Kovar, D. R. and Gould, K. L. (2013a). SIN-dependent phosphoinhibition of formin multimerization controls fission yeast cytokinesis. *Genes Dev* **27**, 2164-77.

Bohnert, K. A., Willet, A. H., Kovar, D. R. and Gould, K. L. (2013b). Formin-based control of the actin cytoskeleton during cytokinesis. *Biochem Soc Trans* **41**, 1750-4.

Bollen, M., Gerlich, D. W. and Lesage, B. (2009). Mitotic phosphatases: from entry guards to exit guides. *Trends Cell Biol* **19**, 531-41.

Bresnick, A. R. (1999). Molecular mechanisms of nonmuscle myosin-II regulation. *Curr Opin Cell Biol* **11**, 26-33.

Bridges, A. A. and Gladfelter, A. S. (2015). Septin Form and Function at the Cell Cortex. *J Biol Chem* **290**, 17173-80.

Bridges, A. A., Jentzsch, M. S., Oakes, P. W., Occhipinti, P. and Gladfelter, A. S. (2016). Micron-scale plasma membrane curvature is recognized by the septin cytoskeleton. *J Cell Biol* **213**, 23-32.

Bridges, A. A., Zhang, H., Mehta, S. B., Occhipinti, P., Tani, T. and Gladfelter, A. S. (2014). Septin assemblies form by diffusion-driven annealing on membranes. *Proc Natl Acad Sci U S A* **111**, 2146-51.

Brill, J. A., Hime, G. R., Scharer-Schuksz, M. and Fuller, M. T. (2000). A phospholipid kinase regulates actin organization and intercellular bridge formation during germline cytokinesis. *Development* **127**, 3855-64.

Brill, J. A., Wong, R. and Wilde, A. (2011). Phosphoinositide function in cytokinesis. *Curr Biol* **21**, R930-4.

Budnar, S., Husain, K. B., Gomez, G. A., Naghibosadat, M., Varma, A., Verma, S., Hamilton, N. A., Morris, R. G. and Yap, A. S. (2019). Anillin Promotes Cell Contractility by Cyclic Resetting of RhoA Residence Kinetics. *Dev Cell* **49**, 894-906 e12.

Burke, T. A., Christensen, J. R., Barone, E., Suarez, C., Sirotkin, V. and Kovar, D. R. (2014). Homeostatic actin cytoskeleton networks are regulated by assembly factor competition for monomers. *Curr Biol* **24**, 579-85.

Buttery, S. M., Kono, K., Stokasimov, E. and Pellman, D. (2012). Regulation of the formin Bnr1 by septins anda MARK/Par1-family septin-associated kinase. *Mol Biol Cell* **23**, 4041-53.

Calonge, T. M., Nakano, K., Arellano, M., Arai, R., Katayama, S., Toda, T., Mabuchi, I. and Perez, P. (2000). Schizosaccharomyces pombe rho2p GTPase regulates cell wall alpha-glucan biosynthesis through the protein kinase pck2p. *Mol Biol Cell* **11**, 4393-401.

Cannon, K. S., Woods, B. L., Crutchley, J. M. and Gladfelter, A. S. (2019). An amphipathic helix enables septins to sense micrometer-scale membrane curvature. *J Cell Biol* **218**, 1128-1137.

Carlier, M. F., Laurent, V., Santolini, J., Melki, R., Didry, D., Xia, G. X., Hong, Y., Chua, N. H. and Pantaloni, D. (1997). Actin depolymerizing factor (ADF/cofilin) enhances the rate of filament turnover: implication in actin-based motility. *J Cell Biol* **136**, 1307-22.

Carnahan, R. H. and Gould, K. L. (2003). The PCH family protein, Cdc15p, recruits two F-actin nucleation pathways to coordinate cytokinetic actin ring formation in Schizosaccharomyces pombe. *J Cell Biol* **162**, 851-62.

Casamayor, A. and Snyder, M. (2003). Molecular dissection of a yeast septin: distinct domains are required for septin interaction, localization, and function. *Mol Cell Biol* **23**, 2762-77.

Caudron, F. and Barral, Y. (2009). Septins and the lateral compartmentalization of eukaryotic membranes. *Dev Cell* **16**, 493-506.

Cauvin, C. and Echard, A. (2015). Phosphoinositides: Lipids with informative heads and mastermind functions in cell division. *Biochim Biophys Acta* **1851**, 832-43.

Celton-Morizur, S., Bordes, N., Fraisier, V., Tran, P. T. and Paoletti, A. (2004). C-terminal anchoring of mid1p to membranes stabilizes cytokinetic ring position in early mitosis in fission yeast. *Mol Cell Biol* **24**, 10621-35.

Celton-Morizur, S., Racine, V., Sibarita, J. B. and Paoletti, A. (2006). Pom1 kinase links division plane position to cell polarity by regulating Mid1p cortical distribution. *J Cell Sci* **119**, 4710-8.

Chalkia, D., Nikolaidis, N., Makalowski, W., Klein, J. and Nei, M. (2008). Origins and evolution of the formin multigene family that is involved in the formation of actin filaments. *Mol Biol Evol* **25**, 2717-33.

Chang, F., Drubin, D. and Nurse, P. (1997). cdc12p, a protein required for cytokinesis in fission yeast, is a component of the cell division ring and interacts with profilin. *J Cell Biol* **137**, 169-82.

Chang, F. and Peter, M. (2002). Cell biology. Formins set the record straight. *Science* **297**, 531-2.

Chang, F., Woollard, A. and Nurse, P. (1996). Isolation and characterization of fission yeast mutants defective in the assembly and placement of the contractile actin ring. *J Cell Sci* **109 (Pt 1)**, 131-42.

Chen, A., Akhshi, T. K., Lavoie, B. D. and Wilde, A. (2015). Importin beta2 Mediates the Spatio-temporal Regulation of Anillin through a Noncanonical Nuclear Localization Signal. *J Biol Chem* **290**, 13500-9.

Chen, C. T., Feoktistova, A., Chen, J. S., Shim, Y. S., Clifford, D. M., Gould, K. L. and McCollum, D. (2008). The SIN kinase Sid2 regulates cytoplasmic retention of the S. pombe Cdc14-like phosphatase Clp1. *Curr Biol* **18**, 1594-9.

Chen, J. S., Broadus, M. R., McLean, J. R., Feoktistova, A., Ren, L. and Gould, K. L. (2013). Comprehensive proteomics analysis reveals new substrates and regulators of the fission yeast clp1/cdc14 phosphatase. *Mol Cell Proteomics* **12**, 1074-86.

Chesarone, M. A., DuPage, A. G. and Goode, B. L. (2010). Unleashing formins to remodel the actin and microtubule cytoskeletons. *Nat Rev Mol Cell Biol* **11**, 62-74.

Clay, L., Caudron, F., Denoth-Lippuner, A., Boettcher, B., Buvelot Frei, S., Snapp, E. L. and Barral, Y. (2014). A sphingolipid-dependent diffusion barrier confines ER stress to the yeast mother cell. *Elife* **3**, e01883.

Clifford, D. M., Wolfe, B. A., Roberts-Galbraith, R. H., McDonald, W. H., Yates, J. R., 3rd and Gould, K. L. (2008). The Clp1/Cdc14 phosphatase contributes to the robustness of cytokinesis by association with anillin-related Mid1. *J Cell Biol* **181**, 79-88.

Coffman, V. C., Nile, A. H., Lee, I. J., Liu, H. and Wu, J. Q. (2009). Roles of formin nodes and myosin motor activity in Mid1p-dependent contractile-ring assembly during fission yeast cytokinesis. *Mol Biol Cell* **20**, 5195-210.

Coffman, V. C., Sees, J. A., Kovar, D. R. and Wu, J. Q. (2013). The formins Cdc12 and For3 cooperate during contractile ring assembly in cytokinesis. *J Cell Biol* **203**, 101-14.

Cortes, J. C., Carnero, E., Ishiguro, J., Sanchez, Y., Duran, A. and Ribas, J. C. (2005). The novel fission yeast (1,3)beta-D-glucan synthase catalytic subunit Bgs4p is essential during both cytokinesis and polarized growth. *J Cell Sci* **118**, 157-74.

Cortes, J. C., Ishiguro, J., Duran, A. and Ribas, J. C. (2002). Localization of the (1,3)beta-D-glucan synthase catalytic subunit homologue Bgs1p/Cps1p from fission yeast suggests that it is involved in septation, polarized growth, mating, spore wall formation and spore germination. *J Cell Sci* **115**, 4081-96.

Cortes, J. C., Konomi, M., Martins, I. M., Munoz, J., Moreno, M. B., Osumi, M., Duran, A. and Ribas, J. C. (2007). The (1,3)beta-D-glucan synthase subunit Bgs1p is responsible for the fission yeast primary septum formation. *Mol Microbiol* **65**, 201-17.

Cortes, J. C., Pujol, N., Sato, M., Pinar, M., Ramos, M., Moreno, B., Osumi, M., Ribas, J. C. and Perez, P. (2015). Cooperation between Paxillin-like Protein Pxl1 and Glucan Synthase Bgs1 Is Essential for Actomyosin Ring Stability and Septum Formation in Fission Yeast. *PLoS Genet* **11**, e1005358.

Cortes, J. C., Ramos, M., Osumi, M., Perez, P. and Ribas, J. C. (2016). Fission yeast septation. *Commun Integr Biol* **9**, e1189045.

Cortes, J. C., Sato, M., Munoz, J., Moreno, M. B., Clemente-Ramos, J. A., Ramos, M., Okada, H., Osumi, M., Duran, A. and Ribas, J. C. (2012). Fission yeast Ags1 confers the essential septum strength needed for safe gradual cell abscission. *J Cell Biol* **198**, 637-56.

Cortes, J. G., Ramos, M., Konomi, M., Barragan, I., Moreno, M. B., Alcaide-Gavilan, M., Moreno, S., Osumi, M., Perez, P. and Ribas, J. C. (2018). Specific detection of fission yeast primary septum reveals septum and cleavage furrow ingression during early anaphase independent of mitosis completion. *PLoS Genet* **14**, e1007388.

Costa, J., Fu, C., Syrovatkina, V. and Tran, P. T. (2013). Imaging individual spindle microtubule dynamics in fission yeast. *Methods Cell Biol* **115**, 385-94.

Cross, R. A. and McAinsh, A. (2014). Prime movers: the mechanochemistry of mitotic kinesins. *Nat Rev Mol Cell Biol* **15**, 257-71.

Cueille, N., Salimova, E., Esteban, V., Blanco, M., Moreno, S., Bueno, A. and Simanis, V. (2001). Flp1, a fission yeast orthologue of the s. cerevisiae CDC14 gene, is not required for cyclin degradation or rum1p stabilisation at the end of mitosis. *J Cell Sci* **114**, 2649-64.

Cullati, S. N. and Gould, K. L. (2019). Spatiotemporal regulation of the Dma1-mediated mitotic checkpoint coordinates mitosis with cytokinesis. *Curr Genet* **65**, 663-668.

D'Avino, P. P. (2009). How to scaffold the contractile ring for a safe cytokinesis - lessons from Anillin-related proteins. *J Cell Sci* **122**, 1071-9.

Daga, R. R. and Chang, F. (2005). Dynamic positioning of the fission yeast cell division plane. *Proc Natl Acad Sci U S A* **102**, 8228-32.

Dambournet, D., Machicoane, M., Chesneau, L., Sachse, M., Rocancourt, M., El Marjou, A., Formstecher, E., Salomon, R., Goud, B. and Echard, A. (2011). Rab35 GTPase and OCRL phosphatase remodel lipids and F-actin for successful cytokinesis. *Nat Cell Biol* **13**, 981-8.

Davie, E. and Petersen, J. (2012). Environmental control of cell size at division. *Curr Opin Cell Biol* **24**, 838-44.

De Virgilio, C., DeMarini, D. J. and Pringle, J. R. (1996). SPR28, a sixth member of the septin gene family in Saccharomyces cerevisiae that is expressed specifically in sporulating cells. *Microbiology* **142 (Pt 10)**, 2897-905.

Dekker, N., Speijer, D., Grun, C. H., van den Berg, M., de Haan, A. and Hochstenbach, F. (2004). Role of the alpha-glucanase Agn1p in fission-yeast cell separation. *Mol Biol Cell* **15**, 3903-14.

DeMay, B. S., Bai, X., Howard, L., Occhipinti, P., Meseroll, R. A., Spiliotis, E. T., Oldenbourg, R. and Gladfelter, A. S. (2011). Septin filaments exhibit a dynamic, paired organization that is conserved from yeast to mammals. *J Cell Biol* **193**, 1065-81.

Deng, L., Baldissard, S., Kettenbach, A. N., Gerber, S. A. and Moseley, J. B. (2014). Dueling kinases regulate cell size at division through the SAD kinase Cdr2. *Curr Biol* **24**, 428-33.

Deng, L., Sugiura, R., Ohta, K., Tada, K., Suzuki, M., Hirata, M., Nakamura, S., Shuntoh, H. and Kuno, T. (2005). Phosphatidylinositol-4-phosphate 5-kinase regulates fission yeast cell integrity through a phospholipase C-mediated protein kinase C-independent pathway. *J Biol Chem* **280**, 27561-8.

Desautels, M., Den Haese, J. P., Slupsky, C. M., McIntosh, L. P. and Hemmingsen, S. M. (2001). Cdc4p, a contractile ring protein essential for cytokinesis in Schizosaccharomyces pombe, interacts with a phosphatidylinositol 4-kinase. *J Biol Chem* **276**, 5932-42.

Dey, S. K. and Pollard, T. D. (2018). Involvement of the septation initiation network in events during cytokinesis in fission yeast. *J Cell Sci* **131**.

Dobbelaere, J. and Barral, Y. (2004). Spatial coordination of cytokinetic events by compartmentalization of the cell cortex. *Science* **305**, 393-6.

Dobbelaere, J., Gentry, M. S., Hallberg, R. L. and Barral, Y. (2003). Phosphorylation-dependent regulation of septin dynamics during the cell cycle. *Dev Cell* **4**, 345-57.

Dolat, L., Hu, Q. and Spiliotis, E. T. (2014). Septin functions in organ system physiology and pathology. *Biol Chem* **395**, 123-41.

Douglas, L. M. and Konopka, J. B. (2014). Fungal membrane organization: the eisosome concept. *Annu Rev Microbiol* **68**, 377-93.

East, D. A., Sousa, D., Martin, S. R., Edwards, T. A., Lehman, W. and Mulvihill, D. P. (2011). Altering the stability of the Cdc8 overlap region modulates the ability of this tropomyosin to bind co-operatively to actin and regulate myosin. *Biochem J* **438**, 265-73.

Echard, A. (2008). Membrane traffic and polarization of lipid domains during cytokinesis. *Biochem Soc Trans* **36**, 395-9.

Echard, A. (2012). Phosphoinositides and cytokinesis: the "PIP" of the iceberg. *Cytoskeleton (Hoboken)* **69**, 893-912.

Echard, A. and Burgess, D. (2014). The changing lipidome during cell division. *Cell* **156**, 394-5.

Echard, A., Hickson, G. R., Foley, E. and O'Farrell, P. H. (2004). Terminal cytokinesis events uncovered after an RNAi screen. *Curr Biol* **14**, 1685-93.

Edwards, M., Zwolak, A., Schafer, D. A., Sept, D., Dominguez, R. and Cooper, J. A. (2014). Capping protein regulators fine-tune actin assembly dynamics. *Nat Rev Mol Cell Biol* **15**, 677-89.

Egelhofer, T. A., Villen, J., McCusker, D., Gygi, S. P. and Kellogg, D. R. (2008). The septins function in G1 pathways that influence the pattern of cell growth in budding yeast. *PLoS One* **3**, e2022.

El Amine, N., Kechad, A., Jananji, S. and Hickson, G. R. (2013). Opposing actions of septins and Sticky on Anillin promote the transition from contractile to midbody ring. *J Cell Biol* **203**, 487-504.

Eluere, R., Varlet, I., Bernadac, A. and Simon, M. N. (2012). Cdk and the anillin homolog Bud4 define a new pathway regulating septin organization in yeast. *Cell Cycle* **11**, 151-8.

Emoto, K., Inadome, H., Kanaho, Y., Narumiya, S. and Umeda, M. (2005). Local change in phospholipid composition at the cleavage furrow is essential for completion of cytokinesis. *J Biol Chem* **280**, 37901-7.

Emoto, K. and Umeda, M. (2000). An essential role for a membrane lipid in cytokinesis. Regulation of contractile ring disassembly by redistribution of phosphatidylethanolamine. *J Cell Biol* **149**, 1215-24.

Eng, K., Naqvi, N. I., Wong, K. C. and Balasubramanian, M. K. (1998). Rng2p, a protein required for cytokinesis in fission yeast, is a component of the actomyosin ring and the spindle pole body. *Curr Biol* **8**, 611-21.

Estey, M. P., Di Ciano-Oliveira, C., Froese, C. D., Bejide, M. T. and Trimble, W. S. (2010). Distinct roles of septins in cytokinesis: SEPT9 mediates midbody abscission. *J Cell Biol* **191**, 741-9.

Ewers, H., Tada, T., Petersen, J. D., Racz, B., Sheng, M. and Choquet, D. (2014). A Septin-Dependent Diffusion Barrier at Dendritic Spine Necks. *PLoS One* **9**, e113916.

Fankhauser, C., Marks, J., Reymond, A. and Simanis, V. (1993). The S. pombe cdc16 gene is required both for maintenance of p34cdc2 kinase activity and regulation of septum formation: a link between mitosis and cytokinesis? *EMBO J* **12**, 2697-704.

Fankhauser, C., Reymond, A., Cerutti, L., Utzig, S., Hofmann, K. and Simanis, V. (1995). The S. pombe cdc15 gene is a key element in the reorganization of F-actin at mitosis. *Cell* **82**, 435-44.

Fankhauser, C. and Simanis, V. (1994). The cdc7 protein kinase is a dosage dependent regulator of septum formation in fission yeast. *EMBO J* **13**, 3011-9.

Feierbach, B. and Chang, F. (2001). Roles of the fission yeast formin for3p in cell polarity, actin cable formation and symmetric cell division. *Curr Biol* **11**, 1656-65.

Feng, B., Schwarz, H. and Jesuthasan, S. (2002). Furrow-specific endocytosis during cytokinesis of zebrafish blastomeres. *Exp Cell Res* **279**, 14-20.

Feoktistova, A., Magnelli, P., Abeijon, C., Perez, P., Lester, R. L., Dickson, R. C. and Gould, K. L. (2001). Coordination between fission yeast glucan formation and growth requires a sphingolipase activity. *Genetics* **158**, 1397-411.

Fernandez, C., Lobo Md Mdel, V., Gomez-Coronado, D. and Lasuncion, M. A. (2004). Cholesterol is essential for mitosis progression and its deficiency induces polyploid cell formation. *Exp Cell Res* **300**, 109-20.

Field, C. M. and Alberts, B. M. (1995). Anillin, a contractile ring protein that cycles from the nucleus to the cell cortex. *J Cell Biol* **131**, 165-78.

Field, C. M., Coughlin, M., Doberstein, S., Marty, T. and Sullivan, W. (2005a). Characterization of anillin mutants reveals essential roles in septin localization and plasma membrane integrity. *Development* **132**, 2849-60.

Field, S. J., Madson, N., Kerr, M. L., Galbraith, K. A., Kennedy, C. E., Tahiliani, M., Wilkins, A. and Cantley, L. C. (2005b). PtdIns(4,5)P2 functions at the cleavage furrow during cytokinesis. *Curr Biol* **15**, 1407-12.

Frazier, J. A., Wong, M. L., Longtine, M. S., Pringle, J. R., Mann, M., Mitchison, T. J. and Field, C. (1998). Polymerization of purified yeast septins: evidence that organized filament arrays may not be required for septin function. *J Cell Biol* **143**, 737-49.

Fremont, S. and Echard, A. (2018). Membrane Traffic in the Late Steps of Cytokinesis. *Curr Biol* **28**, R458-R470.

Fu, C., Ward, J. J., Loiodice, I., Velve-Casquillas, G., Nedelec, F. J. and Tran, P. T. (2009). Phospho-regulated interaction between kinesin-6 Klp9p and microtubule bundler Ase1p promotes spindle elongation. *Dev Cell* **17**, 257-67.

Fujiwara, T., Bandi, M., Nitta, M., Ivanova, E. V., Bronson, R. T. and Pellman, D. (2005). Cytokinesis failure generating tetraploids promotes tumorigenesis in p53-null cells. *Nature* **437**, 1043-7.

Fung, K. Y., Dai, L. and Trimble, W. S. (2014). Cell and molecular biology of septins. *Int Rev Cell Mol Biol* **310**, 289-339.

Garcia-Cortes, J. C. and McCollum, D. (2009). Proper timing of cytokinesis is regulated by Schizosaccharomyces pombe Etd1. *J Cell Biol* **186**, 739-53.

Garcia Cortes, J. C., Ramos, M., Osumi, M., Perez, P. and Ribas, J. C. (2016). The Cell Biology of Fission Yeast Septation. *Microbiol Mol Biol Rev* **80**, 779-91.

Garcia, G., 3rd, Bertin, A., Li, Z., Song, Y., McMurray, M. A., Thorner, J. and Nogales, E. (2011). Subunit-dependent modulation of septin assembly: budding yeast septin Shs1 promotes ring and gauze formation. *J Cell Biol* **195**, 993-1004.

Garcia, I., Jimenez, D., Martin, V., Duran, A. and Sanchez, Y. (2005). The alpha-glucanase Agn1p is required for cell separation in Schizosaccharomyces pombe. *Biol Cell* **97**, 569-76.

Gatta, A. T., Wong, L. H., Sere, Y. Y., Calderon-Norena, D. M., Cockcroft, S., Menon, A. K. and Levine, T. P. (2015). A new family of StART domain proteins at membrane contact sites has a role in ER-PM sterol transport. *Elife* **4**.

Gautier, J., Solomon, M. J., Booher, R. N., Bazan, J. F. and Kirschner, M. W. (1991). cdc25 is a specific tyrosine phosphatase that directly activates p34cdc2. *Cell* **67**, 197-211.

Ge, W. and Balasubramanian, M. K. (2008). Pxl1p, a paxillin-related protein, stabilizes the actomyosin ring during cytokinesis in fission yeast. *Mol Biol Cell* **19**, 1680-92.

Gerganova, V., Floderer, C., Archetti, A., Michon, L., Carlini, L., Reichler, T., Manley, S. and Martin, S. G. (2019). Multi-phosphorylation reaction and clustering tune Pom1 gradient mid-cell levels according to cell size. *Elife* **8**.

Gerien, K. S. and Wu, J. Q. (2018). Molecular mechanisms of contractile-ring constriction and membrane trafficking in cytokinesis. *Biophys Rev* **10**, 1649-1666.

Gladfelter, A. S., Pringle, J. R. and Lew, D. J. (2001). The septin cortex at the yeast mother-bud neck. *Curr Opin Microbiol* **4**, 681-9.

Glomb, O. and Gronemeyer, T. (2016). Septin Organization and Functions in Budding Yeast. *Front Cell Dev Biol* **4**, 123.

Glotzer, M. (2005). The molecular requirements for cytokinesis. *Science* **307**, 1735-9.

Glotzer, M. (2017). Cytokinesis in Metazoa and Fungi. *Cold Spring Harb Perspect Biol* **9**.

Gnad, F., Gunawardena, J. and Mann, M. (2011). PHOSIDA 2011: the posttranslational modification database. *Nucleic Acids Res* **39**, D253-60.

Golbach, P., Wong, R., Beise, N., Sarpal, R., Trimble, W. S. and Brill, J. A. (2010). Stabilization of the Actomyosin Ring Enables Spermatocyte Cytokinesis in Drosophila. *Molecular Biology of the Cell* **21**, 1482–1493.

Goley, E. D. and Welch, M. D. (2006). The ARP2/3 complex: an actin nucleator comes of age. *Nat Rev Mol Cell Biol* **7**, 713-26.

Goss, J. W., Kim, S., Bledsoe, H. and Pollard, T. D. (2014). Characterization of the roles of Blt1p in fission yeast cytokinesis. *Mol Biol Cell* **25**, 1946-57.

Gould, K. L. and Nurse, P. (1989). Tyrosine phosphorylation of the fission yeast cdc2+ protein kinase regulates entry into mitosis. *Nature* **342**, 39-45.

Gould, K. L. and Simanis, V. (1997). The control of septum formation in fission yeast. *Genes Dev* **11**, 2939-51.

Goyal, A. and Simanis, V. (2012). Characterization of ypa1 and ypa2, the Schizosaccharomyces pombe orthologs of the peptidyl proyl isomerases that activate PP2A, reveals a role for Ypa2p in the regulation of cytokinesis. *Genetics* **190**, 1235-50.

Goyal, A., Takaine, M., Simanis, V. and Nakano, K. (2011). Dividing the spoils of growth and the cell cycle: The fission yeast as a model for the study of cytokinesis. *Cytoskeleton (Hoboken)* **68**, 69-88.

Grallert, A., Chan, K. Y., Alonso-Nunez, M. L., Madrid, M., Biswas, A., Alvarez-Tabares, I., Connolly, Y., Tanaka, K., Robertson, A., Ortiz, J. M. et al. (2013). Removal of centrosomal PP1 by NIMA kinase unlocks the MPF feedback loop to promote mitotic commitment in S. pombe. *Curr Biol* **23**, 213-22.

Gregory, S. L., Ebrahimi, S., Milverton, J., Jones, W. M., Bejsovec, A. and Saint, R. (2008). Cell division requires a direct link between microtubule-bound RacGAP and Anillin in the contractile ring. *Curr Biol* **18**, 25-9.

Guertin, D. A., Chang, L., Irshad, F., Gould, K. L. and McCollum, D. (2000). The role of the sid1p kinase and cdc14p in regulating the onset of cytokinesis in fission yeast. *EMBO J* **19**, 1803-15.

Guertin, D. A., Trautmann, S. and McCollum, D. (2002a). Cytokinesis in eukaryotes. *Microbiol Mol Biol Rev* **66**, 155-78.

Guertin, D. A., Venkatram, S., Gould, K. L. and McCollum, D. (2002b). Dma1 prevents mitotic exit and cytokinesis by inhibiting the septation initiation network (SIN). *Dev Cell* **3**, 779-90.

Gupta, S., Govindaraghavan, M. and McCollum, D. (2014). Cross talk between NDR kinase pathways coordinates cytokinesis with cell separation in Schizosaccharomyces pombe. *Eukaryot Cell* **13**, 1104-12.

Guzman-Vendrell, M., Baldissard, S., Almonacid, M., Mayeux, A., Paoletti, A. and Moseley, J. B. (2013). Blt1 and Mid1 provide overlapping membrane anchors to position the division plane in fission yeast. *Mol Cell Biol* **33**, 418-28.

Guzman-Vendrell, M., Rincon, S. A., Dingli, F., Loew, D. and Paoletti, A. (2015). Molecular control of the Wee1 regulatory pathway by the SAD kinase Cdr2. *J Cell Sci* **128**, 2842-53.

Hachet, O., Berthelot-Grosjean, M., Kokkoris, K., Vincenzetti, V., Moosbrugger, J. and Martin, S. G. (2011). A phosphorylation cycle shapes gradients of the DYRK family kinase Pom1 at the plasma membrane. *Cell* **145**, 1116-28.

Hachet, O. and Simanis, V. (2008). Mid1p/anillin and the septation initiation network orchestrate contractile ring assembly for cytokinesis. *Genes Dev* **22**, 3205-16.

Hagan, I. and Yanagida, M. (1990). Novel potential mitotic motor protein encoded by the fission yeast cut7+ gene. *Nature* **347**, 563-6.

Hagan, I. and Yanagida, M. (1992). Kinesin-related cut7 protein associates with mitotic and meiotic spindles in fission yeast. *Nature* **356**, 74-6.

Hagan, I. M. and Grallert, A. (2013). Spatial control of mitotic commitment in fission yeast. *Biochem Soc Trans* **41**, 1766-71.

Hagiwara, A., Tanaka, Y., Hikawa, R., Morone, N., Kusumi, A., Kimura, H. and Kinoshita, M. (2011). Submembranous septins as relatively stable components of actin-based membrane skeleton. *Cytoskeleton (Hoboken)* **68**, 512-25.

Hall, P. A., Russell, H. S. E. and Pringle, J. R. (2008). *The Septins.* Wiley-Blackwell.

Hall, P. A., Todd, C. B., Hyland, P. L., McDade, S. S., Grabsch, H., Dattani, M., Hillan, K. J. and Russell, S. E. (2005). The septin-binding protein anillin is overexpressed in diverse human tumors. *Clin Cancer Res* **11**, 6780-6.

Hartman, M. A. and Spudich, J. A. (2012). The myosin superfamily at a glance. *J Cell Sci* **125**, 1627-32.

Hartwell, L. H. (1971). Genetic control of the cell division cycle in yeast. IV. Genes controlling bud emergence and cytokinesis. *Exp Cell Res* **69**, 265-76.

Haupt, A. and Minc, N. (2016). Gradients of phosphatidylserine contribute to plasma membrane charge localization and cell polarity in fission yeast. *Mol Biol Cell* **28**, 210-220.

Hayashi, M. T. and Karlseder, J. (2013). DNA damage associated with mitosis and cytokinesis failure. *Oncogene* **32**, 4593-601.

Hayles, J. and Nurse, P. (2001). A journey into space. *Nat Rev Mol Cell Biol* **2**, 647-56.

Hayles, J. and Nurse, P. (2018). Introduction to Fission Yeast as a Model System. *Cold Spring Harb Protoc* **2018**.

He, B., Xi, F., Zhang, X., Zhang, J. and Guo, W. (2007). Exo70 interacts with phospholipids and mediates the targeting of the exocyst to the plasma membrane. *EMBO J* **26**, 4053-65.

Hergovich, A., Stegert, M. R., Schmitz, D. and Hemmings, B. A. (2006). NDR kinases regulate essential cell processes from yeast to humans. *Nat Rev Mol Cell Biol* **7**, 253-64.

Hernandez-Rodriguez, Y. and Momany, M. (2012). Posttranslational modifications and assembly of septin heteropolymers and higher-order structures. *Curr Opin Microbiol* **15**, 660-8.

Hickson, G. R. and O'Farrell, P. H. (2008a). Anillin: a pivotal organizer of the cytokinetic machinery. *Biochem Soc Trans* **36**, 439-41.

Hickson, G. R. and O'Farrell, P. H. (2008b). Rho-dependent control of anillin behavior during cytokinesis. *J Cell Biol* **180**, 285-94.

Higgs, H. N. and Pollard, T. D. (2001). Regulation of actin filament network formation through ARP2/3 complex: activation by a diverse array of proteins. *Annu Rev Biochem* **70**, 649-76.

Hochegger, H., Takeda, S. and Hunt, T. (2008). Cyclin-dependent kinases and cell-cycle transitions: does one fit all? *Nat Rev Mol Cell Biol* **9**, 910-6.

Horenkamp, F. A., Valverde, D. P., Nunnari, J. and Reinisch, K. M. (2018). Molecular basis for sterol transport by StART-like lipid transfer domains. *EMBO J* **37**.

Hornbeck, P. V., Kornhauser, J. M., Tkachev, S., Zhang, B., Skrzypek, E., Murray, B., Latham, V. and Sullivan, M. (2012). PhosphoSitePlus: a comprehensive resource for investigating the structure and function of experimentally determined post-translational modifications in man and mouse. *Nucleic Acids Res* **40**, D261-70.

Hotulainen, P. and Lappalainen, P. (2006). Stress fibers are generated by two distinct actin assembly mechanisms in motile cells. *J Cell Biol* **173**, 383-94.

Hu, J., Bai, X., Bowen, J. R., Dolat, L., Korobova, F., Yu, W., Baas, P. W., Svitkina, T., Gallo, G. and Spiliotis, E. T. (2012). Septin-driven coordination of actin and microtubule remodeling regulates the collateral branching of axons. *Curr Biol* **22**, 1109-15.

Hu, Q., Milenkovic, L., Jin, H., Scott, M. P., Nachury, M. V., Spiliotis, E. T. and Nelson, W. J. (2010). A septin diffusion barrier at the base of the primary cilium maintains ciliary membrane protein distribution. *Science* **329**, 436-9.

Huang, J., Huang, Y., Yu, H., Subramanian, D., Padmanabhan, A., Thadani, R., Tao, Y., Tang, X., Wedlich-Soldner, R. and Balasubramanian, M. K. (2012). Nonmedially assembled F-actin cables incorporate into the actomyosin ring in fission yeast. *J Cell Biol* **199**, 831-47.

Huang, Y., Chew, T. G., Ge, W. and Balasubramanian, M. K. (2007). Polarity determinants Tea1p, Tea4p, and Pom1p inhibit division-septum assembly at cell ends in fission yeast. *Dev Cell* **12**, 987-96.

Huang, Y., Yan, H. and Balasubramanian, M. K. (2008). Assembly of normal actomyosin rings in the absence of Mid1p and cortical nodes in fission yeast. *J Cell Biol* **183**, 979-88.

Ihara, M., Kinoshita, A., Yamada, S., Tanaka, H., Tanigaki, A., Kitano, A., Goto, M., Okubo, K., Nishiyama, H., Ogawa, O. et al. (2005). Cortical organization by the septin cytoskeleton is essential for structural and mechanical integrity of mammalian spermatozoa. *Dev Cell* **8**, 343-52.

Iwase, M., Luo, J., Nagaraj, S., Longtine, M., Kim, H. B., Haarer, B. K., Caruso, C., Tong, Z., Pringle, J. R. and Bi, E. (2006). Role of a Cdc42p effector pathway in recruitment of the yeast septins to the presumptive bud site. *Mol Biol Cell* **17**, 1110-25.

Janetopoulos, C., Borleis, J., Vazquez, F., Iijima, M. and Devreotes, P. (2005). Temporal and spatial regulation of phosphoinositide signaling mediates cytokinesis. *Dev Cell* **8**, 467-77.

Janetopoulos, C. and Devreotes, P. (2006). Phosphoinositide signaling plays a key role in cytokinesis. *J Cell Biol* **174**, 485-90.

Jimenez, J. and Oballe, J. (1994). Ethanol-hypersensitive and ethanol-dependent cdc- mutants in Schizosaccharomyces pombe. *Mol Gen Genet* **245**, 86-95.

Jin, Q. W., Zhou, M., Bimbo, A., Balasubramanian, M. K. and McCollum, D. (2006). A role for the septation initiation network in septum assembly revealed by genetic analysis of sid2-250 suppressors. *Genetics* **172**, 2101-12.

Johnson, A. E., McCollum, D. and Gould, K. L. (2012). Polar opposites: Fine-tuning cytokinesis through SIN asymmetry. *Cytoskeleton (Hoboken)* **69**, 686-99.

Johnson, B. F., Yoo, B. Y. and Calleja, G. B. (1973). Cell division in yeasts: movement of organelles associated with cell plate growth of Schizosaccharomyces pombe. *J Bacteriol* **115**, 358-66.

Johnson, E. S. and Blobel, G. (1999). Cell cycle-regulated attachment of the ubiquitin-related protein SUMO to the yeast septins. *J Cell Biol* **147**, 981-94.

Johnson, M., East, D. A. and Mulvihill, D. P. (2014). Formins determine the functional properties of actin filaments in yeast. *Curr Biol* **24**, 1525-30.

Jourdain, I., Brzezinska, E. A. and Toda, T. (2013). Fission yeast Nod1 is a component of cortical nodes involved in cell size control and division site placement. *PLoS One* **8**, e54142.

Juanes, M. A. and Piatti, S. (2016). The final cut: cell polarity meets cytokinesis at the bud neck in S. cerevisiae. *Cell Mol Life Sci* **73**, 3115-36.

Kabeche, R., Baldissard, S., Hammond, J., Howard, L. and Moseley, J. B. (2011). The filament-forming protein Pil1 assembles linear eisosomes in fission yeast. *Mol Biol Cell* **22**, 4059-67.

Kabeche, R., Roguev, A., Krogan, N. J. and Moseley, J. B. (2014). A Pil1-Sle1-Syj1-Tax4 functional pathway links eisosomes with PI(4,5)P2 regulation. *J Cell Sci* **127**, 1318-26.

Kadota, J., Yamamoto, T., Yoshiuchi, S., Bi, E. and Tanaka, K. (2004). Septin ring assembly requires concerted action of polarisome components, a PAK kinase Cla4p, and the actin cytoskeleton in Saccharomyces cerevisiae. *Mol Biol Cell* **15**, 5329-45.

Kang, P. J., Hood-DeGrenier, J. K. and Park, H. O. (2013). Coupling of septins to the axial landmark by Bud4 in budding yeast. *J Cell Sci* **126**, 1218-26.

Karasmanis, E. P., Hwang, D., Nakos, K., Bowen, J. R., Angelis, D. and Spiliotis, E. T. (2019). A Septin Double Ring Controls the Spatiotemporal Organization of the ESCRT Machinery in Cytokinetic Abscission. *Curr Biol* **29**, 2174-2182 e7.

Kartmann, B. and Roth, D. (2001). Novel roles for mammalian septins: from vesicle trafficking to oncogenesis. *J Cell Sci* **114**, 839-44.

Katayama, S., Hirata, D., Arellano, M., Perez, P. and Toda, T. (1999). Fission yeast alpha-glucan synthase Mok1 requires the actin cytoskeleton to localize the sites of growth and plays an essential role in cell morphogenesis downstream of protein kinase C function. *J Cell Biol* **144**, 1173-86.

Kato, T., Watanabe, N., Morishima, Y., Fujita, A., Ishizaki, T. and Narumiya, S. (2001). Localization of a mammalian homolog of diaphanous, mDia1, to the mitotic spindle in HeLa cells. *J Cell Sci* **114**, 775-84.

Kechad, A., Jananji, S., Ruella, Y. and Hickson, G. R. (2012). Anillin acts as a bifunctional linker coordinating midbody ring biogenesis during cytokinesis. *Curr Biol* **22**, 197-203.

Keeney, J. B. and Boeke, J. D. (1994). Efficient targeted integration at leu1-32 and ura4-294 in Schizosaccharomyces pombe. *Genetics* **136**, 849-56.

Kelkar, M. and Martin, S. G. (2015). PKA antagonizes CLASP-dependent microtubule stabilization to re-localize Pom1 and buffer cell size upon glucose limitation. *Nat Commun* **6**, 8445.

Kim, H., Johnson, J. M., Lera, R. F., Brahma, S. and Burkard, M. E. (2017). Anillin Phosphorylation Controls Timely Membrane Association and Successful Cytokinesis. *PLoS Genet* **13**, e1006511.

Kim, M. S., Froese, C. D., Estey, M. P. and Trimble, W. S. (2011). SEPT9 occupies the terminal positions in septin octamers and mediates polymerization-dependent functions in abscission. *J Cell Biol* **195**, 815-26.

Kinoshita, M. (2003a). Assembly of mammalian septins. *J Biochem* **134**, 491-6.

Kinoshita, M. (2003b). The septins. *Genome Biol* **4**, 236.

Kinoshita, M., Field, C. M., Coughlin, M. L., Straight, A. F. and Mitchison, T. J. (2002). Self- and actin-templated assembly of Mammalian septins. *Dev Cell* **3**, 791-802.

Kinoshita, M., Kumar, S., Mizoguchi, A., Ide, C., Kinoshita, A., Haraguchi, T., Hiraoka, Y. and Noda, M. (1997). Nedd5, a mammalian septin, is a novel cytoskeletal component interacting with actin-based structures. *Genes Dev* **11**, 1535-47.

Klose, C., Surma, M. A., Gerl, M. J., Meyenhofer, F., Shevchenko, A. and Simons, K. (2012). Flexibility of a eukaryotic lipidome--insights from yeast lipidomics. *PLoS One* **7**, e35063.

Klose, C., Surma, M. A. and Simons, K. (2013). Organellar lipidomics--background and perspectives. *Curr Opin Cell Biol* **25**, 406-13.

Kobielak, A., Pasolli, H. A. and Fuchs, E. (2004). Mammalian formin-1 participates in adherens junctions and polymerization of linear actin cables. *Nat Cell Biol* **6**, 21-30.

Kovar, D. R. (2006). Molecular details of formin-mediated actin assembly. *Curr Opin Cell Biol* **18**, 11-7.

Kovar, D. R., Kuhn, J. R., Tichy, A. L. and Pollard, T. D. (2003). The fission yeast cytokinesis formin Cdc12p is a barbed end actin filament capping protein gated by profilin. *J Cell Biol* **161**, 875-87.

Kovar, D. R., Sirotkin, V. and Lord, M. (2011). Three's company: the fission yeast actin cytoskeleton. *Trends Cell Biol* **21**, 177-87.

Kozubowski, L., Larson, J. R. and Tatchell, K. (2005). Role of the septin ring in the asymmetric localization of proteins at the mother-bud neck in Saccharomyces cerevisiae. *Mol Biol Cell* **16**, 3455-66.

Krapp, A., Cano, E. and Simanis, V. (2004a). Analysis of the S. pombe signalling scaffold protein Cdc11p reveals an essential role for the N-terminal domain in SIN signalling. *FEBS Lett* **565**, 176-80.

Krapp, A., Gulli, M. P. and Simanis, V. (2004b). SIN and the art of splitting the fission yeast cell. *Curr Biol* **14**, R722-30.

Krapp, A. and Simanis, V. (2008). An overview of the fission yeast septation initiation network (SIN). *Biochem Soc Trans* **36**, 411-5.

Krendel, M. and Mooseker, M. S. (2005). Myosins: tails (and heads) of functional diversity. *Physiology (Bethesda)* **20**, 239-51.

Krokowski, S., Lobato-Marquez, D., Chastanet, A., Pereira, P. M., Angelis, D., Galea, D., Larrouy-Maumus, G., Henriques, R., Spiliotis, E. T., Carballido-Lopez, R. et al. (2018). Septins Recognize and Entrap Dividing Bacterial Cells for Delivery to Lysosomes. *Cell Host Microbe* **24**, 866-874 e4.

Kueh, H. Y. and Mitchison, T. J. (2009). Structural plasticity in actin and tubulin polymer dynamics. *Science* **325**, 960-3.

Kuo, Y. C., Shen, Y. R., Chen, H. I., Lin, Y. H., Wang, Y. Y., Chen, Y. R., Wang, C. Y. and Kuo, P. L. (2015). SEPT12 orchestrates the formation of mammalian sperm annulus by organizing core octameric complexes with other SEPT proteins. *J Cell Sci* **128**, 923-34.

Lacroix, B. and Maddox, A. S. (2012). Cytokinesis, ploidy and aneuploidy. *J Pathol* **226**, 338-51.

Lammers, M., Rose, R., Scrima, A. and Wittinghofer, A. (2005). The regulation of mDia1 by autoinhibition and its release by Rho*GTP. *EMBO J* **24**, 4176-87.

Laplante, C., Berro, J., Karatekin, E., Hernandez-Leyva, A., Lee, R. and Pollard, T. D. (2015). Three myosins contribute uniquely to the assembly and constriction of the fission yeast cytokinetic contractile ring. *Curr Biol* **25**, 1955-65.

Laplante, C., Huang, F., Tebbs, I. R., Bewersdorf, J. and Pollard, T. D. (2016). Molecular organization of cytokinesis nodes and contractile rings by super-resolution fluorescence microscopy of live fission yeast. *Proc Natl Acad Sci U S A* **113**, E5876-E5885.

Laporte, D., Coffman, V. C., Lee, I. J. and Wu, J. Q. (2011). Assembly and architecture of precursor nodes during fission yeast cytokinesis. *J Cell Biol* **192**, 1005-21.

Laporte, D., Ojkic, N., Vavylonis, D. and Wu, J. Q. (2012). alpha-Actinin and fimbrin cooperate with myosin II to organize actomyosin bundles during contractile-ring assembly. *Mol Biol Cell* **23**, 3094-110.

Le Goff, X., Motegi, F., Salimova, E., Mabuchi, I. and Simanis, V. (2000). The S. pombe rlc1 gene encodes a putative myosin regulatory light chain that binds the type II myosins myo3p and myo2p. *J Cell Sci* **113 Pt 23**, 4157-63.

Le Goff, X., Woollard, A. and Simanis, V. (1999). Analysis of the cps1 gene provides evidence for a septation checkpoint in Schizosaccharomyces pombe. *Mol Gen Genet* **262**, 163-72.

Leach, M. D. and Cowen, L. E. (2014). Membrane fluidity and temperature sensing are coupled via circuitry comprised of Ole1, Rsp5, and Hsf1 in Candida albicans. *Eukaryot Cell* **13**, 1077-84.

Lee, I. J., Coffman, V. C. and Wu, J. Q. (2012). Contractile-ring assembly in fission yeast cytokinesis: Recent advances and new perspectives. *Cytoskeleton (Hoboken)* **69**, 751-63.

Lee, I. J. and Wu, J. Q. (2012). Characterization of Mid1 domains for targeting and scaffolding in fission yeast cytokinesis. *J Cell Sci* **125**, 2973-85.

Lee, W. L., Bezanilla, M. and Pollard, T. D. (2000). Fission yeast myosin-I, Myo1p, stimulates actin assembly by Arp2/3 complex and shares functions with WASp. *J Cell Biol* **151**, 789-800.

Lehman, W., Vibert, P., Uman, P. and Craig, R. (1995). Steric-blocking by tropomyosin visualized in relaxed vertebrate muscle thin filaments. *J Mol Biol* **251**, 191-6.

Lhuillier, P., Rode, B., Escalier, D., Lores, P., Dirami, T., Bienvenu, T., Gacon, G., Dulioust, E. and Toure, A. (2009). Absence of annulus in human asthenozoospermia: case report. *Hum Reprod* **24**, 1296-303.

Li, C. R., Au Yong, J. Y., Wang, Y. M. and Wang, Y. (2012). CDK regulates septin organization through cell-cycle-dependent phosphorylation of the Nim1-related kinase Gin4. *J Cell Sci* **125**, 2533-43.

Li, F. and Higgs, H. N. (2003). The mouse Formin mDia1 is a potent actin nucleation factor regulated by autoinhibition. *Curr Biol* **13**, 1335-40.

Li, H., Saucedo-Cuevas, L., Yuan, L., Ross, D., Johansen, A., Sands, D., Stanley, V., Guemez-Gamboa, A., Gregor, A., Evans, T. et al. (2019). Zika Virus Protease Cleavage of Host Protein Septin-2 Mediates Mitotic Defects in Neural Progenitors. *Neuron* **101**, 1089-1098 e4.

Lin, Y. H., Lin, Y. M., Wang, Y. Y., Yu, I. S., Lin, Y. W., Wang, Y. H., Wu, C. M., Pan, H. A., Chao, S. C., Yen, P. H. et al. (2009). The expression level of septin12 is critical for spermiogenesis. *Am J Pathol* **174**, 1857-68.

Lippincott, J. and Li, R. (1998). Sequential assembly of myosin II, an IQGAP-like protein, and filamentous actin to a ring structure involved in budding yeast cytokinesis. *J Cell Biol* **140**, 355-66.

Lippincott, J. and Li, R. (2000). Involvement of PCH family proteins in cytokinesis and actin distribution. *Microsc Res Tech* **49**, 168-72.

Liu, J., Fairn, G. D., Ceccarelli, D. F., Sicheri, F. and Wilde, A. (2012). Cleavage furrow organization requires PIP(2)-mediated recruitment of anillin. *Curr Biol* **22**, 64-9.

Liu, J., Tang, X., Wang, H., Oliferenko, S. and Balasubramanian, M. K. (2002). The localization of the integral membrane protein Cps1p to the cell division site is dependent on the actomyosin ring and the septation-inducing network in Schizosaccharomyces pombe. *Mol Biol Cell* **13**, 989-1000.

Logan, M. R. and Mandato, C. A. (2006). Regulation of the actin cytoskeleton by PIP2 in cytokinesis. *Biol Cell* **98**, 377-88.

Longtine, M. S., DeMarini, D. J., Valencik, M. L., Al-Awar, O. S., Fares, H., De Virgilio, C. and Pringle, J. R. (1996). The septins: roles in cytokinesis and other processes. *Curr Opin Cell Biol* **8**, 106-19.

Loo, T. H. and Balasubramanian, M. (2008). Schizosaccharomyces pombe Pak-related protein, Pak1p/Orb2p, phosphorylates myosin regulatory light chain to inhibit cytokinesis. *J Cell Biol* **183**, 785-93.

Lord, M. and Pollard, T. D. (2004). UCS protein Rng3p activates actin filament gliding by fission yeast myosin-II. *J Cell Biol* **167**, 315-25.

Los, D. A. and Murata, N. (2004). Membrane fluidity and its roles in the perception of environmental signals. *Biochim Biophys Acta* **1666**, 142-57.

Luedeke, C., Frei, S. B., Sbalzarini, I., Schwarz, H., Spang, A. and Barral, Y. (2005). Septin-dependent compartmentalization of the endoplasmic reticulum during yeast polarized growth. *J Cell Biol* **169**, 897-908.

Maddox, A. S., Habermann, B., Desai, A. and Oegema, K. (2005). Distinct roles for two C. elegans anillins in the gonad and early embryo. *Development* **132**, 2837-48.

Maddox, A. S., Lewellyn, L., Desai, A. and Oegema, K. (2007). Anillin and the septins promote asymmetric ingression of the cytokinetic furrow. *Dev Cell* **12**, 827-35.

Makushok, T., Alves, P., Huisman, S. M., Kijowski, A. R. and Brunner, D. (2016). Sterol-Rich Membrane Domains Define Fission Yeast Cell Polarity. *Cell* **165**, 1182-1196.

Mangione, M. C. and Gould, K. L. (2019). Molecular form and function of the cytokinetic ring. *J Cell Sci* **132**.

Marquardt, J., Chen, X. and Bi, E. (2018). Architecture, remodeling, and functions of the septin cytoskeleton. *Cytoskeleton (Hoboken)* **76**, 7-14.

Martin-Cuadrado, A. B., Duenas, E., Sipiczki, M., Vazquez de Aldana, C. R. and del Rey, F. (2003). The endo-beta-1,3-glucanase eng1p is required for dissolution of the primary septum during cell separation in Schizosaccharomyces pombe. *J Cell Sci* **116**, 1689-98.

Martin-Cuadrado, A. B., Morrell, J. L., Konomi, M., An, H., Petit, C., Osumi, M., Balasubramanian, M., Gould, K. L., Del Rey, F. and de Aldana, C. R. (2005). Role of septins and the exocyst complex in the function of hydrolytic enzymes responsible for fission yeast cell separation. *Mol Biol Cell* **16**, 4867-81.

Martın-Garcıa, R., Arribas, V., Coll, P. M., Pinar, M., Viana, R. A., Rincon, S. A., Correa-Bordes, J., Ribas, J. C. a. and Perez, P. (2018). Paxillin-Mediated Recruitment of Calcineurin to the Contractile Ring Is Required for the Correct Progression of Cytokinesis in Fission Yeast. *Cell Reports* **25**, 772–783.

Martin-Garcia, R., Coll, P. M. and Perez, P. (2014). F-BAR domain protein Rga7 collaborates with Cdc15 and Imp2 to ensure proper cytokinesis in fission yeast. *J Cell Sci* **127**, 4146-58.

Martin, S. G. (2009). Microtubule-dependent cell morphogenesis in the fission yeast. *Trends Cell Biol* **19**, 447-54.

Martin, S. G. and Berthelot-Grosjean, M. (2009). Polar gradients of the DYRK-family kinase Pom1 couple cell length with the cell cycle. *Nature* **459**, 852-6.

Martin, S. G., Rincon, S. A., Basu, R., Perez, P. and Chang, F. (2007). Regulation of the formin for3p by cdc42p and bud6p. *Mol Biol Cell* **18**, 4155-67.

Marttinen, M., Kurkinen, K. M., Soininen, H., Haapasalo, A. and Hiltunen, M. (2015). Synaptic dysfunction and septin protein family members in neurodegenerative diseases. *Mol Neurodegener* **10**, 16.

Masters, T. A., Kendrick-Jones, J. and Buss, F. (2016). Myosins: Domain Organisation, Motor Properties, Physiological Roles and Cellular Functions. In *Handbook of Experimental Pharmacology*, (ed. S. I. P. S. 2016).

Matheos, D., Metodiev, M., Muller, E., Stone, D. and Rose, M. D. (2004). Pheromone-induced polarization is dependent on the Fus3p MAPK acting through the formin Bni1p. *J Cell Biol* **165**, 99-109.

Matmati, N. and Hannun, Y. A. (2008). Thematic review series: sphingolipids. ISC1 (inositol phosphosphingolipid-phospholipase C), the yeast homologue of neutral sphingomyelinases. *J Lipid Res* **49**, 922-8.

Matsumura, F. (2005). Regulation of myosin II during cytokinesis in higher eukaryotes. *Trends Cell Biol* **15**, 371-7.

Matsuo, Y., Fisher, E., Patton-Vogt, J. and Marcus, S. (2007). Functional characterization of the fission yeast phosphatidylserine synthase gene, pps1, reveals novel cellular functions for phosphatidylserine. *Eukaryot Cell* **6**, 2092-101.

Mavrakis, M., Azou-Gros, Y., Tsai, F. C., Alvarado, J., Bertin, A., Iv, F., Kress, A., Brasselet, S., Koenderink, G. H. and Lecuit, T. (2014). Septins promote F-actin ring formation by crosslinking actin filaments into curved bundles. *Nat Cell Biol* **16**, 322-34.

May, R. C., Caron, E., Hall, A. and Machesky, L. M. (2000). Involvement of the Arp2/3 complex in phagocytosis mediated by FcgammaR or CR3. *Nat Cell Biol* **2**, 246-8.

McCollum, D. and Gould, K. L. (2001). Timing is everything: regulation of mitotic exit and cytokinesis by the MEN and SIN. *Trends Cell Biol* **11**, 89-95.

McDonald, N. A., Lind, A. L., Smith, S. E., Li, R. and Gould, K. L. (2017). Nanoscale architecture of the Schizosaccharomyces pombe contractile ring. *Elife* **6**.

McDonald, N. A., Vander Kooi, C. W., Ohi, M. D. and Gould, K. L. (2015). Oligomerization but Not Membrane Bending Underlies the Function of Certain F-BAR Proteins in Cell Motility and Cytokinesis. *Dev Cell* **35**, 725-36.

McKillop, D. F. and Geeves, M. A. (1991). Regulation of the acto.myosin subfragment 1 interaction by troponin/tropomyosin. Evidence for control of a specific isomerization between two acto.myosin subfragment 1 states. *Biochem J* **279 (Pt 3)**, 711-8.

McKillop, D. F. and Geeves, M. A. (1993). Regulation of the interaction between actin and myosin subfragment 1: evidence for three states of the thin filament. *Biophys J* **65**, 693-701.

McMurray, M. A. (2019). The long and short of membrane curvature sensing by septins. *J Cell Biol* **218**, 1083-1085.

McMurray, M. A. and Thorner, J. (2009). Septins: molecular partitioning and the generation of cellular asymmetry. *Cell Div* **4**, 18.

McQuilken, M., Jentzsch, M. S., Verma, A., Mehta, S. B., Oldenbourg, R. and Gladfelter, A. S. (2017). Analysis of Septin Reorganization at Cytokinesis Using Polarized Fluorescence Microscopy. *Front. Cell Dev. Biol.* **5**, 42.

Meitinger, F. and Palani, S. (2016). Actomyosin ring driven cytokinesis in budding yeast. *Semin Cell Dev Biol* **53**, 19-27.

Miller, K. G., Field, C. M. and Alberts, B. M. (1989). Actin-binding proteins from Drosophila embryos: a complex network of interacting proteins detected by F-actin affinity chromatography. *J Cell Biol* **109**, 2963-75.

Minet, M., Nurse, P., Thuriaux, P. and Mitchison, J. M. (1979). Uncontrolled septation in a cell division cycle mutant of the fission yeast Schizosaccharomyces pombe. *J Bacteriol* **137**, 440-6.

Mino, A., Tanaka, K., Kamei, T., Umikawa, M., Fujiwara, T. and Takai, Y. (1998). Shs1p: a novel member of septin that interacts with spa2p, involved in polarized growth in saccharomyces cerevisiae. *Biochem Biophys Res Commun* **251**, 732-6.

Mishra, M., Huang, J. and Balasubramanian, M. K. (2014). The yeast actin cytoskeleton. *FEMS Microbiol Rev* **38**, 213-27.

Mishra, M., Karagiannis, J., Trautmann, S., Wang, H., McCollum, D. and Balasubramanian, M. K. (2004). The Clp1p/Flp1p phosphatase ensures completion of cytokinesis in response to minor perturbation of the cell division machinery in Schizosaccharomyces pombe. *J Cell Sci* **117**, 3897-910.

Mishra, M., Kashiwazaki, J., Takagi, T., Srinivasan, R., Huang, Y., Balasubramanian, M. K. and Mabuchi, I. (2013). In vitro contraction of cytokinetic ring depends on myosin II but not on actin dynamics. *Nat Cell Biol* **15**, 853-9.

Mitchell, L., Lau, A., Lambert, J. P., Zhou, H., Fong, Y., Couture, J. F., Figeys, D. and Baetz, K. (2011). Regulation of septin dynamics by the Saccharomyces cerevisiae lysine acetyltransferase NuA4. *PLoS One* **6**, e25336.

Mitchison, J. M. and Nurse, P. (1985). Growth in cell length in the fission yeast Schizosaccharomyces pombe. *J Cell Sci* **75**, 357-76.

Mitra, P., Zhang, Y., Rameh, L. E., Ivshina, M. P., McCollum, D., Nunnari, J. J., Hendricks, G. M., Kerr, M. L., Field, S. J., Cantley, L. C. et al. (2004). A novel phosphatidylinositol(3,4,5)P3 pathway in fission yeast. *J Cell Biol* **166**, 205-11.

Miyake, Y., Kozutsumi, Y., Nakamura, S., Fujita, T. and Kawasaki, T. (1995). Serine palmitoyltransferase is the primary target of a sphingosine-like immunosuppressant, ISP-1/myriocin. *Biochem Biophys Res Commun* **211**, 396-403.

Montagnac, G., Echard, A. and Chavrier, P. (2008). Endocytic traffic in animal cell cytokinesis. *Curr Opin Cell Biol* **20**, 454-61.

Monteiro, P. B., Lataro, R. C., Ferro, J. A. and Reinach Fde, C. (1994). Functional alpha-tropomyosin produced in Escherichia coli. A dipeptide extension can substitute the amino-terminal acetyl group. *J Biol Chem* **269**, 10461-6.

Moreno, S., Klar, A. and Nurse, P. (1991). Molecular genetic analysis of fission yeast Schizosaccharomyces pombe. *Methods Enzymol* **194**, 795-823.

Morrell, J. L., Nichols, C. B. and Gould, K. L. (2004a). The GIN4 family kinase, Cdr2p, acts independently of septins in fission yeast. *J Cell Sci* **117**, 5293-302.

Morrell, J. L., Tomlin, G. C., Rajagopalan, S., Venkatram, S., Feoktistova, A. S., Tasto, J. J., Mehta, S., Jennings, J. L., Link, A., Balasubramanian, M. K. et al. (2004b). Sid4p-Cdc11p assembles the septation initiation network and its regulators at the S. pombe SPB. *Curr Biol* **14**, 579-84.

Mortensen, E. M., McDonald, H., Yates, J., 3rd and Kellogg, D. R. (2002). Cell cycle-dependent assembly of a Gin4-septin complex. *Mol Biol Cell* **13**, 2091-105.

Moseley, J. B. (2014). Actin cytoskeleton: a nucleator face-off. *Curr Biol* **24**, R194-6.

Moseley, J. B., Mayeux, A., Paoletti, A. and Nurse, P. (2009). A spatial gradient coordinates cell size and mitotic entry in fission yeast. *Nature* **459**, 857-60.

Moseley, J. B., Sagot, I., Manning, A. L., Xu, Y., Eck, M. J., Pellman, D. and Goode, B. L. (2004). A conserved mechanism for Bni1- and mDia1-induced actin assembly and dual regulation of Bni1 by Bud6 and profilin. *Mol Biol Cell* **15**, 896-907.

Mostowy, S., Bonazzi, M., Hamon, M. A., Tham, T. N., Mallet, A., Lelek, M., Gouin, E., Demangel, C., Brosch, R., Zimmer, C. et al. (2010). Entrapment of intracytosolic bacteria by septin cage-like structures. *Cell Host Microbe* **8**, 433-44.

Mostowy, S. and Cossart, P. (2012). Septins: the fourth component of the cytoskeleton. *Nat Rev Mol Cell Biol* **13**, 183-94.

Mostowy, S., Janel, S., Forestier, C., Roduit, C., Kasas, S., Pizarro-Cerda, J., Cossart, P. and Lafont, F. (2011). A role for septins in the interaction between the Listeria monocytogenes INVASION PROTEIN InlB and the Met receptor. *Biophys J* **100**, 1949-59.

Mulvihill, D. P. and Hyams, J. S. (2003). Role of the two type II myosins, Myo2 and Myp2, in cytokinetic actomyosin ring formation and function in fission yeast. *Cell Motil Cytoskeleton* **54**, 208-16.

Munoz, J., Cortes, J. C., Sipiczki, M., Ramos, M., Clemente-Ramos, J. A., Moreno, M. B., Martins, I. M., Perez, P. and Ribas, J. C. (2013). Extracellular cell wall beta(1,3)glucan is required to couple septation to actomyosin ring contraction. *J Cell Biol* **203**, 265-82.

Munoz, S., Manjon, E. and Sanchez, Y. (2014). The putative exchange factor Gef3p interacts with Rho3p GTPase and the septin ring during cytokinesis in fission yeast. *J Biol Chem* **289**, 21995-2007.

Murley, A., Sarsam, R. D., Toulmay, A., Yamada, J., Prinz, W. A. and Nunnari, J. (2015). Ltc1 is an ER-localized sterol transporter and a component of ER-mitochondria and ER-vacuole contacts. *J Cell Biol* **209**, 539-48.

Muro, E., Atilla-Gokcumen, G. E. and Eggert, U. S. (2014). Lipids in cell biology: how can we understand them better? *Mol Biol Cell* **25**, 1819-23.

Nakamura, S., Kozutsumi, Y., Sun, Y., Miyake, Y., Fujita, T. and Kawasaki, T. (1996). Dual roles of sphingolipids in signaling of the escape from and onset of apoptosis in a mouse cytotoxic T-cell line, CTLL-2. *J Biol Chem* **271**, 1255-7.

Nakano, K. and Mabuchi, I. (2006). Actin-depolymerizing protein Adf1 is required for formation and maintenance of the contractile ring during cytokinesis in fission yeast. *Mol Biol Cell* **17**, 1933-45.

Nakos, K., Rosenberg, M. and Spiliotis, E. T. (2018). Regulation of microtubule plus end dynamics by septin 9. *Cytoskeleton (Hoboken)* **76**, 83-91.

Neto, H., Collins, L. L. and Gould, G. W. (2011). Vesicle trafficking and membrane remodelling in cytokinesis. *Biochem J* **437**, 13-24.

Nezis, I. P., Sagona, A. P., Schink, K. O. and Stenmark, H. (2010). Divide and ProsPer: the emerging role of PtdIns3P in cytokinesis. *Trends Cell Biol* **20**, 642-9.

Ng, M. M., Chang, F. and Burgess, D. R. (2005). Movement of membrane domains and requirement of membrane signaling molecules for cytokinesis. *Dev Cell* **9**, 781-90.

Nishihama, R., Onishi, M. and Pringle, J. R. (2011). New insights into the phylogenetic distribution and evolutionary origins of the septins. *Biol Chem* **392**, 681-7.

Nurse, P. and Thuriaux, P. (1980). Regulatory genes controlling mitosis in the fission yeast Schizosaccharomyces pombe. *Genetics* **96**, 627-37.

Nurse, P., Thuriaux, P. and Nasmyth, K. (1976). Genetic control of the cell division cycle in the fission yeast Schizosaccharomyces pombe. *Mol Gen Genet* **146**, 167-78.

O`Leary, P. C., Penny, S. A., Dolan, R. T., Kelly, C. M., Madden, S. F., Rexhepaj, E., Brennan, D. J., McCann, A. H., Ponten, F., Uhlen, M. et al. (2013). Systematic antibody generation and validation via tissue microarray technology leading to identification of a novel protein prognostic panel in breast cancer. *BMC Cancer* **13**, 175.

Oegema, K., Savoian, M. S., Mitchison, T. J. and Field, C. M. (2000). Functional analysis of a human homologue of the Drosophila actin binding protein anillin suggests a role in cytokinesis. *J Cell Biol* **150**, 539-52.

Oh, Y. and Bi, E. (2011). Septin structure and function in yeast and beyond. *Trends Cell Biol* **21**, 141-8.

Ohkura, H., Hagan, I. M. and Glover, D. M. (1995). The conserved Schizosaccharomyces pombe kinase plo1, required to form a bipolar spindle, the actin ring, and septum, can drive septum formation in G1 and G2 cells. *Genes Dev* **9**, 1059-73.

Ojkic, N., Wu, J. Q. and Vavylonis, D. (2011). Model of myosin node aggregation into a contractile ring: the effect of local alignment. *J Phys Condens Matter* **23**, 374103.

Okada, H., Wloka, C., Wu, J. Q. and Bi, E. (2019). Distinct Roles of Myosin-II Isoforms in Cytokinesis under Normal and Stressed Conditions. *iScience* **14**, 69-87.

Okada, S., Leda, M., Hanna, J., Savage, N. S., Bi, E. and Goryachev, A. B. (2013). Daughter cell identity emerges from the interplay of Cdc42, septins, and exocytosis. *Dev Cell* **26**, 148-61.

Olakowski, M., Tyszkiewicz, T., Jarzab, M., Krol, R., Oczko-Wojciechowska, M., Kowalska, M., Kowal, M., Gala, G. M., Kajor, M., Lange, D. et al. (2009). NBL1 and anillin (ANLN) genes over-expression in pancreatic carcinoma. *Folia Histochem Cytobiol* **47**, 249-55.

Ong, K., Wloka, C., Okada, S., Svitkina, T. and Bi, E. (2014). Architecture and dynamic remodelling of the septin cytoskeleton during the cell cycle. *Nat Commun* **5**, 5698.

Onishi, M., Koga, T., Hirata, A., Nakamura, T., Asakawa, H., Shimoda, C., Bahler, J., Wu, J. Q., Takegawa, K., Tachikawa, H. et al. (2010). Role of septins in the orientation of forespore membrane extension during sporulation in fission yeast. *Mol Cell Biol* **30**, 2057-74.

Otomo, T., Tomchick, D. R., Otomo, C., Panchal, S. C., Machius, M. and Rosen, M. K. (2005). Structural basis of actin filament nucleation and processive capping by a formin homology 2 domain. *Nature* **433**, 488-94.

Ozsarac, N., Bhattacharyya, M., Dawes, I. W. and Clancy, M. J. (1995). The SPR3 gene encodes a sporulation-specific homologue of the yeast CDC3/10/11/12 family of bud neck microfilaments and is regulated by ABFI. *Gene* **164**, 157-62.

Padmanabhan, A., Bakka, K., Sevugan, M., Naqvi, N. I., D'Souza, V., Tang, X., Mishra, M. and Balasubramanian, M. K. (2011). IQGAP-related Rng2p organizes cortical nodes and ensures position of cell division in fission yeast. *Curr Biol* **21**, 467-72.

Padte, N. N., Martin, S. G., Howard, M. and Chang, F. (2006). The cell-end factor pom1p inhibits mid1p in specification of the cell division plane in fission yeast. *Curr Biol* **16**, 2480-7.

Pan, F., Malmberg, R. L. and Momany, M. (2007). Analysis of septins across kingdoms reveals orthology and new motifs. *BMC Evol Biol* **7**, 103.

Paoletti, A. and Chang, F. (2000). Analysis of mid1p, a protein required for placement of the cell division site, reveals a link between the nucleus and the cell surface in fission yeast. *Mol Biol Cell* **11**, 2757-73.

Paoletti, A. and Chang, F. (2005). Anillins and mid proteins: Organizers of the contractile ring during cytokinesis: Research Signpost.

Park, J. S., Steinbach, S. K., Desautels, M. and Hemmingsen, S. M. (2009). Essential role for Schizosaccharomyces pombe pik1 in septation. *PLoS One* **4**, e6179.

Patzig, J., Erwig, M. S., Tenzer, S., Kusch, K., Dibaj, P., Mobius, W., Goebbels, S., Schaeren-Wiemers, N., Nave, K. A. and Werner, H. B. (2016). Septin/anillin filaments scaffold central nervous system myelin to accelerate nerve conduction. *Elife* **5**.

Pelham, R. J., Jr. and Chang, F. (2001). Role of actin polymerization and actin cables in actin-patch movement in Schizosaccharomyces pombe. *Nat Cell Biol* **3**, 235-44.

Perez, P., Cortes, J. C., Martin-Garcia, R. and Ribas, J. C. (2016). Overview of fission yeast septation. *Cell Microbiol* **18**, 1201-7.

Perez, P., Portales, E. and Santos, B. (2015). Rho4 interaction with exocyst and septins regulates cell separation in fission yeast. *Microbiology* **161**, 948-59.

Perry, S. V. (2001). Vertebrate tropomyosin: distribution, properties and function. *J Muscle Res Cell Motil* **22**, 5-49.

Petersen, J. and Hagan, I. M. (2005). Polo kinase links the stress pathway to cell cycle control and tip growth in fission yeast. *Nature* **435**, 507-12.

Petersen, J. and Nurse, P. (2007). TOR signalling regulates mitotic commitment through the stress MAP kinase pathway and the Polo and Cdc2 kinases. *Nat Cell Biol* **9**, 1263-72.

Petit, C. S., Mehta, S., Roberts, R. H. and Gould, K. L. (2005). Ace2p contributes to fission yeast septin ring assembly by regulating mid2+ expression. *J Cell Sci* **118**, 5731-42.

Piekny, A. J. and Glotzer, M. (2008). Anillin is a scaffold protein that links RhoA, actin, and myosin during cytokinesis. *Curr Biol* **18**, 30-6.

Piekny, A. J. and Maddox, A. S. (2010). The myriad roles of Anillin during cytokinesis. *Semin Cell Dev Biol* **21**, 881-91.

Pike, L. J. (2003). Lipid rafts: bringing order to chaos. *J Lipid Res* **44**, 655-67.

Pinar, M., Coll, P. M., Rincon, S. A. and Perez, P. (2008). Schizosaccharomyces pombe Pxl1 is a paxillin homologue that modulates Rho1 activity and participates in cytokinesis. *Mol Biol Cell* **19**, 1727-38.

Pirruccello, M. and De Camilli, P. (2012). Inositol 5-phosphatases: insights from the Lowe syndrome protein OCRL. *Trends Biochem Sci* **37**, 134-43.

Pollard, T. D. (2007). Regulation of actin filament assembly by Arp2/3 complex and formins. *Annu Rev Biophys Biomol Struct* **36**, 451-77.

Pollard, T. D. and Borisy, G. G. (2003). Cellular motility driven by assembly and disassembly of actin filaments. *Cell* **112**, 453-65.

Pollard, T. D. and Cooper, J. A. (2009). Actin, a central player in cell shape and movement. *Science* **326**, 1208-12.

Pollard, T. D. and O'Shaughnessy, B. (2019). Molecular Mechanism of Cytokinesis. *Annu Rev Biochem*.

Pollard, T. D. and Wu, J. Q. (2010). Understanding cytokinesis: lessons from fission yeast. *Nat Rev Mol Cell Biol* **11**, 149-55.

Pous, C., Klipfel, L. and Baillet, A. (2016). Cancer-Related Functions and Subcellular Localizations of Septins. *Front Cell Dev Biol* **4**, 126.

Proctor, S. A., Minc, N., Boudaoud, A. and Chang, F. (2012). Contributions of turgor pressure, the contractile ring, and septum assembly to forces in cytokinesis in fission yeast. *Curr Biol* **22**, 1601-8.

Pruyne, D., Evangelista, M., Yang, C., Bi, E., Zigmond, S., Bretscher, A. and Boone, C. (2002). Role of formins in actin assembly: nucleation and barbed-end association. *Science* **297**, 612-5.

Rachfall, N., Johnson, A. E., Mehta, S., Chen, J. S. and Gould, K. L. (2014). Cdk1 promotes cytokinesis in fission yeast through activation of the septation initiation network. *Mol Biol Cell* **25**, 2250-9.

Radcliffe, P., Hirata, D., Childs, D., Vardy, L. and Toda, T. (1998). Identification of novel temperature-sensitive lethal alleles in essential beta-tubulin and nonessential alpha 2-tubulin genes as fission yeast polarity mutants. *Mol Biol Cell* **9**, 1757-71.

Rajendran, L. and Simons, K. (2005). Lipid rafts and membrane dynamics. *J Cell Sci* **118**, 1099-102.

Ramalingam, N., Zhao, H., Breitsprecher, D., Lappalainen, P., Faix, J. and Schleicher, M. (2010). Phospholipids regulate localization and activity of mDia1 formin. *Eur J Cell Biol* **89**, 723-32.

Ray, S., Kume, K., Gupta, S., Ge, W., Balasubramanian, M., Hirata, D. and McCollum, D. (2010). The mitosis-to-interphase transition is coordinated by cross talk between the SIN and MOR pathways in Schizosaccharomyces pombe. *J Cell Biol* **190**, 793-805.

Ren, L., Willet, A. H., Roberts-Galbraith, R. H., McDonald, N. A., Feoktistova, A., Chen, J. S., Huang, H., Guillen, R., Boone, C., Sidhu, S. S. et al. (2015). The Cdc15 and Imp2 SH3 domains cooperatively scaffold a network of proteins that redundantly ensure efficient cell division in fission yeast. *Mol Biol Cell* **26**, 256-69.

Renshaw, M. J., Liu, J., Lavoie, B. D. and Wilde, A. (2014). Anillin-dependent organization of septin filaments promotes intercellular bridge elongation and Chmp4B targeting to the abscission site. *Open Biol* **4**, 130190.

Renz, C., Oeljeklaus, S., Grinhagens, S., Warscheid, B., Johnsson, N. and Gronemeyer, T. (2016). Identification of Cell Cycle Dependent Interaction Partners of the Septins by Quantitative Mass Spectrometry. *PLoS One* **11**, e0148340.

Reyes, C. C., Jin, M., Breznau, E. B., Espino, R., Delgado-Gonzalo, R., Goryachev, A. B. and Miller, A. L. (2014). Anillin regulates cell-cell junction integrity by organizing junctional accumulation of Rho-GTP and actomyosin. *Curr Biol* **24**, 1263-70.

Rhind, N. and Russell, P. (2012). Signaling pathways that regulate cell division. *Cold Spring Harb Perspect Biol* **4**.

Ribet, D., Boscaini, S., Cauvin, C., Siguier, M., Mostowy, S., Echard, A. and Cossart, P. (2017). SUMOylation of human septins is critical for septin filament bundling and cytokinesis. *J Cell Biol* **216**, 4041-4052.

Rincon, S. A., Bhatia, P., Bicho, C., Guzman-Vendrell, M., Fraisier, V., Borek, W. E., Alves Fde, L., Dingli, F., Loew, D., Rappsilber, J. et al. (2014). Pom1 regulates the assembly of Cdr2-Mid1 cortical nodes for robust spatial control of cytokinesis. *J Cell Biol* **206**, 61-77.

Rincon, S. A., Estravis, M., Dingli, F., Loew, D., Tran, P. T. and Paoletti, A. (2017). SIN-Dependent Dissociation of the SAD Kinase Cdr2 from the Cell Cortex Resets the Division Plane. *Curr Biol* **27**, 534-542.

Rincon, S. A. and Paoletti, A. (2012). Mid1/anillin and the spatial regulation of cytokinesis in fission yeast. *Cytoskeleton (Hoboken)* **69**, 764-77.

Rincon, S. A. and Paoletti, A. (2016). Molecular control of fission yeast cytokinesis. *Semin Cell Dev Biol* **53**, 28-38.

Rincon, S. A., Ye, Y., Villar-Tajadura, M. A., Santos, B., Martin, S. G. and Perez, P. (2009). Pob1 Participates in the Cdc42 Regulation of Fission Yeast Actin Cytoskeleton. *Molecular Biology of the Cell* **20**, 4390–4399.

Roberts-Galbraith, R. H., Chen, J. S., Wang, J. and Gould, K. L. (2009). The SH3 domains of two PCH family members cooperate in assembly of the Schizosaccharomyces pombe contractile ring. *J Cell Biol* **184**, 113-27.

Roberts-Galbraith, R. H., Ohi, M. D., Ballif, B. A., Chen, J. S., McLeod, I., McDonald, W. H., Gygi, S. P., Yates, J. R., 3rd and Gould, K. L. (2010). Dephosphorylation of F-BAR protein Cdc15 modulates its conformation and stimulates its scaffolding activity at the cell division site. *Mol Cell* **39**, 86-99.

Romero, S., Le Clainche, C., Didry, D., Egile, C., Pantaloni, D. and Carlier, M. F. (2004). Formin is a processive motor that requires profilin to accelerate actin assembly and associated ATP hydrolysis. *Cell* **119**, 419-29.

Roncero, C. and Sanchez, Y. (2010). Cell separation and the maintenance of cell integrity during cytokinesis in yeast: the assembly of a septum. *Yeast* **27**, 521-30.

Ross, J. L., Ali, M. Y. and Warshaw, D. M. (2008). Cargo transport: molecular motors navigate a complex cytoskeleton. *Curr Opin Cell Biol* **20**, 41-7.

Russell, P. and Nurse, P. (1986). cdc25+ functions as an inducer in the mitotic control of fission yeast. *Cell* **45**, 145-53.

Russell, P. and Nurse, P. (1987). Negative regulation of mitosis by wee1+, a gene encoding a protein kinase homolog. *Cell* **49**, 559-67.

Saarikangas, J. and Barral, Y. (2011). The emerging functions of septins in metazoans. *EMBO Rep* **12**, 1118-26.

Saarikangas, J., Zhao, H. and Lappalainen, P. (2010). Regulation of the actin cytoskeleton-plasma membrane interplay by phosphoinositides. *Physiol Rev* **90**, 259-89.

Sacristan, C. and Kops, G. J. (2014). Joined at the hip: kinetochores, microtubules, and spindle assembly checkpoint signaling. *Trends Cell Biol* **25**, 21-8.

Saha, S. and Pollard, T. D. (2012). Anillin-related protein Mid1p coordinates the assembly of the cytokinetic contractile ring in fission yeast. *Mol Biol Cell* **23**, 3982-92.

Salimova, E., Sohrmann, M., Fournier, N. and Simanis, V. (2000). The S. pombe orthologue of the S. cerevisiae mob1 gene is essential and functions in signalling the onset of septum formation. *J Cell Sci* **113 (Pt 10)**, 1695-704.

Sanders, S. L. and Herskowitz, I. (1996). The BUD4 protein of yeast, required for axial budding, is localized to the mother/BUD neck in a cell cycle-dependent manner. *J Cell Biol* **134**, 413-27.

Santos, B., Martin-Cuadrado, A. B., Vazquez de Aldana, C. R., del Rey, F. and Perez, P. (2005). Rho4 GTPase is involved in secretion of glucanases during fission yeast cytokinesis. *Eukaryot Cell* **4**, 1639-45.

Schiel, J. A., Childs, C. and Prekeris, R. (2013). Endocytic transport and cytokinesis: from regulation of the cytoskeleton to midbody inheritance. *Trends Cell Biol* **23**, 319-27.

Schmidt, S., Sohrmann, M., Hofmann, K., Woollard, A. and Simanis, V. (1997). The Spg1p GTPase is an essential, dosage-dependent inducer of septum formation in Schizosaccharomyces pombe. *Genes Dev* **11**, 1519-34.

Sellin, M. E., Sandblad, L., Stenmark, S. and Gullberg, M. (2011). Deciphering the rules governing assembly order of mammalian septin complexes. *Mol Biol Cell* **22**, 3152-64.

Shcheprova, Z., Baldi, S., Frei, S. B., Gonnet, G. and Barral, Y. (2008). A mechanism for asymmetric segregation of age during yeast budding. *Nature* **454**, 728.

Shevchenko, A. and Simons, K. (2010). Lipidomics: coming to grips with lipid diversity. *Nat Rev Mol Cell Biol* **11**, 593-8.

Shortle, D., Haber, J. E. and Botstein, D. (1982). Lethal disruption of the yeast actin gene by integrative DNA transformation. *Science* **217**, 371-3.

Simanis, V. (2003). Events at the end of mitosis in the budding and fission yeasts. *J Cell Sci* **116**, 4263-75.

Simanis, V. (2015). Pombe's thirteen - control of fission yeast cell division by the septation initiation network. *J Cell Sci* **128**, 1465-74.

Singh, N. S., Shao, N., McLean, J. R., Sevugan, M., Ren, L., Chew, T. G., Bimbo, A., Sharma, R., Tang, X., Gould, K. L. et al. (2011). SIN-inhibitory phosphatase complex promotes Cdc11p dephosphorylation and propagates SIN asymmetry in fission yeast. *Curr Biol* **21**, 1968-78.

Sirajuddin, M., Farkasovsky, M., Hauer, F., Kuhlmann, D., Macara, I. G., Weyand, M., Stark, H. and Wittinghofer, A. (2007). Structural insight into filament formation by mammalian septins. *Nature* **449**, 311-5.

Sirotkin, V., Beltzner, C. C., Marchand, J. B. and Pollard, T. D. (2005). Interactions of WASp, myosin-I, and verprolin with Arp2/3 complex during actin patch assembly in fission yeast. *J Cell Biol* **170**, 637-48.

Sirotkin, V., Berro, J., Macmillan, K., Zhao, L. and Pollard, T. D. (2010). Quantitative analysis of the mechanism of endocytic actin patch assembly and disassembly in fission yeast. *Mol Biol Cell* **21**, 2894-904.

Skau, C. T., Neidt, E. M. and Kovar, D. R. (2009). Role of tropomyosin in formin-mediated contractile ring assembly in fission yeast. *Mol Biol Cell* **20**, 2160-73.

Skoumpla, K., Coulton, A. T., Lehman, W., Geeves, M. A. and Mulvihill, D. P. (2007). Acetylation regulates tropomyosin function in the fission yeast Schizosaccharomyces pombe. *J Cell Sci* **120**, 1635-45.

Sladewski, T. E., Previs, M. J. and Lord, M. (2009). Regulation of fission yeast myosin-II function and contractile ring dynamics by regulatory light-chain and heavy-chain phosphorylation. *Mol Biol Cell* **20**, 3941-52.

Slubowski, C. J., Funk, A. D., Roesner, J. M., Paulissen, S. M. and Huang, L. S. (2015). Plasmids for C-terminal tagging in Saccharomyces cerevisiae that contain improved GFP proteins, Envy and Ivy. *Yeast* **32**, 379-87.

Snider, C. E., Willet, A. H., Brown, H. T. and Gould, K. L. (2018). Analysis of the contribution of phosphoinositides to medial septation in fission yeast highlights the importance of PI(4,5)P2 for medial contractile ring anchoring. *Mol Biol Cell* **29**, 2148-2155.

Snider, C. E., Willet, A. H., Chen, J. S., Arpag, G., Zanic, M. and Gould, K. L. (2017). Phosphoinositide-mediated ring anchoring resists perpendicular forces to promote medial cytokinesis. *J Cell Biol* **216**, 3041-3050.

Sohrmann, M., Fankhauser, C., Brodbeck, C. and Simanis, V. (1996). The dmf1/mid1 gene is essential for correct positioning of the division septum in fission yeast. *Genes Dev* **10**, 2707-19.

Somlyo, A. P. and Somlyo, A. V. (2003). Ca2+ sensitivity of smooth muscle and nonmuscle myosin II: modulated by G proteins, kinases, and myosin phosphatase. *Physiol Rev* **83**, 1325-58.

Somma, M. P., Fasulo, B., Cenci, G., Cundari, E. and Gatti, M. (2002). Molecular dissection of cytokinesis by RNA interference in Drosophila cultured cells. *Mol Biol Cell* **13**, 2448-60.

Song, K., Mach, K. E., Chen, C. Y., Reynolds, T. and Albright, C. F. (1996). A novel suppressor of ras1 in fission yeast, byr4, is a dosage-dependent inhibitor of cytokinesis. *J Cell Biol* **133**, 1307-19.

Sparks, C. A., Morphew, M. and McCollum, D. (1999). Sid2p, a spindle pole body kinase that regulates the onset of cytokinesis. *J Cell Biol* **146**, 777-90.

Spiliotis, E. T. (2018). Spatial effects - site-specific regulation of actin and microtubule organization by septin GTPases. *J Cell Sci* **131**.

Stachowiak, M. R., Laplante, C., Chin, H. F., Guirao, B., Karatekin, E., Pollard, T. D. and O'Shaughnessy, B. (2014). Mechanism of cytokinetic contractile ring constriction in fission yeast. *Dev Cell* **29**, 547-561.

Stark, B. C., James, M. L., Pollard, L. W., Sirotkin, V. and Lord, M. (2013). UCS protein Rng3p is essential for myosin-II motor activity during cytokinesis in fission yeast. *PLoS One* **8**, e79593.

Storchova, Z. and Pellman, D. (2004). From polyploidy to aneuploidy, genome instability and cancer. *Nat Rev Mol Cell Biol* **5**, 45-54.

Storck, E. M., Ozbalci, C. and Eggert, U. S. (2018). Lipid Cell Biology: A Focus on Lipids in Cell Division. *Annu Rev Biochem* **87**, 839-869.

Straight, A. F., Field, C. M. and Mitchison, T. J. (2005). Anillin binds nonmuscle myosin II and regulates the contractile ring. *Mol Biol Cell* **16**, 193-201.

Stumpf, C. R., Moreno, M. V., Olshen, A. B., Taylor, B. S. and Ruggero, D. (2013). The translational landscape of the mammalian cell cycle. *Mol Cell* **52**, 574-82.

Suarez, C., Carroll, R. T., Burke, T. A., Christensen, J. R., Bestul, A. J., Sees, J. A., James, M. L., Sirotkin, V. and Kovar, D. R. (2015). Profilin regulates F-actin network homeostasis by favoring formin over Arp2/3 complex. *Dev Cell* **32**, 43-53.

Sun, L., Guan, R., Lee, I. J., Liu, Y., Chen, M., Wang, J., Wu, J. Q. and Chen, Z. (2015). Mechanistic insights into the anchorage of the contractile ring by anillin and Mid1. *Dev Cell* **33**, 413-26.

Suzuki, C., Daigo, Y., Ishikawa, N., Kato, T., Hayama, S., Ito, T., Tsuchiya, E. and Nakamura, Y. (2005). ANLN plays a critical role in human lung carcinogenesis through the activation of RHOA and by involvement in the phosphoinositide 3-kinase/AKT pathway. *Cancer Res* **65**, 11314-25.

Tada, T., Simonetta, A., Batterton, M., Kinoshita, M., Edbauer, D. and Sheng, M. (2007). Role of Septin cytoskeleton in spine morphogenesis and dendrite development in neurons. *Curr Biol* **17**, 1752-8.

Tajadura, V., Garcia, B., Garcia, I., Garcia, P. and Sanchez, Y. (2004). Schizosaccharomyces pombe Rgf3p is a specific Rho1 GEF that regulates cell wall beta-glucan biosynthesis through the GTPase Rho1p. *J Cell Sci* **117**, 6163-74.

Takahashi, Y., Iwase, M., Konishi, M., Tanaka, M., Toh-e, A. and Kikuchi, Y. (1999). Smt3, a SUMO-1 homolog, is conjugated to Cdc3, a component of septin rings at the mother-bud neck in budding yeast. *Biochem Biophys Res Commun* **259**, 582-7.

Takaine, M., Numata, O. and Nakano, K. (2009). Fission yeast IQGAP arranges actin filaments into the cytokinetic contractile ring. *EMBO J* **28**, 3117-31.

Takaine, M., Numata, O. and Nakano, K. (2014). Fission yeast IQGAP maintains F-actin-independent localization of myosin-II in the contractile ring. *Genes Cells* **19**, 161-76.

Takeda, T. and Chang, F. (2005). Role of fission yeast myosin I in organization of sterol-rich membrane domains. *Curr Biol* **15**, 1331-6.

Takeda, T., Kawate, T. and Chang, F. (2004). Organization of a sterol-rich membrane domain by cdc15p during cytokinesis in fission yeast. *Nat Cell Biol* **6**, 1142-4.

Takeya, R., Taniguchi, K., Narumiya, S. and Sumimoto, H. (2008). The mammalian formin FHOD1 is activated through phosphorylation by ROCK and mediates thrombin-induced stress fibre formation in endothelial cells. *EMBO J* **27**, 618-28.

Tanaka-Takiguchi, Y., Kinoshita, M. and Takiguchi, K. (2009). Septin-mediated uniform bracing of phospholipid membranes. *Curr Biol* **19**, 140-5.

Tanaka, K., Nishide, J., Okazaki, K., Kato, H., Niwa, O., Nakagawa, T., Matsuda, H., Kawamukai, M. and Murakami, Y. (1999). Characterization of a fission yeast SUMO-1 homologue, pmt3p, required for multiple nuclear events, including the control of telomere length and chromosome segregation. *Mol Cell Biol* **19**, 8660-72.

Tanaka, K., Petersen, J., MacIver, F., Mulvihill, D. P., Glover, D. M. and Hagan, I. M. (2001). The role of Plo1 kinase in mitotic commitment and septation in Schizosaccharomyces pombe. *EMBO J* **20**, 1259-70.

Tang, C. S. and Reed, S. I. (2002). Phosphorylation of the septin cdc3 in g1 by the cdc28 kinase is essential for efficient septin ring disassembly. *Cell Cycle* **1**, 42-9.

Tao, E. Y., Calvert, M. and Balasubramanian, M. K. (2014). Rewiring Mid1p-independent medial division in fission yeast. *Curr Biol* **24**, 2181-2188.

Tasto, J. J., Morrell, J. L. and Gould, K. L. (2003). An anillin homologue, Mid2p, acts during fission yeast cytokinesis to organize the septin ring and promote cell separation. *J Cell Biol* **160**, 1093-103.

Tebbs, I. R. and Pollard, T. D. (2013). Separate roles of IQGAP Rng2p in forming and constricting the Schizosaccharomyces pombe cytokinetic contractile ring. *Mol Biol Cell* **24**, 1904-17.

Thiyagarajan, S., Munteanu, E. L., Arasada, R., Pollard, T. D. and O'Shaughnessy, B. (2015). The fission yeast cytokinetic contractile ring regulates septum shape and closure. *J Cell Sci* **128**, 3672-81.

Tian, D., Diao, M., Jiang, Y., Sun, L., Zhang, Y., Chen, Z., Huang, S. and Ou, G. (2015). Anillin Regulates Neuronal Migration and Neurite Growth by Linking RhoG to the Actin Cytoskeleton. *Curr Biol* **25**, 1135-45.

Toda, T., Umesono, K., Hirata, A. and Yanagida, M. (1983). Cold-sensitive nuclear division arrest mutants of the fission yeast Schizosaccharomyces pombe. *J Mol Biol* **168**, 251-70.

Tolic-Norrelykke, I. M., Sacconi, L., Stringari, C., Raabe, I. and Pavone, F. S. (2005). Nuclear and division-plane positioning revealed by optical micromanipulation. *Curr Biol* **15**, 1212-6.

Tong, J., Manik, M. K. and Im, Y. J. (2018). Structural basis of sterol recognition and nonvesicular transport by lipid transfer proteins anchored at membrane contact sites. *Proc Natl Acad Sci U S A* **115**, E856-E865.

Tran, P. T., Marsh, L., Doye, V., Inoue, S. and Chang, F. (2001). A mechanism for nuclear positioning in fission yeast based on microtubule pushing. *J Cell Biol* **153**, 397-411.

Trautmann, S., Wolfe, B. A., Jorgensen, P., Tyers, M., Gould, K. L. and McCollum, D. (2001). Fission yeast Clp1p phosphatase regulates G2/M transition and coordination of cytokinesis with cell cycle progression. *Curr Biol* **11**, 931-40.

van Meer, G., Voelker, D. R. and Feigenson, G. W. (2008). Membrane lipids: where they are and how they behave. *Nat Rev Mol Cell Biol* **9**, 112-24.

Vavylonis, D., Kovar, D. R., O'Shaughnessy, B. and Pollard, T. D. (2006). Model of formin-associated actin filament elongation. *Mol Cell* **21**, 455-66.

Vavylonis, D., Wu, J. Q., Hao, S., O'Shaughnessy, B. and Pollard, T. D. (2008). Assembly mechanism of the contractile ring for cytokinesis by fission yeast. *Science* **319**, 97-100.

Versele, M. and Thorner, J. (2004). Septin collar formation in budding yeast requires GTP binding and direct phosphorylation by the PAK, Cla4. *J Cell Biol* **164**, 701-15.

Versele, M. and Thorner, J. (2005). Some assembly required: yeast septins provide the instruction manual. *Trends Cell Biol* **15**, 414-24.

Vicente-Manzanares, M., Ma, X., Adelstein, R. S. and Horwitz, A. R. (2009). Non-muscle myosin II takes centre stage in cell adhesion and migration. *Nat Rev Mol Cell Biol* **10**, 778-90.

Vrabioiu, A. M. and Mitchison, J. M. (2006). Structural insights into yeast septin organization from polarized fluorescence microscopy. *Nature* **443**, 466-469.

Vrabioiu, A. M. and Mitchison, J. M. (2007). Symmetry of Septin Hourglass and Ring Structures. *J. Mol. Biol.* **372**, 37-49.

Wachowicz, P., Chasapi, A., Krapp, A., Cano Del Rosario, E., Schmitter, D., Sage, D., Unser, M., Xenarios, I., Rougemont, J. and Simanis, V. (2015). Analysis of S. pombe SIN protein association to the SPB reveals two genetically separable states of the SIN. *J Cell Sci* **128**, 741-54.

Wachtler, V. and Balasubramanian, M. K. (2006). Yeast lipid rafts?--an emerging view. *Trends Cell Biol* **16**, 1-4.

Wachtler, V., Rajagopalan, S. and Balasubramanian, M. K. (2003). Sterol-rich plasma membrane domains in the fission yeast Schizosaccharomyces pombe. *J Cell Sci* **116**, 867-74.

Wallar, B. J., Stropich, B. N., Schoenherr, J. A., Holman, H. A., Kitchen, S. M. and Alberts, A. S. (2006). The basic region of the diaphanous-autoregulatory domain (DAD) is required for autoregulatory interactions with the diaphanous-related formin inhibitory domain. *J Biol Chem* **281**, 4300-7.

Wang, D., Chadha, G. K., Feygin, A. and Ivanov, A. I. (2015). F-actin binding protein, anillin, regulates integrity of intercellular junctions in human epithelial cells. *Cell Mol Life Sci* **72**, 3185-3200.

Wang, H., Tang, X. and Balasubramanian, M. K. (2003). Rho3p regulates cell separation by modulating exocyst function in Schizosaccharomyces pombe. *Genetics* **164**, 1323-31.

Wang, H., Tang, X., Liu, J., Trautmann, S., Balasundaram, D., McCollum, D. and Balasubramanian, M. K. (2002). The multiprotein exocyst complex is essential for cell separation in Schizosaccharomyces pombe. *Mol Biol Cell* **13**, 515-29.

Wang, J., Neo, S. P. and Cai, M. (2009). Regulation of the yeast formin Bni1p by the actin-regulating kinase Prk1p. *Traffic* **10**, 528-35.

Wang, N., Wang, M., Zhu, Y. H., Grosel, T. W., Sun, D., Kudryashov, D. S. and Wu, J. Q. (2014). The Rho-GEF Gef3 interacts with the septin complex and activates the GTPase Rho4 during fission yeast cytokinesis. *Mol Biol Cell* **26**, 238-55.

Watanabe, S., Ando, Y., Yasuda, S., Hosoya, H., Watanabe, N., Ishizaki, T. and Narumiya, S. (2008). mDia2 induces the actin scaffold for the contractile ring and stabilizes its position during cytokinesis in NIH 3T3 cells. *Mol Biol Cell* **19**, 2328-38.

Watanabe, S., Okawa, K., Miki, T., Sakamoto, S., Morinaga, T., Segawa, K., Arakawa, T., Kinoshita, M., Ishizaki, T. and Narumiya, S. (2010). Rho and anillin-dependent control of mDia2 localization and function in cytokinesis. *Mol Biol Cell* **21**, 3193-204.

White, E. A. and Glotzer, M. (2012). Centralspindlin: at the heart of cytokinesis. *Cytoskeleton (Hoboken)* **69**, 882-92.

Willet, A. H., DeWitt, A. K., Beckley, J. R., Clifford, D. M. and Gould, K. L. (2019). NDR Kinase Sid2 Drives Anillin-like Mid1 from the Membrane to Promote Cytokinesis and Medial Division Site Placement. *Curr Biol* **29**, 1055-1063 e2.

Willet, A. H., McDonald, N. A., Bohnert, K. A., Baird, M. A., Allen, J. R., Davidson, M. W. and Gould, K. L. (2015a). The F-BAR Cdc15 promotes contractile ring formation through the direct recruitment of the formin Cdc12. *J Cell Biol* **208**, 391-9.

Willet, A. H., McDonald, N. A. and Gould, K. L. (2015b). Regulation of contractile ring formation and septation in Schizosaccharomyces pombe. *Curr Opin Microbiol* **28**, 46-52.

Wloka, C., Nishihama, R., Onishi, M., Oh, Y., Hanna, J., Pringle, J. R., Krauss, M. and Bi, E. (2011). Evidence that a septin diffusion barrier is dispensable for cytokinesis in budding yeast. *Biol Chem* **392**, 813-29.

Wolven, A. K., Belmont, L. D., Mahoney, N. M., Almo, S. C. and Drubin, D. G. (2000). In vivo importance of actin nucleotide exchange catalyzed by profilin. *J Cell Biol* **150**, 895-904.

Wu, H., Guo, J., Zhou, Y. T. and Gao, X. D. (2015). The anillin-related region of Bud4 is the major functional determinant for Bud4's function in septin organization during bud growth and axial bud site selection in budding yeast. *Eukaryot Cell* **14**, 241-51.

Wu, J. Q., Bahler, J. and Pringle, J. R. (2001). Roles of a fimbrin and an alpha-actinin-like protein in fission yeast cell polarization and cytokinesis. *Mol Biol Cell* **12**, 1061-77.

Wu, J. Q., Kuhn, J. R., Kovar, D. R. and Pollard, T. D. (2003). Spatial and temporal pathway for assembly and constriction of the contractile ring in fission yeast cytokinesis. *Dev Cell* **5**, 723-34.

Wu, J. Q. and Pollard, T. D. (2005). Counting cytokinesis proteins globally and locally in fission yeast. *Science* **310**, 310-4.

Wu, J. Q., Sirotkin, V., Kovar, D. R., Lord, M., Beltzner, C. C., Kuhn, J. R. and Pollard, T. D. (2006). Assembly of the cytokinetic contractile ring from a broad band of nodes in fission yeast. *J Cell Biol* **174**, 391-402.

Wu, J. Q., Ye, Y., Wang, N., Pollard, T. D. and Pringle, J. R. (2010). Cooperation between the septins and the actomyosin ring and role of a cell-integrity pathway during cell division in fission yeast. *Genetics* **186**, 897-915.

Wurzenberger, C. and Gerlich, D. W. (2011). Phosphatases: providing safe passage through mitotic exit. *Nat Rev Mol Cell Biol* **12**, 469-82.

Xu, Y., Moseley, J. B., Sagot, I., Poy, F., Pellman, D., Goode, B. L. and Eck, M. J. (2004). Crystal structures of a Formin Homology-2 domain reveal a tethered dimer architecture. *Cell* **116**, 711-23.

Yam, C., He, Y., Zhang, D., Chiam, K. H. and Oliferenko, S. (2011). Divergent strategies for controlling the nuclear membrane satisfy geometric constraints during nuclear division. *Curr Biol* **21**, 1314-9.

Yarmola, E. G. and Bubb, M. R. (2006). Profilin: emerging concepts and lingering misconceptions. *Trends Biochem Sci* **31**, 197-205.

Ye, Y., Lee, I. J., Runge, K. W. and Wu, J. Q. (2012). Roles of putative Rho-GEF Gef2 in division-site positioning and contractile-ring function in fission yeast cytokinesis. *Mol Biol Cell* **23**, 1181-95.

Yonetani, A. and Chang, F. (2010). Regulation of cytokinesis by the formin cdc12p. *Curr Biol* **20**, 561-6.

Yonetani, A., Lustig, R. J., Moseley, J. B., Takeda, T., Goode, B. L. and Chang, F. (2008). Regulation and targeting of the fission yeast formin cdc12p in cytokinesis. *Mol Biol Cell* **19**, 2208-19.

Zhang, D., Vjestica, A. and Oliferenko, S. (2010). The cortical ER network limits the permissive zone for actomyosin ring assembly. *Curr Biol* **20**, 1029-34.

Zhang, D., Vjestica, A. and Oliferenko, S. (2012). Plasma membrane tethering of the cortical ER necessitates its finely reticulated architecture. *Curr Biol* **22**, 2048-52.

Zhang, J., Kong, C., Xie, H., McPherson, P. S., Grinstein, S. and Trimble, W. S. (1999). Phosphatidylinositol polyphosphate binding to the mammalian septin H5 is modulated by GTP. *Curr Biol* **9**, 1458-67.

Zhang, Y., Sugiura, R., Lu, Y., Asami, M., Maeda, T., Itoh, T., Takenawa, T., Shuntoh, H. and Kuno, T. (2000). Phosphatidylinositol 4-phosphate 5-kinase Its3 and calcineurin Ppb1 coordinately regulate cytokinesis in fission yeast. *J Biol Chem* **275**, 35600-6.

Zhao, W. M. and Fang, G. (2005). Anillin is a substrate of anaphase-promoting complex/cyclosome (APC/C) that controls spatial contractility of myosin during late cytokinesis. *J Biol Chem* **280**, 33516-24.

Zheng, S., Dong, F., Rasul, F., Yao, X., Jin, Q. W., Zheng, F. and Fu, C. (2018). Septins regulate the equatorial dynamics of the separation initiation network kinase Sid2p and glucan synthases to ensure proper cytokinesis. *FEBS J* **285**, 2468-2480.

Zhou, W., Wang, Z., Shen, N., Pi, W., Jiang, W., Huang, J., Hu, Y., Li, X. and Sun, L. (2015a). Knockdown of ANLN by lentivirus inhibits cell growth and migration in human breast cancer. *Mol Cell Biochem* **398**, 11-9.

Zhou, Z., Munteanu, E. L., He, J., Ursell, T., Bathe, M., Huang, K. C. and Chang, F. (2015b). The contractile ring coordinates curvature-dependent septum assembly during fission yeast cytokinesis. *Mol Biol Cell* **26**, 78-90.

Zhu, Y. H., Ye, Y., Wu, Z. and Wu, J. Q. (2013). Cooperation between Rho-GEF Gef2 and its binding partner Nod1 in the regulation of fission yeast cytokinesis. *Mol Biol Cell* **24**, 3187-204.

Zigmond, S. H. (2004). Formin-induced nucleation of actin filaments. *Curr Opin Cell Biol* **16**, 99-105.

Zimmermann, D., Homa, K. E., Hocky, G. M., Pollard, L. W., De La Cruz, E. M., Voth, G. A., Trybus, K. M. and Kovar, D. R. (2017). Mechanoregulated inhibition of formin facilitates contractile actomyosin ring assembly. *Nat Commun* **8**, 703.

ABSTRACT

Cell division is an essential process required for the proliferation of unicellular organisms, for the development of multicellular organisms, as well as for cell renewal within tissues and organs. Defective control of cell division can either lead to cell death, or to cell hyper-proliferation and contribute to cancer progression. Cell division is therefore under the control of very tight regulatory mechanisms. In animals and fungi, its final step, cytokinesis, requires an acto-myosin-based contractile ring that constricts to promote sister cell cleavage. Modifications in the lipid composition of the plasma membrane take place during cell division, with functional impact on cytokinesis.

Fission yeast is a simple single cell eukaryotic organism which has been extensively used to study cell division because of its stereotyped rode shape, easy genetics and short generation time. In particular, this model system has proved very powerful for the molecular dissection of contractile ring assembly. However remarkably little is known on how membrane lipids regulate contractile ring assembly. In the first part of my PhD, my objective was to study how lipids could regulate contractile ring positioning in fission yeast. I have combined fission yeast genetics with live-cell imaging of contractile ring assembly from precursor nodes to understand how ergosterol levels affect division plane positioning. I have found that increased ergosterol levels prevent F-actin assembly from cytokinetic precursor nodes by the formin Cdc12, avoiding their compaction into a medially placed contractile ring. Since the stability of F-actin cables was not altered altogether and the phenotype could be partially rescued by inhibition of the Arp2/3 complex which competes with formins, we propose that increasing ergosterol levels in the plasma membrane may inhibit the activity of the formin Cdc12.

In addition to the contractile ring, cytokinesis involves an additional component of the cytoskeleton, the septins, which form filaments at the division site. Septins are a family of conserved GTP binding proteins whose deletion leads to cytokinetic defects. They also serve as scaffolds for protein-protein interactions and/or as diffusion barriers for protein compartmentalization in cytokinesis and beyond. In fission yeast, in contrast to budding yeast, septins are late at the division site and are only involved in late stages of cytokinesis, to promote sister cell separation. In the second part of my PhD, I decided to explore the dynamic behavior of septins and decipher how they are regulated. Using live cell imaging and precise cell cycle timers, I have identified a new step in the recruitment of septin to the cell cortex in the proximity of the contractile acto-myosin ring, in a broad meshwork that then compacts into a tight ring. I have also found evidence that the anillin-like protein Mid2 is necessary to promote this compaction and may act as a bundler for septin filaments. However, analysis of mutants blocked in mitosis shows that this protein is not sufficient to accomplish this task. Moreover, I have determined that high Cdk activity allows septins and Mid2 initial recruitment and assembly, but the SIN pathway also plays a role in promoting their recruitment at the cell middle and is then required to drive their compaction. Additionally, I have found that PIP2 levels influence not only the amount of septins and Mid2 filaments associated at the medial cortex together with their compaction but also the timing of septin and mid2 recruitment to the division site. This demonstrates that septin assembly relies on complex regulations coordinated by the cell cycle machinery.

KEYWORDS

Cytokinesis, fission yeast, lipids, septins